

Utilizing Catalytic mTOR Inhibition in Preclinical Models of Huntington Disease

Dissertation

der Mathematisch-Naturwissenschaftlichen Fakultät

der Eberhard Karls Universität Tübingen

zur Erlangung des Grades eines

Doktors der Naturwissenschaften

(Dr. rer. nat.)

vorgelegt von

Elisabeth Singer-Mikosch, geb. Singer

aus Pawlodar/Kasachstan

Tübingen

2021

Gedruckt mit Genehmigung der Mathematisch-Naturwissenschaftlichen Fakultät der Eberhard Karls Universität Tübingen.

Tag der mündlichen Qualifikation: 11.07.2022

Dekan: Prof. Dr. Thilo Stehle

1. Berichterstatter: Prof. Dr. Huu Phuc Nguyen

2. Berichterstatter: Prof. Dr. Tassula Proikas-Cezanne

TABLE OF CONTENTS

Abbreviations	iv
Zusammenfassung.....	v
Summary.....	vi
Introduction	1
Huntington Disease	1
disease aetiology	1
pathogenesis of Huntington disease	2
Molecular Mechanisms of Neurodegeneration	3
shared mechanisms in neurodegeneration	4
the PolyQ effect.....	4
protein quality control and the autophagosomal lysosomal pathway.....	7
Autophagy in HD.....	9
pathway alterations in HD	9
Huntingtin – an autophagy protein?	11
models to study autophagy in HD	11
Therapeutic approaches for HD.....	13
therapeutic approaches to increase autophagy in HD.....	13
Objectives	15
Results and Discussion	16
Characterization of the STHdh cell model	16
Publication # 1: Reduced cell size, chromosomal aberration and altered proliferation rates are characteristics and confounding factors in the <i>STHdh</i> cell model of Huntington disease.....	16
In vitro and in vivo characterization of PIQUR compounds.....	24

Publication # 5: Brain-penetrant PQR620 mTOR and PQR530 PI3K/mTOR inhibitor reduce huntingtin levels in cell models of HD (Singer <i>et al.</i> , 2019).....	24
unpublished manuscript # 1: PQR530 and PQR620 reduce aggregation in the R6/2 mouse model but fail to ameliorate behavioural phenotype (Singer <i>et al.</i> , 2020).....	24
Options & Perspectives.....	37
References.....	39
Appendix: Publication #1 - #6.....	53

ABBREVIATIONS

4E-BP1	Eukaryotic translation initiation factor 4E-binding protein 1	IGF-1	Insulin-like growth factor 1
AD	Alzheimer Disease	IPSC	induced pluripotent stem cells
ADP	Adenosine diphosphate	LC3-II.....	Microtubule-associated proteins 1A/1B light chain 3B
ALP...	autophagosomal lysosomal pathway	mHTT	mutant huntingtin
ALS.....	Amyotrophic lateral sclerosis	MITOC.....	microtubule organizing centre
AMPK	AMP-activated protein kinase	MSCs.....	mesenchymal stem cells
ASO	antisense oligonucleotides	mTOR.....	mechanistic target of rapamycin
BBB	blood brain barrier	NGF.....	Nerve growth factor
BDNF.....	Brain-derived neurotrophic factor	PD	Parkinson Disease
CR	caloric restriction	PI3K.....	Phosphoinositide 3-kinase
CSF	cerebrospinal fluid	RAN.....	repeat-associated non-ATG
DRPLA.....	Dentatorubral–pallidoluysian atrophy	Rheb.....	Ras homolog enriched in brain
ER	endoplasmatic reticulum	Rhes.....	Ras homolog enriched in striatum
HD	Huntington Disease	RNAi	RNA interference
Hdh.....	Huntingtin (mouse)	RPS6K.....	Ribosomal protein S6 kinase
HDKI.....	Huntington Disease Knock-in	S6RP	ribosomal protein S6
HEAT....	found in HTT, elongation factor 3, phosphatase 2A and TOR1	SBMA.	spinal and bulbar muscular atrophy
HPRT.....	Hypoxanthine Phosphoribosyltransferase	SCA3.....	spinocerebellar ataxia type 3
HTT	Huntingtin	ULK1.....	Unc-51 like autophagy activating kinase
		UPS	ubiquitin proteasome system

ZUSAMMENFASSUNG

Die vorliegende Arbeit befasst sich mit dem experimentellen Therapieansatz, Autophagie zu nutzen, um pathologische Veränderungen der Huntington Erkrankung abzuschwächen. Die Huntington Erkrankung ist eine erbliche, neurodegenerative Erkrankung, die schon bevor sie ausbricht zu Veränderungen in Neuronen führt. Das krankheitsverursachende Protein, Huntingtin, kann seine ursprünglichen Funktionen nicht ausreichend erfüllen und nimmt daher unerwünschte Eigenschaften an. Es akkumuliert in den Zellen, wodurch es zu einer Dysbalance auf zellulärer und neuronaler Ebene kommt. Kann das Gleichgewicht zwischen Zellstress und protektiven Prozessen nicht aufrechterhalten werden, so kommt es zum Zelltod.

Die Autophagie (Makroautophagie) ist ein Proteinabbauprozess und beseitigt solche akkumulierenden und nicht funktionalen Proteine und speist die dabei entstehenden Grundbausteine wieder in anabole Prozesse der Zelle ein. Eine Erhöhung der Rate abgebauten zellulären Materials zeigte positive Effekte in Tiermodellen für die Huntington Erkrankung. Jedoch ist die pharmakologische Induktion der Autophagie bisher mit Nebenwirkungen und einer eingeschränkten Bioverfügbarkeit im Gehirn verbunden. Um diese Nachteile zu umgehen, wurden für diese Arbeit zwei neue, gehirngängige *mechanistic target of rapamycin* (mTOR)-Inhibitoren herangezogen, die auf ihre Fähigkeit hin untersucht wurden, Autophagie in Modellen der Huntington Erkrankung zu induzieren. Um diese Wirkstoffe im Zellmodell testen zu können, wurden aus *Huntington Disease Knock-in* (HDKI) – Mäusen generierte Zelllinien charakterisiert, welche das mutierte *Huntingtin* Gen tragen. Darauf aufbauend wurde die Wirkung in einem transgenen Mausmodell (R6/2) der Huntington Erkrankung untersucht, welches einen starken Phänotyp entwickelt. Während gezeigt werden konnte, dass die Inhibition mTORs mittels oraler Gabe die Akkumulation des Huntingtins in den Neuronen der Mäuse reduzieren konnte, so wie es auch im Zellmodell beobachtet wurde, konnte der verheerende Krankheitsverlauf dieses Modells nicht aufgehalten oder verlangsamt werden. Damit wurde ein weiterer Schritt gemacht, um die optimale Therapieform mittels mTOR Inhibitoren zu ermitteln.

SUMMARY

Huntington Disease is a neurodegenerative, monogenetic disorder that affects neuronal health long before patients become aware of symptoms. The disease-causing protein, Huntingtin – when mutated – is no longer able to fulfil its cellular functions and moreover acquires features by the mutation that further impose stress to the cell. The mutated protein accumulates in the cell, leading to a disbalance on the cellular and neuronal level. If the cell is no longer able to mitigate the stress levels, cell death occurs.

Autophagy (macroautophagy) is one of the cell's pathways to reduce protein accumulations of excess, long-lived and unfunctional proteins. Proteolysis of these cellular waste deposits feeds then into newly synthesised proteins and anabolic processes. Increasing the throughput of this recycling mechanism has been shown to have beneficial effects on animal models of Huntington Disease. By lowering the amount of the mutated protein, cell viability and functions are improved. However, the pharmacological stimulation of autophagy is accompanied by side effects and limited bioavailability in the brain. To circumvent these obstacles, for the here described studies two novel, brain-penetrant mechanistic target of rapamycin (mTOR) inhibitors have been chosen to evaluate their potential to ameliorate pathological features of Huntington disease in cell and animal models of Huntington disease. For evaluating these compounds, Huntington Disease knock-in (HDKI) mice-derived cell lines have been characterized, which carry the Huntington mutation and the new mTOR inhibiting compounds have been evaluated for their ability to induce autophagy and to reduce Huntingtin accumulations. Based on the findings in this cell model, mTOR inhibition has been further studied in a transgenic mouse model of Huntington Disease (R6/2 mice), which develop a very fast and severe phenotype. While it could be shown that mTOR inhibition, in line with the *in vitro* findings, reduced Huntingtin accumulations in neurons, the fast progressive phenotype could not be ameliorated.

Therefore, with this study another tool has been made available to investigate the therapeutic potential of autophagy inducing compounds for Huntington Disease by providing information on the effects on Huntingtin levels *in vitro* and *in vivo*.

INTRODUCTION

HUNTINGTON DISEASE

disease aetiology

Huntington disease (HD), is a fatal, autosomal dominantly inherited, neurodegenerative disorder (Vonsattel & DiFiglia, 1998). It was named after George Huntington, who provided one of the first descriptions of the disease in 1872, mentioning many of the clinical features and the hereditary nature (Huntington, 2003; Walker, 2007). The disease-causing gene, *Huntingtin (HTT)*, was identified in 1993 (The Huntington's Disease Collaborative Research Group, 1993). The gene consists of 67 exons, of which exon 1 is the best studied, as it contains the CAG nucleotide repeat region, the mutated locus. Healthy individuals most commonly carry 19 or 20 CAG triplet repeats, which code for the amino acid glutamine (Q) stretch (PolyQ), within exon1 in the N-terminus of Huntingtin protein (HTT). A multiplication of the CAG repeats to more than 39 results in full penetrance (Rubinsztein *et al.*, 1996), mostly with onset in mid-life of patients (Vonsattel & DiFiglia, 1998). Age of onset is inversely correlated with the number of CAGs (Duyao *et al.*, 1993; Stine *et al.*, 1993) and an expansion of the polyglutamine repeats to over 60 leads to the juvenile form, which is characterized by onset in childhood or adolescence and symptoms distinct

from the adult form with rigidity and seizures (Nance & Myers, 2001). CAG length accounts for 50 – 70 % of the variance in age of onset, which is further modulated by genetic modifiers and environmental factors (GeM-HD, 2015; Ross & Tabrizi, 2011; Zuccato *et al.*, 2010). The disorder is inherited by autosomal dominant transmission and affects approximately 5 -10 to 10 - 14 individuals in 100,000 in western populations (McColgan & Tabrizi, 2018; Saudou & Humbert, 2016).

pathogenesis of Huntington disease

clinical features of HD

Huntington disease is characterized by a triad of motor, psychiatric and cognitive symptoms. The diagnosis is based on genetic testing for the mutation and the evaluation of motor symptoms. A pre-diagnosis (pre-manifest) phase precedes disease onset, in which already years earlier mild symptoms can be detected, without the awareness of the patients (Tabrizi *et al.*, 2009) and degeneration of brain structures and pathological processes precede even this period (Caron *et al.*, 2018). Once the disease manifests, it presents with a hyperkinetic phase with chorea and involuntary movements, which progresses to a hypokinetic phase, where patients suffer from dystonia, balance and gait disturbances (McColgan & Tabrizi, 2018). Psychiatric and cognitive symptoms amongst others are apathy, depression, and irritability in premanifest and manifest stages and impaired emotion recognition and processing speed. The underlying neuropathology is loss and atrophy in the caudate and putamen (Walker, 2007) with a specific loss of medium spiny neurons in the striatum (Ferrante *et al.*, 1987; Graveland *et al.*, 1985; Reiner *et al.*, 1988), extending to the cortex and other brain regions upon disease progression. The brain is the most vulnerable organ to the disease, but also pathological alterations in peripheral tissues, metabolic function and weight loss are characteristics (Ciammola *et al.*, 2006; Zielonka *et al.*, 2014). Patients die 15 - 20 years after manifestation from disease complications.

wild type huntingtin

Huntingtin is evolutionary conserved from fly to mammals and expressed throughout the entire lifetime in all tissues, with highest expression in brain and testes (Landwehrmeyer *et al.*, 1995; Saudou & Humbert, 2016). It is essential during

development, as the knockout results in embryonic lethality (Zeitlin *et al.*, 1995). Conditional knockout after birth has been shown to cause milder deficits in peripheral tissues that resemble some features of HD (Cattaneo *et al.*, 2001).

Within the large protein (348 kDa) are several HEAT domains (found in HTT, elongation factor 3, phosphatase 2A and TOR1), which are often found in large, complex forming proteins, involved in cytoplasmic trafficking (Andrade & Bork, 1995). Wildtype HTT is found mainly in the cytoplasm, where it interacts with various organelles, vesicle membranes and transport structures (Rubinsztein & Carmichael, 2003). Even though more than 350 interaction partners have been proposed to interact with wildtype HTT, alone, the understanding of HTT's function in the cell is not yet complete (Kaltenbach *et al.*, 2007; Ratovitski *et al.*, 2012; Saudou & Humbert, 2016). HTT is involved in vesicle trafficking (Caviston & Holzbaur, 2009), endocytosis (Cattaneo *et al.*, 2001), cell division (Godin *et al.*, 2010), transcription regulation (Kegel *et al.*, 2002) and wildtype huntingtin overexpression was shown to be anti-apoptotic (Leavitt *et al.*, 2006; Rigamonti *et al.*, 2000; Wild & Tabrizi, 2017). The plethora of functional entities HTT can adopt is multiplied by several cleavage sites for proteolytic modifications as well as post-translational modifications, which prime HTT for distinct biological functions. For example, the cleavage of HTT at two sites in combination with myristylation, results in increased autophagy (Martin *et al.*, 2014). By the mutation of the CAG repeat many of the physiological functions and interactions of the protein are affected, contributing to the pathogenesis (Cattaneo *et al.*, 2005), as well as the gain of function of other toxic functions of the mutant Huntingtin (mHTT) protein.

MOLECULAR MECHANISMS OF NEURODEGENERATION

Increasing life expectancy worldwide poses great challenges to the elderly and to communities (United Nations, 2018). With this increase in lifetime the risk factor aging contributes to increased prevalence of neurodegenerative disorders (Checkoway *et al.*, 2011; Heemels, 2016; Maiese, 2016). Many of the late-onset disorders share common mechanisms, as for example abnormal protein aggregation of a disease specific protein: β -amyloid plaques in Alzheimer disease (AD), α -synuclein inclusions in Parkinson disease (PD), huntingtin in HD or ataxin-3 in

spinocerebellar ataxia type 3 (SCA3), which result in divergent, yet sometimes overlapping, clinical features, depending on the affected brain structure (Gan *et al.*, 2018). Huntington disease can be considered a model disease for other neurodegenerative disorders. First, it is the most common of the polyglutamine disorders and second, the monogenetic nature allows modelling in animals and cell culture. As CAG length is a reliable marker for disease onset, but not disease progression (Ross & Tabrizi, 2011), underlying mechanism need to be elucidated and measures need to be found to slow the pathogenic processes.

shared mechanisms in neurodegeneration

Common pathomechanisms in AD, PD, Amyotrophic lateral sclerosis (ALS) and HD are promising targets for treatment. In all of the disorders protein aggregation is found in different regions and neuronal decline is promoted by dysfunctional protein folding and degradation, inflammation, altered post translational modifications, mitochondrial dysfunction and excitotoxicity (Caron *et al.*, 2018; Ehrnhoefer *et al.*, 2011b; Gan *et al.*, 2018). Polyglutamine disorders are caused by the expansion of a repetitive CAG repeat over a certain size that is specific for each of the ten disorders: HD, SCA1, SCA2, SCA3, SCA6, SCA7, SCA12, SCA17, spinal and bulbar muscular atrophy (SBMA) and Dentatorubral–pallidolusian atrophy (DRPLA). All these disorders show protein aggregation that is not compensated for by degradation (Walker, 2007), which is in common with Alzheimer and Parkinson disease.

the PolyQ effect

Even though the above mentioned polyglutamine disorders are caused by structurally distinct and functionally independent genes, they all show neurodegeneration in distinct brain regions (Gan *et al.*, 2018). The addition of the PolyQ repeat to the HTT protein is a relatively late event (after the protostome-deuterostome divergence) in evolution, as it is not or only rudimentary present in *Drosophila* and sea urchin (Tartari *et al.*, 2007; Zheng *et al.*, 2010). The mutation in the *HTT* gene, the expansion of the glutamine (Q) stretch to pathogenic lengths, leads to an alteration of protein function. This is on the one hand a loss of function of HTT, supported by the observation that models of HD have a more severe phenotype when homozygous for the mutation (Reddy *et al.*, 1998; Wheeler *et al.*,

1999) and also HD patients who, very rarely, carry both alleles with elongated CAGs show an accelerated disease progression (Squitieri *et al.*, 2003). On the other hand, the elongation of the PolyQ tract impacts the protein structure, solubility, and interaction behaviour, leading to a gain of function, which includes PolyQ specific effects and effects that are a result of altered protein conformation. This was shown by the introduction of a polyglutamine stretch into the Hypoxanthine Phosphoribosyltransferase (HPRT) gene, which has no functional overlap with the PolyQ-disorders, but leads to a neurodegeneration phenotype in HPRT-PolyQ mice (Ordway *et al.*, 1997) and most of the transgenic models of HD, express the mutated gene in addition to the endogenous, while presenting the disease phenotype. The PolyQ tract is further not essential in mouse models of HD and the deletion improves metabolic and behavioural parameters (Clabough & Zeitlin, 2006) and increases autophagy (Zheng *et al.*, 2010). Accordingly, such a general role of the polyglutamine expansion has implications for the other polyglutamine disorders.

mutant huntingtin's effect on cellular mechanisms

The cause (CAG expansion) leads to the effect (cell death), but the mechanisms by which loss of wildtype function and simultaneous toxic gain of function of the mutant protein leads to cell death are not yet completely understood and it remains difficult to distinguish primary and secondary effects. Beginning from the transcription, RNA transcripts from exon 1 (Li *et al.*, 2008; Sathasivam *et al.*, 2013) of the protein have been implicated in disease pathology, as well as the unconventional translation of proteins from repeat-associated non-ATG (RAN) translation (Bañez-Coronel *et al.*, 2015; Zu *et al.*, 2011). The mutation further affects protein structure and function. The length of the PolyQ repeat determines interaction capability and strength (Harjes & Wanker, 2003), which can lead to the loss of binding and sequestration of e.g. pro-apoptotic complex components (Gervais *et al.*, 2002) or the sequestration and suppression of signalling components by increased binding (Ravikumar *et al.*, 2004). Many different cellular functions are affected by the mutation. These involve calcium handling deficits and excitotoxicity, mitochondrial energy metabolism and dynamics, the sequestration of transcription factors, defects in vesicular trafficking and declining protein quality control amongst others (Martin *et al.*, 2015; Panov *et al.*, 2002; Petersén *et al.*, 2001; Quintanilla & Johnson, 2009; Seong *et al.*, 2005; Sugars & Rubinsztein) (Figure 1).

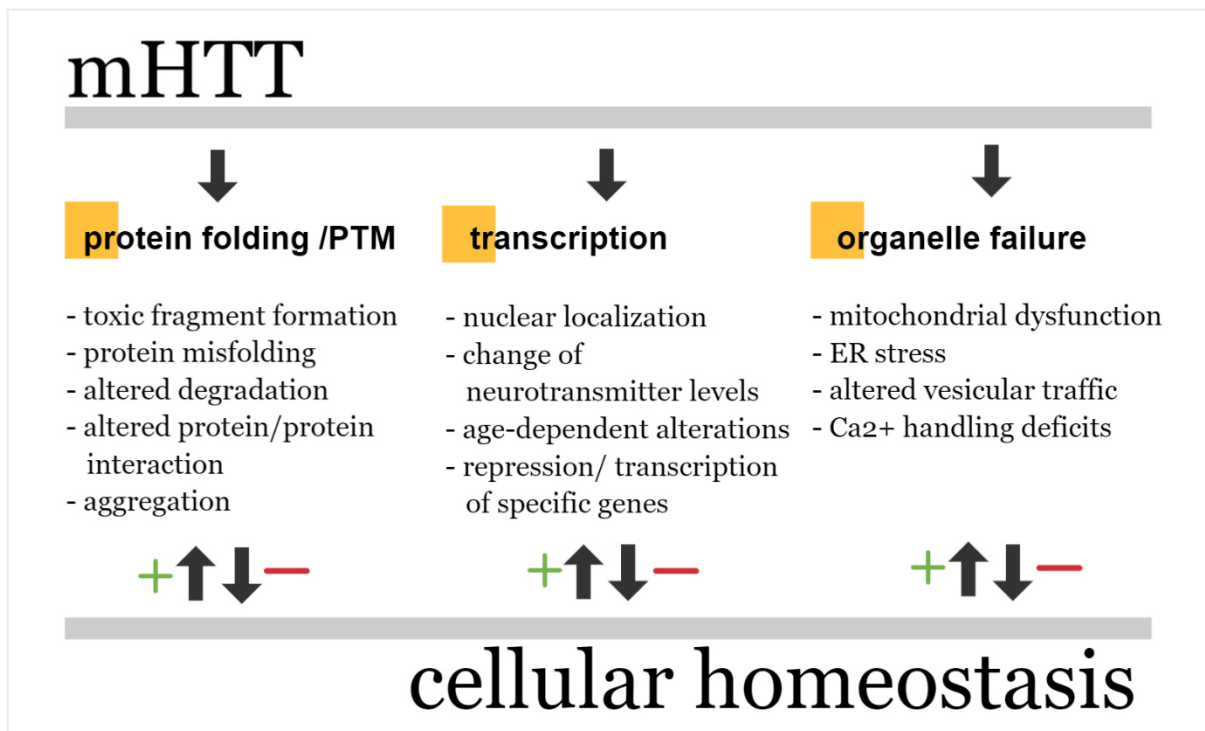


Figure 1: Hierarchical effects of mutant Huntingtin on cellular homeostasis. Pathogenic mechanisms in HD involve protein folding, protein modifications, protein function, transcription and organelle failure. All these effects can partially be compensated for by repair mechanisms, but with increasing burden by accumulating huntingtin, ultimately cellular homeostasis cannot be upheld. At this point the cells undergo cell death.

protein seeding and aggregation

One of the hallmarks of polyglutamine disorders are the aggregates that are formed from the disease proteins. They are found in affected brain areas in patients and in many of the disease models (Kosinski *et al.*, 1999; Taufiqua Islam *et al.*, 2014; Taylor *et al.*, 2002). The length of the PolyQ repeat determines the propensity to aggregate and the age of onset. As well as the density of aggregates is correlated to the CAG length (Becher *et al.*, 1998; Chen *et al.*, 2002). Aggregates can be found as nuclear inclusions, in the cytoplasm or in neuropils (Gutekunst *et al.*, 1999; Kazantsev *et al.*, 1999). The presence of aggregates is just another example of cause and epiphenomena where the roles are not yet allocated (Michalik & Van Broeckhoven, 2003). While many studies have directly correlated aggregation with cell death (Bucciantini *et al.*, 2002; Davies *et al.*, 1997; DiFiglia *et al.*, 1997), it has become accepted that the mere presence of aggregates does not equal the cell harming action (Arrasate *et al.*, 2004). It is rather the intermediate products from the

soluble, monomeric, non-cleaved and non-modified gene product to the highly aggregation prone, β -sheet rich, truncated protein fragments that are sequestered into aggregates, which are most toxic to the cells (Davies *et al.*, 1997; Graham *et al.*, 2006; Saudou *et al.*, 1998). Nonetheless, aggregation load has been a reliable measure for the efficiency of the reduction of mHTT in treatment approaches, as their presence is an indicator of homeostasis dysregulation and as the reduction correlates with an improvement of symptoms.

protein quality control and the autophagosomal lysosomal pathway

A major contributing factor to cellular homeostasis are two protein degrading systems that ensure the removal of misfolded or damaged proteins. The ubiquitin proteasome system (UPS) and the autophagosomal lysosomal pathway (ALP) (Ciechanover & Kwon, 2015; Lilienbaum, 2013). The UPS is active at a constitutively high rate in the nucleus and cytosol and breaks down proteins that are accessible to the proteasomal pore into peptides (Ciechanover, 2005). Via the ALP cytosolic content, as big as lipid droplets, aggregates and even organelles are degraded into single amino acids by the fusion of double-membraned vesicles with lysosomes (macroautophagy) in order to supply the cell with nutrients or to ensure homeostasis (Mizushima, 2007). The word “autophagy” is a Graecism built from the two words “self” and “eating”, a literal description of the process (Klionsky, 2007). The material transport into the lysosome can, next to macroautophagy, be a direct engulfment at the lysosomal membrane (microautophagy) (Li *et al.*, 2012) or via chaperones (chaperone-mediated autophagy), due to a specific targeting sequence (Kaushik & Cuervo, 2012). There is an imminent importance to flawless function of protein turnover, as the failure leads to accumulation of undegradable protein species, which is a feature in many neurodegenerative disorders, e.g., HD, PD, AD and ALS (Gan *et al.*, 2018; Nedelsky *et al.*, 2008). The importance of the ALP was shown by experiments by Hara and Komatsu in 2006. By conditionally knocking out autophagic genes and thereby abolishing the degradative functions (knockout of core autophagic genes is neonatal or embryonically lethal (Kuma *et al.*, 2004)), they found abnormal protein aggregation and cell death in neurons of mice and symptoms that resembled neurodegeneration (Hara, 2006). Under physiological conditions autophagy is regulated through the energetic/ nutritional status of the cell. A lack of

adenosine triphosphate (ATP), or more precise, a shifted ATP/ adenosine diphosphate (ADP) ratio activates AMP-activated protein kinase (AMPK). Amino acids and growth factor signalling (e.g. Insulin-like growth factor 1; IGF-1) is integrated via the mechanistic target of rapamycin (mTOR), which regulates cell growth, survival, protein translation and autophagy (Laplante & Sabatini, 2009; Swiech *et al.*, 2008). Interconnected with the two before mentioned regulators of autophagy, the depletion of cytosolic acetyl CoA induces autophagy, as well (Mariño *et al.*, 2014). Autophagy serves as a response to stress, e.g., in the removal of unfunctional organelles or a form of adaptation mechanism, e.g. in situations of altered energy requirements, like differentiation (Levine & Klionsky, 2004). The then initiated ALP consists of many multistep conjugation and signalling events, which can be summarized in their sequential order (reviewed in (Mizushima & Komatsu, 2011)): 1. nucleation and pre-autophagosomal structure formation – upon environmental/ cellular cues isolation membranes are formed *de novo* at the endoplasmic reticulum (ER), which grow into cup-shaped vesicles engulfing cellular material; 2. cargo loading and traffic to the microtubule organizing centre (MITOC) – the engulfment of the cargo can be mediated by specific adaptors (e.g. p62, OPTN) which enables selective autophagy (Stolz *et al.*, 2014). Formed autophagosomes are trafficked to the MITOC, where they fuse with lysosomes, and 3. lysosomal degradation – the cathepsins in the autolysosome degrade proteins into single amino acids in the acidic pH of this compartment and these amino acids can re-enter anabolic processes. In different neurodegenerative disorders individual steps of this pathway are affected, ultimately leading to protein accumulations (Menziés *et al.*, 2017; Wong & Cuervo, 2010). The elucidation of the specific deficits is critical for any treatment approach.

AUTOPHAGY IN HD

pathway alterations in HD

Autophagy is an essential part in the upkeeping of cellular homeostasis and therefore involved in many different disease classes, ranging from metabolic diseases to cancer and neurodegeneration (Choi *et al.*, 2013). Different process alteration have been described in HD models and patients. A graphic summary is shown in Figure 2. Early descriptions mention increased autophagosomes (Sapp *et al.*, 1997; Tellez-Nagel *et al.*, 1974) and increased numbers of autophagosomes

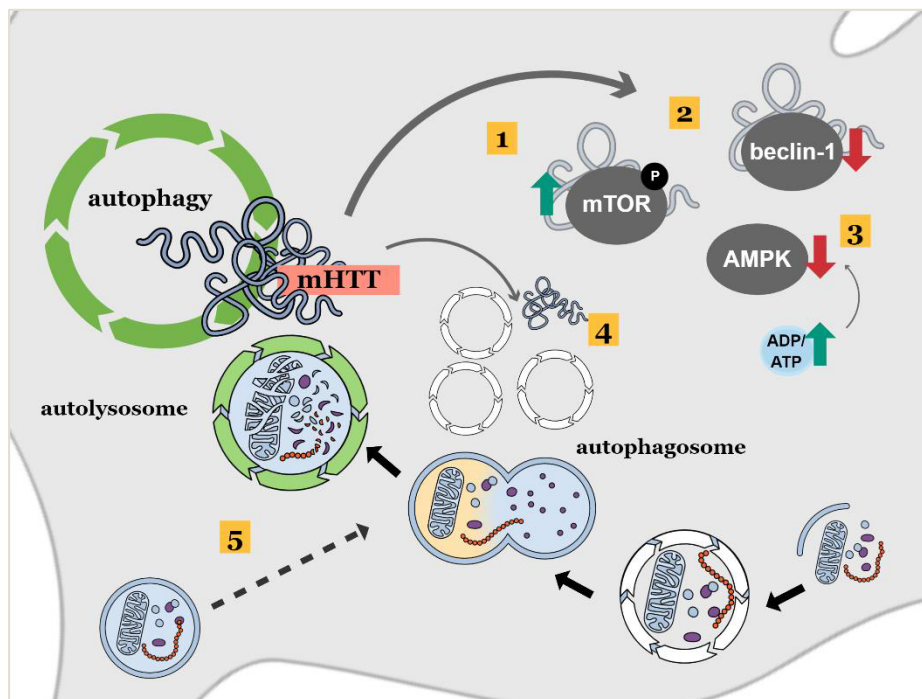


Figure 2: autophagy pathway alterations in HD are found at distinct levels of the process. Initiating signaling components show altered levels/activity [1-3]. Models of HD show increased mTOR phosphorylation, indicative of increased mTOR activity [1], an age-dependent decline of beclin-1 levels [2], and decreased AMPK signaling [3]. mTOR and beclin-1 are additionally sequestered into mHTT aggregates [1 and 2]. The autophagic flux is normal in HD, but mHTT is inefficiently targeted to the forming autophagosomes [4], which are formed at higher rates in HD, thereby avoiding clearance. Another contributing factor to inefficient clearance is the disturbed retrograde transport of autophagosomes along microtubules [5], where autophagosomes fuse with lysosomes to form autolysosomes, where the cargo is degraded.

have been found in HD patients brain samples and in lymphoblasts (Nagata *et al.*,

2004). This finding was confirmed in cell and animal models of HD (Lee *et al.*, 2011). Also, the flux, the rate by which autolysosomes are effectively cleared from the system, is normal or even higher in HD than in wildtype controls (Kegel *et al.*, 2000; Martinez-Vicente *et al.*, 2010; Petersén *et al.*, 2005). As depicted in Figure 2 the autophagosomes in HD are often “empty”, a consequence of a cargo loading deficit (Martinez-Vicente *et al.*, 2010). Cargo receptors that selectively shuttle designated cargo to the autophagosomes have also been found to be dysregulated in a HD mouse model (Rue *et al.*, 2013).

On the regulatory level autophagic deficits in HD are characterized by an age-dependent decline of autophagy inducing signalling components, like beclin-1, which expression declines with age (Shibata *et al.*, 2006). Additionally, altered protein interactions between HTT and autophagy inducing proteins are disrupted by the mutation. It has been proposed that the binding of Ras homologue enriched in striatum (Rhes), which activates autophagy through the binding to beclin-1, is hindered by mHTT (Mealer *et al.*, 2014). Furthermore, mTOR, as well as beclin-1, is sequestered into mHTT aggregates, thereby losing its autophagy inhibiting function (Ravikumar *et al.*, 2004; Sarkar & Rubinsztein, 2008b) and the initiation complex formation (Shibata *et al.*, 2006). The decrease in mTOR activity was linked to the observed phenotype of increased autophagosomes in HD. In HD models mTOR hyperactivation has been described (Pryor *et al.*, 2014). Regulating proteins of mTOR are, for example, phosphoinositide 3-kinase (PI3K), which integrates growth factor signalling (Heras-Sandoval *et al.*, 2014). mTOR forms at least two multi-protein complexes, that exert different functions in the cell. In mTORC1 (mTOR complex 1), under normal conditions the level of mTOR phosphorylation are high and autophagy is inhibited. The inhibition of mTOR and therefore the induction of autophagy has been shown to be neuroprotective in hypoxia-ischemia induced brain injury (Balduini *et al.*, 2012), under excitotoxicity (Kulbe *et al.*, 2014; Saliba *et al.*, 2017), spinal cord injury (Sekiguchi *et al.*, 2012), prion disease (Jeong *et al.*, 2012) and in HD (Ravikumar *et al.*, 2004), PD (Malagelada *et al.*, 2010) and AD (Spilman *et al.*, 2010).

Huntingtin – an autophagy protein?

Bioinformatic studies have revealed that huntingtin shares structurally related sequences with autophagy genes (Atgs). More precise, it represents the fusion of three Atg proteins, Atg11, Atg23 and Vac8 – responsible for the initiation of autophagy through the interaction with Unc-51 like autophagy activating kinase 1 (ULK1) and beclin-1 (Steffan, 2010). Knocking out huntingtin postnatally, specifically in the brain, results in the accumulation of p62, lipofuscin and ubiquitin, markers of failed autophagic clearance (Ochaba *et al.*, 2014), suggesting a functional role of HTT in autophagy, which has been confirmed by others (Rui *et al.*, 2015a; Rui *et al.*, 2015b). The best studied region of HTT, the polyglutamine stretch, has been implicated in the regulation of autophagy, too. The deletion of the polyglutamine stretch in a HD mouse model (Hdh140Q/ΔQ) increased autophagy, decreased aggregation and increased survival in this model (Zheng *et al.*, 2010). Also, the PolyQ stretch in the androgen receptor, the SBMA causing gene, was found to have an autophagy regulating role (Yang & Yamamoto, 2014). On the contrary, investigating the role of the polyglutamine region in ataxin-3, it has been found to interact with beclin-1, leading to autophagy induction when ataxin-3 was deubiquitinating beclin-1 and therefore autophagy was reduced upon elimination of the PolyQ (Ashkenazi *et al.*, 2017). However, this interaction and role of the PolyQ region in ataxin-3 has been questioned in a recent report (Herzog *et al.*, 2019).

models to study autophagy in HD

Different angles have been tried to elucidate the role and relationship between HD and autophagy. On the genetic level, a disease modifying SNP in the Atg7 protein has been found to affect age of onset in HD (Metzger *et al.*, 2013). And a role of autophagy in neuronal function has been established by knock-out models of Atg proteins, which display a neurological phenotype (Hara, 2006; Komatsu *et al.*, 2007). On the protein level, various markers have been identified to measure autophagic clearance (Klionsky *et al.*, 2016). And different aspects of autophagy dysregulation have been described in cell and animal models of HD (Figure 2) (Martin *et al.*, 2015; Menzies *et al.*, 2017). With the identification of the HD causing mutation and advances in molecular genetics, many animal models have been created to investigate HD-related disease mechanisms and to evaluate therapeutics in pre-

clinical trials. Most frequently used are rodent models, but also large animal models exist (Li & Li, 2015). Animal models are classified by the method used to introduce the mutation and the sequence of the mutated gene into three types of animal models: (1) transgenic fragment models, which exhibit a fast progressive phenotype and often a decreased lifespan. Only an N-terminal fragment is introduced, containing the CAG repeat expansion. The most commonly used pre-clinical animal model, R6/2 mice, belongs to this group (Mangiarini *et al.*, 1996). (2) transgenic full-length models, which express an additional copy of the *HTT* gene. These transgenes are introduced with the help of yeast or bacterial artificial chromosomes (YAC/BAC). BACHD mice and rats are well characterized models of this group (Abada *et al.*, 2013; Yu-Taeger *et al.*, 2012). And (3), HD gene knock-in (HDKI) models, where only the mutation is knocked-in into the endogenous *HTT* gene locus. While these animals possess endogenous regulatory elements and expression levels, the observed phenotypes are mild and slowly progressing (Menalled, 2005).

While expression differences in autophagic proteins and process alterations have been identified in HD models (Figure 2), measuring the dynamics of autophagy - more precisely autophagic flux - reliably is challenging. This is because of the dynamic nature of this process. The reaction on environmental/ pharmacological cues happens within minutes and transcriptional and protein markers are subject to great variation within different cells and tissues. Useful tools are proton pump inhibitors which stop the autophagic degradation process at a defined step, allowing snap-shot detections of the level of autophagy (Mizushima & Yoshimori, 2007). This is, however, more practical in *in vitro* investigations, as the use of these substances in animals results in toxicity and circadian and inter-animal variations make large animal groups necessary. Also fluorescently labelled autophagy proteins, like LC3-II, are valuable tools. It can be expressed *in vitro* and *in vivo*. Crossing of transgenic GFP-LC3 mice to other animal models is a valuable genetic tool, to study the autophagic process (Mizushima, 2009). But still limitations exist on the insights obtained from these animal studies. Most important to mention the proof of principle in humans, as there are no biomarkers of autophagy induction available. Only an intervention study combined with the proof of principle in animal models is feasible (Klionsky *et al.*, 2016). Therefore, the use of cell models is an invaluable tool in autophagy flux determination.

THERAPEUTIC APPROACHES FOR HD

Treatment of Huntington patients is currently limited to the management of motor and psychiatric symptoms (Dickey & La Spada, 2018). The treatment approaches so far targeting cellular processes, affected by mHTT (reviewed in (Ross & Tabrizi, 2011) and (Wild & Tabrizi, 2014)) have not proven beneficial yet in humans. Naturally, there is a wide gap in the translation of positive findings in preclinical studies to clinical trials. In Huntington disease this is further complicated by the complexity of the human CNS and the difficulties in the exact measurement of clinical improvement in a slow and individually progressing disorder. However, there is hope that the possibility of lowering the disease-causing protein by antisense oligonucleotides (ASOs) and RNA interference (RNAi) will be ameliorating disease burden in patients (Wild & Tabrizi, 2017). Promising results were obtained in a first clinical trial (Tabrizi *et al.*, 2019b)

therapeutic approaches to increase autophagy in HD

Autophagy has been shown to be a druggable target in HD (Galluzzi *et al.*, 2017). The first autophagy inducing compound tested in HD was rapamycin (Ravikumar *et al.*, 2002). It is approved for clinical use for immunosuppression, but limited induction of autophagy in mammalian cells, rapamycin-resistant protein translation and side effects have favoured the search for alternative compounds (Soefje *et al.*, 2011; Thoreen *et al.*, 2009). Rapamycin and its derivatives further lack sufficient brain penetration (Wong, 2013). A plethora of small molecules and other autophagy inducers have been described, but all of them have not yet made their way out of pre-clinical studies (Menzies *et al.*, 2017; Sarkar & Rubinsztein, 2008a). One clinical trial is currently running for resveratrol, which also affects autophagy, but mainly acts through SIRT1. Moreover, other compounds approved for clinical use with autophagy inducing properties have been found, whereas the mechanism of action varies (Menzies *et al.*, 2017). A summary of supplements and drugs approved for clinical use and studied in models of HD can be found in Table 1. The compounds used in this study, PQR530 and PQR620, PI3K/mTOR and mTOR inhibitors,

respectively, are designed as anti-cancer drugs that are in pre-clinical safety evaluation (Singer *et al.*, 2019). Their improved solubility allows these substances to pass the blood brain barrier (BBB), which makes them optimal candidates for pre-clinical studies in neurodegenerative disorders.

OBJECTIVES

Autophagy induction through the inhibition of mTOR is a desirable treatment approach in Huntington disease. mTOR inhibitors approved for clinical use are however unsuited, due to side effects and inefficient brain penetration. Two novel brain-penetrant compounds, currently in pre-clinical investigation for cancer therapy have been tested for their applicability in HD. For this:

1. a neuronal progenitor-derived cell model of Huntington disease (*STHdh*) was characterized. The cells either carrying wildtype or mutant alleles, differ in size, proliferation and have genetically diverged since their first description. Especially size differences and the altered proliferation rates were important to be defined prior to screening autophagy inducing compounds in this cell line.
2. mTOR inhibiting compounds, which have improved pharmacokinetics and allow penetration of the brain, were tested for their therapeutic value in Huntington disease. They have been tested *in vitro* in two cell models of HD, one of which is the above mentioned *STHdh* cell line. They have been further used in a treatment study in a transgenic mouse line of HD.

RESULTS AND DISCUSSION

CHARACTERIZATION OF THE STHDH CELL MODEL

Publication # 1: Reduced cell size, chromosomal aberration and altered proliferation rates are characteristics and confounding factors in the *STHdh* cell model of Huntington disease

We have characterized a cell model commonly used in many pre-clinical studies for Huntington treatment (Jiang *et al.*, 2012; Jin *et al.*, 2016; Lu *et al.*, 2014), which has diverged from its original description in ours and other laboratories. Whilst the mutant cell line is genetically and phenotypically more distinct from the wildtype counterpart than just the disease-causing mutation, we found the *STHdh* cells to present other HD related phenotypes that were not described previously. Most important, the HD cells are smaller and proliferate more rapidly, both cellular characteristics that are found in other cell and animal models of HD. It remains to be elucidated to what extent the cell size and proliferation phenotype are relevant to the pathology of HD.

Finding appropriate models to study molecular mechanisms of disease is of great interest in the field of Huntington disease research. *In vitro* models have been used to investigate molecular pathways and mechanism that can only be controlled under the consistent environment of a petri dish. Modelling HD has been often achieved through the overexpression of fragments - or less often - of full-length huntingtin. While this is a very useful tool and the protein can be tagged by fluorophores, the genetic context does not represent the situation in patients. Primary neurons of HD

animal models are a very useful model as the cell type is the most relevant to HD, in contrast to other cell models that are tumour derived or isolated from peripheral organs. Clearly, they are genetically identical to the models they derive from and therefore copy their advantages and disadvantages. But they are a limited resource and cannot be expanded much, as cell death occurs early. Immortalization of cell lines derived from HD animal models therefore provides models that are of neuronal origin but can be passaged and expanded to a higher number. As patient fibroblasts are not isogenic with their controls, also wild type and mutant cells generated from animal models differ. *STHdh* cells derive from HDKI mice. HDKI models are genetically precise, as the mutation is introduced into the mouse locus of the *Hdh* gene by homologous recombination. Different HDKI models exist varying in the sequence – human, mouse or chimeric – that was introduced.

We sought to characterize these immortalized cell lines that are derived from HDKI mice. SV40 large T-antigen was used for the immortalization of the *STHdh* cell lines. This has several disadvantages to the integrity of the cell. The karyotype is altered by this form of viral transformation and other molecular regulators, as p53 show altered expression patterns. Also, in our cell lines we found these alterations, which highlights the importance of a thorough characterization of each cell line, as differences in the karyotypes can affect protein levels and molecular mechanisms. Interestingly, the cells showed characteristics that differed between wildtype and mutant cell line and were found to be not solely a by-product of immortalization, but rather a HD phenotype.

A common feature to different HD models is reduced cell size. It has been previously described in striatal neurons of HD animal models (Chopra *et al.*, 2007; Levine *et al.*, 1999; Rubinsztein, 2002; Slow *et al.*, 2003) and is speculated for HD patients, but there exist only limited reports about the cell size of neurons from HD patients (Rajkowska *et al.*, 1998; Vonsattel *et al.*, 2008). The cell size phenotype observed in the *STHdh*^{Q111/Q111} cells (Singer *et al.*, 2017), has been further confirmed in a human derived model of HD since the publication of this study (Hung *et al.*, 2018). Some reports mention the cell size reduction to be a direct pre-apoptotic effect of fragment expression in cell models of HD (Orozco-Díaz *et al.*, 2019; Wyttenbach *et al.*, 2001). On the contrary, the expression of N171-82Q fragments resulted in larger HEK293 cells (Pryor *et al.*, 2014). To date, no mechanistic

explanation for the reduced size has been found. Recently, a mechanistic explanation for the growth deficit of a yeast HD model has been proposed. This model shows a growth defect upon the expression of 103Q-exon1 constructs that is neither linked to PolyQ induced toxicity nor explained by altered proliferation (Jiang *et al.*, 2019; Meriin *et al.*, 2002). The authors found the SAGA/NuA4 complex to be involved in chromatin remodelling and upon mHTT expression, upregulating TRA1, which is involved in cell size regulation and ribosomal biogenesis under protein misfolding stress (Jiang *et al.*, 2019).

Epigenetic dysfunction is another pathomechanism caused by toxic functions of the HD mutation, leading to altered post-translational modifications on histones through e.g. the sequestration and inactivation of acetyltransferases (Steffan *et al.*, 2000). As a result, a remodelling of chromatin on these histones occurs. Lee and colleagues have found the activity of ETDB1/ESET, a histone methyltransferase, to be a druggable target for HD therapy. In their study *drosophila* expressing 127Q, had significantly smaller eyes. This could be rescued by reducing the protein amount. Moreover, the pharmaceutical regulation of Setdb1/Eset protein levels, which are upregulated in cell and animal models of HD, led to an increase in neuronal size in the R6/2 mouse model (Lee *et al.*, 2017).

Interestingly, the size difference between HD and control is not restricted to the cellular level but is also observed on the organismal level. In children, carrying the HD mutation in the premanifest stage of the disease, a smaller head circumference was found, even when corrected for height (Lee *et al.*, 2012). In a larger cohort of premanifest HD patients, intracranial volume was found to be reduced in male participants, while it was only tendentially reduced in females (Nopoulos *et al.*, 2011). The fact that size differences are already seen in children, decades before disease manifestation, could imply that there is a preceding developmental alteration caused by the HD mutation. One possible explanation for the abnormal development could be an altered metabolic phenotype where mHTT affects the mitochondria leading to abnormalities in energy metabolism and in growth (Lee *et al.*, 2012). Another explanation is altered caspase activation, which is crucial for development. In the BACHD rat model (Yu-Taeger *et al.*, 2012), which also shows reduced body size, the olfactory bulb in both lines of this model, TG5 and TG9, is reduced (see co-authored publication #3: olfactory bulb atrophy and caspase activation observed in the

BACHD rat models of Huntington disease (Lessard-Beaudoin *et al.*, 2019)). Aggregation of mHTT has been shown in the olfactory bulb of HD patients and patients also show olfactory deficits (Highet *et al.*, 2020; Larsson *et al.*, 2006; Moberg & Doty, 1997). In young rats (3 months) the size difference was already present and the size increment over age was reduced in both HD lines in comparison to wildtype animals, while cell death was observed at the oldest age observed (12 months). The reduced size at the earlier age was found to correlate with caspase 3, 8 and potentially caspase 6 activation, which could argue for a developmental deficit, as caspase activation is essential in neurogenesis in the olfactory bulb (Mouret *et al.*, 2009). Weight is also affected in HD, the phenotypes, however, diverge between patients and animal models. Whereas weight loss is the predominant symptom in later stages of disease in humans, transgenic models often show increased fat mass. Weight loss is also observed in some models, e.g. R6/2 model (Fain *et al.*, 2001). Noteworthy, in the BACHD rat, despite similar body weight, the body composition is massively changed. BACHD rats have smaller heads, increased fat mass and reduced lean mass, compared to wildtype littermates (Jansson *et al.*, 2014). Like the BACHD model, R6/2 mice display an overall growth retardation with an accompanied body fat increase. This transgenic fragment model shows cachexia and muscle atrophy towards the end of disease progression at approximately 12 weeks of age (Fain *et al.*, 2001). The growth phenotype is therefore more pronounced among the different animal models, than the body composition phenotype.

In general, organismal and cell size is genetically programmed and relies less on environmental factors. The exact determinants are not clearly understood, especially regarding the maintenance of cellular size in the different phases of development and different tissues. Even though adult neurons are in a post-mitotic state, cell size maintenance is a constantly ongoing process (Lloyd, 2013). Sensory neurons supplied with nerve growth factor (NGF) and a protein synthesis inhibitor maintain their cell size, whereas they shrink in the absence of NGF. This is explained by the increased degradation of long-lived proteins upon the increase of growth factors by degradation pathways (Franklin & Johnson Jr, 1998). One limiting factor of cell size is the availability of IGF-1. Increased IGF-1 signalling results in larger cell size (Saucedo & Edgar, 2002). Interestingly, the levels of IGF-1 were found to be lower

in males, which also exhibit a stronger body composition alteration compared to wild-type animals than females. The main signalling axis for IGF is the PI3K/AKT/mTOR axis. The artificial activation of mTOR, as it can be achieved through high levels of IGF-1, leads to an increment in size. A combination of several environmental cues (growth factor, energy, amino acids) is needed to promote cell size via the integration hub mTOR, which simultaneously regulates cell size through feedback loops. In the *STHdh* cells the situation is surprisingly inversed. We, in accordance with others, have found increased mTOR and mTOR target phosphorylation levels in the HD cells that represent increased mTOR activity, despite the smaller size in *STHdh*^{Q111/Q111} cells (Creus-Muncunill *et al.*, 2019; Pryor *et al.*, 2014; Walter *et al.*, 2016). As the presence of mHTT increases mTOR activity, one could propose a model, in which the HTT mutation results in decreased cell size, whereas it simultaneously activates mTOR, as a form of compensation. Autophagy induction on the other hand, by the inhibition of mTOR, decreases cell size (Hosokawa *et al.*, 2006), which is in line with the finding of increased autophagy in HD models (Heng *et al.*, 2010; Kegel *et al.*, 2000; Martinez-Vicente *et al.*, 2010). This conundrum is yet to be solved, though difficult as the external conditions *in vitro* are most likely too artificial to resemble the state of a cell in a functioning organ. In *Hdh*Q111 mice, only brain volume has been assessed, showing a region-specific volume reduction at unchanged cell numbers (Kovalenko *et al.*, 2018). Many aspects, like mechanical sensing by cilia, cell contacts and tissue specificity play an essential role in the regulation of cell size and are difficult to model in a petri dish (Orhon *et al.*, 2016; Pavel *et al.*, 2018). In the specific case of HTT and mTOR it would be interesting to see if and how HTT is interconnected to cell size regulation. For this, *in vivo* studies are needed. The observation of decreased size and increased proliferation argue for an involvement of mTOR in the HD cell's phenotype. Therefore, the *STHdh* cells represent a valuable model to further investigate HTT's role in cell size regulation, as they have been used to model other HD phenotypes (Figure 3). So far, the treatment of mutant *STHdh* cells with mTOR inhibitors lead to a clear reduction of proliferation (Singer *et al.*, 2019) and cell size was reduced upon mTOR inhibition in preliminary experiments (unpublished data, not included). These findings need to be further confirmed in different models. It remains unclear what role HTT plays in the manifestation of the cell / body size phenotype of HD. For cell size HTT's role in the

cytoskeletal organization might play a role. It is also supported that HTT plays a crucial role in metabolic (Fain *et al.*, 2001) and developmental processes and therefore the mutation could affect cell size, as well as crucial differentiation steps within development, adding up to the observed phenotype.

Cell size regulation and cell division are interconnected processes, both regulated by mTOR and the dysregulation of cell division, can lead to altered cell size and cell numbers. Re-entry into the cell cycle is a proposed mechanism contributing to neurodegeneration and has been shown in various models and HD post-mortem tissue (Fernandez-Fernandez *et al.*, 2011; Folch *et al.*, 2012; Pelegrí *et al.*, 2008). Increased proliferation rates in dividing cells, carrying the mutation are therefore considered to be a pathological mechanism caused by the HD mutation. HD patient fibroblasts show increased proliferation (Goetz *et al.*, 1981). Recently, fibroblasts collected from 48 months old tgHD minipigs showed increased proliferation in contrast to wildtype controls (Šmatlíková, 2019). The TruHD fibroblast cell lines, created by Claudia Hung and colleagues, also showed increased proliferation in cells carrying the expanded CAG repeat. These cell lines are derived from HD patients and show several molecular phenotypes of HD (Hung *et al.*, 2018). miRNAs were proposed to alter - and when differently expressed in the mutant cell lines - disrupt the proliferation process, leading to replication stress and cell death, as well in the *STHdh* cell model (Bucha *et al.*, 2015; Das *et al.*, 2013; Das, 2014). Genetic modification through CRISPR and similar technologies and the availability of induced pluripotent stem cells (iPSC) from HD patients has led to the generation of isogenic iPSC lines. Because these cell lines solely differ by the CAG length, they provide an exciting new model to study neurodevelopmental and cell type specific aspects of the HD pathology (Dabrowska *et al.*, 2020; Ooi *et al.*, 2019)

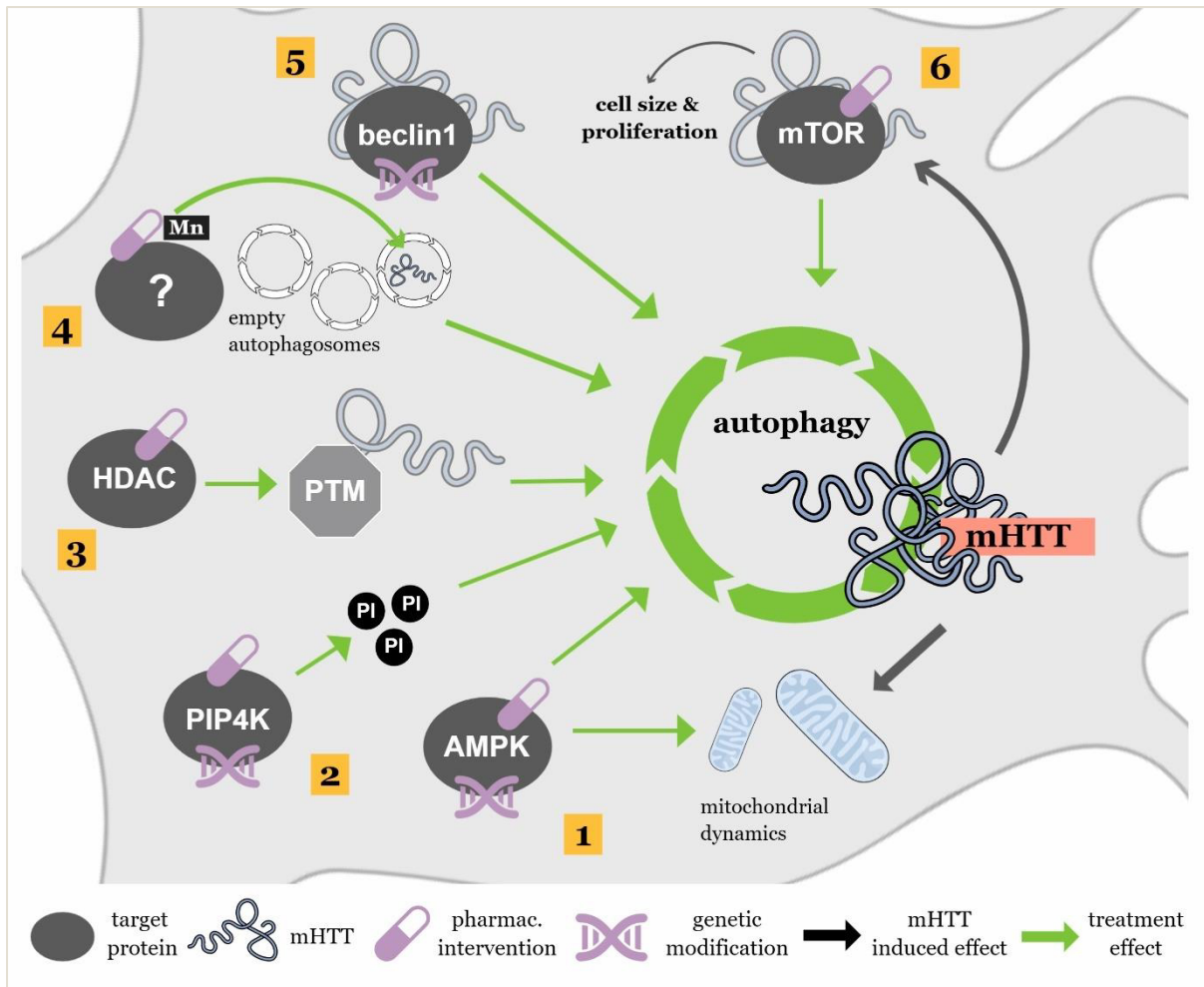


Figure 3: targets of autophagy induction in the *STHdh* cells. (1) genetic or pharmacological activation of AMPK induces autophagy and improves mitochondrial dynamics (Jin et al., 2016; Walter et al., 2016). (2) PIP4Ky inhibition modulates phosphoinositol (PI) levels in the cell and lead to the induction of autophagy and mHTT reduction (Al-Ramahi et al., 2017) (3) HDAC inhibition alters PTMs and increases autophagic clearance of mHTT (Jia et al., 2012). (4) Manganese (Mn) elicits autophagy and corrects autophagosome loading via an unknown mechanism (Bryan et al., 2019). (5) Beclin-1 overexpression, to counteract the age-dependent decline and sequestration by mHTT of the autophagy initiating protein, leads to the reduction of mHTT (Shibata et al., 2006). (6) Inhibition of mTOR leads to the induction of autophagy and the reduction of mHTT levels (Singer et al., 2019).

The *STHdh* cell lines represent phenotypes that can be attributed to the HD mutation, however especially the cell size and proliferation differences between mutant and wildtype cell lines need to be considered in experimental design. The full length HTT gene is a valuable feature of these cell lines. On the downside, the lines are not isogenic, and the mutant *huntingtin* contains a chimeric sequence with a CAG length that is not comparable to patients. The HDKI mice from which these cells derive display a very mild phenotype only manifesting at a very old age, a common feature of HDKI animals. Only long CAG repeats elicit behavioural phenotypes, which is

commonly observed in animal models of HD. Nonetheless many pathogenic mechanisms found in other models are replicated in this cell model. Relevant to this work, the *STHdh* cell lines have been used for several studies to investigate autophagy inducing therapy options (Figure 3), highlighting the relevance of autophagy induction as a therapy for HD. Our study on this cell line has helped us better understand how to work with these cells, avoiding direct comparisons between mutant and wildtype cell line and differentiating the cells to minimize effects of proliferation differences in experiments. These findings have been translated to the *in vitro* characterization of two novel catalytic mTOR inhibitors (Singer *et al.*, 2019). Collectively, both studies confirm, the *STHdh* cell lines are a useful and valid model of Huntington disease.

IN VITRO AND IN VIVO CHARACTERIZATION OF PIQR COMPOUNDS

Publication # 5: Brain-penetrant PQR620 mTOR and PQR530 PI3K/mTOR inhibitor reduce huntingtin levels in cell models of HD (Singer *et al.*, 2019)

and

unpublished manuscript # 1: PQR530 and PQR620 reduce aggregation in the R6/2 mouse model but fail to ameliorate behavioural phenotype (Singer *et al.*, 2020)

Figure 3 shows a summary of studies where *STHdh* cells have been used to investigate autophagy phenotypes and related treatment options for HD, ranging from overexpression of autophagy inducing proteins, like beclin-1 and AMPK to pharmacological approaches, boosting autophagy through different cellular targets. The goal of these therapies is to prolong the healthy lifetime of neurons, by boosting cellular coping mechanism against proteotoxic stress and thereby to postpone cellular demise and phenotypic signs of neurodegeneration (Figure 4). The classical way of inducing autophagy is through the inhibition of mTOR. mTOR overactivation is a common theme in neurodegeneration and cancer (Laplante & Sabatini, 2012; Tian *et al.*, 2019). Through sequencing efforts many mutations in the PI3K/mTOR/AKT pathway have been identified in cancers and rare genetic disorders, so called overgrowth syndromes, which are caused by mTOR overactivation. These disorders, which have a neurological component, could benefit from the development of brain penetrant PI3K/mTOR inhibitors (Hillmann & Fabbro, 2019). Although contradictory at first thought, a link between cancer and neurodegeneration might exist. mTOR overactivation was described in HD patient fibroblasts and different cell (Walter *et al.*, 2016) and animal models (Abd-Elrahman & Ferguson, 2019; Ravikumar *et al.*, 2004). Following this hypothesis, there might be therapies available for neurodegenerative disorders, which were developed for cancer. The improvement of HD phenotypes in animal models has been achieved previously in

animal models with rapalogs (Ravikumar *et al.*, 2002; Ravikumar & Rubinsztein, 2006; Sarkar *et al.*, 2009) and with ATP competitive inhibitors in a cell model of HD (Rosic *et al.*, 2011). Despite the already proven efficacy of mTOR inhibition, ameliorating HD symptoms in rodent models, side effects and the low brain-penetrance of classical mTOR inhibitors have made them impractical and hard to translate from animal models to potential clinical trials. We have therefore tested two compounds that pass the BBB due to increased lipophilic properties. Testing substances which previously demonstrated safety in other disorders has the advantage that they enter clinical trials for additional applications faster and often the mechanisms of action are known. mTOR dependent and independent inducers of autophagy are listed in table 1. For our study ATP-competitive PI3K/mTOR and mTOR inhibitors, PQR530 and PQR 620, respectively, were chosen. The *in vitro* testing of these compounds was performed in the *STHdh* cell lines and a transient transfection fragment model, where both compounds showed cytostatic effects and reduced the amount of soluble and aggregated huntingtin protein species (Singer *et al.*, 2019). The compounds effectively inhibited mTOR in brain, spread throughout the brain and reduced aggregation *in vitro* and *in vivo*. In the R6/2 mice PQR530 reduced the amounts of aggregates in striatum, but neither compound was able to rescue the motoric and behavioural phenotype of the animals (Singer *et al.*, 2020). In

parallel, PQR compounds have been tested in a model of epilepsy, where they as well effectively crossed the BBB and reduced seizures (Brandt *et al.*, 2018).

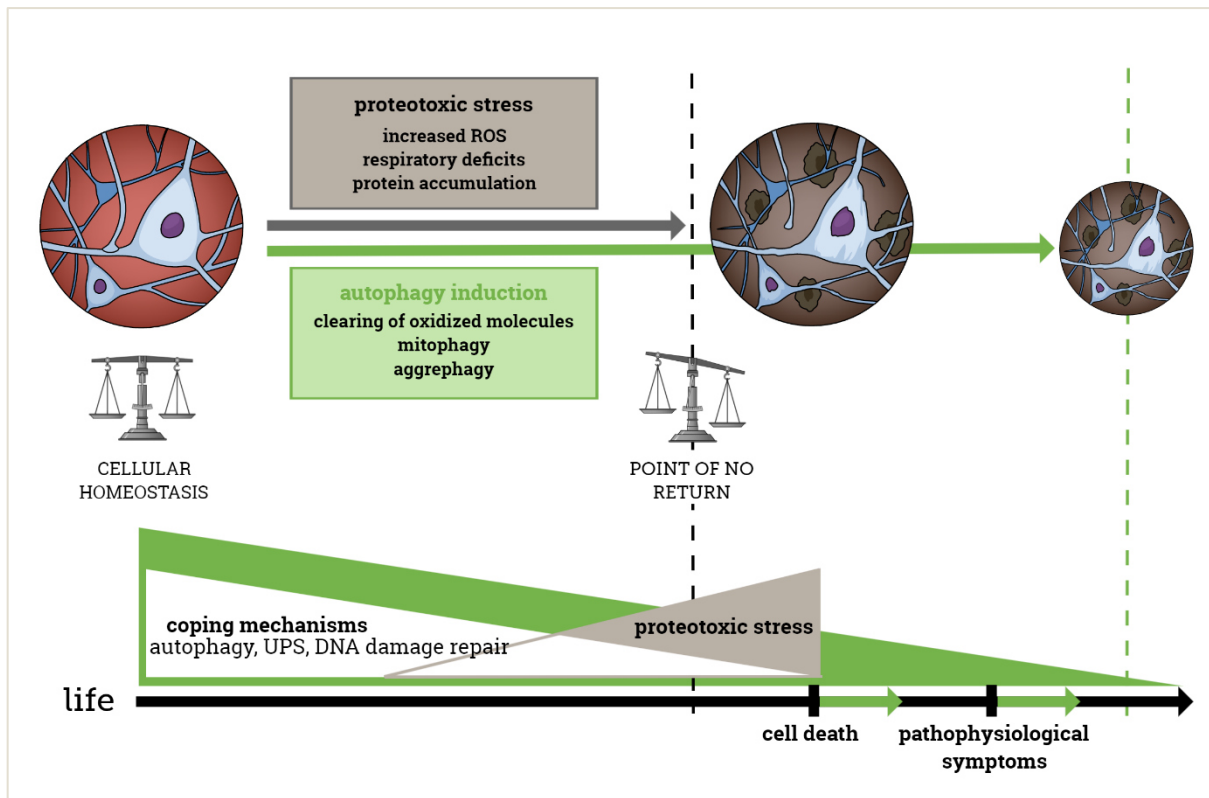


Figure 4: autophagy-based therapy outcome. By inducing autophagy (pharmacologically or e.g. through fasting or exercise) at a point in life when healthy neuronal networks still exist and coping mechanisms against proteotoxic insults and effects of protein malformations are not limited by the age-dependent decline of their functionality, increased induction of autophagy and at later stages the maintained rate of autophagy could help push the point-of-no-return that decides the fate of every single cell, when the balance between cellular survival and damage to the cell cannot be sustained anymore. Therefore, the health-span of cells could be extended, and the appearance of pathophysiological symptoms would be, consequently, delayed, as they appear after gross neuronal loss.

Oxidative stress and DNA damage force cells, also neurons, to re-enter the cell-cycle (Folch *et al.*, 2012). While in cancer, this could lead to autonomous cell population growth, in neurons it leads to apoptosis. A role for cell-cycle alterations has first been proposed for Alzheimer (Nagy *et al.*, 1998) and was confirmed in other neurodegenerative disorders including Huntington disease (Pelegri *et al.*, 2008). As mentioned before, in our characterization of the *STHdh* cell lines the cause of the altered proliferation in the *Hdh*^{Q111/Q111} cell line was not investigated on the molecular level, and it is not clear whether it might be a rescue effect to repair DNA damage, as no apoptosis was observed, or if proliferation is favoured because of other functions HTT exerts on the cell cycle. Nonetheless, those cell lines present a druggable

phenotype that could lead to reduced cell-cycle progression when treated with mTOR inhibitors, which exert cytostatic effects (Wander *et al.*, 2011). In cancer therapy the lack of cytotoxicity of mTOR inhibitors is considered a downside, due to limited treatment success (Sabatini, 2006). By using these inhibitors in a setting where cytotoxicity needs to be prevented, a disadvantage of mTOR inhibition in cancer therapy can be exploited. A naturally occurring, mTOR inhibiting compound that targets cell-cycle progression and has been proposed as a treatment for neurodegenerative disorders is Resveratrol, which has been attributed various beneficial effects and also blocks mHTT toxicity by increasing SIRT1 activity and inducing cell cycle arrest (Sharma *et al.*, 2017; Tellone *et al.*, 2015). It has been proven effective in different HD models (Maher *et al.*, 2011) and a clinical trial has been conducted and completed in 2020. However, results have not been published.

Contradictory to the findings of increased mTOR activity in HD and the treatment effects in models of neurodegeneration, reduced mTOR levels in HD patients have been found (Hodges *et al.*, 2006). Treatment strategies overexpressing one component of mTOR complex 1, Ras homolog enriched in brain or striatum, Rheb and Rhes, respectively, have been shown to be beneficial in HD models as well (Child *et al.*, 2018; Lee *et al.*, 2015). While the therapeutic effect of Rhes or Rheb substitution has been demonstrated in these studies, they fail to demonstrate the underlying deficit being caused by inactive mTOR, as mTOR phosphorylation levels are not assessed. Child *et al.* demonstrate a reduction of ribosomal protein S6 (S6RP) and eukaryotic translation initiation factor 4E-binding protein 1 (4E-BP1) phosphorylation in cardiac tissue of HD mouse models, which can be explained by mTOR inhibition. Nonetheless, there are other mechanisms by which Rheb could improve HD pathologies, e.g. by Rheb binding beclin-1 and inducing autophagy mTOR independently, which has been shown for Rhes (Mealer *et al.*, 2014). There seems to be a role for Rheb/Rhes in HD pathology, as mHTT binds Rhes with higher affinity (Subramaniam *et al.*, 2009) and reduced Rhes levels are found in HD patient's caudate nuclei (Hodges *et al.*, 2006). Reduction of Rheb protein levels, negatively affected myelination and postnatal brain development (Zou *et al.*, 2011). The knock-out of Rhes also negatively affected brain weight in Rhes KO mice (Baiamonte *et al.*, 2013), which show deficits in some behavioural aspects and motor coordination (Spano *et al.*, 2004). But the part it plays in the pathogenesis is

controversial. Rhes knock-out was neuroprotective in a neurotoxin model (Mealer *et al.*, 2013) and delayed motor symptom onset in R6/1 mice (Baiamonte *et al.*, 2013).

mTOR dysregulation has been targeted as well by other means. In the zQ175 mouse model increased mTOR(S2448) levels have been normalized by treatment with CTEB, a negative allosteric mGluR5 modulator (Abd-Elrahman & Ferguson, 2019). This had a positive effect on aggregation and disease progression (Abd-Elrahman *et al.*, 2017) by ULK1 activation and brain-derived neurotrophic factor (BDNF) transcription facilitation (Abd-Elrahman & Ferguson, 2019). In line with this, efforts have been made to find other targets within the autophagy regulating circuits that have less pleiotropic effects in the cell and on the entire organism. It is quite clear that this form of therapy will come at a cost, due to side effects and it is unclear how long treatment effects might persist before resistances occur. Here it needs to be mentioned that catalytic mTOR inhibition, results as well in inhibition of mTORC2, which reacts to growth factor signalling and phosphorylates AKT. While mTORC2 also promotes autophagy inhibiting signalling, its pleiotropic and less studied functions in the cell could lead to undesirable effects (Ballesteros-Álvarez & Andersen, 2021; Querfurth & Lee, 2021). Despite other effects on cellular processes, one effect of mTOR inhibition is the subsequent inhibition of protein synthesis. A recent report has shown that inhibition of 4EBP-1 phosphorylation, a downstream effector of mTOR - and therefore protein biosynthesis inhibition - has a beneficial effect in the R6/1 model of HD. The authors found increased phospho-4E-BP1 levels in different HD models, which is concordant with our findings and the hypothesis that mTOR signalling is increased in HD. Further they have shown that the inhibition of protein biosynthesis by blocking 4E-BP1 is sufficient to improve the R6/1 phenotype and therefore the increased protein translation in HD can be considered a pathogenic mechanism (Creus-Muncunill *et al.*, 2019). While 4E-BP1 inhibition was achieved through intracranial injections of compounds, such an effect can as well be expected from mTOR inhibition (Wang & Proud, 2006) and was shown for both PQR compounds in the *STHdh* cells (Singer *et al.*, 2019). Previous work in our group has shown that the *STHdh*^{Q111/Q111} cell line also shows HD related autophagic deficits and characteristics. Increased microtubule-associated proteins 1A/1B light chain 3B (LC3-II) expression and mTOR activity was found, as well as increased mTOR phosphorylation levels in combination with increased downstream phosphorylation of

target proteins like S6RP and 4E-BP1. Additionally, empty autophagosomes were observed (Walter *et al.*, 2016).

The inhibition of mHTT transcription is a desirable goal and has been demonstrated for metformin (Arnoux *et al.*, 2018). Metformin is prescribed today as a type II diabetic drug and in clinical use for already more than 60 years, without complete knowledge about the mechanism of action (Rena *et al.*, 2017). Many cellular targets have been proposed: metformin accumulates in mitochondria and blocks Complex I of the respiratory chain, thereby repressing ATP production and regulating gluconeogenesis (Doran & Halestrap, 2000). Metformin activates the cell's energy sensor AMP-activated protein kinase (AMPK), thereby also affecting gluconeogenesis and lifespan (Zhou *et al.*, 2001). Metformin induces autophagy by activating AMPK, a known mechanism in lifespan expansion and a proposed treatment strategy for neurodegeneration (Rubinsztein *et al.*, 2012) and improved cognitive function in HD patients (Hervás *et al.*, 2017). Also, a mTOR dependent, metformin mediated effect on longevity has been described in *C.elegans* (Howell *et al.*, 2017). It has been shown before that mHTT transcription is regulated by a complex formed by mTOR/MID1/PP2A in a CAG dependent manner. MID1 binds specifically to the elongated CAG of mHTT transcripts leading to an enhanced translation (Krauß *et al.*, 2013). Recently, in the 150Q knock-in model of HD, a regulating role on mHTT transcription was found for metformin. Administration of the drug for 11 weeks showed a significant reduction of mHTT levels in cortical tissue in combination with a reduction of S6K phosphorylation. Also, a reversal of the pathological neuronal network activity and beneficial effects in open field were observed (Arnoux *et al.*, 2018). These results are of special interest, as they have been carried out in mice that are in the VFOD (very far from disease onset) state of disease. Reversing mHTT damage before irreversible damage to the brain occurs is probably the only treatment strategy that could delay or relieve classical HD symptoms occurring in the symptomatic phase of disease with motor and cognitive symptoms. In cases with a family history of HD, genetic testing at an early age would allow for this kind of intervention. It remains to be clarified, whether it is possible to delay symptoms by treating patients in the pre-symptomatic phase, or even before that.

Next to the inhibition of mHTT accumulation through transcription inhibition, the expected mechanism of action of mTOR inhibition by which the amelioration of aggregate burden is expected to be achieved is through the induction of autophagy. But it needs to be critically assessed, whether the induction of autophagy by inhibiting a certain component of the cascade, is a desirable mode of action. This is relevant because a) inhibiting one step in a cascade can be compensated for by resistance feedback loops and b) single components, as mTOR or AMPK fulfil various functions in the cell. Especially, since both compounds evaluated do not only inhibit mTORC1, but all mTOR complexes. Therefore, beneficial outcomes could be either too low or too short-timed and detrimental outcomes might not be separable from beneficial ones. Even though the combination of PI3K and mTOR inhibition (with PQR530) was effective in reducing the aggregation load in the R6/2 model, the detrimental peripheral/ motor phenotype was not ameliorated. Similarly, everolimus, a first-generation mTOR inhibitor that effectively ameliorated HD phenotypes in other mice models, was unable to reduce protein accumulations and motor phenotypes in the R6/2 model (Fox *et al.*, 2010). Target inhibition in both cases - our study and the study by Fox *et al.* - was persistent at the end of the experiment. It remains to be clarified, whether the treatment was unable to reduce behavioural phenotypes because the course was already set to fatal processes before it started. This wouldn't be unexpected in the R6/2 model, which shows early neuropathological symptoms and would explain why the same treatment was beneficial in other HD models. In this regard it is interesting to mention that autophagy was originally considered a cell death mechanism, because autophagosomes were observed in excessive numbers in dying cells. Only much later the sensitizing of autophagy mutants to cell death, led to the delineation that this was not cause and effect, but a survival mechanism, unable to halt the already initiated death program of the cell (Kroemer & Levine, 2008). On the other hand, trehalose, a disaccharide was shown to decrease PolyQ aggregation and extend life-span in R6/2 mice (Tanaka *et al.*, 2004). It is unclear, whether this effect can be solely attributed to the polyglutamine binding properties of trehalose or whether its induction of autophagy was adding to the beneficial effect. Trehalose creates a starvation-like state in the cell by blocking glucose transporters, thereby activating AMPK (DeBosch *et al.*, 2016). Initially trehalose was found to act independent of mTOR (Sarkar *et al.*, 2007), whereas later

mTOR's inhibitory phosphorylation on ULK1 was found to be decreased upon trehalose treatment (DeBosch *et al.*, 2016). Independent of autophagy as a treatment approach, treating R6/2 mice with mesenchymal stem cells (MSCs), beginning at the same age as in our PQR-treatment study, was successful in our group (Yu-Taeger *et al.*, 2019). R6/2 mice were intranasally treated with MSCs, which are known to show regenerative properties and to migrate to damaged tissues. MSC treatment improved neuropathological changes and improved sleep disturbance of R6/2 mice. Further, MSC treated mice showed a trend towards improved motor performance on the rotarod and microglial marker, Iba1, was restored in the striatum of treated mice (see co-authored publication #4: Intranasal Administration of Mesenchymal Stem Cells Ameliorates the Abnormal Dopamine Transmission System and Inflammatory Reaction in the R6/2 Mouse Model of Huntington Disease (Yu-Taeger *et al.*, 2019)). While for this study female mice were used, in the PQR-treatment study male mice were used. This could be one possible explanation for the differential treatment outcome, as male R6/2 mice experience more severe body weight loss (Yu-Taeger, in submission). Also, a sex specific difference in mTOR target phosphorylation was found in the BACHD rat model, which shows the same gender difference in weight loss, as the R6/2 mouse model. Ribosomal protein S6 kinase (RPS6K), a target of mTOR and a marker for mTOR activity, was significantly increased in male BACHD rats (TG5) in comparison to female BACHD rats (data not shown, unpublished). Further these findings highlight that mTOR inhibition will not have regenerative effects, but can only be applicable as a prophylactic, possibly health span extending treatment approach. In line with this, mTOR is also interconnected to life span extension by non-pharmacological interventions, however mTOR is only one piece of many interconnected metabolic pathways, involved in longevity promoting processes.

The induction of autophagy, by e.g. inhibiting mTOR, activating AMPK and changing the acetylation state of proteins as a natural response to the lack of nutrients and energy, has become a desirable approach to counteract effects of aging (Madeo *et al.*, 2019) and has found its way into the general public's perception in recent years. This is based on the findings of prolonged longevity in various model organisms, from *C.elegans* to primates (Bodkin *et al.*, 2003; Hansen *et al.*, 2008; Roth *et al.*, 2001) that goes far beyond the treatment of diseases and a great interest in caloric

restriction (CR) and intermittent fasting protocols for a whole palette of conditions exists, ranging from simple weight loss and all the associated disorders linked to obesity, to the prolongation of healthy life span and longevity (Maiuri & Kroemer, 2019; Stekovic *et al.*, 2019). The terminology on different fasting regimens is not always precise and can refer to divergent fasting periods and calory consumption (Longo *et al.*, 2021). For HD patients, who cannot tolerate a too low body mass index, caloric restriction mimetics (compounds that trigger signalling, normally induced by the lack of nutrients) promise beneficial effects of CR without the need to reduce the calorie intake by approximately half and remain a treatment option for patients who aren't able to maintain such a rigorous, resource demanding lifestyle (Madeo *et al.*, 2019). Intermittent fasting (time-restricted, reduced calory intake) on the other hand comes with the promise that no external drug needs to be administered and no toxicity needs to be considered, because the beneficial effects of CR can be achieved by fasting in a timely manner alone. But also, this comes at a price. Weight loss, fatigue and repressed immune response are just a few to name. In healthy individuals alter nate day fasting has shown promising results as health parameters were improved while eating every other day was safe for the participants (Stekovic *et al.*, 2019). In this study the overall calorie reduction was approximately 40%. This would need to be adapted to HD patients, who show severe weight loss at late stages of disease (van der Burg *et al.*, 2009). In HD mice, intermittent fasting was beneficial and reduced the levels of mHTT (Ehrnhoefer *et al.*, 2018).

Table 1: supplements and drugs approved for clinical use with autophagy inducing properties

<i>mechanism</i>	<i>treatment</i>	<i>target</i>	<i>model/ group</i>	<i>reference</i>
mTOR dependent	fasting	mTOR/SIRT1	HD mice	(Ehrnhoefer <i>et al.</i> , 2017)
	rapamycin	mTORC1	cell & fly models of HD	(Ravikumar <i>et al.</i> , 2002)
	CCI-779 (temsirolimus)	mTORC1	fly & mouse models of HD	(Ravikumar <i>et al.</i> , 2004)
		mTORC1/ GSK3 β	AD mice	(Jiang <i>et al.</i> , 2014)
		mTORC1	SCA3 mice	(Menziez, 2010)
resveratrol	mTOR/ ATP competition Atg4 SIRT1/ antioxidant	AD mice	(Kou & Chen, 2017)	
		SH-SY5Y cells	(Vidoni <i>et al.</i> , 2018)	
		HD patients	NCT02336633 ¹	
mTOR independent	Rilmenidine	activation of ADRA2/ α 2 and I ₁ R	HD mice	(Rose <i>et al.</i> , 2010)
		induction of autophagy	HD patients	(Underwood <i>et al.</i> , 2017)
	metformin	AMPK	<i>C.elegans</i> , HD cell models, HD mice	(Vázquez-Manrique <i>et al.</i> , 2015)
		AMPK	HD patients	(Ma <i>et al.</i> , 2007)
		diabetes control, improved cognition		(Hervás <i>et al.</i> , 2017)
trehalose	mTOR independent/ exact mechanism unknown aggregation/autophagy induction	PC-12 cells	(Sarkar <i>et al.</i> , 2007)	
		HD mice	(Tanaka <i>et al.</i> , 2004)	
		SCA17 mice	(Chen <i>et al.</i> , 2015)	

¹ ClinicalTrials.gov Identifier

One interesting finding of the study by Ehrnhoefer *et al.* was that it was not necessary to restrict the caloric intake in mice, to reduce the protein, but rather the forced timing of food intake was essential. A finding that was also confirmed in healthy mice, which had - when on a feeding regimen - much better tolerance towards a high fat diet, in comparison to littermates, who ate similar amounts without the timely restriction (Dedual *et al.*, 2019).

Even though the metabolism of mice and men cannot be compared, the potential of lifestyle changes should be exploited in order to investigate possible additional treatment strategies for HD patients. One such treatment strategy, which is also connected to the induction of autophagy, is physical exercise, which has been shown to improve brain function (He *et al.*, 2012; Mattson, 2012). Meta-studies found preliminary support of beneficial effects on the level of strengthening motor control and improving fitness in HD (Fritz *et al.*, 2017) and similar results were found for AD (Heyn *et al.*, 2004). Most studies investigating the effects of exercise in HD models were performed in the R6/1 model. A transgenic mouse model, expressing 115 – 150 CAG repeats, showing severe motor symptoms and reduced life span (Mangiarini *et al.*, 1996). In this model exercise delayed disease onset (Pang *et al.*, 2006; van Dellen *et al.*, 2008) and modulated neuropathological processes, as BDNF release and mitochondrial respiratory capacity (Herbst & Holloway, 2015; Pang *et al.*, 2006). Findings on motor symptoms were mixed, which can be attributed to different exercise protocols (Caldwell *et al.*, 2019; Harrison *et al.*, 2013). Interestingly, aggregate size and number of intranuclear aggregates was increased in exercised R6/1 mice, whereas the number of extra-nuclear inclusions was decreased (Harrison *et al.*, 2013). One could speculate that this finding is a result of autophagy's predominant clearance in the cytoplasm (Luo *et al.*, 2016). While exercise has been shown to be beneficial as well in R6/2 mice (Wood *et al.*, 2011) and the quinolinic acid induced rat model of HD (Kim *et al.*, 2015), no benefits were observed in the N171-82Q mouse model (Potter *et al.*, 2010).

One could also think of other forms of treatments that would affect and increase autophagy, but without the direct manipulation of the signalling cascades components. One possibility to exploit autophagy induction is to engage the calpain system. Calpains are calcium dependent proteolytic enzymes involved in the formation of toxic N-terminal mHTT fragments. These proteases are overactivated in

HD patients and their genetic or pharmacological inhibition leads to a reduction of aggregate formation and amelioration of motor phenotypes in several models of neurodegeneration (Diepenbroek *et al.*, 2014; Haacke *et al.*, 2007; Simões *et al.*, 2012). An off-target effect of calpain inhibition is the induction of autophagy. Therefore, lowering the fragmentation of the mutant protein additionally benefits its degradation (see co-authored publication #2: Killing Two Angry Birds with One Stone: Autophagy Activation by Inhibiting Calpains in Neurodegenerative Diseases and Beyond (Weber *et al.*, 2019)). This effect was described by Fiona Menzies in a HD model (Menzies *et al.*, 2015). Genetic inhibition of calpains in HD mice led to improvement of HD phenotypes in an autophagy dependent manner. This is explained by the modulatory function of calpains on autophagy proteins, e.g. Atg5 or beclin-1 (Russo *et al.*, 2011; Yousefi *et al.*, 2006). A similar mode of action has been proposed for caspases. Caspases are cysteine proteases, which are the regulating proteins of apoptosis. Caspase 6, as one example, has been proposed to be connected to the cleavage of mHTT, while mHTT activates caspase 6 (Graham *et al.*, 2006; Martin *et al.*, 2015) and the absence of caspase 6 activates autophagy whereby HTT is degraded (Gafni *et al.*, 2012). Moreover caspase 6 has been attributed autophagy protein cleaving, similar to calpains (Norman *et al.*, 2010). It is important to note, that other posttranslational modifications, as ubiquitination, myristylation or acetylation also regulate the degradation of HTT (Ehrnhoefer *et al.*, 2011a; Martin *et al.*, 2015). In line with this, increased caspase activity has been found in HD patients and animal models (see also co-authored publication #3: olfactory bulb atrophy and caspase activation observed in the BACHD rat models of Huntington disease). In line with this, also wild-type HTT functions in the induction of autophagy need to be considered, when reducing mutant and wild-type of the protein at the same time by pharmacological means, RNAi or ASOs. This becomes evident, considering the many studies where the lack of wild-type HTT has been shown to negatively affect autophagy induction and function (Pircs *et al.*, 2021; Wu *et al.*, 2012). Interestingly, it has also been shown that autophagy activation can enhance the efficacy of ASO mediated gene silencing, through the endocytosis/lysosomal pathway (Ochaba *et al.*, 2019).

One feature that all studies investigating the mTOR/autophagy axis *in vivo* lack, is the reliable measurement of autophagy. While there have been advantages with

artificial reporters like fluorescently labelled LC3, chemical inhibitors of autophagosome degradation and genetic knock-out controls of key autophagic genes, a reliable biomarker of autophagy, something that could be a marker of treatment efficacy and proof of principle in clinical trials is missing. It is not only missing to translate pre-clinical into clinical studies, but it is also missing to gain a full understanding about autophagy in humans (Yoshii & Mizushima, 2017). Open questions revolve about the magnitude of the inducing effect. The autophagic answer in the body is an answer to the lack of nutrients. Naturally, this is an oscillating process, having high amplitudes when there are little nutrients and energy supply. But it remains elusive what happens to the magnitude of a response to inducers and how and when this induction can be most effective and if a constant higher level is something that can be sustained. So far most studies have looked at tissue biopsies (Gassen *et al.*, 2014) or have analysed post-mortem samples (Sittler *et al.*, 2018). This however can, at best, be indicative of a biological meaningful alteration but fails to be a practical and reliable measure of the basal and treated state, especially throughout different tissues. An optimal “autophagometer” has not been found yet (Rubinsztein *et al.*, 2009). So far, the best measure of an effective selective autophagy induction, is the measurement of its target’s degradation. In the case of Huntington disease, the reduction of mHTT can be used as a biomarker, however HTT levels are regulated on the transcriptional levels and affected by many cellular processes, not only autophagy. The mutant protein can be measured in cerebrospinal fluid (CSF), blood and even saliva and the amount of protein, correlates with disease progression in terms of clinical stage, phenotype and disease burden (Byrne & Wild, 2016; Killoran & Biglan, 2016; Weiss *et al.*, 2012). Measuring mHTT in the CSF has the advantage of the direct connection to the brain. Currently the reduction by huntingtin lowering strategies in clinical trials is assessed by measuring CSF mHTT levels and previous studies have shown that lowering mHTT levels directly in the brain, correlates with decreasing mHTT CSF levels (Byrne & Wild, 2016; Tabrizi *et al.*, 2019a). mHTT being the disease-causing protein makes it a very interesting model and marker, as well for autophagy inducing therapies.

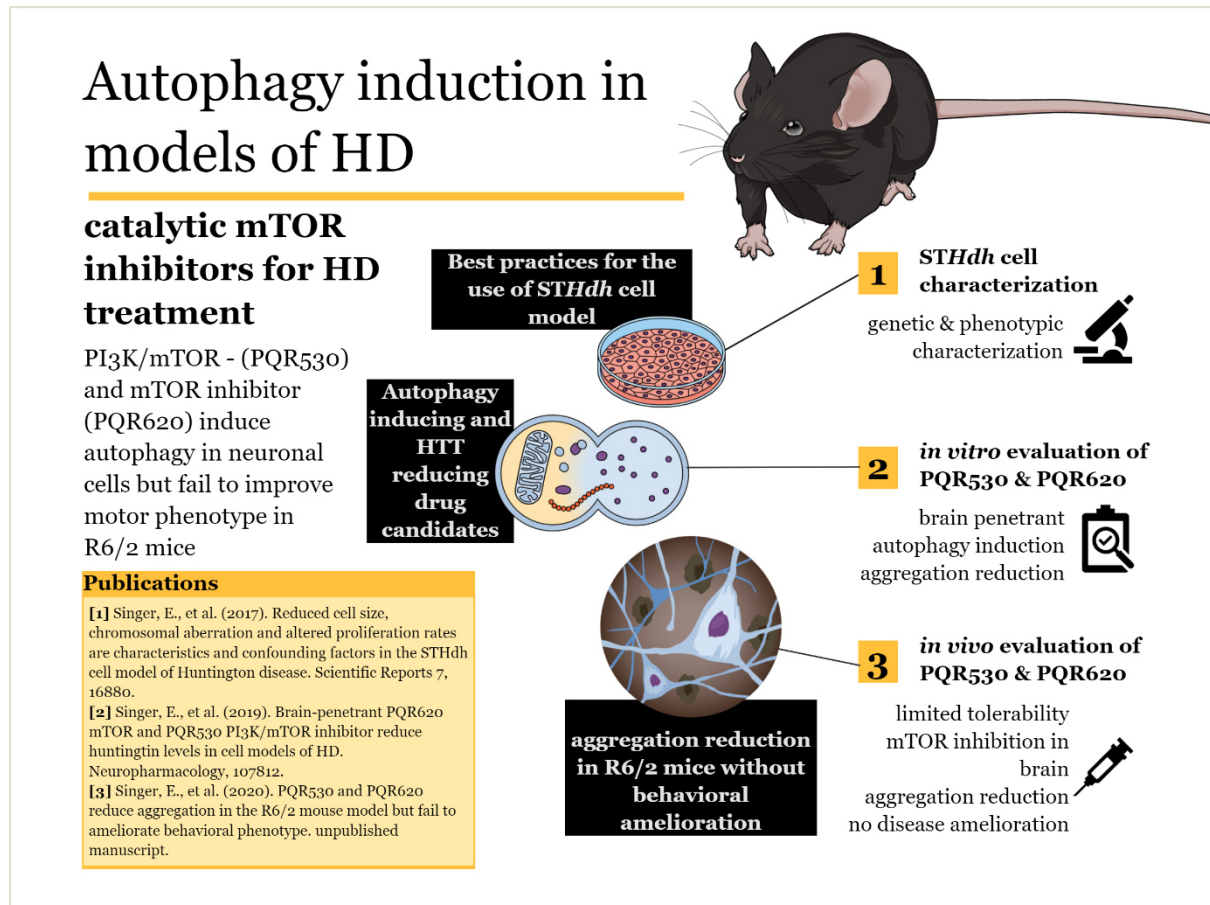


Figure 5: summary of obtained results. The characterization of STHdh cell lines (1) has laid the groundwork for their use as an in vitro HD model for evaluation of autophagy inducing compounds (2). Both brain-penetrant compounds (PQR530 and PQR620) have been tested in the R6/2 model of HD (3). Despite reduction of the aggregation load, no amelioration of the motor deficits or the weight loss phenotype was observed.

Options & Perspectives

The identification of cellular processes affected by the HD mutation has led to the development of many different treatment strategies. Next to established but only symptomatic treatment regimens for patients targeting motor symptoms, e.g. Tetrabenazine and Deutetrabenazine (Claassen *et al.*, 2017), other interventions for patients currently evaluated in clinical trials range from physiotherapy, cognitive training and transcranial magnetic stimulation to stem cell transplantation and deep brain stimulation (Rodrigues & Wild, 2018b). All aiming at improving life quality with the disease. Clinical trials evaluating substances aiming at restoring mHTT induced cellular dysfunctions have not been successful yet, as in preceding examples with studies evaluating coenzyme Q10 (McGarry *et al.*, 2017) or pridopidine (De Yebenes *et al.*, 2011). The most promising strategy is the reduction of the mutant protein by

means of ASOs (Rodrigues & Wild, 2018a) or RNA interference (RNAi) (Grondin *et al.*, 2012), as the production of the mutant protein, the upstream cause of the pathogenic process, is targeted. The optimal distribution in the brain, time point of intervention and effects from haploinsufficiency are yet to be evaluated and for this, great effort is made to determine optimal lowering strategies (Caron *et al.*, 2018; Wild & Tabrizi, 2017). Currently non-allele specific ASOs therapy is in clinical trial and patients are recruited for what could be for the first time a disease-slowing treatment and results are awaited (Tabrizi *et al.*, 2019b). On the way to a “one-shot” treatment, ideally before any symptoms occur, the intricacies of the pathogenic mechanisms in neurodegeneration are yet to be determined. mTOR inhibition and autophagy induction has a fundamental role in promoting longevity and could be a measure to increase life quality of HD patients. Further knowledge about the delicate mechanism is needed to determine whether autophagy induction could be beneficial in men and whether boosting autophagy can provide sufficient clearance of proteins that cause neurodegeneration. Despite the lack of an autophagometer and knowledge about the basal autophagic clearance in humans for the future, autophagy induction could become an addition to treatment plans for HD patients. Optimal form of induction - by lifestyle changes or pharmacologically – and especially the optimal therapeutic window remain to be established.

More than 25 years after the discovery of Huntingtin, knowledge on the disease mechanism has expanded rapidly and new gene therapy tools promise to give more insight on how the disease can be ultimately treatable.

REFERENCES

- Abada, Y.-s. K., Schreiber, R. & Ellenbroek, B. (2013).** Motor, emotional and cognitive deficits in adult BACHD mice: A model for Huntington's disease. *Behavioural Brain Research* **238**, 243-251.
- Abd-Elrahman, K. S., Hamilton, A., Hutchinson, S. R., Liu, F., Russell, R. C. & Ferguson, S. S. (2017).** mGluR5 antagonism increases autophagy and prevents disease progression in the zQ175 mouse model of Huntington's disease. *Sci Signal* **10**, eaan6387.
- Abd-Elrahman, K. S. & Ferguson, S. S. G. (2019).** Modulation of mTOR and CREB pathways following mGluR5 blockade contribute to improved Huntington's pathology in zQ175 mice. *Molecular Brain* **12**, 35.
- Al-Ramahi, I., Giridharan, S. S. P., Chen, Y.-C. & other authors (2017).** Inhibition of PIP4K γ ameliorates the pathological effects of mutant huntingtin protein. *Elife* **6**, e29123.
- Andrade, M. A. & Bork, P. (1995).** HEAT repeats in the Huntington's disease protein. *Nature genetics* **11**, 115-116.
- Arnoux, I., Willam, M., Griesche, N. & other authors (2018).** Metformin reverses early cortical network dysfunction and behavior changes in Huntington's disease. *Elife* **7**, e38744.
- Arrasate, M., Mitra, S., Schweitzer, E. S., Segal, M. R. & Finkbeiner, S. (2004).** Inclusion body formation reduces levels of mutant huntingtin and the risk of neuronal death. *Nature* **431**, 805.
- Ashkenazi, A., Bento, C. F., Ricketts, T. & other authors (2017).** Polyglutamine tracts regulate beclin 1-dependent autophagy. *Nature* **545**, 108.
- Baiamonte, B. A., Lee, F. A., Brewer, S. T., Spano, D. & LaHoste, G. J. (2013).** Attenuation of Rhes Activity Significantly Delays the Appearance of Behavioral Symptoms in a Mouse Model of Huntington's Disease. *PLOS ONE* **8**, e53606.
- Balduini, W., Carloni, S. & Buonocore, G. (2012).** Autophagy in hypoxia-ischemia induced brain injury. *The journal of maternal-fetal & neonatal medicine* **25**, 30-34.
- Ballesteros-Álvarez, J. & Andersen, J. K. (2021).** mTORC2: The other mTOR in autophagy regulation. *Aging Cell* **20**, e13431.
- Bañez-Coronel, M., Ayhan, F., Tarabochia, A. D. & other authors (2015).** RAN translation in Huntington disease. *Neuron* **88**, 667-677.
- Becher, M. W., Kotzok, J. A., Sharp, A. H., Davies, S. W., Bates, G. P., Price, D. L. & Ross, C. A. (1998).** Intranuclear Neuronal Inclusions in Huntington's Disease and Dentatorubral and Pallidolusian Atrophy: Correlation between the Density of Inclusions and IT15CAG Triplet Repeat Length. *Neurobiology of disease* **4**, 387-397.
- Bodkin, N. L., Alexander, T. M., Ortmeyer, H. K., Johnson, E. & Hansen, B. C. (2003).** Mortality and Morbidity in Laboratory-maintained Rhesus Monkeys and Effects of Long-term Dietary Restriction. *The Journals of Gerontology: Series A* **58**, B212-B219.
- Brandt, C., Hillmann, P., Noack, A. & other authors (2018).** The novel, catalytic mTORC1/2 inhibitor PQR620 and the PI3K/mTORC1/2 inhibitor PQR530 effectively cross the blood-brain barrier and increase seizure threshold in a mouse model of chronic epilepsy. *Neuropharmacology* **140**, 107-120.
- Bryan, M. R., O'Brien, M. T., Nordham, K. D. & other authors (2019).** Acute manganese treatment restores defective autophagic cargo loading in Huntington's disease cell lines. *Human Molecular Genetics* **28**, 3825-3841.
- Bucciantini, M., Giannoni, E., Chiti, F. & other authors (2002).** Inherent toxicity of aggregates implies a common mechanism for protein misfolding diseases. *nature* **416**, 507.
- Bucha, S., Mukhopadhyay, D. & Bhattacharyya, N. P. (2015).** Regulation of mitochondrial morphology and cell cycle by microRNA-214 targeting Mitofusin2. *Biochemical and Biophysical Research Communications* **465**, 797-802.

- Byrne, L. M. & Wild, E. J. (2016).** Cerebrospinal fluid biomarkers for Huntington's disease. *J Huntingtons Dis* **5**, 1-13.
- Caldwell, C. C., Petzinger, G. M., Jakowec, M. W. & Cadenas, E. (2019).** Treadmill exercise rescues mitochondrial function and motor behavior in the CAG(140) knock-in mouse model of Huntington's disease. *Chem Biol Interact* **315**, 108907-108907.
- Caron, N. S., Dorsey, E. R. & Hayden, M. R. (2018).** Therapeutic approaches to Huntington disease: from the bench to the clinic. *Nature Reviews Drug Discovery* **17**, 729.
- Cattaneo, E., Rigamonti, D., Goffredo, D., Zuccato, C., Squitieri, F. & Sipione, S. (2001).** Loss of normal huntingtin function: new developments in Huntington's disease research. *Trends in neurosciences* **24**, 182-188.
- Cattaneo, E., Zuccato, C. & Tartari, M. (2005).** Normal huntingtin function: an alternative approach to Huntington's disease. *Nat Rev Neurosci* **6**, 919-930.
- Caviston, J. P. & Holzbaaur, E. L. (2009).** Huntingtin as an essential integrator of intracellular vesicular trafficking. *Trends in cell biology* **19**, 147-155.
- Checkoway, H., Lundin, J. I. & Kelada, S. N. (2011).** Neurodegenerative diseases. *IARC scientific publications*, 407-419.
- Chen, S., Ferrone, F. A. & Wetzel, R. (2002).** Huntington's disease age-of-onset linked to polyglutamine aggregation nucleation. *Proceedings of the National Academy of sciences* **99**, 11884-11889.
- Chen, Z.-Z., Wang, C.-M., Lee, G.-C. & other authors (2015).** Trehalose attenuates the gait ataxia and gliosis of spinocerebellar ataxia type 17 mice. *Neurochemical research* **40**, 800-810.
- Child, D. D., Lee, J. H., Pascua, C. J., Chen, Y. H., Mas Monteys, A. & Davidson, B. L. (2018).** Cardiac mTORC1 Dysregulation Impacts Stress Adaptation and Survival in Huntington's Disease. *Cell Reports* **23**, 1020-1033.
- Choi, A. M. K., Ryter, S. W. & Levine, B. (2013).** Autophagy in human health and disease. *N Engl J Med* **368**, 651-662.
- Chopra, V., Fox, J. H., Lieberman, G. & other authors (2007).** A small-molecule therapeutic lead for Huntington's disease: Preclinical pharmacology and efficacy of C2-8 in the R6/2 transgenic mouse. *Proceedings of the National Academy of Sciences* **104**, 16685-16689.
- Ciammola, A., Sassone, J., Alberti, L., Meola, G., Mancinelli, E., Russo, M. A., Squitieri, F. & Silani, V. (2006).** Increased apoptosis, Huntingtin inclusions and altered differentiation in muscle cell cultures from Huntington's disease subjects. *Cell death and differentiation* **13**, 2068-2078.
- Ciechanover, A. (2005).** Proteolysis: from the lysosome to ubiquitin and the proteasome. *Nat Rev Mol Cell Biol* **6**, 79-87.
- Ciechanover, A. & Kwon, Y. T. (2015).** Degradation of misfolded proteins in neurodegenerative diseases: therapeutic targets and strategies. *Experimental & molecular medicine* **47**, e147.
- Claassen, D. O., Carroll, B., De Boer, L. M., Wu, E., Ayyagari, R., Gandhi, S. & Stamler, D. (2017).** Indirect tolerability comparison of Deutetrabenazine and Tetrabenazine for Huntington disease. *Journal of clinical movement disorders* **4**, 3.
- Clabough, E. B. & Zeitlin, S. O. (2006).** Deletion of the triplet repeat encoding polyglutamine within the mouse Huntington's disease gene results in subtle behavioral/motor phenotypes in vivo and elevated levels of ATP with cellular senescence in vitro. *Human molecular genetics* **15**, 607-623.
- Creus-Muncunill, J., Badillos-Rodríguez, R., Garcia-Forn, M. & other authors (2019).** Increased translation as a novel pathogenic mechanism in Huntington's disease. *Brain* **142**, 3158-3175.
- Dabrowska, M., Ciolak, A., Kozłowska, E., Fiszer, A. & Olejniczak, M. (2020).** Generation of New Isogenic Models of Huntington's Disease Using CRISPR-Cas9 Technology. *International Journal of Molecular Sciences* **21**, 1854.
- Das, E., Jana, N. R. & Bhattacharyya, N. P. (2013).** MicroRNA-124 targets CCNA2 and regulates cell cycle in STHdhQ111/HdhQ111 cells. *Biochemical and Biophysical Research Communications* **437**, 217-224.
- Das, E. (2014).** Regulation of cell cycle autophagy and neuronal differentiation by micro RNA.
- Davies, S. W., Turmaine, M., Cozens, B. A. & other authors (1997).** Formation of Neuronal Intranuclear Inclusions Underlies the Neurological Dysfunction in Mice Transgenic for the HD Mutation. *Cell* **90**, 537-548.

- De Yebenes, J. G., Landwehrmeyer, B., Squitieri, F. & other authors (2011).** Pridopidine for the treatment of motor function in patients with Huntington's disease (MermaiHD): a phase 3, randomised, double-blind, placebo-controlled trial. *The Lancet Neurology* **10**, 1049-1057.
- DeBosch, B. J., Heitmeier, M. R., Mayer, A. L. & other authors (2016).** Trehalose inhibits solute carrier 2A (SLC2A) proteins to induce autophagy and prevent hepatic steatosis. *Science Signaling* **9**, ra21-ra21.
- Dedual, M. A., Wueest, S., Borsigova, M. & Konrad, D. (2019).** Intermittent fasting improves metabolic flexibility in short-term high-fat diet-fed mice. *American Journal of Physiology-Endocrinology and Metabolism* **317**, E773-E782.
- Dickey, A. S. & La Spada, A. R. (2018).** Therapy development in Huntington disease: From current strategies to emerging opportunities. *American journal of medical genetics Part A* **176**, 842-861.
- Diepenbroek, M., Casadei, N., Esmer, H. & other authors (2014).** Overexpression of the calpain-specific inhibitor calpastatin reduces human alpha-Synuclein processing, aggregation and synaptic impairment in [A30P] α Syn transgenic mice. *Human Molecular Genetics* **23**, 3975-3989.
- DiFiglia, M., Sapp, E., Chase, K. O., Davies, S. W., Bates, G. P., Vonsattel, J. P. & Aronin, N. (1997).** Aggregation of huntingtin in neuronal intranuclear inclusions and dystrophic neurites in brain. *Science* **277**, 1990-1993.
- Doran, E. & Halestrap, A. P. (2000).** Evidence that metformin exerts its anti-diabetic effects through inhibition of complex 1 of the mitochondrial respiratory chain. *Biochemical Journal* **348**, 607-614.
- Duyao, M., Ambrose, C., Myers, R. & other authors (1993).** Trinucleotide repeat length instability and age of onset in Huntington's disease. *Nat Genet* **4**, 387-392.
- Ehrnhoefer, D. E., Sutton, L. & Hayden, M. R. (2011a).** Small changes, big impact: posttranslational modifications and function of huntingtin in Huntington disease. *The Neuroscientist* **17**, 475-492.
- Ehrnhoefer, D. E., Wong, B. K. & Hayden, M. R. (2011b).** Convergent pathogenic pathways in Alzheimer's and Huntington's diseases: shared targets for drug development. *Nature reviews Drug discovery* **10**, 853.
- Ehrnhoefer, D. E., Martin, D. D., Qiu, X. & other authors (2017).** Feeding Schedule And Proteolysis Regulate Autophagic Clearance Of Mutant Huntingtin. *bioRxiv*.
- Ehrnhoefer, D. E., Martin, D. D. O., Schmidt, M. E. & other authors (2018).** Preventing mutant huntingtin proteolysis and intermittent fasting promote autophagy in models of Huntington disease. *Acta Neuropathologica Communications* **6**, 16.
- Fain, J. N., Del Mar, N. A., Meade, C. A., Reiner, A. & Goldowitz, D. (2001).** Abnormalities in the functioning of adipocytes from R6/2 mice that are transgenic for the Huntington's disease mutation. *Human Molecular Genetics* **10**, 145-152.
- Fernandez-Fernandez, M. R., Ferrer, I. & Lucas, J. J. (2011).** Impaired ATF6 α processing, decreased Rheb and neuronal cell cycle re-entry in Huntington's disease. *Neurobiology of Disease* **41**, 23-32.
- Ferrante, R. J., Kowall, N. W., Beal, M. F., Martin, J. B., Bird, E. D. & Richardson, E. P., Jr. (1987).** Morphologic and histochemical characteristics of a spared subset of striatal neurons in Huntington's disease. *Journal of neuropathology and experimental neurology* **46**, 12-27.
- Folch, J., Junyent, F., Verdaguer, E., Auladell, C., Pizarro, J. G., Beas-Zarate, C., Pallàs, M. & Camins, A. (2012).** Role of Cell Cycle Re-Entry in Neurons: A Common Apoptotic Mechanism of Neuronal Cell Death. *Neurotoxicity Research* **22**, 195-207.
- Fox, J. H., Connor, T., Chopra, V. & other authors (2010).** The mTOR kinase inhibitor Everolimus decreases S6 kinase phosphorylation but fails to reduce mutant huntingtin levels in brain and is not neuroprotective in the R6/2 mouse model of Huntington's disease. *Mol Neurodegener* **5**.
- Franklin, J. L. & Johnson Jr, E. M. (1998).** Control of neuronal size homeostasis by trophic factor-mediated coupling of protein degradation to protein synthesis. *The Journal of cell biology* **142**, 1313-1324.
- Fritz, N. E., Rao, A. K., Kegelmeyer, D., Kloos, A., Busse, M., Hartel, L., Carrier, J. & Quinn, L. (2017).** Physical Therapy and Exercise Interventions in Huntington's Disease: A Mixed Methods Systematic Review. *J Huntingtons Dis* **6**, 217-235.
- Gafni, J., Papanikolaou, T., Degiacomo, F. & other authors (2012).** Caspase-6 activity in a BACHD mouse modulates steady-state levels of mutant huntingtin protein but is not necessary for production of a 586 amino acid proteolytic fragment. *The Journal of neuroscience : the official journal of the Society for Neuroscience* **32**, 7454-7465.

- Galluzzi, L., Bravo-San Pedro, J. M., Levine, B., Green, D. R. & Kroemer, G. (2017).** Pharmacological modulation of autophagy: therapeutic potential and persisting obstacles. *Nature reviews Drug discovery* **16**, 487-511.
- Gan, L., Cookson, M. R., Petrucelli, L. & La Spada, A. R. (2018).** Converging pathways in neurodegeneration, from genetics to mechanisms. *Nature neuroscience* **21**, 1300-1309.
- Gassen, N. C., Hartmann, J., Zschocke, J. & other authors (2014).** Association of FKBP51 with priming of autophagy pathways and mediation of antidepressant treatment response: evidence in cells, mice, and humans. *PLoS medicine* **11**, e1001755.
- GeM-HD, C. (2015).** Identification of Genetic Factors that Modify Clinical Onset of Huntington's Disease. *Cell* **162**, 516-526.
- Gervais, F. G., Singaraja, R., Xanthoudakis, S. & other authors (2002).** Recruitment and activation of caspase-8 by the Huntingtin-interacting protein Hip-1 and a novel partner Hipp1. *Nature cell biology* **4**, 95.
- Godin, J. D., Colombo, K., Molina-Calavita, M. & other authors (2010).** Huntingtin is required for mitotic spindle orientation and mammalian neurogenesis. *Neuron* **67**, 392-406.
- Goetz, I. E., Roberts, E. & Warren, J. (1981).** Skin fibroblasts in Huntington disease. *American journal of human genetics* **33**, 187.
- Graham, R. K., Deng, Y., Slow, E. J. & other authors (2006).** Cleavage at the caspase-6 site is required for neuronal dysfunction and degeneration due to mutant huntingtin. *Cell* **125**, 1179-1191.
- Graveland, G. A., Williams, R. S. & DiFiglia, M. (1985).** Evidence for degenerative and regenerative changes in neostriatal spiny neurons in Huntington's disease. *Science* **227**, 770-773.
- Gronkin, R., Kaytor, M. D., Ai, Y. & other authors (2012).** Six-month partial suppression of Huntingtin is well tolerated in the adult rhesus striatum. *Brain* **135**, 1197-1209.
- Gutekunst, C. A., Li, S. H., Yi, H. & other authors (1999).** Nuclear and neuropil aggregates in Huntington's disease: relationship to neuropathology. *J Neurosci* **19**, 2522-2534.
- Haacke, A., Hartl, F. U. & Breuer, P. (2007).** Calpain inhibition is sufficient to suppress aggregation of polyglutamine-expanded ataxin-3. *Journal of Biological Chemistry* **282**, 18851-18856.
- Hansen, M., Chandra, A., Mitic, L. L., Onken, B., Driscoll, M. & Kenyon, C. (2008).** A role for autophagy in the extension of lifespan by dietary restriction in *C. elegans*. *PLoS genetics* **4**, e24.
- Hara, T. (2006).** Suppression of basal autophagy in neural cells causes neurodegenerative disease in mice. *Nature* **441**, 885-889.
- Harjes, P. & Wanker, E. E. (2003).** The hunt for huntingtin function: interaction partners tell many different stories. *Trends Biochem Sci* **28**, 425-433.
- Harrison, D. J., Busse, M., Openshaw, R., Rosser, A. E., Dunnett, S. B. & Brooks, S. P. (2013).** Exercise attenuates neuropathology and has greater benefit on cognitive than motor deficits in the R6/1 Huntington's disease mouse model. *Experimental neurology* **248**, 457-469.
- He, C., Bassik, M. C., Moresi, V. & other authors (2012).** Exercise-induced BCL2-regulated autophagy is required for muscle glucose homeostasis. *Nature* **481**, 511.
- Heemels, M.-T. (2016).** Neurodegenerative diseases. *Nature* **539**, 179.
- Heng, M. Y., Duong, D. K., Albin, R. L., Tallaksen-Greene, S. J., Hunter, J. M. & Lesort, M. J. (2010).** Early autophagic response in a novel knock-in model of Huntington disease. *Hum Mol Genet* **19**.
- Heras-Sandoval, D., Pérez-Rojas, J. M., Hernández-Damián, J. & Pedraza-Chaverri, J. (2014).** The role of PI3K/AKT/mTOR pathway in the modulation of autophagy and the clearance of protein aggregates in neurodegeneration. *Cellular Signalling* **26**, 2694-2701.
- Herbst, E. & Holloway, G. (2015).** Exercise training normalizes mitochondrial respiratory capacity within the striatum of the R6/1 model of Huntington's disease. *Neuroscience* **303**, 515-523.
- Hervás, D., Fornés-Ferrer, V., Gómez-Escribano, A. P., Sequedo, M. D., Peiró, C., Millán, J. M. & Vázquez-Manrique, R. P. (2017).** Metformin intake associates with better cognitive function in patients with Huntington's disease. *PLOS ONE* **12**, e0179283.
- Herzog, L. K., Kevei, É., Marchante, R. & other authors (2019).** The Machado-Joseph disease deubiquitylase ataxin-3 interacts with LC3C/GABARAP and promotes autophagy. *Aging Cell* **n/a**, e13051.

- Heyn, P., Abreu, B. C. & Ottenbacher, K. J. (2004).** The effects of exercise training on elderly persons with cognitive impairment and dementia: A meta-analysis. *Archives of Physical Medicine and Rehabilitation* **85**, 1694-1704.
- Highet, B., Dieriks, B. V., Murray, H. C., Faull, R. L. M. & Curtis, M. A. (2020).** Huntingtin Aggregates in the Olfactory Bulb in Huntington's Disease. *Frontiers in aging neuroscience* **12**, 261-261.
- Hillmann, P. & Fabbro, D. (2019).** PI3K/mTOR Pathway Inhibition: Opportunities in Oncology and Rare Genetic Diseases. *International journal of molecular sciences* **20**, 5792.
- Hodges, A., Strand, A. D., Aragaki, A. K. & other authors (2006).** Regional and cellular gene expression changes in human Huntington's disease brain. *Human molecular genetics* **15**, 965-977.
- Hosokawa, N., Hara, Y. & Mizushima, N. (2006).** Generation of cell lines with tetracycline-regulated autophagy and a role for autophagy in controlling cell size. *FEBS Letters* **580**, 2623-2629.
- Howell, J. J., Hellberg, K., Turner, M. & other authors (2017).** Metformin inhibits hepatic mTORC1 signaling via dose-dependent mechanisms involving AMPK and the TSC complex. *Cell metabolism* **25**, 463-471.
- Hung, C. L., Maiuri, T., Bowie, L. E. & other authors (2018).** A Patient-Derived Cellular Model for Huntington's Disease Reveals Phenotypes at Clinically Relevant CAG Lengths. *bioRxiv*, 291575.
- Huntington, G. (2003).** On Chorea. *The Journal of Neuropsychiatry and Clinical Neurosciences* **15**, 109-112.
- Jansson, E. K. H., Clemens, L. E., Riess, O. & Nguyen, H. P. (2014).** Reduced Motivation in the BACHD Rat Model of Huntington Disease Is Dependent on the Choice of Food Deprivation Strategy. *PLOS ONE* **9**, e105662.
- Jeong, J.-K., Moon, M.-H., Bae, B.-C., Lee, Y.-J., Seol, J.-W., Kang, H.-S., Kim, J.-S., Kang, S.-J. & Park, S.-Y. (2012).** Autophagy induced by resveratrol prevents human prion protein-mediated neurotoxicity. *Neuroscience research* **73**, 99-105.
- Jia, H., Kast, R. J., Steffan, J. S. & Thomas, E. A. (2012).** Selective histone deacetylase (HDAC) inhibition imparts beneficial effects in Huntington's disease mice: implications for the ubiquitin–proteasomal and autophagy systems. *Human Molecular Genetics* **21**, 5280-5293.
- Jiang, M., Wang, J., Fu, J. & other authors (2012).** Neuroprotective role of Sirt1 in mammalian models of Huntington's disease through activation of multiple Sirt1 targets. *Nature medicine* **18**, 153.
- Jiang, T., Yu, J.-T., Zhu, X.-C. & other authors (2014).** Temsirolimus attenuates tauopathy in vitro and in vivo by targeting tau hyperphosphorylation and autophagic clearance. *Neuropharmacology* **85**, 121-130.
- Jiang, Y., Berg, M. D., Genereaux, J., Ahmed, K., Duennwald, M. L., Brandl, C. J. & Lajoie, P. (2019).** Sfp1 links TORC1 and cell growth regulation to the yeast SAGA-complex component Tra1 in response to polyQ proteotoxicity. *Traffic* **20**, 267-283.
- Jin, J., Gu, H., Anders, N. M., Ren, T., Jiang, M., Tao, M., Peng, Q., Rudek, M. A. & Duan, W. (2016).** Metformin Protects Cells from Mutant Huntingtin Toxicity Through Activation of AMPK and Modulation of Mitochondrial Dynamics. *NeuroMolecular Medicine* **18**, 581-592.
- Kaltenbach, L. S., Romero, E., Becklin, R. R. & other authors (2007).** Huntingtin interacting proteins are genetic modifiers of neurodegeneration. *PLoS Genet* **3**, e82.
- Kaushik, S. & Cuervo, A. M. (2012).** Chaperone-mediated autophagy: a unique way to enter the lysosome world. *Trends in cell biology* **22**, 407-417.
- Kazantsev, A., Preisinger, E., Dranovsky, A., Goldgaber, D. & Housman, D. (1999).** Insoluble detergent-resistant aggregates form between pathological and nonpathological lengths of polyglutamine in mammalian cells. *Proc Natl Acad Sci U S A* **96**, 11404-11409.
- Kegel, K. B., Kim, M., Sapp, E., McIntyre, C., Castaño, J. G., Aronin, N. & DiFiglia, M. (2000).** Huntingtin Expression Stimulates Endosomal–Lysosomal Activity, Endosome Tubulation, and Autophagy. *The Journal of Neuroscience* **20**, 7268-7278.
- Kegel, K. B., Meloni, A. R., Yi, Y. & other authors (2002).** Huntingtin is present in the nucleus, interacts with the transcriptional corepressor C-terminal binding protein, and represses transcription. *Journal of Biological Chemistry* **277**, 7466-7476.
- Killoran, A. & Biglan, K. (2016).** Biomarkers for Huntington's disease: A brief overview. *J Rare Dis Res Treat*.

- Kim, Y.-M., Ji, E.-S., Kim, S.-H., Kim, T.-W., Ko, I.-G., Jin, J.-J., Kim, C.-J., Kim, T.-W. & Kim, D.-H. (2015).** Treadmill exercise improves short-term memory by enhancing hippocampal cell proliferation in quinolinic acid-induced Huntington's disease rats. *J Exerc Rehabil* **11**, 5-11.
- Klionsky, D. J. (2007).** Autophagy: from phenomenology to molecular understanding in less than a decade. *Nat Rev Mol Cell Biol* **8**, 931-937.
- Klionsky, D. J., Abdelmohsen, K., Abe, A. & other authors (2016).** Guidelines for the use and interpretation of assays for monitoring autophagy. *Autophagy* **12**, 1-222.
- Komatsu, M., Wang, Q. J., Holstein, G. R., Friedrich, V. L., Jr., Iwata, J., Kominami, E., Chait, B. T., Tanaka, K. & Yue, Z. (2007).** Essential role for autophagy protein Atg7 in the maintenance of axonal homeostasis and the prevention of axonal degeneration. *Proc Natl Acad Sci U S A* **104**, 14489-14494.
- Kosinski, C. M., Cha, J. H., Young, A. B., Mangiarini, L., Bates, G., Schiefer, J. & Schwarz, M. (1999).** Intranuclear inclusions in subtypes of striatal neurons in Huntington's disease transgenic mice. *Neuroreport* **10**, 3891-3896.
- Kou, X. & Chen, N. (2017).** Resveratrol as a Natural Autophagy Regulator for Prevention and Treatment of Alzheimer's Disease. *Nutrients* **9**, 927.
- Kovalenko, M., Milnerwood, A., Giordano, J. & other authors (2018).** HttQ111/+ Huntington's Disease Knock-in Mice Exhibit Brain Region-Specific Morphological Changes and Synaptic Dysfunction. *J Huntingtons Dis* **7**, 17-33.
- Krauß, S., Griesche, N., Jastrzebska, E. & other authors (2013).** Translation of HTT mRNA with expanded CAG repeats is regulated by the MID1-PP2A protein complex. *Nature communications* **4**, 1511.
- Kroemer, G. & Levine, B. (2008).** Autophagic cell death: the story of a misnomer. *Nat Rev Mol Cell Biol* **9**, 1004-1010.
- Kulbe, J. R., Levy, J. M. M., Coultrap, S. J., Thorburn, A. & Bayer, K. U. (2014).** Excitotoxic glutamate insults block autophagic flux in hippocampal neurons. *Brain research* **1542**, 12-19.
- Kuma, A., Hatano, M., Matsui, M., Yamamoto, A., Nakaya, H., Yoshimori, T., Ohsumi, Y., Tokuhashi, T. & Mizushima, N. (2004).** The role of autophagy during the early neonatal starvation period. *Nature* **432**, 1032.
- Landwehrmeyer, G. B., McNeil, S. M., Dure, L. S. t. & other authors (1995).** Huntington's disease gene: regional and cellular expression in brain of normal and affected individuals. *Ann Neurol* **37**, 218-230.
- Laplante, M. & Sabatini, D. M. (2009).** mTOR signaling at a glance. *Journal of Cell Science* **122**, 3589-3594.
- Laplante, M. & Sabatini, David M. (2012).** mTOR Signaling in Growth Control and Disease. *Cell* **149**, 274-293.
- Larsson, M., Lundin, A. & Robins Wahlin, T.-B. (2006).** Olfactory functions in asymptomatic carriers of the Huntington disease mutation. *Journal of clinical and experimental neuropsychology* **28**, 1373-1380.
- Leavitt, B. R., van Raamsdonk, J. M., Shehadeh, J., Fernandes, H., Murphy, Z., Graham, R. K., Wellington, C. L., Raymond, L. A. & Hayden, M. R. (2006).** Wild - type huntingtin protects neurons from excitotoxicity. *Journal of neurochemistry* **96**, 1121-1129.
- Lee, H., Noh, J.-Y., Oh, Y. & other authors (2011).** IRE1 plays an essential role in ER stress-mediated aggregation of mutant huntingtin via the inhibition of autophagy flux. *Human Molecular Genetics* **21**, 101-114.
- Lee, J., Hwang, Y. J., Kim, Y. & other authors (2017).** Remodeling of heterochromatin structure slows neuropathological progression and prolongs survival in an animal model of Huntington's disease. *Acta Neuropathologica* **134**, 729-748.
- Lee, J. H., Tecedor, L., Chen, Y. H., Monteys, A. M., Sowada, M. J., Thompson, L. M. & Davidson, B. L. (2015).** Reinstating aberrant mTORC1 activity in Huntington's disease mice improves disease phenotypes. *Neuron* **85**, 303-315.
- Lee, J. K., Mathews, K., Schlaggar, B., Perlmutter, J., Paulsen, J. S., Epping, E., Burmeister, L. & Nopoulos, P. (2012).** Measures of growth in children at risk for Huntington disease. *Neurology* **79**, 668-674.
- Lessard-Beaudoin, M., Yu-Taeger, L., Laroche, M., Singer, E., Riess, O., Nguyen, H. H. P. & Graham, R. K. (2019).** Olfactory bulb atrophy and caspase activation observed in the BACHD rat models of Huntington disease. *Neurobiology of disease* **125**, 219-231.
- Levine, B. & Klionsky, D. J. (2004).** Development by Self-Digestion: Molecular Mechanisms and Biological Functions of Autophagy. *Developmental Cell* **6**, 463-477.

- Levine, M. S., Klapstein, G. J., Koppel, A. & other authors (1999).** Enhanced sensitivity to N-methyl-D-aspartate receptor activation in transgenic and knockin mouse models of Huntington's disease. *J Neurosci Res* **58**, 515-532.
- Li, L.-B., Yu, Z., Teng, X. & Bonini, N. M. (2008).** RNA toxicity is a component of ataxin-3 degeneration in *Drosophila*. *Nature* **453**, 1107.
- Li, W.-w., Li, J. & Bao, J.-k. (2012).** Microautophagy: lesser-known self-eating. *Cellular and Molecular Life Sciences* **69**, 1125-1136.
- Li, X.-J. & Li, S. (2015).** Large Animal Models of Huntington's Disease. *Curr Top Behav Neurosci* **22**, 149-160.
- Lilienbaum, A. (2013).** Relationship between the proteasomal system and autophagy. *International journal of biochemistry and molecular biology* **4**, 1-26.
- Lloyd, Alison C. (2013).** The Regulation of Cell Size. *Cell* **154**, 1194-1205.
- Longo, V. D., Di Tano, M., Mattson, M. P. & Guidi, N. (2021).** Intermittent and periodic fasting, longevity and disease. *Nature Aging* **1**, 47-59.
- Lu, X.-H., Mattis, V. B., Wang, N. & other authors (2014).** Targeting ATM ameliorates mutant Huntingtin toxicity in cell and animal models of Huntington's disease. *Science translational medicine* **6**, 268ra178-268ra178.
- Luo, M., Zhao, X., Song, Y., Cheng, H. & Zhou, R. (2016).** Nuclear autophagy: An evolutionarily conserved mechanism of nuclear degradation in the cytoplasm. *Autophagy* **12**, 1973-1983.
- Ma, T. C., Buescher, J. L., Oatis, B., Funk, J. A., Nash, A. J., Carrier, R. L. & Hoyt, K. R. (2007).** Metformin therapy in a transgenic mouse model of Huntington's disease. *Neurosci Lett* **411**, 98-103.
- Madeo, F., Carmona-Gutierrez, D., Hofer, S. J. & Kroemer, G. (2019).** Caloric Restriction Mimetics against Age-Associated Disease: Targets, Mechanisms, and Therapeutic Potential. *Cell Metabolism* **29**, 592-610.
- Maher, P., Dargusch, R., Bodai, L., Gerard, P. E., Purcell, J. M. & Marsh, J. L. (2011).** ERK activation by the polyphenols fisetin and resveratrol provides neuroprotection in multiple models of Huntington's disease. *Hum Mol Genet* **20**, 261-270.
- Maiese, K. (2016).** Targeting molecules to medicine with mTOR, autophagy and neurodegenerative disorders. *British Journal of Clinical Pharmacology* **82**, 1245-1266.
- Maiuri, M. C. & Kroemer, G. (2019).** Therapeutic modulation of autophagy: Which disease comes first.
- Malagelada, C., Jin, Z. H., Jackson-Lewis, V., Przedborski, S. & Greene, L. A. (2010).** Rapamycin Protects against Neuron Death in In Vitro and In Vivo Models of Parkinson's Disease. *Journal of Neuroscience* **30**, 1166-1175.
- Mangiarini, L., Sathasivam, K., Seller, M. & other authors (1996).** Exon 1 of the HD gene with an expanded CAG repeat is sufficient to cause a progressive neurological phenotype in transgenic mice. *Cell* **87**, 493-506.
- Mariño, G., Pietrocola, F., Eisenberg, T. & other authors (2014).** Regulation of autophagy by cytosolic acetyl-coenzyme A. *Molecular cell* **53**, 710-725.
- Martin, D. D. O., Heit, R. J., Yap, M. C., Davidson, M. W., Hayden, M. R. & Berthiaume, L. G. (2014).** Identification of a post-translationally myristoylated autophagy-inducing domain released by caspase cleavage of Huntingtin. *Human Molecular Genetics* **23**, 3166-3179.
- Martin, D. D. O., Ladha, S., Ehrnhoefer, D. E. & Hayden, M. R. (2015).** Autophagy in Huntington disease and huntingtin in autophagy. *Trends in Neurosciences* **38**, 26-35.
- Martinez-Vicente, M., Talloczy, Z., Wong, E. & other authors (2010).** Cargo recognition failure is responsible for inefficient autophagy in Huntington's disease. *Nature neuroscience* **13**, 567-576.
- Mattson, Mark P. (2012).** Energy Intake and Exercise as Determinants of Brain Health and Vulnerability to Injury and Disease. *Cell Metabolism* **16**, 706-722.
- McColgan, P. & Tabrizi, S. J. (2018).** Huntington's disease: a clinical review. *European Journal of Neurology* **25**, 24-34.
- McGarry, A., McDermott, M., Kiebert, K. & other authors (2017).** A randomized, double-blind, placebo-controlled trial of coenzyme Q10 in Huntington disease. *Neurology* **88**, 152-159.
- Mealer, R. G., Subramaniam, S. & Snyder, S. H. (2013).** Rhes Deletion Is Neuroprotective in the 3-Nitropropionic Acid Model of Huntington's Disease. *The Journal of Neuroscience* **33**, 4206-4210.

- Mealer, R. G., Murray, A. J., Shahani, N., Subramaniam, S. & Snyder, S. H. (2014).** Rhes, a striatal-selective protein implicated in Huntington disease, binds beclin-1 and activates autophagy. *J Biol Chem* **289**, 3547-3554.
- Menalled, L. B. (2005).** Knock-In Mouse Models of Huntington's Disease. *NeuroRX* **2**, 465-470.
- Menzies, F. M. (2010).** Autophagy induction reduces mutant ataxin-3 levels and toxicity in a mouse model of spinocerebellar ataxia type 3. *Brain* **133**, 93-104.
- Menzies, F. M., Garcia-Arencibia, M., Imarisio, S. & other authors (2015).** Calpain inhibition mediates autophagy-dependent protection against polyglutamine toxicity. *Cell death and differentiation* **22**, 433-444.
- Menzies, F. M., Fleming, A., Caricasole, A. & other authors (2017).** Autophagy and neurodegeneration: pathogenic mechanisms and therapeutic opportunities. *Neuron* **93**, 1015-1034.
- Meriin, A. B., Zhang, X., He, X., Newnam, G. P., Chernoff, Y. O. & Sherman, M. Y. (2002).** Huntingtin toxicity in yeast model depends on polyglutamine aggregation mediated by a prion-like protein Rnq1. *The Journal of Cell Biology* **157**, 997-1004.
- Metzger, S., Walter, C., Riess, O., Roos, R. A. C., Nielsen, J. E., Craufurd, D., Network, R. I. o. t. E. H. s. D. & Nguyen, H. P. (2013).** The V471A Polymorphism in Autophagy-Related Gene ATG7 Modifies Age at Onset Specifically in Italian Huntington Disease Patients. *PLOS ONE* **8**, e68951.
- Michalik, A. & Van Broeckhoven, C. (2003).** Pathogenesis of polyglutamine disorders: aggregation revisited. *Human molecular genetics* **12**, R173-R186.
- Mizushima, N. (2007).** Autophagy: process and function. *Genes & development* **21**, 2861-2873.
- Mizushima, N. & Yoshimori, T. (2007).** How to interpret LC3 immunoblotting. *Autophagy* **3**, 542-545.
- Mizushima, N. (2009).** Chapter 2 Methods for Monitoring Autophagy Using GFP - LC3 Transgenic Mice. In *Methods in Enzymology*, pp. 13-23: Academic Press.
- Mizushima, N. & Komatsu, M. (2011).** Autophagy: renovation of cells and tissues. *Cell* **147**, 728-741.
- Moberg, P. J. & Doty, R. L. (1997).** Olfactory function in Huntington's disease patients and at-risk offspring. *International Journal of Neuroscience* **89**, 133-139.
- Mouret, A., Lepousez, G., Gras, J., Gabellec, M.-M. & Lledo, P.-M. (2009).** Turnover of newborn olfactory bulb neurons optimizes olfaction. *Journal of Neuroscience* **29**, 12302-12314.
- Nagata, E., Sawa, A., Ross, C. A. & Snyder, S. H. (2004).** Autophagosome-like vacuole formation in Huntington's disease lymphoblasts. *NeuroReport* **15**, 1325-1328.
- Nagy, Z., Esiri, M. & Smith, A. (1998).** The cell division cycle and the pathophysiology of Alzheimer's disease. *Neuroscience* **87**, 731-739.
- Nance, M. A. & Myers, R. H. (2001).** Juvenile onset Huntington's disease--clinical and research perspectives. *Ment Retard Dev Disabil Res Rev* **7**, 153-157.
- Nedelsky, N. B., Todd, P. K. & Taylor, J. P. (2008).** Autophagy and the ubiquitin-proteasome system: collaborators in neuroprotection. *Biochimica et Biophysica Acta (BBA)-Molecular Basis of Disease* **1782**, 691-699.
- Nopoulos, P. C., Aylward, E. H., Ross, C. A. & other authors (2011).** Smaller intracranial volume in prodromal Huntington's disease: evidence for abnormal neurodevelopment. *Brain* **134**, 137-142.
- Norman, J. M., Cohen, G. M. & Bampton, E. T. W. (2010).** The in vitro cleavage of the hAtg proteins by cell death proteases. *Autophagy* **6**, 1042-1056.
- Ochaba, J., Lukacsovich, T., Csikos, G. & other authors (2014).** Potential function for the Huntingtin protein as a scaffold for selective autophagy. *Proc Natl Acad Sci U S A* **111**, 16889-16894.
- Ochaba, J., Powers, A. F., Tremble, K. A., Greenlee, S., Post, N. M., Matson, J. E., MacLeod, A. R., Guo, S. & Aghajan, M. (2019).** A novel and translational role for autophagy in antisense oligonucleotide trafficking and activity. *Nucleic acids research* **47**, 11284-11303.
- Ooi, J., Langley, S. R., Xu, X. & other authors (2019).** Unbiased profiling of isogenic Huntington disease hPSC-derived CNS and peripheral cells reveals strong cell-type specificity of CAG length effects. *Cell reports* **26**, 2494-2508. e2497.
- Ordway, J. M., Tallaksen-Greene, S., Gutekunst, C.-A. & other authors (1997).** Ectopically expressed CAG repeats cause intranuclear inclusions and a progressive late onset neurological phenotype in the mouse. *Cell* **91**, 753-763.

- Orhon, I., Dupont, N., Zaidan, M. & other authors (2016).** Primary-cilium-dependent autophagy controls epithelial cell volume in response to fluid flow. *Nature cell biology* **18**, 657-667.
- Orozco-Díaz, R., Sánchez-Álvarez, A., Hernández-Hernández, J. M. & Tapia-Ramírez, J. (2019).** The interaction between RE1-silencing transcription factor (REST) and heat shock protein 90 as new therapeutic target against Huntington's disease. *PLoS one* **14**, e0220393-e0220393.
- Pang, T., Stam, N., Nithianantharajah, J., Howard, M. L. & Hannan, A. (2006).** Differential effects of voluntary physical exercise on behavioral and brain-derived neurotrophic factor expression deficits in Huntington's disease transgenic mice. *Neuroscience* **141**, 569-584.
- Panov, A. V., Gutekunst, C. A., Leavitt, B. R., Hayden, M. R., Burke, J. R., Strittmatter, W. J. & Greenamyre, J. T. (2002).** Early mitochondrial calcium defects in Huntington's disease are a direct effect of polyglutamines. *Nature neuroscience* **5**, 731-736.
- Pavel, M., Renna, M., Park, S. J. & other authors (2018).** Contact inhibition controls cell survival and proliferation via YAP/TAZ-autophagy axis. *Nature communications* **9**, 2961.
- Pelegrí, C., Duran-Vilaregut, J., del Valle, J., Crespo-Biel, N., Ferrer, I., Pallàs, M., Camins, A. & Vilaplana, J. (2008).** Cell cycle activation in striatal neurons from Huntington's disease patients and rats treated with 3-nitropropionic acid. *International Journal of Developmental Neuroscience* **26**, 665-671.
- Petersén, Å., Renström, E., Sundler, F. & other authors (2005).** The R6/2 transgenic mouse model of Huntington's disease develops diabetes due to deficient β -cell mass and exocytosis. *Human Molecular Genetics* **14**, 565-574.
- Petersén, A. s., Larsen, K. E., Behr, G. G., Romero, N., Przedborski, S., Brundin, P. & Sulzer, D. (2001).** Expanded CAG repeats in exon 1 of the Huntington's disease gene stimulate dopamine-mediated striatal neuron autophagy and degeneration. *Human Molecular Genetics* **10**, 1243-1254.
- Piracs, K., Drouin-Ouellet, J., Gil, J. & other authors (2021).** Distinct sub-cellular autophagy impairments occur independently of protein aggregation in induced neurons from patients with Huntington's disease. *bioRxiv*, 2021.2003.2001.433433.
- Potter, M. C., Yuan, C., Ottenritter, C., Mughal, M. & van Praag, H. (2010).** Exercise is not beneficial and may accelerate symptom onset in a mouse model of Huntington's disease. *PLoS currents* **2**, RRN1201-RRN1201.
- Pryor, W. M., Biagioli, M., Shahani, N., Swarnkar, S., Huang, W. C., Page, D. T., MacDonald, M. E. & Subramaniam, S. (2014).** Huntingtin promotes mTORC1 signaling in the pathogenesis of Huntington's disease. *Sci Signal* **7**, ra103.
- Querfurth, H. & Lee, H.-K. (2021).** Mammalian/mechanistic target of rapamycin (mTOR) complexes in neurodegeneration. *Molecular neurodegeneration* **16**, 44.
- Quintanilla, R. A. & Johnson, G. V. (2009).** Role of mitochondrial dysfunction in the pathogenesis of Huntington's disease. *Brain Res Bull* **80**, 242-247.
- Rajkowska, G., Selemon, L. D. & Goldman-Rakic, P. S. (1998).** Neuronal and glial somal size in the prefrontal cortex: A postmortem morphometric study of schizophrenia and huntington disease. *Archives of General Psychiatry* **55**, 215-224.
- Ratovitski, T., Chighladze, E., Arbez, N., Boronina, T., Herbrich, S., Cole, R. N. & Ross, C. A. (2012).** Huntingtin protein interactions altered by polyglutamine expansion as determined by quantitative proteomic analysis. *Cell Cycle* **11**, 2006-2021.
- Ravikumar, B., Duden, R. & Rubinsztein, D. C. (2002).** Aggregate-prone proteins with polyglutamine and polyalanine expansions are degraded by autophagy. *Hum Mol Genet* **11**.
- Ravikumar, B., Vacher, C., Berger, Z., Davies, J. E., Luo, S. & Oroz, L. G. (2004).** Inhibition of mTOR induces autophagy and reduces toxicity of polyglutamine expansions in fly and mouse models of Huntington disease. *Nat Genet* **36**.
- Ravikumar, B. & Rubinsztein, D. C. (2006).** Role of autophagy in the clearance of mutant huntingtin: A step towards therapy? *Molecular Aspects of Medicine* **27**, 520-527.
- Reddy, P. H., Williams, M., Charles, V., Garrett, L., Pike-Buchanan, L., Whetsell Jr, W. O., Miller, G. & Tagle, D. A. (1998).** Behavioural abnormalities and selective neuronal loss in HD transgenic mice expressing mutated full-length HD cDNA. *Nature genetics* **20**, 198.
- Reiner, A., Albin, R. L., Anderson, K. D., D'Amato, C. J., Penney, J. B. & Young, A. B. (1988).** Differential loss of striatal projection neurons in Huntington disease. *Proc Natl Acad Sci U S A* **85**, 5733-5737.

- Rena, G., Hardie, D. G. & Pearson, E. R. (2017).** The mechanisms of action of metformin. *Diabetologia* **60**, 1577-1585.
- Rigamonti, D., Bauer, J. H., De-Fraja, C. & other authors (2000).** Wild-type huntingtin protects from apoptosis upstream of caspase-3. *Journal of Neuroscience* **20**, 3705-3713.
- Rodrigues, F. B. & Wild, E. J. (2018a).** Huntington's Disease Clinical Trials Corner: February 2018. *J Huntingtons Dis* **7**, 89-98.
- Rodrigues, F. B. & Wild, E. J. (2018b).** Huntington's Disease Clinical Trials Corner: August 2018. *J Huntingtons Dis* **7**, 279-286.
- Roscic, A., Baldo, B., Crochemore, C., Marcellin, D. & Paganetti, P. (2011).** Induction of autophagy with catalytic mTOR inhibitors reduces huntingtin aggregates in a neuronal cell model. *Journal of Neurochemistry* **119**, 398-407.
- Rose, C., Menzies, F. M., Renna, M., Acevedo-Arozena, A., Corrochano, S., Sadiq, O., Brown, S. D. & Rubinsztein, D. C. (2010).** Rilmenidine attenuates toxicity of polyglutamine expansions in a mouse model of Huntington's disease. *Human molecular genetics* **19**, 2144-2153.
- Ross, C. A. & Tabrizi, S. J. (2011).** Huntington's disease: from molecular pathogenesis to clinical treatment. *Lancet Neurol* **10**, 83-98.
- Roth, G. S., Ingram, D. K. & Lane, M. A. (2001).** Caloric restriction in primates and relevance to humans. *Annals of the New York Academy of Sciences* **928**, 305-315.
- Rubinsztein, D., Cuervo, A., Ravikumar, B., Sarkar, S., Korolchuk, V., Kaushik, S. & Klionsky, D. (2009).** In search of an "autophagometer". *Autophagy* **5**, 585-589.
- Rubinsztein, D. C., Leggo, J., Coles, R. & other authors (1996).** Phenotypic characterization of individuals with 30-40 CAG repeats in the Huntington disease (HD) gene reveals HD cases with 36 repeats and apparently normal elderly individuals with 36-39 repeats. *Am J Hum Genet* **59**, 16-22.
- Rubinsztein, D. C. (2002).** Lessons from animal models of Huntington's disease. *Trends Genet* **18**, 202-209.
- Rubinsztein, D. C. & Carmichael, J. (2003).** Huntington's disease: molecular basis of neurodegeneration. *Expert Rev Mol Med* **5**, 1-21.
- Rubinsztein, D. C., Codogno, P. & Levine, B. (2012).** Autophagy modulation as a potential therapeutic target for diverse diseases. *Nat Rev Drug Discov* **11**, 709-730.
- Rue, L., Lopez-Soop, G., Gelpi, E., Martinez-Vicente, M., Alberch, J. & Perez-Navarro, E. (2013).** Brain region- and age-dependent dysregulation of p62 and NBR1 in a mouse model of Huntington's disease. *Neurobiol Dis* **52**, 219-228.
- Rui, Y.-N., Xu, Z., Patel, B., Chen, Z., Chen, D. & Tito, A. (2015a).** Huntingtin functions as a scaffold for selective macroautophagy. *Nat Cell Biol* **17**.
- Rui, Y. N., Xu, Z., Patel, B., Cuervo, A. M. & Zhang, S. (2015b).** HTT/Huntingtin in selective autophagy and Huntington disease: A foe or a friend within? *Autophagy* **11**, 858-860.
- Russo, R., Berliocchi, L., Adornetto, A. & other authors (2011).** Calpain-mediated cleavage of Beclin-1 and autophagy deregulation following retinal ischemic injury in vivo. *Cell death & disease* **2**, e144.
- Sabatini, D. M. (2006).** mTOR and cancer: insights into a complex relationship. *Nature Reviews Cancer* **6**, 729-734.
- Saliba, S. W., Vieira, E. L. M., de Melo Santos, R. P., Candelario-Jalil, E., Fiebich, B. L., Vieira, L. B., Teixeira, A. L. & de Oliveira, A. C. P. (2017).** Neuroprotective effects of intrastriatal injection of rapamycin in a mouse model of excitotoxicity induced by quinolinic acid. *Journal of neuroinflammation* **14**, 25.
- Sapp, E., Schwarz, C., Chase, K., Bhide, P. G., Young, A. B., Penney, J., Vonsattel, J. P., Aronin, N. & DiFiglia, M. (1997).** Huntingtin localization in brains of normal and Huntington's disease patients. *Annals of Neurology* **42**, 604-612.
- Sarkar, S., Davies, J. E., Huang, Z., Tunnacliffe, A. & Rubinsztein, D. C. (2007).** Trehalose, a novel mTOR-independent autophagy enhancer, accelerates the clearance of mutant huntingtin and α -synuclein. *J Biol Chem* **282**, 5641-5652.
- Sarkar, S. & Rubinsztein, D. C. (2008a).** Small molecule enhancers of autophagy for neurodegenerative diseases. *Molecular BioSystems* **4**, 895-901.

- Sarkar, S. & Rubinsztein, D. C. (2008b).** Huntington's disease: degradation of mutant huntingtin by autophagy. *FEBS Journal* **275**, 4263-4270.
- Sarkar, S., Ravikumar, B., Floto, R. A. & Rubinsztein, D. C. (2009).** Rapamycin and mTOR-independent autophagy inducers ameliorate toxicity of polyglutamine-expanded huntingtin and related proteinopathies. *Cell Death Differ* **16**, 46-56.
- Sathasivam, K., Neueder, A., Gipson, T. A. & other authors (2013).** Aberrant splicing of HTT generates the pathogenic exon 1 protein in Huntington disease. *Proceedings of the National Academy of Sciences* **110**, 2366-2370.
- Saucedo, L. J. & Edgar, B. A. (2002).** Why size matters: altering cell size. *Current Opinion in Genetics & Development* **12**, 565-571.
- Saudou, F., Finkbeiner, S., Devys, D. & Greenberg, M. E. (1998).** Huntingtin Acts in the Nucleus to Induce Apoptosis but Death Does Not Correlate with the Formation of Intranuclear Inclusions. *Cell* **95**, 55-66.
- Saudou, F. & Humbert, S. (2016).** The Biology of Huntingtin. *Neuron* **89**, 910-926.
- Sekiguchi, A., Kanno, H., Ozawa, H., Yamaya, S. & Itoi, E. (2012).** Rapamycin promotes autophagy and reduces neural tissue damage and locomotor impairment after spinal cord injury in mice. *Journal of neurotrauma* **29**, 946-956.
- Seong, I. S., Ivanova, E., Lee, J. M. & other authors (2005).** HD CAG repeat implicates a dominant property of huntingtin in mitochondrial energy metabolism. *Hum Mol Genet* **14**, 2871-2880.
- Sharma, R., Kumar, D., Jha, N. K., Jha, S. K., Ambasta, R. K. & Kumar, P. (2017).** Re-expression of cell cycle markers in aged neurons and muscles: Whether cells should divide or die? *Biochimica et Biophysica Acta (BBA) - Molecular Basis of Disease* **1863**, 324-336.
- Shibata, M., Lu, T., Furuya, T., Degterev, A., Mizushima, N., Yoshimori, T., MacDonald, M., Yankner, B. & Yuan, J. (2006).** Regulation of Intracellular Accumulation of Mutant Huntingtin by Beclin 1. *Journal of Biological Chemistry* **281**, 14474-14485.
- Simões, A. T., Gonçalves, N., Koeppen, A., Déglon, N., Kügler, S., Duarte, C. B. & Pereira de Almeida, L. (2012).** Calpastatin-mediated inhibition of calpains in the mouse brain prevents mutant ataxin 3 proteolysis, nuclear localization and aggregation, relieving Machado–Joseph disease. *Brain* **135**, 2428-2439.
- Singer, E., Walter, C., Weber, J. J., Krahl, A.-C., Mau-Holzmann, U. A., Rischert, N., Riess, O., Clemensson, L. E. & Nguyen, H. P. (2017).** Reduced cell size, chromosomal aberration and altered proliferation rates are characteristics and confounding factors in the STHdh cell model of Huntington disease. *Scientific Reports* **7**, 16880.
- Singer, E., Walter, C., Fabbro, D. & other authors (2019).** Brain-penetrant PQR620 mTOR and PQR530 PI3K/mTOR inhibitor reduce huntingtin levels in cell models of HD. *Neuropharmacology*, 107812.
- Singer, E., Bambynek-Dziuk, P., Yu-Taeger, L., Fabbro, D., Rageot, D., Beaufils, F., Riess, O., Hillmann, P. & Nguyen, H. P. (2020).** PQR530 and PQR620 reduce aggregation in the R6/2 mouse model but fail to ameliorate behavioral phenotype. *unpublished manuscript*.
- Sittler, A., Muriel, M. P., Marinello, M., Brice, A., den Dunnen, W. & Alves, S. (2018).** Deregulation of autophagy in postmortem brains of Machado - Joseph disease patients. *Neuropathology* **38**, 113-124.
- Slow, E. J., van Raamsdonk, J., Rogers, D. & other authors (2003).** Selective striatal neuronal loss in a YAC128 mouse model of Huntington disease. *Human Molecular Genetics* **12**, 1555-1567.
- Šmatlíková, P. (2019).** Gradual Molecular Changes in Primary Porcine Cells Expressing Mutated Huntingtin.
- Soefje, S. A., Karnad, A. & Brenner, A. J. (2011).** Common toxicities of mammalian target of rapamycin inhibitors. *Targeted Oncology* **6**, 125-129.
- Spano, D., Branchi, I., Rosica, A. & other authors (2004).** Rhes is involved in striatal function. *Molecular and cellular biology* **24**, 5788-5796.
- Spilman, P., Podlitskaya, N., Hart, M. J., Debnath, J., Gorostiza, O., Bredesen, D., Richardson, A., Strong, R. & Galvan, V. (2010).** Inhibition of mTOR by rapamycin abolishes cognitive deficits and reduces amyloid- β levels in a mouse model of Alzheimer's disease. *PLoS one* **5**, e9979.
- Squitieri, F., Gellera, C., Cannella, M. & other authors (2003).** Homozygosity for CAG mutation in Huntington disease is associated with a more severe clinical course. *Brain* **126**, 946-955.


- Steffan, J. S., Kazantsev, A., Spasic-Boskovic, O. & other authors (2000).** The Huntington's disease protein interacts with p53 and CREB-binding protein and represses transcription. *Proceedings of the National Academy of Sciences* **97**, 6763-6768.
- Steffan, J. S. (2010).** Does Huntingtin play a role in selective macroautophagy? *Cell Cycle* **9**, 3401-3413.
- Stekovic, S., Hofer, S. J., Tripolt, N. & other authors (2019).** Alternate Day Fasting Improves Physiological and Molecular Markers of Aging in Healthy, Non-obese Humans. *Cell Metabolism* **30**, 462-476.e465.
- Stine, O. C., Pleasant, N., Franz, M. L., Abbott, M. H., Folstein, S. E. & Ross, C. A. (1993).** Correlation between the onset age of Huntington's disease and length of the trinucleotide repeat in IT-15. *Hum Mol Genet* **2**, 1547-1549.
- Stolz, A., Ernst, A. & Dikic, I. (2014).** Cargo recognition and trafficking in selective autophagy. *Nature cell biology* **16**, 495.
- Subramaniam, S., Sixt, K. M., Barrow, R. & Snyder, S. H. (2009).** Rhes, a striatal specific protein, mediates mutant-huntingtin cytotoxicity. *Science* **324**, 1327-1330.
- Sugars, K. L. & Rubinsztein, D. C.** Transcriptional abnormalities in Huntington disease. *Trends in Genetics* **19**, 233-238.
- Swiech, L., Perycz, M., Malik, A. & Jaworski, J. (2008).** Role of mTOR in physiology and pathology of the nervous system. *Biochim Biophys Acta* **1784**, 116-132.
- Tabrizi, S. J., Langbehn, D. R., Leavitt, B. R. & other authors (2009).** Biological and clinical manifestations of Huntington's disease in the longitudinal TRACK-HD study: cross-sectional analysis of baseline data. *The Lancet Neurology* **8**, 791-801.
- Tabrizi, S. J., Leavitt, B. R., Landwehrmeyer, G. B. & other authors (2019a).** Targeting Huntingtin expression in patients with Huntington's Disease. *New England Journal of Medicine*.
- Tabrizi, S. J., Leavitt, B. R., Landwehrmeyer, G. B. & other authors (2019b).** Targeting Huntingtin Expression in Patients with Huntington's Disease. *New England Journal of Medicine* **380**, 2307-2316.
- Tanaka, M., Machida, Y., Niu, S., Ikeda, T., Jana, N. R., Doi, H., Kurosawa, M., Nekooki, M. & Nukina, N. (2004).** Trehalose alleviates polyglutamine-mediated pathology in a mouse model of Huntington disease. *Nature Medicine* **10**, 148-154.
- Tartari, M., Gissi, C., Lo Sardo, V., Zuccato, C., Picardi, E., Pesole, G. & Cattaneo, E. (2007).** Phylogenetic comparison of huntingtin homologues reveals the appearance of a primitive polyQ in sea urchin. *Molecular biology and evolution* **25**, 330-338.
- Taufiqul Islam, A. M., Kwak, J., Jung, Y. & Kee, Y. (2014).** Animal models of amyotrophic lateral sclerosis and Huntington's disease. *Genes & Genomics* **36**, 399-413.
- Taylor, J. P., Hardy, J. & Fischbeck, K. H. (2002).** Toxic Proteins in Neurodegenerative Disease. *Science* **296**, 1991-1995.
- Tellez-Nagel, I., Johnson, A. B. & Terry, R. D. (1974).** Studies on brain biopsies of patients with Huntington's chorea. *Journal of neuropathology and experimental neurology* **33**.
- Tellone, E., Galtieri, A., Russo, A., Giardina, B. & Ficarra, S. (2015).** Resveratrol: A Focus on Several Neurodegenerative Diseases. *Oxidative Medicine and Cellular Longevity* **2015**, 14.
- The Huntington's Disease Collaborative Research Group (1993).** A novel gene containing a trinucleotide repeat that is expanded and unstable on Huntington's disease chromosomes. The Huntington's Disease Collaborative Research Group. *Cell* **72**, 971-983.
- Thoreen, C. C., Kang, S. A., Chang, J. W. & other authors (2009).** An ATP-competitive Mammalian Target of Rapamycin Inhibitor Reveals Rapamycin-resistant Functions of mTORC1. *Journal of Biological Chemistry* **284**, 8023-8032.
- Tian, T., Li, X. & Zhang, J. (2019).** mTOR Signaling in Cancer and mTOR Inhibitors in Solid Tumor Targeting Therapy. *International Journal of Molecular Sciences* **20**, 755.
- Underwood, B. R., Green-Thompson, Z. W., Pugh, P. J. & other authors (2017).** An open-label study to assess the feasibility and tolerability of rilmenidine for the treatment of Huntington's disease. *J Neurol* **264**, 2457-2463.
- United Nations (2018).** World Population Ageing 2017 Highlights.

- van Dellen, A., Cordery, P. M., Spires, T. L., Blakemore, C. & Hannan, A. J. (2008). Wheel running from a juvenile age delays onset of specific motor deficits but does not alter protein aggregate density in a mouse model of Huntington's disease. *BMC Neuroscience* **9**, 34.
- van der Burg, J. M., Björkqvist, M. & Brundin, P. (2009). Beyond the brain: widespread pathology in Huntington's disease. *The Lancet Neurology* **8**, 765-774.
- Vázquez-Manrique, R. P., Farina, F., Cambon, K., Dolores Sequedo, M., Parker, A. J., Millán, J. M., Weiss, A., Déglon, N. & Neri, C. (2015). AMPK activation protects from neuronal dysfunction and vulnerability across nematode, cellular and mouse models of Huntington's disease. *Human Molecular Genetics* **25**, 1043-1058.
- Vidoni, C., Secomandi, E., Castiglioni, A., Melone, M. A. B. & Isidoro, C. (2018). Resveratrol protects neuronal-like cells expressing mutant Huntingtin from dopamine toxicity by rescuing ATG4-mediated autophagosome formation. *Neurochem Int* **117**, 174-187.
- Vonsattel, J. P. & DiFiglia, M. (1998). Huntington disease. *Journal of neuropathology and experimental neurology* **57**, 369-384.
- Vonsattel, J. P. G., Keller, C. & Pilar Amaya, M. d. (2008). Neuropathology of Huntington's Disease. *Handbook of Clinical Neurology* **89**, 599-618.
- Walker, F. O. (2007). Huntington's disease. *Lancet* **369**, 218-228.
- Walter, C., Clemens, L. E., Muller, A. J., Fallier-Becker, P., Proikas-Cezanne, T., Riess, O., Metzger, S. & Nguyen, H. P. (2016). Activation of AMPK-induced autophagy ameliorates Huntington disease pathology in vitro. *Neuropharmacology* **108**, 24-38.
- Wander, S. A., Hennessy, B. T. & Slingerland, J. M. (2011). Next-generation mTOR inhibitors in clinical oncology: how pathway complexity informs therapeutic strategy. *The Journal of clinical investigation* **121**, 1231-1241.
- Wang, X. & Proud, C. G. (2006). The mTOR Pathway in the Control of Protein Synthesis. *Physiology* **21**, 362-369.
- Weber, J. J., Pereira Sena, P., Singer, E. & Nguyen, H. P. (2019). Killing Two Angry Birds with One Stone: Autophagy Activation by Inhibiting Calpains in Neurodegenerative Diseases and Beyond. *BioMed research international* **2019**.
- Weiss, A., Träger, U., Wild, E. J. & other authors (2012). Mutant huntingtin fragmentation in immune cells tracks Huntington's disease progression. *The Journal of clinical investigation* **122**, 3731-3736.
- Wheeler, V. C., Auerbach, W., White, J. K. & other authors (1999). Length-dependent gametic CAG repeat instability in the Huntington's disease knock-in mouse. *Human molecular genetics* **8**, 115-122.
- Wild, E. J. & Tabrizi, S. J. (2014). Targets for future clinical trials in Huntington's disease: What's in the pipeline? *Movement Disorders* **29**, 1434-1445.
- Wild, E. J. & Tabrizi, S. J. (2017). Therapies targeting DNA and RNA in Huntington's disease. *The Lancet Neurology* **16**, 837-847.
- Wong, E. & Cuervo, A. M. (2010). Autophagy gone awry in neurodegenerative diseases. *Nature Neurosci* **13**, 805-811.
- Wong, M. (2013). Mammalian target of rapamycin (mTOR) pathways in neurological diseases. *Biomed J* **36**, 40-50.
- Wood, N. I., Glynn, D. & Morton, A. J. (2011). "Brain training" improves cognitive performance and survival in a transgenic mouse model of Huntington's disease. *Neurobiology of Disease* **42**, 427-437.
- Wu, J.-c., Qi, L., Wang, Y., Kegel, K. B., Yoder, J., DiFiglia, M., Qin, Z.-h. & Lin, F. (2012). The regulation of N-terminal Huntingtin (Htt552) accumulation by Beclin1. *Acta Pharmacologica Sinica* **33**, 743-751.
- Wytenbach, A., Swartz, J., Kita, H. & other authors (2001). Polyglutamine expansions cause decreased CRE-mediated transcription and early gene expression changes prior to cell death in an inducible cell model of Huntington's disease. *Human Molecular Genetics* **10**, 1829-1845.
- Yang, X. W. & Yamamoto, A. (2014). CLEARance wars: PolyQ strikes back. *Nature neuroscience* **17**, 1140.
- Yoshii, S. R. & Mizushima, N. (2017). Monitoring and Measuring Autophagy. *International Journal of Molecular Sciences* **18**, 1865.

- Yousefi, S., Perozzo, R., Schmid, I., Ziemecki, A., Schaffner, T., Scapozza, L., Brunner, T. & Simon, H.-U. (2006).** Calpain-mediated cleavage of Atg5 switches autophagy to apoptosis. *Nature cell biology* **8**, 1124.
- Yu-Taeger, L., Petrasch-Parwez, E., Osmand, A. P. & other authors (2012).** A novel BACHD transgenic rat exhibits characteristic neuropathological features of Huntington disease. *Journal of Neuroscience* **32**, 15426-15438.
- Yu-Taeger, L., Stricker-Shaver, J., Arnold, K. & other authors (2019).** Intranasal Administration of Mesenchymal Stem Cells Ameliorates the Abnormal Dopamine Transmission System and Inflammatory Reaction in the R6/2 Mouse Model of Huntington Disease. *Cells* **8**, 595.
- Zeitlin, S., Liu, J. P., Chapman, D. L., Papaioannou, V. E. & Efstratiadis, A. (1995).** Increased apoptosis and early embryonic lethality in mice nullizygous for the Huntington's disease gene homologue. *Nat Genet* **11**, 155-163.
- Zheng, S., Clabough, E. B. D., Sarkar, S., Futter, M., Rubinsztein, D. C. & Zeitlin, S. O. (2010).** Deletion of the Huntingtin Polyglutamine Stretch Enhances Neuronal Autophagy and Longevity in Mice. *PLoS Genet* **6**, e1000838.
- Zhou, G., Myers, R., Li, Y. & other authors (2001).** Role of AMP-activated protein kinase in mechanism of metformin action. *The Journal of clinical investigation* **108**, 1167-1174.
- Zielonka, D., Piotrowska, I., Marcinkowski, J. T. & Mielcarek, M. (2014).** Skeletal muscle pathology in Huntington's disease. *Frontiers in Physiology* **5**, 380.
- Zou, J., Zhou, L., Du, X.-X. & other authors (2011).** Rheb1 Is Required for mTORC1 and Myelination in Postnatal Brain Development. *Developmental Cell* **20**, 97-108.
- Zu, T., Gibbens, B., Doty, N. S. & other authors (2011).** Non-ATG-initiated translation directed by microsatellite expansions. *Proceedings of the National Academy of Sciences* **108**, 260-265.
- Zuccato, C., Valenza, M. & Cattaneo, E. (2010).** Molecular Mechanisms and Potential Therapeutical Targets in Huntington's Disease. *Physiological Reviews* **90**, 905.
-


APPENDIX: PUBLICATION #1 - #6

SCIENTIFIC REPORTS



OPEN

Reduced cell size, chromosomal aberration and altered proliferation rates are characteristics and confounding factors in the *STHdh* cell model of Huntington disease

Elisabeth Singer^{1,2}, Carolin Walter^{1,2}, Jonasz J. Weber^{1,2}, Ann-Christin Krahl³, Ulrike A. Mau-Holzmann¹, Nadine Rischert^{1,2}, Olaf Riess^{1,2}, Laura E. Clemensson^{1,2} & Huu P. Nguyen ^{1,2}

Huntington disease is a fatal neurodegenerative disorder caused by a CAG repeat expansion in the gene encoding the huntingtin protein. Expression of the mutant protein disrupts various intracellular pathways and impairs overall cell function. In particular striatal neurons seem to be most vulnerable to mutant huntingtin-related changes. A well-known and commonly used model to study molecular aspects of Huntington disease are the striatum-derived *STHdh* cell lines generated from wild type and *huntingtin* knock-in mouse embryos. However, obvious morphological differences between wild type and mutant cell lines exist, which have rarely been described and might not have always been considered when designing experiments or interpreting results. Here, we demonstrate that *STHdh* cell lines display differences in cell size, proliferation rate and chromosomal content. While the chromosomal divergence is considered to be a result of the cells' tumour characteristics, differences in size and proliferation, however, were confirmed in a second non-immortalized Huntington disease cell model. Importantly, our results further suggest that the reported phenotypes can confound other study outcomes and lead to false conclusions. Thus, careful experimental design and data analysis are advised when using these cell models.

Huntington disease (HD) is an inherited, fatal, neurodegenerative disorder. It results from a CAG repeat expansion in the gene *HTT*, coding for the huntingtin protein. The mutation is translated into an elongated polyglutamine repeat in huntingtin, which leads to the disruption of various cellular signalling pathways and results in impaired cell function and ultimately cell death, particularly of striatal neurons^{1,2}. To study cellular and molecular mechanisms contributing to the HD pathogenesis, numerous cell and animal models have been generated. The *STHdh* cell lines were generated from an HD knock-in mouse model³, which carries the endogenous *Hdh* gene (mouse Huntington disease gene homolog) with a chimeric exon 1⁴ and is characterized by a mild behavioural phenotype and neuropathological features⁵. These cell lines derive from striatal primordia³ and express wild-type and mutant huntingtin at endogenous levels⁶. The precise genetic context and the striatal origin of the cells make the *STHdh* cell lines a widely used model in HD research. By comparing immortalized striatal precursor cells from wild type mice (*STHdh*^{Q7/Q7} cells) to precursor cells derived from heterozygous and homozygous *Hdh*^{Q111} knock-in mice (*STHdh*^{Q7/Q111} and *STHdh*^{Q111/Q111} cells), differences in a variety of HD-related cellular pathways have been discovered or confirmed, for instance an involvement of huntingtin in calcium handling deficits and mitochondrial dysfunction^{7–11} or effects on various signalling cascades^{12–14}. Despite the to date unquestioned usefulness and importance of this model, obvious but rarely reported differences in size¹¹, shape¹⁵ and proliferation

¹Institute of Medical Genetics and Applied Genomics, University of Tuebingen, 72076, Tuebingen, Germany. ²Centre for Rare Diseases, University of Tuebingen, 72076, Tuebingen, Germany. ³Paediatric Haematology and Oncology, University Children's Hospital Tuebingen, 72076, Tuebingen, Germany. Elisabeth Singer, Carolin Walter, Jonasz J. Weber, Laura E. Clemensson and Huu P. Nguyen contributed equally to this work. Correspondence and requests for materials should be addressed to H.P.N. (email: hoa.nguyen@med.uni-tuebingen.de)

rate might demand caution when using the *STHdh* cell lines. The origin of these differences, their importance for HD, as well as the consequences for the interpretation of study outcomes remains largely unaddressed.

In this study, we show that the *STHdh* cell lines exhibit divergent characteristics, which interfere with commonly used assays and hamper the direct comparison of both cell lines. We further show that these features are partially shared by mouse embryonic fibroblast (*MEFHdh*) cell lines generated from the same animal model and their wild type littermates, which implies a common, HD-related mechanism beyond immortalization artefacts. Overall, these findings argue for a thorough characterization of every cell line used and the inclusion of such confounding factors in the experimental design.

Results

Reduced cell size is a characteristic of *STHdh*^{Q111/Q111} and *MEFHdh*^{Q111/Q111} cells. We performed a morphometric analysis of homozygous *STHdh*^{Q111/Q111} (STQ111) and wild type *STHdh*^{Q7/Q7} (STQ7) cells by light microscopy and flow cytometry analysis. Measurement of the surface area of cells attached to the culture dish revealed a significantly smaller cell surface area in the mutant *STHdh* cells (Fig. 1a and b; $P < 0.001$). The smaller cell size of *STHdh*^{Q111/Q111} was also found in detached cells, both when measuring the surface area from microscopic images (Supplementary Fig. S1) and on a larger scale by flow cytometry analysis (Fig. 1c and d). Here, the relative mean forward-scatter area (FSC-A), which is positively related to cell size, was 32% lower in *STHdh*^{Q111/Q111} than in *STHdh*^{Q7/Q7} cells (Fig. 1d; $P = 0.013$). Similar differences were also observed after differentiation into neuron-like cells (Supplementary Fig. S2).

To assess whether this cell size phenotype is cell line-specific or whether it might be considered a general feature of HD, we performed the same set of experiments in a fibroblast cell line established from the same mouse model (*MEFHdh* cells). Like in the *STHdh* cells, the mutant *MEFHdh*^{Q111/Q111} (*MEFQ111*) cells had a smaller cell surface area compared to the wild type *MEFHdh*^{Q7/Q7} (*MEFQ7*) cells, when the cells were attached to the culture dish (Fig. 1f; $P = 0.03$). Although the difference did not reach statistical significance when manually analysing cell surface area in detached cells (Supplementary Fig. S1; $P = 0.13$), it was detected again via flow cytometry analysis (Fig. 1g and h; $P = 0.002$). The relative mean FSC-A of *MEFHdh*^{Q111/Q111} cells was 31% lower compared to *MEFHdh*^{Q7/Q7} cells, comparable to the values retrieved for *STHdh* cells (Fig. 1h). Flow cytometry analysis further revealed a higher heterogeneity of the *MEFHdh* cell population compared to *STHdh* cells, as represented by a broader distribution of cell sizes and two distinct peaks in the FSC-A plot (Fig. 1g), possibly due to the biological origin of these cell lines¹⁶.

***STHdh* but not *MEFHdh* cells show considerable chromosome abnormalities.** As changes in DNA content can lead to alterations in cell size^{17,18} and are a common feature of cell line stabilization¹⁹ and cell passaging^{20,21}, we performed a karyotype analysis to clarify whether the cell size differences observed in both cell lines are explained by changes in ploidy.

Karyotyping revealed a variety of chromosomal abnormalities in *STHdh* cells. Even more importantly, the chromosomal changes differed between *STHdh*^{Q111/Q111} and *STHdh*^{Q7/Q7} cells in qualitative and quantitative terms (Fig. 2a and b). In detail, *STHdh*^{Q7/Q7} cells showed a hyperpentaploid, female, murine karyotype with chromosome numbers between 104 and 115. Different numerical anomalies as well as a variable number of additional, structurally abnormal chromosomes (three to eight marker chromosomes) were detected. About 40% of the cells showed at least one, but up to four additional copies of chromosome 3, 8, 9, 10, 14, 16 and 17. Interestingly, nearly 100% of the analysed cells showed two to six additional copies of chromosome 15, 18 and 19. Loss of at least one, but up to four copies was found for chromosome 4, 6, 7, 11, 12 and 13 in 40% of the cells. In contrast, *STHdh*^{Q111/Q111} cells showed a hypo- to hypertetraploid, female, murine karyotype (77–82 chromosomes) with a high number (seven to nine) of marker chromosomes. Loss of one to four copies was found for chromosome 1, 4, 6, 7, 12, 14 and 18 - similar to *STHdh*^{Q7/Q7} cells. Nearly all cells had one to three additional copies of chromosome 15 and 19. The total number of chromosomes was significantly lower in *STHdh*^{Q111/Q111} cells compared to *STHdh*^{Q7/Q7} cells (Fig. 2c; $P < 0.001$).

In contrast, *MEFHdh* cells did not show marked chromosomal abnormalities (Fig. 2d and e). In detail, *MEFHdh*^{Q7/Q7} cells showed a mainly diploid, murine, male karyotype with only some tetraploid cells (Fig. 2d). Apart from a small number of single cell anomalies, no chromosomal losses were detected. A few cells showed additional copies of chromosome 16 and 17. *MEFHdh*^{Q111/Q111} cells showed a mainly diploid, female, murine karyotype and only a few tetraploid cells (Fig. 2e). Nearly all cells showed a numerically normal karyotype. About 50% of the cells were found to have an additional chromosome 17. The total number of chromosomes did not differ between *MEFHdh*^{Q111/Q111} and *MEFHdh*^{Q7/Q7} cells (Fig. 2f).

***STHdh*^{Q111/Q111} and *MEFHdh*^{Q111/Q111} cells show a higher proliferation rate.** We further examined the proliferation rate of *STHdh* and *MEFHdh* cells, as both mutant cell lines appeared to proliferate at different rates during regular passaging.

Quantification of the increase in cell number after 3 days of cultivation revealed an elevated proliferation rate of *STHdh*^{Q111/Q111} compared to *STHdh*^{Q7/Q7} cells (Fig. 3a, $P = 0.02$). A trend towards increased proliferation rate was detected in *MEFHdh*^{Q111/Q111} compared to *MEFHdh*^{Q7/Q7} cells after 7 days of cultivation (Fig. 3b; $P = 0.073$), although both *MEFHdh* cell lines did not proliferate as much as *STHdh* cells.

In order to clarify whether the enhanced proliferation had been the result of increased cell division or reduced cell death, we performed a cell cycle analysis and measured the amount of viable and apoptotic cells.

First, the proportion of cells in the different phases of the cell cycle was analysed by measuring the DNA content via DAPI staining intensity in detached, fixed cells. This assay confirmed the difference in ploidy between *STHdh*^{Q7/Q7} and *STHdh*^{Q111/Q111} cells, as there was a noticeable right shift in the curve obtained for *STHdh*^{Q7/Q7}

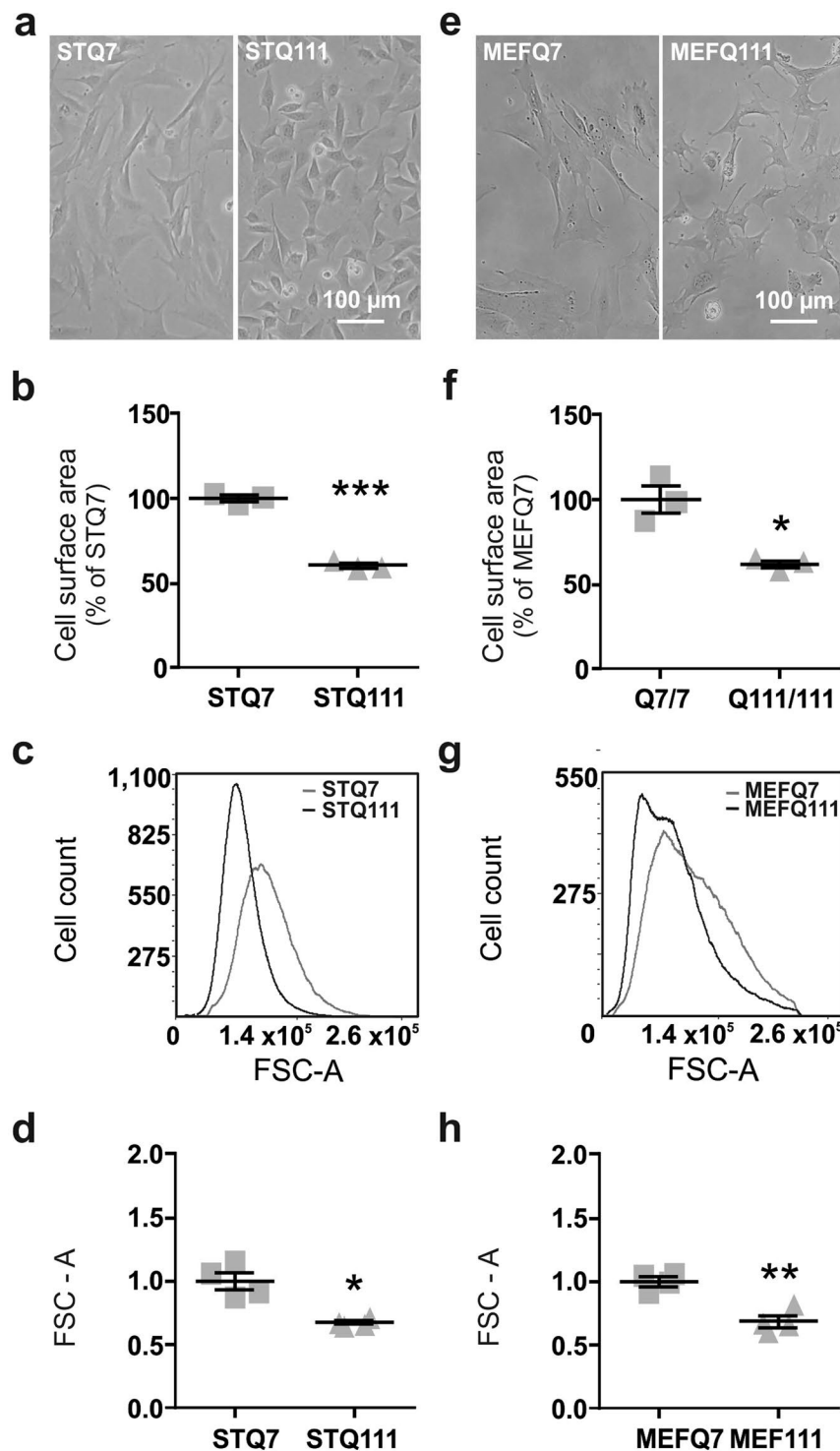


Figure 1. Cell size difference in Q111 knock-in cells. (a) Representative pictures of *STHdh*^{Q7/Q7} (STQ7) and *STHdh*^{Q111/Q111} (STQ111) cells, and (b) ImageJ-based surface area quantification of *STHdh* cells attached to the culture dish surface n = 3 experiments, unpaired *t*-tests; ****P* < 0.001. (c) Representative histograms of *STHdh* cells and (d) quantification of the cell size of live cells in suspension, based on the relative mean forward scatter area (FSC-A); n = 4 experiments, unpaired *t*-tests; **P* < 0.05. (e–h) Results of size determination for *MEFHdh*^{Q7/Q7} (MEFQ7) and *MEFHdh*^{Q111/Q111} (MEFQ111) cells, respectively; **P* < 0.05, ***P* < 0.01.

cells, corresponding to an overall increased DNA content (Fig. 3c). This shift, however, made the automated analysis by the analysis software unreliable, and was therefore not quantified. *MEFHdh* cells, on the other hand and in line with their similar karyograms, exhibited similar distribution patterns of cell populations with different DNA

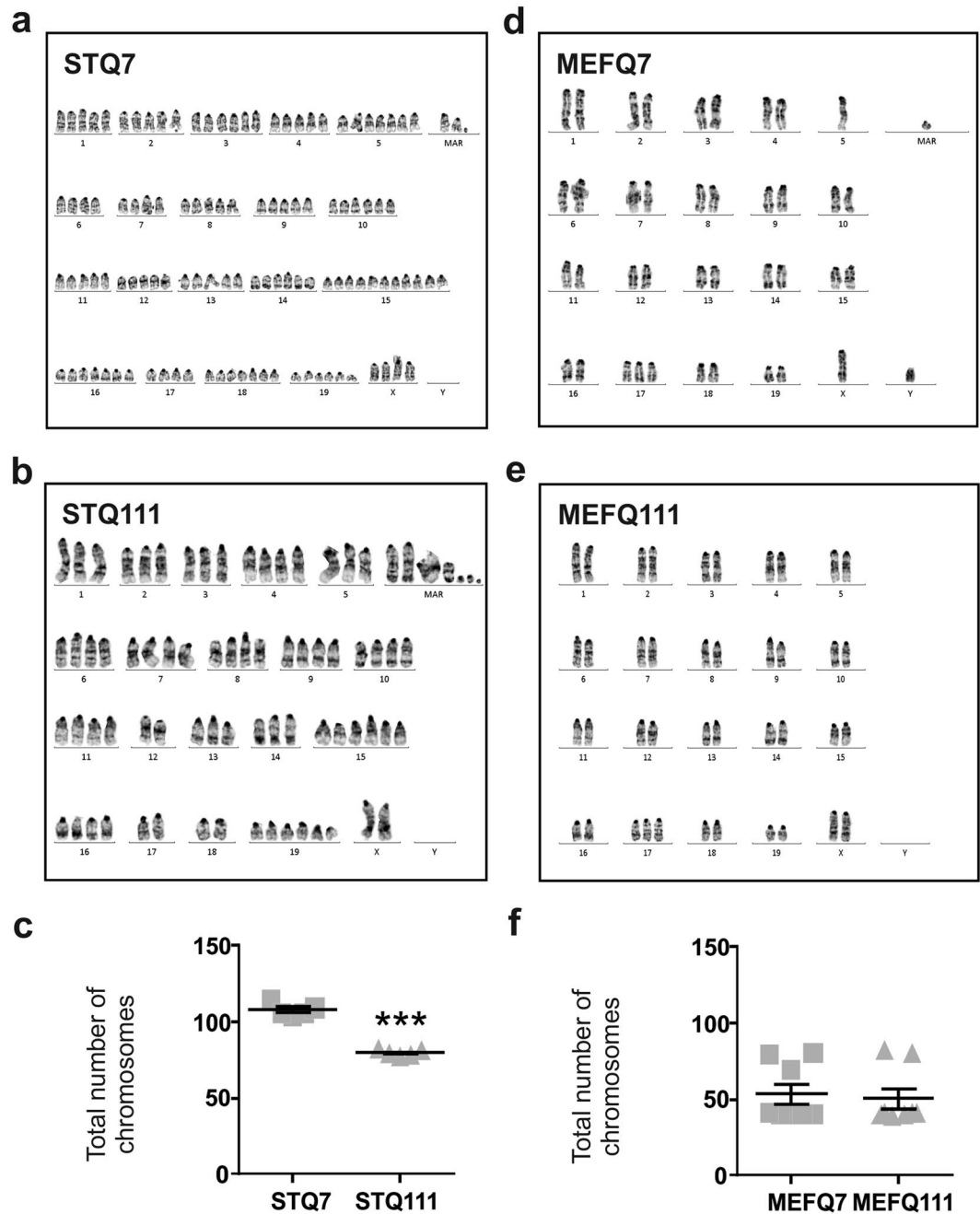


Figure 2. *STHdh* cells display marked and divergent chromosome abnormalities. (a) Representative karyograms from *STHdh*^{Q7/Q7} (STQ7) and (b) *STHdh*^{Q111/Q111} (STQ111) cells with (c) quantification of the chromosome numbers; n = 5 experiments, unpaired *t*-tests; ****P* < 0.001. (d–f) Result of karyogram analysis for *MEFHdh*^{Q7/Q7} (MEFQ7) and *MEFHdh*^{Q111/Q111} (MEFQ111) cells, respectively; n = 8 experiments.

content (Fig. 3d). In this case, the analysis showed a significant decrease in cells in the G₀/G₁ phase (*MEFHdh*^{Q7/Q7} 65.73 ± 2; *MEFHdh*^{Q111/Q111} 39.17 ± 1; *P* = 0.0003), alongside a tendency to an increase in cells in the S (*MEFHdh*^{Q7/Q7} 4.1 ± 2; *MEFHdh*^{Q111/Q111} 8.2 ± 0.2; *P* = 0.07) and G₂/M phase (*MEFHdh*^{Q7/Q7} 22.9 ± 4; *MEFHdh*^{Q111/Q111} 38.1 ± 0.2; *P* = 0.03). The observed differences in cell cycle progression were in line with the observation that *MEFHdh* cells containing the *huntingtin* knock-in mutation proliferate more than wild type cells.

Second, we analysed the amount of viable and apoptotic cells by flow cytometry analysis (Fig. 4). We found *STHdh*^{Q111/Q111} cells to have a higher proportion of viable cells (Fig. 4b, *P* = 0.047), and in turn a lower proportion of apoptotic cells compared to *STHdh*^{Q7/Q7} cells, although the latter did not reach statistical significance. Similar results were obtained for *MEFHdh* cells, showing a significantly higher proportion of viable cells (Fig. 4e; *P* = 0.026) and, in this case, a significantly lower number of apoptotic cells (Fig. 4f; *P* = 0.017) in *MEFHdh*^{Q111/Q111} cells compared to their wild type control.

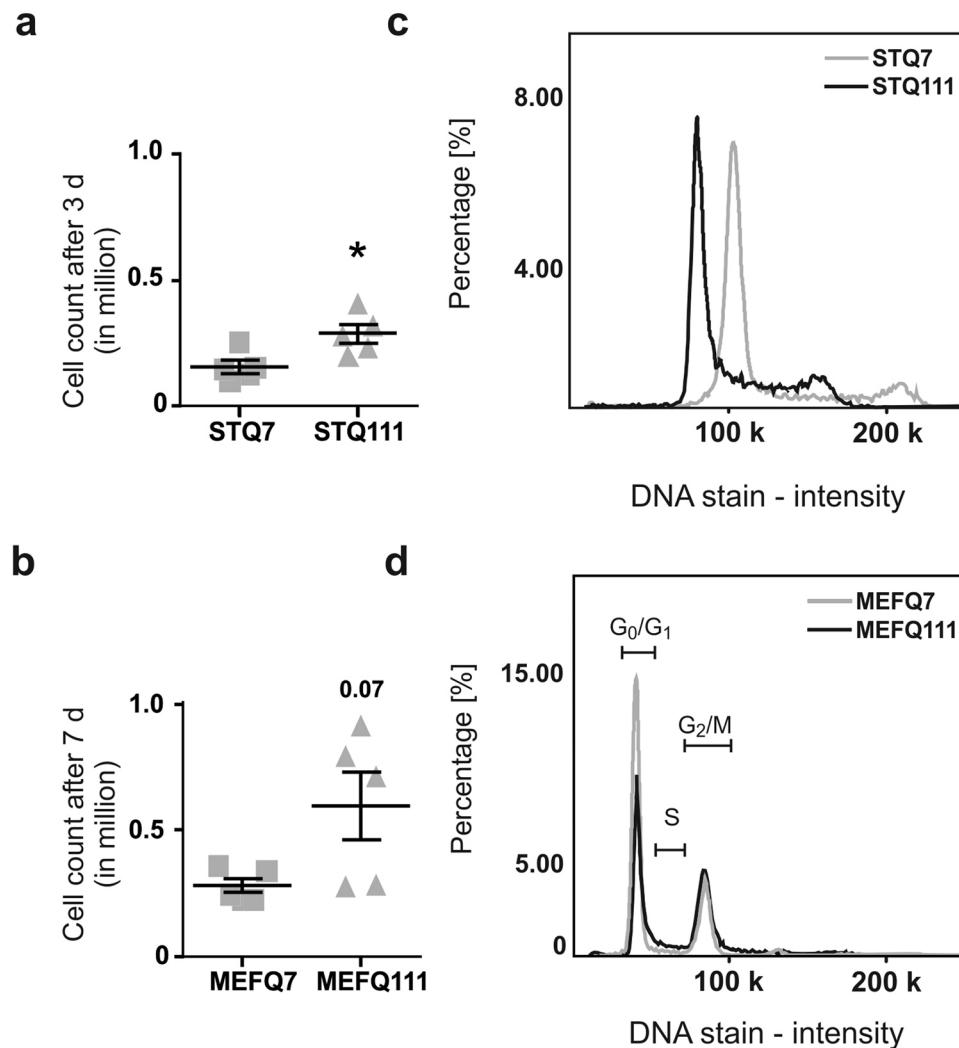


Figure 3. Both mutant cell lines exhibit increased proliferation rates. (a) Manually determined cell count of *STHdh* cells after 3 days; $n = 5$ experiments, unpaired t -tests; $*P < 0.05$ and (b) manually determined cell count of *MEFHdh* cells after 7 days; $n = 5$ experiments; unpaired t -tests. (c) Representative overlays of signal intensity of *STHdh*^{Q7/Q7} and *STHdh*^{Q111/Q111} DAPI-stained cells and (d) representative overlay of signal intensity of *MEFHdh*^{Q7/Q7} and *MEFHdh*^{Q111/Q111} DAPI-stained cells with exemplary indication of cell cycle; $n = 3$.

The cell size and proliferation phenotypes in *STHdh*^{Q111/Q111} cells might impede the interpretation of standard cell viability assays.

When investigating cell viability in our study, we used flow cytometry, a method that should theoretically be independent of cell size and cell proliferation. However, common cell viability tests depend considerably on these parameters. Thus, we reassessed cell viability and cell death using the standard cell viability assays, PrestoBlue[®] and LDH assay, respectively (Fig. 5).

Analysis of the data revealed contradicting results when compared to the outcomes from flow cytometry. The PrestoBlue[®] assay consistently showed lower signals in *STHdh*^{Q111/Q111} cells (Fig. 5a; $P = 0.031$) and the LDH assay revealed increased LDH release in *STHdh*^{Q111/Q111} compared to *STHdh*^{Q7/Q7} cells (Fig. 5b; $P = 0.022$), suggesting that mutant cells are characterized by reduced viability and increased cell death, in contrast to the first findings. Differentiation of *STHdh* cells led to a similar readout as flow cytometry (Supplementary Fig. S3).

The results obtained for *MEFHdh* cells differed from the results obtained for *STHdh* cells. *MEFHdh*^{Q111/Q111} cells had similar signals as *MEFHdh*^{Q7/Q7} cells in the PrestoBlue[®] assay (Fig. 5c; $P = 0.656$), but showed reduced LDH release (Fig. 5d; $P = 0.034$). These findings were comparable to the results obtained by flow cytometry.

Chromosomal abnormalities in *STHdh*^{Q111/Q111} cells might impede the interpretation of western blot analyses.

Since we observed that *STHdh*^{Q111/Q111} cells differ markedly from the control *STHdh*^{Q7/Q7} cell line in terms of chromosomal constitution, we investigated possible consequences of these alterations on the protein levels of commonly used loading controls for western blot analysis. The four proteins, β -actin (*Actb*, chromosome 5), GAPDH (*Gapdh*, chromosome 6), α -tubulin (*Tuba1a*, chromosome 15) and vinculin (*Vcl*, chromosome 14) are located on different chromosomes.

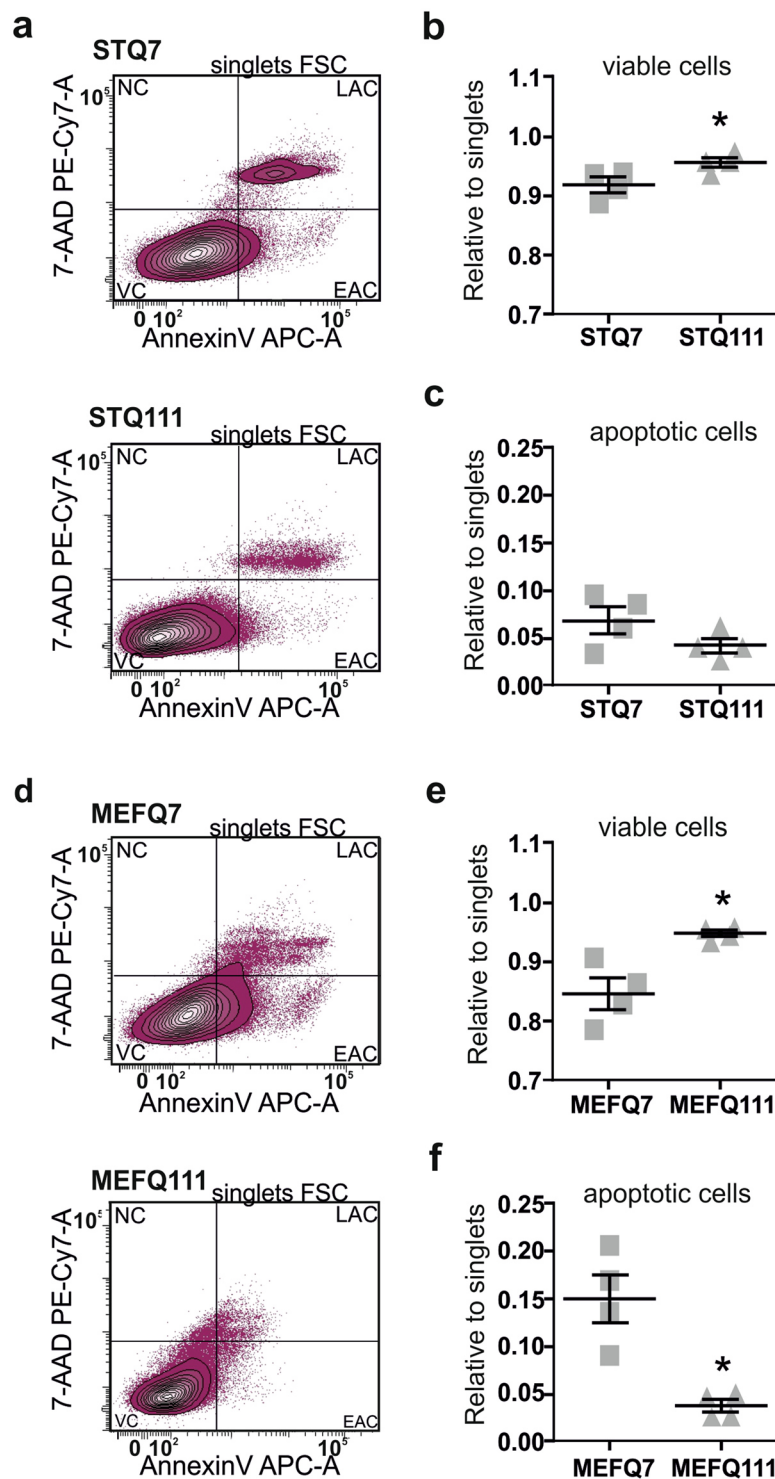


Figure 4. Cell viability is not reduced in *STHdh* and *MEFHdh* mutant cell lines. Results from cell size- and cell number-independent flow cytometry analysis: **(a)** Representative scatterplots of flow cytometry analysis of *STHdh* cells and **(b)** and **(c)** quantification from flow cytometry analysis of Annexin V/7'AAD staining; $n = 4$ experiments. VC: viable cells, EAC: early apoptotic cells, LAC: late apoptotic cells, NC: necrotic cells. Quantification of apoptotic cells combines results for EAC and LAC; unpaired t -tests; * $P < 0.05$. **(d–f)** Results of *MEFHdh* cells, respectively; unpaired t -tests; * $P < 0.05$.

Western blot analysis of RIPA cell lysates revealed strong trends toward decreased levels of α -tubulin and vinculin in *STHdh*^{Q111/Q111} cells compared to *STHdh*^{Q7/Q7} cells (Fig. 6b and c; $P = 0.06$, $P = 0.03$), in accordance with the reduced number of chromosomes 15 and 14 in *STHdh*^{Q111/Q111} cells. In contrast, these differences were

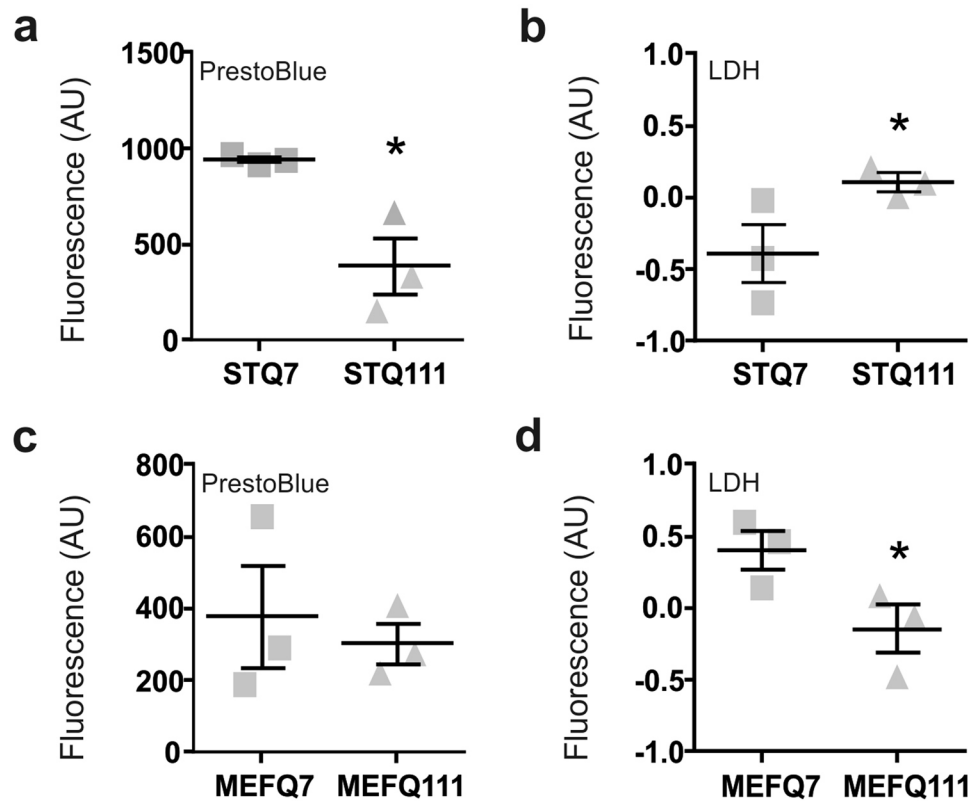


Figure 5. The cell size and proliferation phenotypes in *STHdh*^{Q111/Q111} cells impede the interpretation of standard cell viability assays. Results from the cell size- and cell number-dependent tests for *STHdh* cells: (a) PrestoBlue®, n = 3 experiments and (b) LDH assay, n = 3 experiments. Unpaired *t*-tests; **P* < 0.05. (c and d) Results from size- and cell number-dependent tests for *MEFHdh* cells, respectively; unpaired *t*-tests; **P* < 0.05.

not found in *MEFHdh* cells (Fig. 6e and f), where no differences in the number of chromosomes 15 and 14 were detected. Furthermore, the levels of β -actin were comparable in *STHdh*^{Q111/Q111} and *STHdh*^{Q7/Q7} cells (Fig. 6b and c) as well as in *MEFHdh*^{Q111/Q111} and *MEFHdh*^{Q7/Q7} cells (Fig. 6e and f), in accordance with the similar numbers of chromosome 5 in mutant and control cell lines. Interestingly, despite equal numbers of chromosome 6, levels of GAPDH were elevated in *STHdh*^{Q111/Q111} and tendentially in *MEFHdh*^{Q111/Q111} cell lines, compared to their wild type counterparts (Fig. 6b,c; *P* = 0.06, e and f; *P* = 0.02).

Discussion

STHdh cells represent a widely used cell culture model for studying cellular and molecular aspects of HD. Differences in cell morphology, growth and differentiation have previously been mentioned by other groups^{15,22}, but to date, these differences have not been assessed quantitatively. Our study demonstrates clear differences in cell size, proliferation and ploidy between mutant and wild type *STHdh* cells, and suggests a strong influence of these phenotypes on other readouts.

In the first description of the *STHdh* cell lines, it was stated that *STHdh*^{Q111/Q111} cells are of similar size as *STHdh*^{Q7/Q7} cells, while cell proliferation was even decreased in the mutant cells and accompanied by an increase in DNA content³. Later studies, however, either do mention a reduced cell size of *STHdh*^{Q111/Q111} cells^{11,15}, or the results are at least suggestive of such a phenotype (although not specifically discussed in these papers)^{23–25}. This might indicate that the phenotypes observed in our study had developed over time, possibly due to the tumour character of the cell lines. On the other hand, a reduced cell size was also found in our *MEFHdh*^{Q111/Q111} cell line compared to the respective control, despite the absence of large scale chromosomal changes. In addition, cell size differences in striatal neurons have been reported for the R6/2 model^{26,27} and the YAC128 model²⁸, two transgenic mouse models of HD, and it has been suspected for HD patients²⁹. It remains uncertain, if the reduced cell size should be considered an artefact or could be an HD-related feature, although it might be concluded that huntingtin is at least somehow involved in cell size regulation, as it is, as well, known to interact with cytoskeletal proteins³⁰.

The multiple numerical anomalies and structurally abnormal chromosomes we found in both *STHdh* cell lines are typical for stable cell lines and long-term passaging^{19–21}. Importantly, these abnormalities were found in cell populations that had been passaged for a maximum of six times between their purchase and the respective karyogram analysis. As this is a normal amount of passages required to carry out experiments, the abnormalities are likely to appear in other laboratories in a similar magnitude. Thus, users should be aware that the cell lines might not show the characteristics according to the original publication.

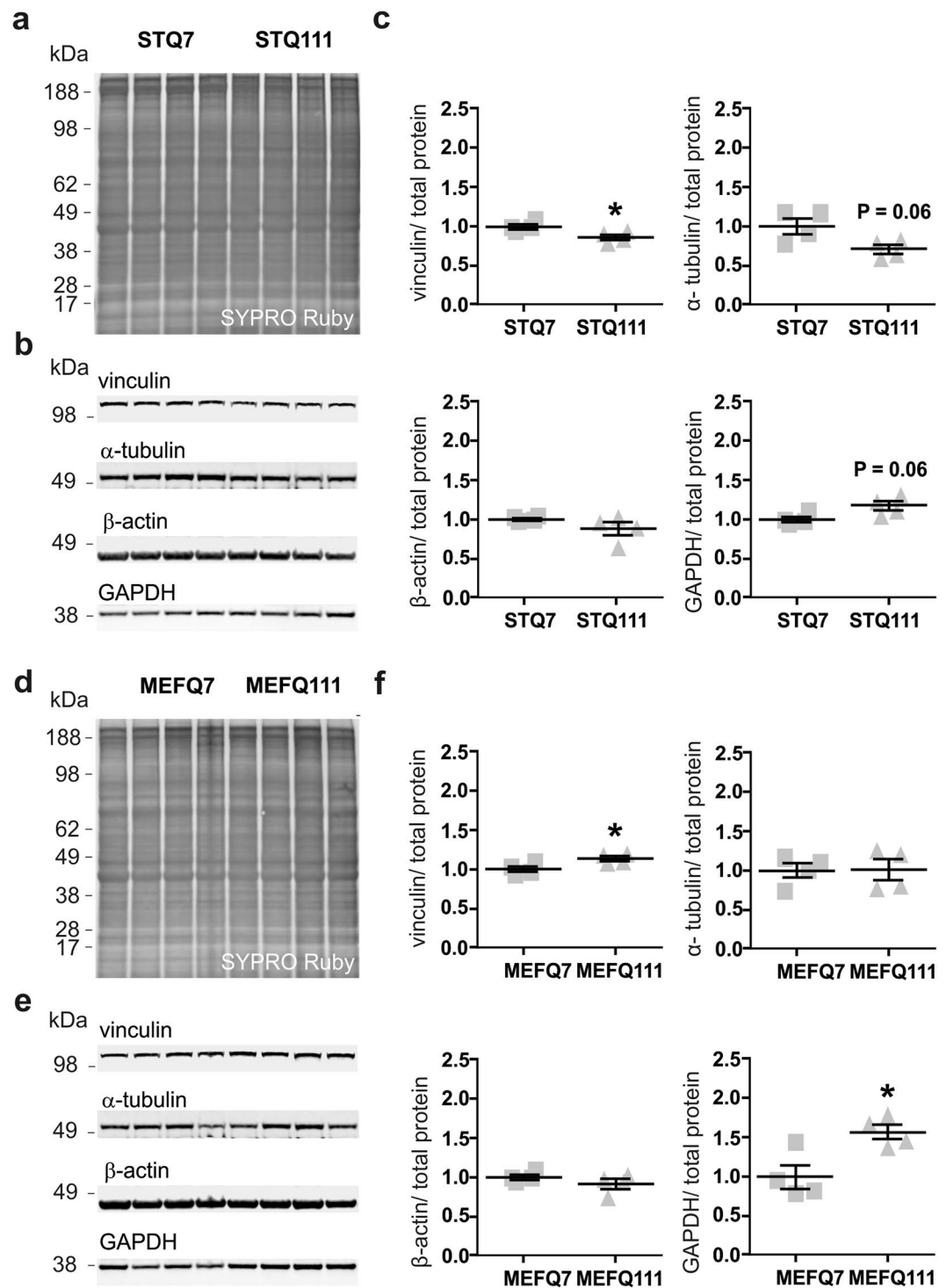


Figure 6. Chromosomal abnormalities impede the interpretation of western blot results in *STHdh* cells. (a) SYPRO Ruby staining, (b) western blots and (c) corresponding quantification of marker proteins in *STHdh* cells. Unpaired *t*-tests; * $P < 0.05$. (d) SYPRO Ruby staining, (e) western blots and (f) corresponding quantification of marker proteins in *MEFHdh* cells. Unpaired *t*-tests; * $P < 0.05$.

We further found the *STHdh*^{Q111/Q111} as well as *MEFHdh*^{Q111/Q111} cells to have an increased proliferation rate. It had been reported earlier that mutant huntingtin is involved in cell division in cell models and *Drosophila*³¹, as well as *Hdh*^{Q111/111} knock-in mice, *STHdh*^{Q111/Q111} cells and *MEFHdh*^{Q111/Q111} cells, as it alters the orientation of the mitotic spindle³². Although cell proliferation had not been measured in that study, the authors demonstrate that this leads to changes in neurogenesis in the developing cortex, highlighting the importance of this phenotype.

It is perceivable that differences in cell size, proliferation rate and chromosomal content might constitute confounding factors, and might complicate the interpretation of study outcomes due to adding several variables

which cannot properly be controlled for. We demonstrated that assays based on cell size and number, such as the PrestoBlue[®] and LDH assay, revealed lower basal cell viability and increased cell mortality in *STHdh*^{Q111/Q111} cells. Similar results have previously been published by others using the same assays^{33–35} or comparable methods⁷. However, the results could not be recreated in an assay that was likely to not depend on cell size or cell number. Thus, the earlier reported baseline difference in cell viability between *STHdh*^{Q111/Q111} and *STHdh*^{Q7/Q7} cells is questionable. Interestingly, our results were even indicative of increased cell viability in both, *STHdh*^{Q111/Q111} and *MEFHdh*^{Q111/Q111}. Effects on pro-survival functions in *STHdh*^{Q111/Q111} cells would need to be further investigated, as they have been reported to be reduced for other cell models of HD^{36,37}, whereas Akt signalling, implicated in neuronal survival³⁸, has been shown to be increased in mutant *STHdh* cells¹⁴. Clearly, *STHdh* cells do not represent the hallmarks of the advanced disease. Intranuclear inclusions, amongst others, found in *in vitro* and *in vivo* models, are not found in *STHdh* cells³. Therefore, the disease stage they model might not necessarily be characterized by a reduction in cell viability under normal conditions.

Confounding effects of the chromosomal abnormalities found in the *STHdh* cell lines were further expected for western blot analyses. Our investigations revealed important aspects to be considered when choosing a loading control for western blot analysis in *STHdh* cells. The protein levels of α -tubulin and vinculin were lower in *STHdh*^{Q111/Q111}, but not in *MEFHdh*^{Q111/Q111}, when compared to their respective controls and can be interpreted as a direct effect of the lower copy number of the chromosomes 14 and 15 in the *STHdh*^{Q111/Q111} cells. These observations correspond to previous studies, which reported on analogous proteomic changes resulting from variations of the gene copy number in cancer cells or aneuploid cell lines^{39,40}. On the other hand, our observation of an elevated GAPDH expression in both *STHdh*^{Q111/Q111} and *MEFHdh*^{Q111/Q111} cells has already been shown in other HD models. As GAPDH is a well-known interaction partner of huntingtin, these results further render GAPDH as an inadequate loading control in HD research^{41–43}.

Although our study is important, as it demonstrates features of the extensively used *STHdh* model that need to be considered when working with this cell model, and as it highlights the *MEFHdh* cells as useful controls in *in vitro* studies, there are some limitations that we would like to point out. First, our *MEFHdh* cells were generated from embryos of different sex. The *MEFHdh* cells were generated 12 days after a 48-hour breeding period, and sex differentiation in the mouse embryo begins as early as E10⁴⁴. Therefore, although we consider the influence of sex determination on cell size, proliferation rate and chromosomal content at that point negligible, we cannot rule it out. Thus, we highly recommend the generation of sex-matched *MEFHdh* cell lines for further studies. Second, the two cell lines characterized here originate from the same HD animal model. As such, they share several drawbacks that need to be considered. *Hdh*^{Q111} knock-in mice, like most other animal models of HD, are designed to express mutant huntingtin with high numbers of polyglutamine repeats to provoke possibly early and strong phenotypes (reviewed by Ferrante *et al.*⁴⁵), even though such high repeat numbers are only found in patients with the rare juvenile form of HD. In this regard, it should be noted that cell models⁴⁶ and animal models⁴⁷ with lower CAG-repeats have been generated to recapitulate the commonly found mutation lengths. Furthermore, both *STHdh* and *MEFHdh* cell lines are not isogenic. Q7 alleles represent the wild type mouse alleles, while Q111 alleles are human mouse chimera of exon 1. For this reason, there are additional differences in the gene sequence between Q7 and Q111 alleles than the CAG repeat expansion. On the other hand, *STHdh* and *MEFHdh* cells differ fundamentally regarding immortalization and biological origin. *STHdh* cells are comparable to other immortalized cell lines with regard to immortalization artefacts^{19–21,48}, as shown here by the altered chromosome numbers. This is a drawback, as the supposedly complementary Q7 and Q111 cell lines have apparently acquired divergent features over time. Moreover, it needs to be considered that p53, a tumour suppressor protein affected in immortalized cell lines^{49,50}, is a transcriptional regulator of *huntingtin*⁵¹ and implicated in the pathogenesis of HD⁵². In this regard, the *MEFHdh* cells used here represent a better cell model, as these were not immortalized and therefore the genetic integrity was less corrupted. However, the *MEFHdh* cells presented milder phenotypes regarding cell size and proliferation, which is likely to be due to their heterogeneous cell composition¹⁶. In this regard, the clonal and neuronal character of *STHdh* cells might lead to stronger and more robust phenotypes than embryonic fibroblasts. The clonal character, however, once more underscores the importance of an additional model, to exclude artefacts. Finally, it would always be advantageous to confirm phenotypes in cell and animal models of HD that are based on a different genetic background.

In summary, *STHdh* cell lines are a generally useful model to study mechanisms behind the molecular pathogenesis of HD, because they provide the proper cellular as well as genetic context of HD due to their striatal origin and the knock-in model they derive from. However, the possible bias due to differences in cell size, proliferation and chromosomal content need to be considered when planning and interpreting results. In this regard, assays in which cell size and cell number play an important role for the outcome, and cannot be controlled for, should be avoided. Differentiation of the *STHdh* cells into neuron-like cells might at least overcome the problem regarding cell proliferation. Nevertheless, for time-course experiments the increased proliferation rate, as it was, as well, observed in *MEFHdh* cells needs to be considered. A simple solution for treatment studies would be to not directly compare results from *STHdh*^{Q7/Q7} to *STHdh*^{Q111/Q111}, but to rather compare treatment effects in the two cell lines independently. Finally, using a second *in vitro* or an *in vivo* model to confirm results is beneficial to determine the HD-dependency of the phenotype investigated. Our study emphasizes that it is of importance to regularly check the basic characteristics of an employed cell model and to consider putative alterations for experimental design and analysis.

Methods

Ethics Statement. Experiments for the generation of *MEFHdh* cells were performed at the University of Tuebingen. The protocol was approved by the local ethics committee at Regierungspraesidium Tuebingen and carried out in accordance with the German Animal Welfare Act and the guidelines of the Federation of European Laboratory Animal Science Associations, based on European Union legislation (Directive 2010/63/EU).

STHdh cells. *STHdh* cell lines, originally generated at the laboratory of Dr. Marcy MacDonald (Harvard Medical School, Boston)³, were purchased from Coriell Cell Repositories (Coriell Institute for Medical Research). Cell passages 4–12 were used for the experiments.

MEFHdh cells. A heterozygous breeding of *Hdh*^{Q111} knock-in mice was set up and maintained for 48 hours. After 12 days, the pregnant female was sacrificed by inhalation of CO₂. The embryos were extracted by caesarean sectioning, decapitated immediately and placed individually in sterile, ice-cold, Dulbecco's phosphate-buffered saline (DPBS) (Invitrogen). Limbs, brain and visceral organs were removed. The remaining tissue was transferred into a sterile well of a 6-well plate with fresh DPBS, which was then replaced by 2 ml of culture media (Dulbecco's Modified Eagle Medium (DMEM) with 1% penicillin/streptomycin and 10% fetal calf serum (FCS), Gibco®, Thermo Fisher Scientific). The tissue was incubated for 1 h at 37 °C and 5% CO₂. After this, the tissue was transferred into a 100 mm dish with 10 ml culture media (pre-warmed to 37 °C), and minced with a scalpel. Pieces were transferred to a T75 cell culture flask with 10 ml of fresh media and incubated at 37 °C and 5% CO₂ for 3 days. Afterwards, media was changed and the cells were incubated until they reached 90% confluency. Cells were then trypsinized (1 ml 0.25% trypsin-EDTA (Invitrogen) for 5 min at 37 °C and 5% CO₂) and gently resuspended using a 1 ml pipette for subcultivation. For the experiments, a wild type and a homozygous culture were picked.

Cell handling and treatment. *STHdh* and *MEFHdh* cells were maintained in DMEM supplemented with 10% FCS (Gibco™) and 1% penicillin/streptomycin (Gibco™) at 37 °C in 5% CO₂. *STHdh* media was additionally complemented by adding 1% geneticin (A2912, Biochrome). Both, *STHdh* and *MEFHdh* cells were routinely tested negative for contamination by mycoplasma using the Venor®*GeM* Mycoplasma detection kit (Merck). Unless specifically stated differently, *STHdh* cells were undifferentiated. For differentiation into neuron-like cells a previously described differentiation protocol³ was used. For this, cells were incubated in differentiation cocktail for 24–48 h.

Flow cytometry. Undifferentiated *STHdh* and *MEFHdh* cells were recorded using a flow cytometry LSR II cytofluorometer (BD Bioscience). A total of 200,000 ungated events were analysed with the flow cytometry-DIVA software version 6.1.3 (BD Bioscience) and overlays were processed with FCS Express software version 4.0.230 (De Novo Software). Differentiated *STHdh* cells were recorded with a CyAn™ ADP flow cytometer (Beckman Coulter). A total of 20,000 ungated events were analysed with Summit V4.3.01 software (Dako Colorado, Inc.).

Cell size determination. Cells were seeded in 6-well plates and grown to 60–70% confluency. Cell size was measured for cells attached to the surface of the culture dish as well as for detached cells after trypsinization each with 3 replicates per cell line. A total of 270 cells per genotype were analysed in 3 independent experiments (30 cells/well; 3 wells/experiment). Pictures of the cells were taken using an Eclipse TS100 Inverted Routine microscope (Nikon) with a digital camera at 20x magnification and analysed with ImageJ v1.47⁵³. For attached cells, the area of the cells was approximated by measuring the area of a polygon that was assigned to each cell. For detached cells, the area of a round shape was measured that was applied to each cell individually. The scale was determined by the length of the counting chamber grid.

Chromosome analysis. Chromosome preparations from cultured cells and GTG-banding were performed using standard techniques. For each cell line, 17 mitoses were numerically analysed and 5–8 mitoses were structurally analysed. For cytogenetic analyses, for all cell lines, cells from early passages (P4–P6) were harvested using a standard protocol and was followed by G-banding. Images of well spread metaphase chromosomes were captured using a CCD camera. Karyotyping was performed using the IKAROS software (MetaSystems, Altlußheim, Germany). Chromosome classification followed the guidelines of the International Committee on Standardized Genetics nomenclature for mice⁵⁴.

Determination of proliferation rate. Three replicates of *STHdh* (40,000 cells per well) and *MEFHdh* cells (100,000 cells per well) were seeded in 6-well plates. After 3 days (*STHdh*) or 7 days (*MEFHdh*), cells were harvested by trypsinization (250 µl 0.25% trypsin-EDTA (Gibco™) for 5 min at 37 °C and 5% CO₂), washed and counted again. At least three independent experiments were performed.

Determination of DNA content. DNA content was measured using the NucleoView NC-3000 (ChemoMetec). Reagents were provided by the manufacturer and cells were treated according to the manufacturer's instructions. In brief, cells were detached from the culture flask, washed with DPBS (Gibco™) and lysed. The cells were stained with DAPI, at a saturating concentration (10 µg/ml), stabilized and immediately analysed with the device. Data was analysed with the NucleoView NC-3000 software, Version 2.1.25.12 (ChemoMetec).

Viability assays. Cell viability and cell death were determined using commercially available kits (PrestoBlue® cell viability reagent, Invitrogen™; Cytotoxicity Detection Kit (LDH), Roche), following the provider's instructions. Briefly, 10,000 cells were seeded in a 96-well plate and incubated overnight. Culture media was transferred into a new 96 well plate for the LDH assay. Cells left in the original plate received fresh media containing PrestoBlue®. The fluorescence intensity (PrestoBlue® assay) was measured after 1 h; the absorption (LDH assay) was measured according to manufacturer's instructions, using the plate reader MWGt Synergy HT (BioTek Instruments) and the software Gen5 2.01 (BioTek).

In addition, cell viability and cell death were measured using flow cytometry. For this, cells were grown in 75 ml culture flasks and harvested by gentle trypsinization (0.25% Trypsin-EDTA; Gibco®, Thermo Fisher Scientific). Cells were centrifuged at 400 × g for 5 min and washed twice with 1 × Annexin V Binding Buffer (eBioscience). Cells were labelled with Alexa Fluor® 647 Annexin V (Biolegend) and 7-Amino-Actinomycin (7'AAD) (BD Pharmingen). Data was recorded by flow cytometry to determine the number of Annexin V/7'AAD-positive cells.

Cell lysate preparation. For preparation of lysates, *STHdh* and *MEFHdh* cells were trypsinized and collected by centrifugation at $350 \times g$ for 5 min. The pellet was washed once with cold DPBS (Gibco[®], Thermo Fisher Scientific), centrifuged again and lysed in RIPA buffer (50 mM Tris pH 7.5, 150 mM NaCl, 0.1% SDS, 0.5% sodium deoxycholate and 1% Triton X-100, containing protease inhibitors) for 25 min on ice, while vortexing briefly every 5 min. Afterwards, samples were centrifuged at $13,200 \times g$ for 15 min at 4 °C. Supernatant was pipetted into a pre-cooled reaction tube, adding glycerol to final concentration of 10%, and stored at -80 °C until further analysis.

Western blotting, SYPRO Ruby staining and immunodetection. Protein concentrations of RIPA lysates were determined spectrophotometrically using Bradford reagent (Bio-Rad Laboratories). Western blot analysis was performed following standard procedures. Briefly, 30 μ g of protein were separated electrophoretically using 10% Bolt[®] Bis-Tris Plus Gels (Thermo Fisher Scientific). Proteins were transferred on Amersham[™] Protran[™] Premium 0.2 μ m nitrocellulose membranes (GE Healthcare) using a TE22 Transfer Tank (Hoefer).

After transfer, total protein was stained with SYPRO Ruby Protein Blot Stain (Thermo Fisher Scientific) according to manufacturer's instructions and detected at 600 nm using the LI-COR ODYSSEY[®] FC imaging system (LI-COR Biosciences).

After SYPRO Ruby staining, membranes were blocked with 5% Slimfast in TBS at room temperature for 1 h and probed overnight at 4 °C with the following primary antibodies: mouse anti- β -actin (1:10,000; clone AC-15, A5441, Sigma Aldrich), mouse anti-GAPDH (1:1000; clone GA1R, ab125247, Abcam), mouse anti- α -tubulin (1:5000; clone DM1A, CP06, EMD Millipore) and rabbit anti-vinculin (1:1000; clone E1E9V, #13901, Cell signaling). Afterwards, membranes were incubated at room temperature for 1 h with the respective secondary IRDye antibodies goat anti-mouse 680LT and goat anti-rabbit 800CW (all 1:10,000; LI-COR Biosciences). Fluorescence signals were detected with the LI-COR ODYSSEY[®] FC and quantified with ODYSSEY[®] Server software version 4.1 (LI-COR Biosciences). Quantified signals were normalized to total protein as detected before using SYPRO Ruby Protein Stain.

Statistical Analysis and Data availability. All data are presented as individual measurements (grey shapes) with mean and standard error of the mean (SEM). Statistical analysis was performed with GraphPad Prism 6.00 for Windows (GraphPad Software, Inc). Statistical significance of two group data sets was determined using two-tailed, unpaired Student's *t*-test, with Welch's correction. The significance threshold was set to $P < 0.05$. The datasets generated during and/or analysed during the current study are available from the corresponding author on reasonable request.

References

- Vonsattel, J. P. *et al.* Neuropathological classification of Huntington's disease. *Journal of neuropathology and experimental neurology* **44**, 559–577 (1985).
- Zuccato, C. & Cattaneo, E. Brain-derived neurotrophic factor in neurodegenerative diseases. *Nat Rev Neurol* **5**, 311–322 (2009).
- Trettel, F. *et al.* Dominant phenotypes produced by the HD mutation in *STHdh*(Q111) striatal cells. *Hum Mol Genet* **9**, 2799–2809 (2000).
- Menalled, L. B. Knock-In Mouse Models of Huntington's Disease. *NeuroRX* **2**, 465–470 (2005).
- Wheeler, V. C. *et al.* Early phenotypes that presage late-onset neurodegenerative disease allow testing of modifiers in *Hdh* CAG knock-in mice. *Human Molecular Genetics* **11**, 633–640, <https://doi.org/10.1093/hmg/11.6.633> (2002).
- Wheeler, V. C. *et al.* Long glutamine tracts cause nuclear localization of a novel form of huntingtin in medium spiny striatal neurons in *Hdh*Q92 and *Hdh*Q111 knock-in mice. *Human Molecular Genetics* **9**, 503–513, <https://doi.org/10.1093/hmg/9.4.503> (2000).
- Gines, S. *et al.* Specific progressive cAMP reduction implicates energy deficit in presymptomatic Huntington's disease knock-in mice. *Human Molecular Genetics* **12**, 497–508, <https://doi.org/10.1093/hmg/ddg046> (2003).
- Oliveira, J. M. A. *et al.* Mitochondrial-Dependent Ca²⁺ Handling in Huntington's Disease Striatal Cells: Effect of Histone Deacetylase Inhibitors. *The Journal of Neuroscience* **26**, 11174–11186, <https://doi.org/10.1523/jneurosci.3004-06.2006> (2006).
- Choo, Y. S., Johnson, G. V., MacDonald, M., Detloff, P. J. & Lesort, M. Mutant huntingtin directly increases susceptibility of mitochondria to the calcium-induced permeability transition and cytochrome c release. *Hum Mol Genet* **13**, 1407–1420, <https://doi.org/10.1093/hmg/ddh162> (2004).
- Seong, I. S. *et al.* HD CAG repeat implicates a dominant property of huntingtin in mitochondrial energy metabolism. *Hum Mol Genet* **14**, 2871–2880, <https://doi.org/10.1093/hmg/ddi319> (2005).
- Milakovic, T. & Johnson, G. V. Mitochondrial respiration and ATP production are significantly impaired in striatal cells expressing mutant huntingtin. *J Biol Chem* **280**, 30773–30782, <https://doi.org/10.1074/jbc.M504749200> (2005).
- Xifro, X., Garcia-Martinez, J. M., Del Toro, D., Alberch, J. & Perez-Navarro, E. Calcineurin is involved in the early activation of NMDA-mediated cell death in mutant huntingtin knock-in striatal cells. *J Neurochem* **105**, 1596–1612, <https://doi.org/10.1111/j.1471-4159.2008.05252.x> (2008).
- Ferrante, A. *et al.* Expression, pharmacology and functional activity of adenosine A1 receptors in genetic models of Huntington's disease. *Neurobiol Dis* **71**, 193–204, <https://doi.org/10.1016/j.nbd.2014.08.013> (2014).
- Gines, S., Ivanova, E., Seong, I. S., Saura, C. A. & MacDonald, M. E. Enhanced Akt signaling is an early pro-survival response that reflects N-methyl-D-aspartate receptor activation in Huntington's disease knock-in striatal cells. *J Biol Chem* **278**, 50514–50522, <https://doi.org/10.1074/jbc.M309348200> (2003).
- Reis, S. A. *et al.* Striatal neurons expressing full-length mutant huntingtin exhibit decreased N-cadherin and altered neurogenesis. *Hum Mol Genet* **20**, 2344–2355, <https://doi.org/10.1093/hmg/ddr127> (2011).
- Singhal, P. K. *et al.* Mouse embryonic fibroblasts exhibit extensive developmental and phenotypic diversity. *Proc Natl Acad Sci USA* **113**, 122–127, <https://doi.org/10.1073/pnas.1522401112> (2016).
- Lee, H. O., Davidson, J. M. & Duronio, R. J. Endoreplication: polyploidy with purpose. *Genes & Development* **23**, 2461–2477, <https://doi.org/10.1101/gad.1829209> (2009).
- Gregory, T. R. Coincidence, coevolution, or causation? DNA content, cell size, and the C-value enigma. *Biological Reviews* **76**, 65–101, doi:undefined (2001).
- Stewart, N. & Bacchetti, S. Expression of SV40 large T antigen, but not small t antigen, is required for the induction of chromosomal aberrations in transformed human cells. *Virology* **180**, 49–57 (1991).

20. Gaztelumendi, N. & Nogués, C. Chromosome Instability in mouse Embryonic Stem Cells. *Scientific Reports* **4**, 5324, <https://doi.org/10.1038/srep05324> (2014).
21. Wang, Y. *et al.* Long-term cultured mesenchymal stem cells frequently develop genomic mutations but do not undergo malignant transformation. *Cell Death Dis* **4**, e950, <https://doi.org/10.1038/cddis.2013.480> (2013).
22. Lim, D. *et al.* Calcium homeostasis and mitochondrial dysfunction in striatal neurons of Huntington disease. *J Biol Chem* **283**, 5780–5789, <https://doi.org/10.1074/jbc.M704704200> (2008).
23. Acuna, A. I. *et al.* A failure in energy metabolism and antioxidant uptake precede symptoms of Huntington's disease in mice. *Nature communications* **4**, 2917, <https://doi.org/10.1038/ncomms3917> (2013).
24. Blazquez, C. *et al.* Loss of striatal type 1 cannabinoid receptors is a key pathogenic factor in Huntington's disease. *Brain* **134**, 119–136, <https://doi.org/10.1093/brain/awq278> (2011).
25. Lajoie, P. & Snapp, E. L. Changes in BiP availability reveal hypersensitivity to acute endoplasmic reticulum stress in cells expressing mutant huntingtin. *J Cell Sci* **124**, 3332–3343, <https://doi.org/10.1242/jcs.087510> (2011).
26. Chopra, V. *et al.* A small-molecule therapeutic lead for Huntington's disease: Preclinical pharmacology and efficacy of C2-8 in the R6/2 transgenic mouse. *Proceedings of the National Academy of Sciences* **104**, 16685–16689, <https://doi.org/10.1073/pnas.0707842104> (2007).
27. Levine, M. S. *et al.* Enhanced sensitivity to N-methyl-D-aspartate receptor activation in transgenic and knockin mouse models of Huntington's disease. *J Neurosci Res* **58**, 515–532 (1999).
28. Slow, E. J. *et al.* Selective striatal neuronal loss in a YAC128 mouse model of Huntington disease. *Human Molecular Genetics* **12**, 1555–1567, <https://doi.org/10.1093/hmg/ddg169> (2003).
29. Vonsattel, J. P. G., Keller, C. & Pilar Amaya, Md Neuropathology of Huntington's Disease. *Handbook of Clinical Neurology* **89**, 599–618 (2008).
30. Munsie, L. *et al.* Mutant huntingtin causes defective actin remodeling during stress: defining a new role for transglutaminase 2 in neurodegenerative disease. *Human Molecular Genetics* **20**, 1937–1951, <https://doi.org/10.1093/hmg/ddr075> (2011).
31. Godin, J. D. *et al.* Huntingtin Is Required for Mitotic Spindle Orientation and Mammalian Neurogenesis. *Neuron* **67**, 392–406, <https://doi.org/10.1016/j.neuron.2010.06.027>.
32. Molina-Calavita, M. *et al.* Mutant Huntingtin Affects Cortical Progenitor Cell Division and Development of the Mouse Neocortex. *The Journal of Neuroscience* **34**, 10034–10040, <https://doi.org/10.1523/jneurosci.0715-14.2014> (2014).
33. Ribeiro, M., Silva, A. C., Rodrigues, J., Naia, L. & Rego, A. C. Oxidizing effects of exogenous stressors in Huntington's disease knock-in striatal cells—protective effect of cystamine and creatine. *Toxicol Sci* **136**, 487–499, <https://doi.org/10.1093/toxsci/kft199> (2013).
34. Oliveira, A. M. *et al.* Protective effects of 3-alkyl luteolin derivatives are mediated by Nrf2 transcriptional activity and decreased oxidative stress in Huntington's disease mouse striatal cells. *Neurochemistry International* **91**, 1–12 (2015).
35. Ruiz, C. *et al.* Protection by glia-conditioned medium in a cell model of Huntington disease. *PLoS Currents* **4**, e4fbca54a2028b, <https://doi.org/10.1371/4fbca54a2028b> (2012).
36. Rigamonti, D. *et al.* Wild-type huntingtin protects from apoptosis upstream of caspase-3. *Journal of Neuroscience* **20**, 3705–3713 (2000).
37. Li, S.-H., Cheng, A. L., Li, H. & Li, X.-J. Cellular Defects and Altered Gene Expression in PC12 Cells Stably Expressing Mutant Huntingtin. *The Journal of Neuroscience* **19**, 5159–5172 (1999).
38. Dudek, H. *et al.* Regulation of Neuronal Survival by the Serine-Threonine Protein Kinase Akt. *Science* **275**, 661 (1997).
39. Geiger, T., Cox, J. & Mann, M. Proteomic changes resulting from gene copy number variations in cancer cells. *PLoS Genet* **6**, e1001090, <https://doi.org/10.1371/journal.pgen.1001090> (2010).
40. Stingle, S. *et al.* Global analysis of genome, transcriptome and proteome reveals the response to aneuploidy in human cells. *Mol Syst Biol* **8**, 608, <https://doi.org/10.1038/msb.2012.40> (2012).
41. Bae, B. I. *et al.* Mutant huntingtin: nuclear translocation and cytotoxicity mediated by GAPDH. *Proc Natl Acad Sci USA* **103**, 3405–3409, <https://doi.org/10.1073/pnas.0511316103> (2006).
42. Burke, J. R. *et al.* Huntingtin and DRPLA proteins selectively interact with the enzyme GAPDH. *Nat Med* **2**, 347–350 (1996).
43. Senatorov, V. V., Charles, V., Reddy, P. H., Tagle, D. A. & Chuang, D. M. Overexpression and nuclear accumulation of glyceraldehyde-3-phosphate dehydrogenase in a transgenic mouse model of Huntington's disease. *Mol Cell Neurosci* **22**, 285–297 (2003).
44. Eggers, S. & Sinclair, A. Mammalian sex determination—insights from humans and mice. *Chromosome Research* **20**, 215–238, <https://doi.org/10.1007/s10577-012-9274-3> (2012).
45. Ferrante, R. J. Mouse Models of Huntington's Disease and Methodological Considerations for Therapeutic Trials. *Biochimica et biophysica acta* **1792**, 506–520, <https://doi.org/10.1016/j.bbdis.2009.04.001> (2009).
46. Maiuri, T. *et al.* Huntingtin is a scaffolding protein in the ATM oxidative DNA damage response complex. *Human Molecular Genetics* **26**, 395–406, <https://doi.org/10.1093/hmg/ddw395> (2017).
47. von Horsten, S. *et al.* Transgenic rat model of Huntington's disease. *Hum Mol Genet* **12**, 617–624 (2003).
48. Mittelman, D. & Wilson, J. H. The fractured genome of HeLa cells. *Genome Biology* **14**, 111, <https://doi.org/10.1186/gb-2013-14-4-111> (2013).
49. Segawa, K., Minowa, A., Sugasawa, K., Takano, T. & Hanaoka, F. Abrogation of p53-mediated transactivation by SV40 large T antigen. *Oncogene* **8**, 543–548 (1993).
50. Ali, S. H. & DeCaprio, J. A. Cellular transformation by SV40 large T antigen: interaction with host proteins. *Seminars in Cancer Biology* **11**, 15–22, <https://doi.org/10.1006/scbi.2000.0342> (2001).
51. Feng, Z. *et al.* p53 tumor suppressor protein regulates the levels of huntingtin gene expression. *Oncogene* **25**, 1 (2006).
52. Bae, B. I. *et al.* p53 mediates cellular dysfunction and behavioral abnormalities in Huntington's disease. *Neuron* **47**, 29–41, <https://doi.org/10.1016/j.neuron.2005.06.005> (2005).
53. Abramoff, M. D. M., Paulo, J. & Ram, Sunanda, J. Image Processing with ImageJ. *Biophotonics International* (2004).
54. Eppig, J. T. *Rules for Nomenclature of Mouse Chromosome Aberrations*, <http://www.informatics.jax.org/mgihome/nomen/anomalies.shtml> (2015).

Acknowledgements

J.J.W. was funded by the Baden-Wuerttemberg Foundation (research grant number P-BWS-SPII/3-08). The work was supported by the European Union 7th Framework Program (FP7/2012), Project “SWITCH-HD”, under grant agreement No. 324495 to H.P.N. L.E.C. was a postdoctoral fellow of the SWITCH-HD project. We are grateful to Alissa Mitnik and Tanja Wlodkowski for making the first cell size analyses in *STHdh* cells, Midea Ortiz Rios for supportive cell culture work and Eva Haydt for harvesting the different cultures for karyotyping as well as Jeannette Schoene for technical assistance.

Author Contributions

L.E.C., C.W., J.J.W., O.R. and H.P.N. developed the conceptual framework for the study. E.S., C.W., A.-C.K. and L.E.C. performed cell size and proliferation analyses. U.A.M.-H. performed karyotyping. J.J.W. performed the analysis of protein markers. E.S., C.W., A.-C.K., N.R. and L.E.C. determined cell viability. L.E.C., C.W., J.J.W., E.S., U.A.M.-H., and H.P.N. interpreted the data. L.E.C., C.W., J.J.W. and E.S. prepared the Figures. L.E.C., E.S., C.W., J.J.W. and H.P.N. wrote the manuscript. All authors reviewed the manuscript.

Additional Information

Supplementary information accompanies this paper at <https://doi.org/10.1038/s41598-017-17275-4>.

Competing Interests: The authors declare that they have no competing interests.

Publisher's note: Springer Nature remains neutral with regard to jurisdictional claims in published maps and institutional affiliations.



Open Access This article is licensed under a Creative Commons Attribution 4.0 International License, which permits use, sharing, adaptation, distribution and reproduction in any medium or format, as long as you give appropriate credit to the original author(s) and the source, provide a link to the Creative Commons license, and indicate if changes were made. The images or other third party material in this article are included in the article's Creative Commons license, unless indicated otherwise in a credit line to the material. If material is not included in the article's Creative Commons license and your intended use is not permitted by statutory regulation or exceeds the permitted use, you will need to obtain permission directly from the copyright holder. To view a copy of this license, visit <http://creativecommons.org/licenses/by/4.0/>.

© The Author(s) 2017

Review Article

Killing Two Angry Birds with One Stone: Autophagy Activation by Inhibiting Calpains in Neurodegenerative Diseases and Beyond

Jonasz Jeremiasz Weber ¹, Priscila Pereira Sena ¹,
Elisabeth Singer,¹ and Huu Phuc Nguyen^{1,2}

¹Institute of Medical Genetics and Applied Genomics, University of Tübingen, Calwerstraße 7, 72076 Tübingen, Germany

²Department of Human Genetics, Ruhr-University Bochum, Universitätsstraße 150, 44801 Bochum, Germany

Correspondence should be addressed to Jonasz Jeremiasz Weber; jonasz.weber@med.uni-tuebingen.de

Received 31 October 2018; Accepted 27 January 2019; Published 14 February 2019

Academic Editor: Gessica Sala

Copyright © 2019 Jonasz Jeremiasz Weber et al. This is an open access article distributed under the Creative Commons Attribution License, which permits unrestricted use, distribution, and reproduction in any medium, provided the original work is properly cited.

Proteolytic machineries execute vital cellular functions and their disturbances are implicated in diverse medical conditions, including neurodegenerative diseases. Interestingly, calpains, a class of Ca^{2+} -dependent regulatory proteases, can modulate the degradational system of autophagy by cleaving proteins involved in this pathway. Moreover, both machineries are common players in many molecular pathomechanisms and have been targeted individually or together, as a therapeutic strategy in experimental setups. In this review, we briefly introduce calpains and autophagy, with their roles in health and disease, and focus on their direct pathologically relevant interplay in neurodegeneration and beyond. The modulation of calpain activity may comprise a promising treatment approach to attenuate the deregulation of these two essential mechanisms.

1. Introduction

Proteolytic machineries of eukaryotic cells are key players in the regulation of protein function or the maintenance of cell homeostasis. Importantly, they act as modifiers of numerous neurodegenerative proteopathies, including classical medical conditions such as Alzheimer disease (AD), Parkinson disease (PD), and the group of polyglutamine (polyQ) disorders. This link is evident as the nature of these diseases, i.e., the occurrence of structurally abnormal toxic proteins, provokes an overload of these systems, leading to their disruption, loss of cellular integrity, and eventually neuronal demise [1]. Beyond neurodegeneration, proteostatic processes are implicated in further medical conditions like, for instance, cancer, cardiovascular disorders, and diabetes [2–4]. This multifarious involvement emphasizes the value of targeting these machineries therapeutically.

In this review, we focus on two major proteolytic machineries of the cell, the calpain protease system and autophagy, which both have been scrutinized in the context

of neurodegenerative disorders and other diseases for the last two decades. As often the case with complex cellular pathways, both proteolytic machineries are strongly interconnected and the deregulation of one of them inevitably leads to repercussion on the other. By shedding new light on the impact of calpains on autophagy and vice versa, we aim to work out points of vantage for therapeutic applications, which only target one but may hit both compromised proteolytic systems. Consequently, future disease-treating approaches may kill those rather angry birds, namely overactivated calpains and impaired autophagy, with only one stone.

2. Calpains and Autophagy in Neurodegeneration and Other Medical Conditions

2.1. Calpains

2.1.1. Calpain Basics. The regulation of protein structure, function, localization, or lifetime is mediated by a vast range

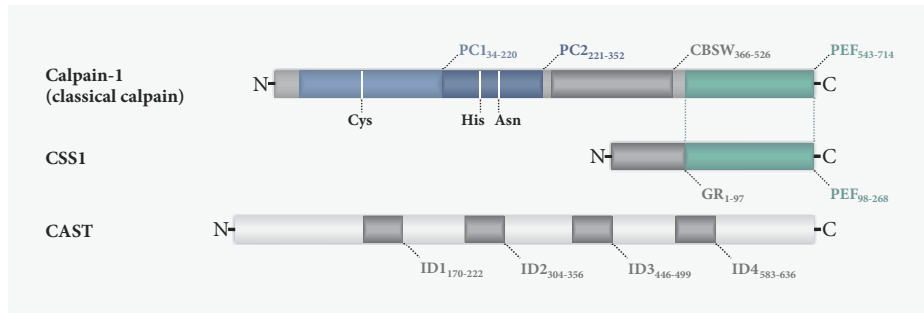


FIGURE 1: *Domain composition and structure of calpain-1, CSS1, and CAST.* Conventional classical calpains are present as a large protease unit, such as the here depicted calpain-1, and the calpain small subunit 1 (CSS1). Both share a C-terminal Ca^{2+} -binding penta-EF-hand (PEF) domain. Calpain-1 further contains an N-terminal proteolytic CysPc domain, consisting of core domains PC1 and PC2, which also bind Ca^{2+} ions. Amino acid positions of the catalytic triad of calpain-1 are indicated by vertical white lines. In addition, a calpain-like β -sandwich domain (CBSW) is located between the CysPc and the PEF domain. CSS1 features, moreover, an N-terminal glycine-rich (GR) hydrophobic domain. The endogenous inhibitor calpastatin (CAST) contains four structurally flexible inhibitory domains (ID1-4) of which each can inhibit one calpain molecule. Illustrations of calpain-1, CSS1, and CAST are based on data retrieved from the UniProt database (respective identifiers P07384-1, P04632-1, and P20810-1).

of posttranslational modifications (PTMs). Amongst those, proteolytic processing constitutes a profound mechanism, which spans from the removal of single amino acids to longer peptides or whole domains of the targeted protein. One class of enzymes responsible for this modification is calpains, firstly described as a Ca^{2+} -activated neutral proteinase in rat brain [5]. The later-promoted term ‘calpain’ is a portmanteau, which consists of the two syllables ‘cal’ in reference to Ca^{2+} or Ca^{2+} -binding proteins and ‘pain’ as an allusion to structurally related cysteine proteases like papain from plants or clostripain from *Clostridium* [6]. Calpain and their homologs can be found in unicellular and multicellular organisms, from animals, over plants, fungi, yeast, and down to bacteria [4].

Structurally, all calpains are characterized by their conserved proteolytic domain (CysPc), which is subdivided in the two protease core domains PC1 and PC2. Together with more than 40 different other protein domains or motifs, the CysPc domain forms multiple variants of calpains in a modular principle. The human genome encodes 15 different calpains, divided into two main groups: classical (calpains-1-14) and nonclassical calpains (calpain-5, calpain-6, calpain-7, calpain-10, calpain-15, and calpain-16). Classical calpains feature a C-terminal Ca^{2+} -binding penta-EF-hand (PEF) domain. Via this domain, members like calpain-1 and calpain-2, which are referred to as conventional classical calpains, exhibit a vital interaction with the regulatory calpain small subunit 1 (CSS1, formerly known as calpain-4) [7, 8]. Nonclassical calpains lack both the PEF domain and the interaction with a regulatory subunit [4, 8, 9]. The direct antagonist of these proteases is calpastatin (CAST), the only known endogenous, ubiquitously expressed, and highly specific proteinaceous inhibitor of classical calpains. Altogether, calpains, regulatory subunits, and CAST form the intracellular calpain system [10, 11]. A structural representation of calpain-1, CSS1, and CAST is shown in Figure 1. Calpain expression depends largely on the respective isoform: calpain-1, together with the regulatory subunit CSS1, is expressed ubiquitously, and isoforms such as calpain-2,

calpain-5, and calpain-10 are found in most cells. However, other calpains, like the skeletal muscle-specific calpain-3, show expression patterns restricted to distinct tissues [8].

The activation mechanism of calpains has been controversially discussed and led to the formulation of different explanatory scenarios [12]. However, X-ray crystallography of Ca^{2+} -bound calpain-2 together with CSS1 and CAST shed light on the precise mechanism: in a fully activated state, calpain-2-CSS1 heterodimer binds ten Ca^{2+} ions, of which eight are bound to the two PEF domains, and one Ca^{2+} is bound at each PC domain. The Ca^{2+} -binding induces structural rearrangements, which then allows the connection of the PC1 and PC2 core domains to a closed active state [13, 14]. *In vitro* studies demonstrated that Ca^{2+} concentrations necessary for activation of calpains were in a micro- to millimolar range, which is rather far beyond the nanomolar Ca^{2+} levels in cells under normal physiological conditions. Yet, this apparent contradiction is resolved, as the cellular microenvironment may provide the sufficient Ca^{2+} concentration [12].

Calpains feature a wide range of cellular functions and act in a regulatory way by performing limited proteolysis of substrates, such as enzymes and structural proteins [15, 16]. Their functional involvement ranges from remodeling cytoskeletal elements, regulating cell motility, cell cycle control, and proliferation, via controlling gene expression, inflammation, autophagy, and apoptosis, through to tuning signal transduction and synaptic plasticity in neurons [7, 17–19].

2.1.2. Calpains in Health and Disease. The important role of calpains in a healthy biological system becomes even clearer in the light of the wide-ranging implications of their malfunction in a multitude of human diseases. The deregulation of calpain function and mediation of molecular pathomechanisms by calpains were described in medical conditions such as myopathies, ophthalmic maladies, cardiovascular disorders, cancer, and neurodegeneration.

A whole group of diseases which are based on the direct dysfunctions of calpains was termed *calpainopathies*, comprising a wide spectrum of pathological manifestations [8]. Limb-girdle muscular dystrophy 2A (LGMD2A) was the first-described calpainopathy, which is caused by mutations in the gene encoding muscular calpain-3 (*CAPN3*) [20, 21]. Missense mutations in the calpain-5 gene (*CAPN5*) were associated with an autosomal-dominant form of neovascular inflammatory vitreoretinopathy (ADNIV) [22]. In cardiovascular injuries, mitochondrial calpain-1 was shown to mediate apoptotic effects [23–25]. Moreover, an intriguing association of calpains was made with diabetes, when calpain-10 was identified as a susceptibility gene for type 2 diabetes [26]. Mutations in the skin-specific calpain-12 were shown to worsen the clinical manifestation of autosomal recessive congenital ichthyosis [27].

Calpains also play a role in tumorigenesis by diversely acting on cancer cell migration, survival, and death, rendering these proteases a potential therapeutic target in oncology [28]. The proteases were shown to contribute to tumor progression and to exhibit deregulated expression patterns on one hand. On the other, calpains are acting as executioners of apoptotic cancer cell death, activated by anticancer drugs [29]. For instance, calpain-1 and calpain-2 demonstrated protumorigenic roles in HER2⁺ breast cancer models, as conditional deletion or knockout of *CSS1*, which is crucial for the activity of these conventional calpains, blocked or delayed tumorigenesis [30]. High calpain-2 expression was associated with the adverse clinical outcome of basal-like and triple-negative invasive breast cancer [31]. However, the proapoptotic or antineoplastic activity of capsaicin was found to be based on increased Ca²⁺ levels and, thereby, calpain-1 and calpain-2 activation, in models of human small cell lung cancer [32, 33].

Lastly, calpains are also implicated in neuronal injury, neurodegenerative disorders, and neuronal aging processes [1, 34]. For instance, these proteases execute Wallerian degeneration and mediate degenerative effects in traumatic brain injury [35–37]. A detrimental calpain overactivation has been detected in many neurodegenerative disorders such as AD, amyotrophic lateral sclerosis (ALS), PD, or the group of polyQ disorders [38–41]. Interestingly, calpains were associated with fragmentation of the respective disease proteins, leading to the generation of breakdown products with an increased toxicity compared to the full-length protein. This includes α -synuclein in PD or transactivation response element DNA-binding protein 43 (TDP-43) in ALS, as well as the polyQ disease proteins huntingtin in Huntington disease (HD) and ataxin-3 in Machado-Joseph disease (MJD). Resulting protein fragments were shown to be more harmful to cells or to readily form disease protein aggregates [42–46]. Consequently, inhibition of cleavage by genetically and pharmacologically targeting calpains or by rendering disease proteins cleavage-resistant ameliorated disease-related molecular and behavioral characteristics in respective models of those diseases [46–51]. Overexpression of CAST in animal models of AD and ALS showed beneficial effects by counteracting the intrinsic calpain overactivation [52–54]. Most recently, a neuronal calpainopathy was identified which is

caused by *CAPN1*-null mutations, leading to cerebellar ataxia and limb spasticity [55]. Furthermore, calpain-1 and calpain-2 seem to have opposing roles in neuronal function, mediating synaptic plasticity, and neuroprotection versus neurodegenerative effects [17]. Therefore, these circumstances have to be considered when targeting calpains for therapeutic purposes.

2.2. Autophagy

2.2.1. Autophagy Basics. Cellular homeostasis is the result of constantly ongoing self-renewing processes that assure elimination of malfunctioning or nonfunctional components, from proteins to organelles. These highly conserved processes feed into recycling mechanisms that provide the cell with nutrients and metabolites. PTMs, typically ubiquitination, can mark proteins for destruction, if they are nonfunctioning, aggregating, or long-lived, eventually handing them over to the cell's major protein-degradation pathways: the ubiquitin-proteasome system (UPS) and the autophagy lysosome pathway (ALP) [56, 57].

Classically, UPS targets are tagged with K48-linked ubiquitin chains, recognized by the 19S regulatory cap of the 26S proteasome, unfolded, and then cleaved in the 20S proteolytic core, generating small peptides [58, 59]. ALP, the other degradational system, allows specific as well as bulk degradation under energy- and nutrient-deficient conditions. This system can be subdivided into three different mechanisms: chaperone-mediated autophagy (CMA), microautophagy, and (macro-)autophagy. All of them have the shuttling of cargo to the lysosome in common, where hydrolases break the content down to single amino acids. Whereas CMA relies on a specific KFERQ pentapeptide recognition sequence for the chaperone-mediated transport to the lysosomal transporters [60, 61], microautophagy is a rather unspecific engulfment of cytoplasmic content at the lysosomal membrane [62].

Macroautophagy is characterized by the *de novo* formation of double-membrane structures that are formed in the vicinity of the endoplasmic reticulum (ER), at nucleation sites, even though the origin of the membranes is still not entirely resolved [63]. Membrane structures are created that form the phagophore (isolation membrane) by a steady growth into the vesicular structure, engulfing cellular material from proteins up to organelles. The mature autophagosomes finally fuse with lysosomes to autolysosomes, where the cargo is degraded [64]. The genes responsible for this process (autophagy-related genes, ATGs) have been found by reverse genetics in *Saccharomyces cerevisiae* and a multitude of homologues were shown to be conserved throughout many species and in humans [65]. The sensory components of this degradation mechanism are the mechanistic target of rapamycin complex 1 (mTORC1) and AMP-activated protein kinase (AMPK), which integrate signals about nutritional cues and growth factors or the energetic status of the cell, respectively. This leads to the rapid adaptation of anabolic processes and to the release of amino acids, through recycling of cellular material by their differential regulation of the

serine/threonine-protein kinase ULK1 [66, 67]. The formation of the autophagosome is classically initiated by the ULK1 (Atg1 in yeast) complex under nutrient deprivation. Beclin-1 is phosphorylated by ULK1 and VPS34 (Class III phosphatidylinositol 3-kinase (PI3K) in humans) is activated [68, 69]. In complex with VPS34, beclin-1 and ATG14 are involved in the nucleation of the phagophore and maturation of the autophagosome. The phagophore membranes are elongated via two ubiquitin-like systems (ATG12 and ATG8) by the reversible conjugation of several ATG gene products, which prime the growing ends for further protein interactions [70]. ATG5-conjugated ATG12 binds to ATG16L (E3-like protein) by E1-like (ATG7) and E2-like (ATG10) proteins. This complex at the extending phagophore allows the recruitment of the second ubiquitin-like system [71]. For this, ATG4-cleaved microtubule-associated protein 1 light chain 3 (LC3, Atg8 in yeast) is lipidated with phosphatidylethanolamine (PE). These modifications generate LC3-II [72], which is then incorporated into the double membrane. ATG7 and ATG3 function as E1-like and E2-like proteins, respectively, and LC3-II is conjugated to the ATG5/12/16L complex by ATG3, which drives the growth of the phagophore membrane [73, 74].

Autophagosomes can selectively engulf diverse forms of autophagic cargo, ranging from single proteins, over protein aggregates (aggrephagy), to whole organelles like mitochondria (mitophagy) and even proteasomes (proteaphagy) [75–78]. Cargo designated for degradation is detected by p62/SQSTM1, neighbor of BRCA1 gene 1 (NBR1), optineurin, Toll-interacting protein (TOLLIP), or other receptor proteins [78–80]. These receptors preferentially bind K63-polyubiquitin-tagged substrates and bring them in contact with the autophagosomes via a LC3-interacting region (LIR). The specific binding and the capacity of some proteins to act additionally as scaffolds for the recruitment of autophagic complexes ensure selective degradation [81].

Lastly, the mature autophagosomes fuse with lysosomes. This process requires several components, such as lysosome-associated membrane proteins (LAMPs) [82]. The degradation in the lysosome proceeds to the breakdown of proteinaceous cargo into single amino acids by cathepsins. Dysfunction of both degradative systems has been associated with neuronal aging and degeneration, bringing it into focus for therapeutic research [83].

2.2.2. Autophagy in Health and Disease. In line with its essential role in cellular homeostasis, autophagy is involved in major disease classes like cardiovascular, infectious, and metabolic disorders as well as cancer [84]. It has been generally challenging to delineate the exact roles of autophagy in cell survival and cell death [85]. Whilst this mechanism can have cell protective functions in regard to genomic integrity [86] and autophagy induction is a common therapeutic strategy in cancer, inhibition of this pathway has also shown its applicability in tumor treatment. This is mainly because autophagy can represent an escape mechanism for tumor cells and may be responsible for the development of resistances [87].

In the healthy nervous system, autophagy relieves neurons of protein and organelle damage. Moreover, it plays an important role in developmental organization processes [88], ensuring axonal homeostasis [89] and sustaining the pool of neuronal stem cells [90]. Autophagy is most vital during the neonatal starvation period and thus ubiquitous deletion of ATG core proteins results in neonatal or embryonic lethality [91]. In brain injury by hypoxia or trauma, autophagy is a critical and protective factor in cell survival, underlining its important role in the survival of neurons [92, 93]. Conditional knockout of core autophagy genes leads to decreased life span and phenotypes resembling neurodegeneration [94, 95]. Successful aging is especially relevant in postmitotic cells such as neurons [96]. The accumulation of long-lived organelles and proteins, as well as the reduced ability of cells to cope with stress imposed by those, is believed to be a major cause for late onset neurodegenerative diseases. As many different pathomechanisms may lead to neurodegeneration, various disease-specific deregulations of the autophagic pathway have been suggested [81, 97].

In several neurodegenerative disorders of the brain, an accumulation of autophagosomes and autophagic markers has been observed [84, 98, 99]. Importantly, the mere finding of an increased number of autophagosomes gives no information on whether the autophagic flux is increased or the elimination of autophagosomes is just inhibited [100]. Observations in HD have shown that patient brain and lymphoblasts feature increased numbers of autophagosomes [101, 102]. This upregulation of autophagosome formation is caused by the sequestration and inactivation of mTOR by mutant huntingtin [103] and is accompanied by a defect in cargo loading [104]. Further, critical autophagy regulating genes, such as beclin-1 and Ras homolog enriched in striatum (Rhes), show reduced function and protein levels in HD brain [105–107]. Despite an already increased autophagy and functionally disturbed autophagosomes, genetic or pharmacological induction of autophagy has, however, been proven effective in different HD models [108, 109] and comparable results were obtained for other polyQ disorders as well as for AD and PD [110–113]. On the other hand, lysosomal cathepsins, which are responsible for the degradation of cargo proteins in autophagy, were associated with cleavage of mutant huntingtin in HD or APP in AD and, thus, formation of toxic fragments. In this regard, inhibition of these proteases led to beneficial effects on the molecular disease phenotype [114, 115]. Interestingly, not only have the disease-causing proteins in polyQ disorders been found to be degraded by autophagy, but also accumulated evidence suggests a direct role of proteins like huntingtin or MJD's ataxin-3 in autophagy regulation. Huntingtin itself represents a very special case since its structure is related to several ATG proteins. Consequently, it has been implicated in the induction of autophagy [116, 117]. Huntingtin, in its physiological function, is proposed to act as a scaffold, which recruits autophagy-initiating factors and adapter proteins [117, 118]. More recent studies have also found ataxin-3 to be a regulator of autophagy initiation. Wild-type ataxin-3 is a deubiquitinase that is thought to cleave polyubiquitin chains from beclin-1, thereby saving it from

degradation and enabling autophagy [119]. By contrast, in MJD patient-derived fibroblasts, beclin-1 and autophagy levels were reduced, and beclin-1 overexpression rescued the deficit in autophagosome formation [120]. Interestingly, reduced beclin-1 levels are commonly detected in neurodegenerative disorders and aging brains, representing a limiting factor in autophagy induction and a driving factor in late onset proteinopathies [106, 121, 122].

Aside from polyQ disorders, different levels of autophagy deregulation have been reported for AD, PD, and ALS. An increased PI3K/AKT/mTOR signaling was shown in AD, as well as a defect in lysosomal clearance caused by A β [63, 121]. Autophagy induction by various means has been successfully tested in animal models of AD, and several substances have been evaluated in clinical trials [112, 123, 124]. All types of autophagy have been implicated in PD pathogenesis and macroautophagy, in particular, has been linked to mitochondrial dysfunction, due to ineffective mitophagy [125]. The PINK/parkin pathway, which is based on two proteins known to be causative for PD when mutated, regulates mitophagy and, therefore, controls mitochondrial number and quality. Moreover, the accumulation of α -synuclein has been found to interfere with mitochondrial turnover [126]. The genetic activation of autophagy by beclin-1 expression as well as pharmacological approaches were able to rescue disease phenotypes in PD animal models [113, 127, 128]. In ALS, the E478G mutation in the autophagy receptor optineurin leads to defective degradation of mitochondria [129]. Also, for the protein C9orf72, a regulatory function in autophagy induction has been proposed [130].

The general translation of findings on autophagy's role in cell and animal disease models to human patients and clinical applications poses a big challenge. Open questions remain about the exact dynamics of deregulation in autophagic processes in different neurodegenerative disorders, e.g., in terms of aging and tissue specificity. Furthermore, treatment approaches targeting mTOR and AMPK signaling pathways suffer from complications, such as pleiotropic effects or occurring toxicities. Thus, despite its compromised functionality in diseases, it is still unclear to which extent the autophagic clearance can be therapeutically exploited. In the pursuit of new targets for autophagy modulation, the calpain system could represent an approach to indirectly upregulate autophagy and thereby reestablish cell homeostasis.

2.3. Interplay between the Autophagy Pathway and the Calpain System

2.3.1. Impact of Calpains on Autophagy. Due to their limited proteolytic activity and intrinsic substrate specificity, calpains are considered as modulator proteases, allowing them to regulate protein functions and, thereby, various cellular pathways. It is, therefore, obvious that calpains exert respective modulatory effects on autophagy. In many disease conditions and models, calpains were shown to negatively regulate autophagy, making enhanced calpain activation a conceivable contributory factor in the impaired activation of this degradation pathway.

Diverse studies have shown that the impact of calpains on autophagy occurs on multiple levels, as summarized in Figure 2. For instance, the α -subunit of heterotrimeric G proteins ($G_{s\alpha}$) appears to be a substrate for calpains. Cleavage leads to its activation, which in turn activates adenylyl cyclase. This results in an accumulation of cAMP, which then culminates in the inhibition of phagophore formation through activation of phospholipase C and, consequently, increased generation of inositol triphosphate (IP₃) [131, 132]. Furthermore, ATG5 is cleaved and inactivated by calpains, leading to a disturbance of the ATG12-ATG5 complex formation and, as a consequence, of the expansion of the phagophore membrane [133, 134]. Interestingly, calpain-cleaved ATG5 was shown to translocate to mitochondria and induce apoptosis by blocking the antiapoptotic function of Bcl-xL. Thus, calpain cleavage of ATG5 constitutes a switch between autophagy and apoptosis [134]. Moreover, calpain overactivation as a result of anoxia-reoxygenation in cells or ischemia-reperfusion injuries *in vivo* demonstrated detrimental effects on autophagy via breakdown of beclin-1, ATG3, or ATG7, while calpain knockdown or overexpression of respective substrates counteracted the autophagic impairments [135–137]. Nearly all ATG proteins were shown to be cleaved by calpains *in vitro*, without characterizing, however, the biological relevance of their proteolysis [138]. Aside from proteins implicated in the proper formation of autophagosomes, calpains also target autophagy receptors, such as p62/SQSTM1 and optineurin, which may lead to a compromised cargo binding [138–140]. Autophagosome maturation might also be affected by calpains, as LAMP2 was shown to be cleaved by these proteases, leading to lysosomal permeabilization [141, 142]. Finally, due to their well-established role in microfilament dynamics, it was hypothesized that calpains may interfere with the dynamic changes of the cytoskeleton coupled to autophagosome formation [143]. Of note, the HD disease protein huntingtin, which is involved in autophagic processes, is a known calpain substrate, suggesting functional repercussions when proteolytically fragmented [43, 117, 118]. Interestingly, depletion of CSS1, whose knockout leads to early embryonic lethality in mice, induced lysosomal defects and blocked autophagy in cell-based experiments. The latter effect was attributed to the substantial calpain cleavage of Bif-1, which allows the scission of Golgi components and their targeting to nascent autophagosomes [144–146].

As neurodegenerative conditions, cancer, cardiovascular diseases, and diabetes have in common a reported deregulation of proteases and disturbances of the autophagic flux, further studies on the involvement of calpains in autophagy are of particular relevance. In the following sections, we will discuss the interplay between calpains and autophagy in a choice of those maladies.

2.3.2. Interplay of Calpains and Autophagy in Diabetes, Ischemia and Cancer. Both calpain activation and deregulated autophagy are implicated in the molecular pathomechanisms of many common health conditions with unsolved or complex etiologies. Myriads of them feature an impaired Ca²⁺ homeostasis as a primary trigger for these disturbances.

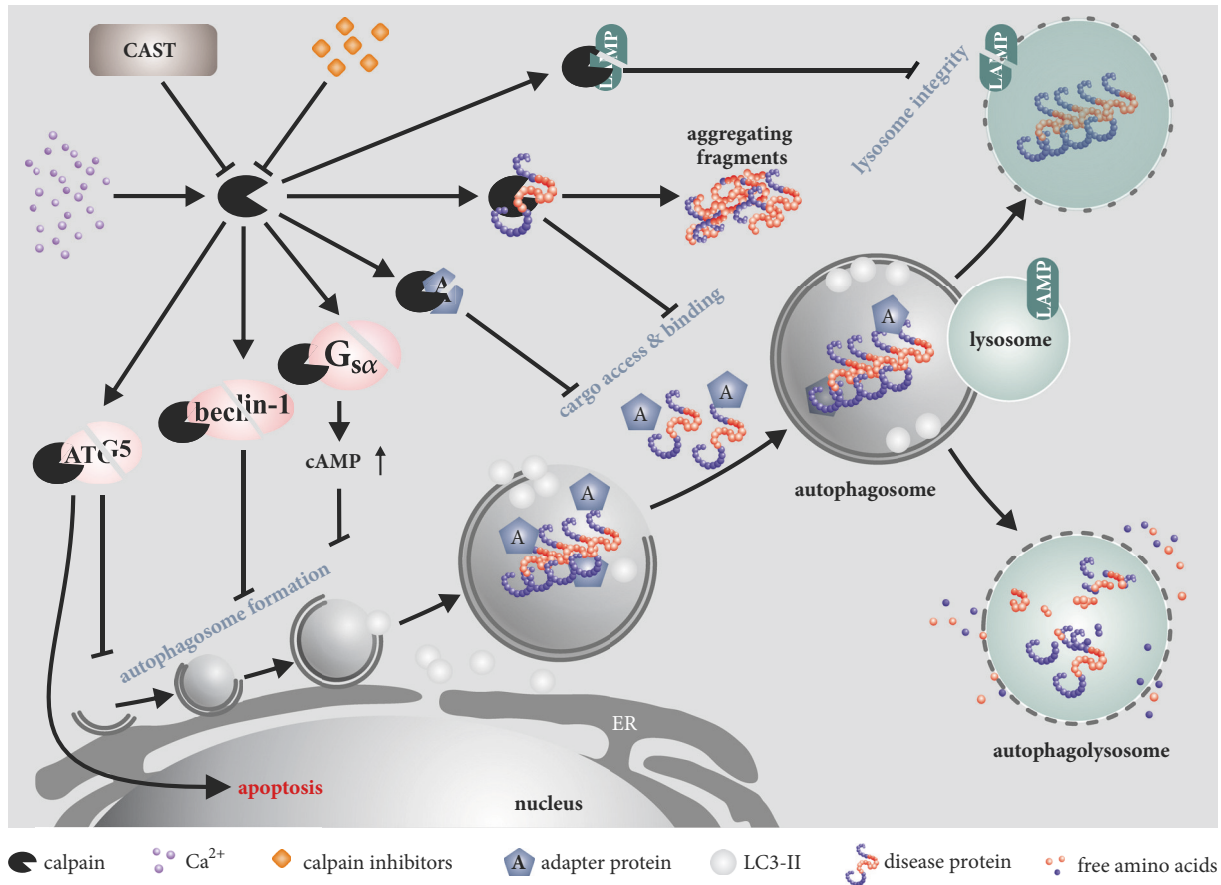


FIGURE 2: Calpain targets in the autophagic machinery. Calpains can impair protein clearance on different levels of the ALP. By cleaving signal transduction molecules, like G_{α} , or autophagic proteins, like beclin-1 and ATG5, calpains lead to a reduction of autophagy initiation and can, in the case of ATG5 cleavage, act as a switch from autophagy to apoptosis. Moreover, the cleavage of adapter proteins (optineurin, p62/SQSTM1), cargo (e.g., disease proteins), or lysosome-associated proteins (LAMPs) can change the dynamics of cargo degradation, thereby causing a defect in protein homeostasis. The inhibitory function of CAST reduces calpain activity and thereby leads to increased autophagy levels. Additionally, it prevents the cleavage of disease proteins into toxic or strongly aggregating fragments, rendering more soluble, full-length forms of the protein more accessible to autophagy.

In type 2 diabetes (T2D), amylin (or islet amyloid polypeptide, IAPP), a peptide hormone which is cosecreted with insulin in a ratio 1:100, was shown to accumulate in affected pancreatic β cells, forming amyloid deposits and, eventually, leading to cell death [147]. Autophagy has been suggested as a defending mechanism in β cells against the proteotoxicity of amylin, and a known dysfunction of the ALP in T2D may further contribute to detrimental effects [148, 149]. Interestingly, toxic amylin oligomers were shown to lead to intracellular membrane disruption, increased cytoplasmic Ca^{2+} concentrations, and, consequently, overactivation of the calpain system, specifically calpain-2, in cell models, mice, and pancreatic tissues from humans with T2D [150, 151]. This overactivation ultimately leads to critical autophagic dysfunctions [150].

Calpain overactivation is a general response during ischemia-reperfusion in many different tissues, when anaerobic metabolism decreases the active Ca^{2+} efflux and limits its reuptake by the ER, thereby producing Ca^{2+} overload in

the cell. In the eye, heart, or liver, for instance, this overload leads to the deleterious overactivation of calpains, which then excessively cleave structural and functional proteins [152–154]. Following retinal ischemic injury *in vivo*, calpains were shown to fragment and inactivate beclin-1, resulting in the deregulation of autophagy [136]. A direct impact of calpains on autophagy remains unproven in the heart muscle; however, in fatty livers, calpain-2 inhibited autophagy by cleaving ATG3 and ATG7, thereby contributing to ischemia-reperfusion injuries [137]. In livers of obese mice, a baseline impairment of autophagy, due to ATG7 depletion, was associated with a dramatic increase in calpain-2 protein expression [155].

In cancer cells, calpains are often mediating the switch between protective autophagy and desired apoptosis (e.g., via ATG5). Inhibiting their activity may be disadvantageous in anticancer treatments, whereas activating them may be beneficial [156, 157]. Investigations on human metastatic melanoma cells treated with cisplatin revealed that this

chemotherapeutic induces calpain activation and inhibits basal autophagy, while autophagy activation by calpain inhibition acts as a prosurvival response [158, 159]. A nonclassical calpain demonstrated a different effect regarding the control of the autophagy system in sarcoma cells. Knockdown of calpain-6, which is strongly upregulated in cells with tumor-initiating and metastatic capacities, suppressed autophagy as well as hypoxia-dependent prevention of senescence entry [160, 161]. The Kaposi sarcoma-associated herpesvirus inhibits autophagy and impairs monocyte differentiation into dendritic cells as an immune evasion strategy, by reducing CAST expression and consequently leading to decreased ATG5 levels [162].

2.3.3. Linking Calpain Activation and Autophagy in Neurodegeneration. The neurodegenerative disorders AD, ALS, HD, MJD, and PD exhibit an overactivation of calpains and disturbances of the autophagic pathway [1, 8, 81]. Considering the known implications of calpains in autophagy, a link between both pathways is also apparent in neurodegeneration.

In HD, calpains have been early identified as a disease modifier, being overactivated in the disease context and leading to cleavage of polyQ-expanded huntingtin [43, 49]. Likewise, a deregulation of autophagy was shown for HD, which is further emphasized by wild-type huntingtin's physiological involvement in this pathway [117, 118, 163]. A direct connection between calpain overactivation and autophagy deregulation has yet not been made for HD; however, the knockdown of a calpain homologue in an HD *Drosophila* model and CAST overexpression in HD mice reduced polyQ toxicity of an N-terminal huntingtin fragment and improved behavioral signs, by activating autophagy [164]. This upregulation of the autophagic pathway was attributed to cleavage inhibition of the calpain substrate G_{sc} , as shown earlier in cell and zebrafish models of HD [131]. Respective effects also cannot be ruled out as a contributing factor in two of our preclinical studies, where we treated two HD animal models with the experimental drug olesoxime, thereby not only reducing calpain overactivation, huntingtin fragmentation, and aggregate formation, but also ameliorating the behavioral phenotype [47, 165]. In an MJD zebrafish model, calpain inhibition reduced polyQ-expanded ataxin-3 levels in an autophagy-dependent manner [166]. In a conditional α -synuclein-expressing mouse model of PD, the environmental neurotoxin paraquat was shown to activate calpains, leading to inhibition of autolysosomal clearance and, thereby, accumulation of both calpain-cleaved and insoluble α -synuclein species [167].

Calpains were, furthermore, suggested to act as a switch between two modes of cell death in hippocampal neural stem cells, as low calpain activity triggered by insulin deprivation resulted in a preference for autophagic cell death over apoptosis [168]. In cortical neurons, autophagy was shown to fail preventing glucose deprivation/reintroduction-induced neuronal death due to lysosomal permeabilization, which resulted from a calpain-mediated LAMP2 cleavage [141].

2.4. Activating Autophagy via Calpain Inhibition as a Therapeutic Approach

2.4.1. Genetic Approaches for Calpain Inhibition to Stimulate Autophagy. In the previous paragraphs we have highlighted the relevance of calpains and autophagy in various human medical conditions, as well as the interplay of both proteolytic machineries. The fact that calpains have a direct regulatory impact on the autophagic system suggests the assumption that exclusively targeting these proteases may target both their deregulation and the autophagic dysfunction. Not having reached clinical applicability yet, multiple cell-based or *in vivo* disease models have delivered general proofs of concept using genetic or pharmacological approaches.

Typical genetic strategies comprise the overexpression of the endogenous calpain inhibitor CAST, or the knockdown and knockout of calpain isoforms as well as of CSS1. In a human IAPP transgenic mouse model of T2D, overexpression of CAST was shown to be protective against the loss and dysfunction of pancreatic β cells and preventing diabetes onset by restoring the vital ALP [150]. Moreover, the intravitreal injection of siRNA directed against CSS1 reduced calpain activation and beclin-1 cleavage in an *in vivo* model for retinal ischemic injuries [136]. In a mouse model for bone sarcoma, knockdown of the nonclassical calpain-6 blocked tumor development, and overexpression of this protease in an osteosarcoma cell line increased autophagic flux, which could rather favor tumorigenesis [161].

In models of neurodegenerative disorders, CAST overexpression and calpain knockdown were protective against toxicity of the respective disease proteins. RNAi-mediated knockdown of the calpain homologue *CalpA* in *Drosophila* models of HD and tauopathy ameliorated the disease-related phenotypes in an autophagy-dependent manner [164]. HD mice transgenic for CAST showed an activation of autophagy, leading to reduced mutant huntingtin protein and aggregate levels, attenuating disease symptoms, such as tremor and motor phenotype [164]. In line with these findings, our group showed that HD mice with ablated CAST expression presented, in addition to calpain overactivation and the consequent increase of huntingtin cleavage and aggregation, disturbances in autophagy [169]. Analogously, positive effects of CAST overexpression as well as negative consequences of an CAST knockout on disease protein toxicity were shown in further cell and mouse models of neurodegenerative disorders, such as ALS, PD, and SCA3, without, however, linking it directly to autophagy [44, 45, 48, 50, 52–54, 170].

Excessively calpain inhibition can be, nevertheless, detrimental, as the inhibition of calpain activity by CAST overexpression in mouse hearts resulted in a progressive cardiomyopathy characterized by accumulation of protein aggregates, formation of autophagosomes, and disruption of sarcomere integrity [171]. Moreover, in CAST transgenic mice, postinfarct scar healing was impaired, leading to an increased mortality [172].

2.4.2. Pharmacological Approaches for Calpain Inhibition to Stimulate Autophagy. Pharmacological inhibition of calpains for stimulating autophagy can be achieved in two modes: first,

by targeting calpains directly with specific inhibitors and, second, by aiming at calpain-activating mechanisms (i.e., primary elements of the cellular Ca^{2+} homeostasis). Accordingly, studies in different fields of clinical investigations have tested these respective approaches.

In a model for retinal ischemic injuries, administration of calpain inhibitors MDL 28170 and SJA6017 prevented calpain overactivation and cleavage of beclin-1 [136]. Pharmacological inhibition of calpain-2, not calpain-1, suppressed anoxia-reoxygenation-induced loss of autophagy proteins beclin-1 and ATG7, avoiding the onset of mitochondrial permeability transition and decreasing cell death after reoxygenation in rat hepatocytes [135]. Similar results were achieved by preventing a Ca^{2+} overload in mouse livers after ischemia-reperfusion, using the anticonvulsant/antiepileptic drug carbamazepine, which suppressed the calpain-mediated autophagic flux impairment and likewise prevented the loss of beclin-1 and ATG7 [173]. Furthermore, inhibition of calpain-2 in steatotic livers restored autophagic flux both in livers from obese rats, after ischemia-reperfusion, and in free fatty acid-treated hepatocytes [174]. In obese mice, administration of calpain inhibitors MDL 28170 and PD150606 resulted in rescued ATG7 level, eventuating in lower ER stress, enhanced hepatic insulin action, and systemic glucose tolerance [155].

In the field of polyQ diseases, diverse approved compounds have been rising as a promising reliever, through calpain inhibition, for those disorders. In PC12 and neuroblastoma cells expressing an exon 1 fragment of mutant huntingtin, inhibition of L-type Ca^{2+} ion channels (e.g., with verapamil) enhanced the autophagic clearance of the soluble and aggregated disease protein in a calpain-inhibiting manner. These effects could also be observed by direct inhibition of calpains using calpeptin [131]. In line with this, treatment of an MJD zebrafish model with calpeptin resulted in lowered mutant ataxin-3 expression by increased autophagy, which furthermore ameliorated the model's motor phenotype [166]. With regard to its significant effects on calpain activation and mutant huntingtin aggregation in two animal models of HD, the voltage-dependent anion channel-targeting experimental drug olesoxime may most likely exert positive effects on autophagy. However, respective evidence still needs to be provided [47, 165].

3. Conclusions

As presented in this review, many *in vivo* and *in vitro* studies have furnished evidence for the crosstalk between calpains and autophagy, two important proteolytic cell machineries. The interaction is grounded on calpains' functional role as *modulator proteases*, which cleave and modify the activity of multiple substrate proteins, in this context, involved in the autophagy pathway. Thereby, calpains regulate autophagy by influencing autophagosome formation, substrate recognition, and cargo degradation.

This direct mechanistic impact highlights calpains as a point of vantage for therapeutically targeting autophagy. Especially in neurodegenerative diseases, but also other medical conditions such as diabetes or ischemia, where calpains

are known to be overactivated, genetic or pharmacological strategies to inhibit these proteases can attenuate concomitant autophagic disturbances. Still, a further and broader dissection of the interplay is necessary, which may cover its potential involvement in other diseases and additional underinvestigated processes along the autophagy pathway. Notwithstanding the known detrimental effects of an exhaustive calpain inhibition or an excessive autophagy activation, the general role of calpains in autophagy regulation may present downstream advantages, either by increasing cell viability such as in diabetes and neurodegeneration, or by facilitating apoptotic cell death upon chemotherapy in cancer.

For this reason, a broad discernment on both proteolytic machineries and their intersections may be useful for understanding deregulation of calpains and autophagy in neurodegenerative diseases and beyond, thereby contributing to the development of additional treatment strategies for a multitude of medical conditions.

Conflicts of Interest

The authors declare that there are no conflicts of interest regarding the publication of this article.

Authors' Contributions

All authors contributed equally to this study.

Acknowledgments

Priscila Pereira Sena received funding from CNPq (Brazil; Process no. 229957/2013-7).

References

- [1] M. P. Mattson and T. Magnus, "Ageing and neuronal vulnerability," *Nature Reviews Neuroscience*, vol. 7, no. 4, pp. 278–294, 2006.
- [2] E.-L. Eskelinen and P. Saftig, "Autophagy: a lysosomal degradation pathway with a central role in health and disease," *Biochimica et Biophysica Acta*, vol. 1793, no. 4, pp. 664–673, 2009.
- [3] E. Jankowska, J. Stoj, P. Karpowicz, P. A. Osmulski, and M. Gaczynska, "The proteasome in health and disease," *Current Pharmaceutical Design*, vol. 19, no. 6, pp. 1010–1028, 2013.
- [4] H. Sorimachi, S. Hata, and Y. Ono, "Calpain chronicle—an enzyme family under multidisciplinary characterization," *Proceedings of the Japan Academy Series B: Physical and Biological Sciences*, vol. 87, no. 6, pp. 287–327, 2011.
- [5] G. Guroff, "A Neutral, calcium-activated proteinase from the soluble fraction of rat brain," *Journal of Biological Chemistry*, vol. 239, pp. 149–55, 1964.
- [6] T. Murachi, K. Tanaka, M. Hatanaka, and T. Murakami, "Intracellular Ca^{2+} -dependent protease (CALPAIN) and its high-molecular-weight endogenous inhibitor (CALPASTATIN)," *Advances in Enzyme Regulation*, vol. 19, pp. 407–424, 1980.
- [7] D. E. Goll, V. F. Thompson, H. Q. Li, W. Wei, and J. Y. Cong, "The calpain system," *Physiological Reviews*, vol. 83, no. 3, pp. 731–801, 2003.

- [8] Y. Ono, T. C. Saido, and H. Sorimachi, "Calpain research for drug discovery: Challenges and potential," *Nature Reviews Drug Discovery*, vol. 15, no. 12, pp. 854–876, 2016.
- [9] W. R. Dayton, D. E. Goll, M. G. Zeece, R. M. Robson, and W. J. Reville, "A Ca²⁺-activated protease possibly involved in myofibrillar protein turnover. purification from porcine muscle," *Biochemistry*, vol. 15, no. 10, pp. 2150–2158, 1976.
- [10] I. Nishiura, K. Tanaka, S. Yamato, and T. Murachi, "The occurrence of an inhibitor of Ca²⁺-dependent neutral protease in rat liver," *The Journal of Biochemistry*, vol. 84, no. 6, pp. 1657–1659, 1978.
- [11] A. Wendt, V. F. Thompson, and D. E. Goll, "Interaction of calpastatin with calpain: A review," *Biological Chemistry*, vol. 385, no. 6, pp. 465–472, 2004.
- [12] R. L. Campbell and P. L. Davies, "Structure-function relationships in calpains," *Biochemical Journal*, vol. 447, no. 3, pp. 335–351, 2012.
- [13] R. A. Hanna, R. L. Campbell, and P. L. Davies, "Calcium-bound structure of calpain and its mechanism of inhibition by calpastatin," *Nature*, vol. 456, no. 7220, pp. 409–412, 2008.
- [14] T. Moldoveanu, K. Gehring, and D. R. Green, "Concerted multi-pronged attack by calpastatin to occlude the catalytic cleft of heterodimeric calpains," *Nature*, vol. 456, no. 7220, pp. 404–408, 2008.
- [15] D. A. duVerle, Y. Ono, H. Sorimachi, and H. Mamitsuka, "Calpain cleavage prediction using multiple kernel learning," *PLoS ONE*, vol. 6, no. 5, p. e19035, 2011.
- [16] P. Tompa, P. Buzder-Lantos, A. Tantos et al., "On the sequential determinants of calpain cleavage," *The Journal of Biological Chemistry*, vol. 279, no. 20, pp. 20775–20785, 2004.
- [17] M. Baudry and X. Bi, "Calpain-1 and calpain-2: the yin and yang of synaptic plasticity and neurodegeneration," *Trends in Neurosciences*, vol. 39, no. 4, pp. 235–245, 2016.
- [18] J. Ji, L. Su, and Z. Liu, "Critical role of calpain in inflammation," *Biomedical Reports*, vol. 5, no. 6, pp. 647–652, 2016.
- [19] B. Ravikumar, S. Sarkar, J. E. Davies et al., "Regulation of mammalian autophagy in physiology and pathophysiology," *Physiological Reviews*, vol. 90, no. 4, pp. 1383–1435, 2010.
- [20] E. Gallardo, A. Saenz, and I. Illa, "Limb-girdle muscular dystrophy 2A," *Handbook of Clinical Neurology*, vol. 101, pp. 97–110, 2011.
- [21] I. Richard, O. Broux, V. Allamand et al., "Mutations in the proteolytic enzyme calpain 3 cause limb-girdle muscular dystrophy type 2A," *Cell*, vol. 81, no. 1, pp. 27–40, 1995.
- [22] V. B. Mahajan, J. M. Skeie, A. G. Bassuk et al., "Calpain-5 mutations cause autoimmune uveitis, retinal neovascularization, and photoreceptor degeneration," *PLoS Genetics*, vol. 8, no. 10, p. e1003001, 2012.
- [23] Q. Chen, M. Paillard, L. Gomez et al., "Activation of mitochondrial μ -calpain increases AIF cleavage in cardiac mitochondria during ischemia-reperfusion," *Biochemical and Biophysical Research Communications*, vol. 415, no. 4, pp. 533–538, 2011.
- [24] M. A. Smith and R. G. Schnellmann, "Calpains, mitochondria, and apoptosis," *Cardiovascular Research*, vol. 96, no. 1, pp. 32–37, 2012.
- [25] J. Thompson, Y. Hu, E. J. Lesnfsky, and Q. Chen, "Activation of mitochondrial calpain and increased cardiac injury: beyond AIF release," *American Journal of Physiology-Heart and Circulatory Physiology*, vol. 310, no. 3, pp. H376–H384, 2016.
- [26] Y. Horikawa, N. Oda, N. J. Cox et al., "Genetic variation in the gene encoding calpain-10 is associated with type 2 diabetes mellitus," *Nature Genetics*, vol. 26, no. 2, pp. 163–175, 2000.
- [27] R. Bochner, L. Samuelov, O. Sarig et al., "Calpain 12 function revealed through the study of an atypical case of autosomal recessive congenital ichthyosis," *Journal of Investigative Dermatology*, vol. 137, no. 2, pp. 385–393, 2017.
- [28] S. J. Storr, N. O. Carragher, M. C. Frame, T. Parr, and S. G. Martin, "The calpain system and cancer," *Nature Reviews Cancer*, vol. 11, no. 5, pp. 364–374, 2011.
- [29] D. Moretti, B. Del Bello, G. Allavena, and E. Maellaro, "Calpains and cancer: Friends or enemies?" *Archives of Biochemistry and Biophysics*, vol. 564, pp. 26–36, 2014.
- [30] J. A. MacLeod, Y. Gao, C. Hall, W. J. Muller, T. S. Gujral, and P. A. Greer, "Genetic disruption of calpain-1 and calpain-2 attenuates tumorigenesis in mouse models of HER2+ breast cancer and sensitizes cancer cells to doxorubicin and lapatinib," *Oncotarget*, vol. 9, no. 70, pp. 33382–33395, 2018.
- [31] S. J. Storr, K. W. Lee, C. M. Woolston et al., "Calpain system protein expression in basal-like and triple-negative invasive breast cancer," *Annals of Oncology*, vol. 23, no. 9, pp. 2289–2296, 2012.
- [32] J. R. Friedman, H. E. Perry, K. C. Brown et al., "Capsaicin synergizes with camptothecin to induce increased apoptosis in human small cell lung cancers via the calpain pathway," *Biochemical Pharmacology*, vol. 129, pp. 54–66, 2017.
- [33] J. K. Lau, K. C. Brown, A. M. Dom et al., "Capsaicin induces apoptosis in human small cell lung cancer via the TRPV6 receptor and the calpain pathway," *Apoptosis*, vol. 19, no. 8, pp. 1190–1201, 2014.
- [34] R. A. Nixon, "The calpains in aging and aging-related diseases," *Ageing Research Reviews*, vol. 2, no. 4, pp. 407–418, 2003.
- [35] M. Ma, T. A. Ferguson, K. M. Schoch et al., "Calpains mediate axonal cytoskeleton disintegration during Wallerian degeneration," *Neurobiology of Disease*, vol. 56, pp. 34–46, 2013.
- [36] K. E. Saatman, J. Creed, and R. Raghupathi, "Calpain as a therapeutic target in traumatic brain injury," *Neurotherapeutics*, vol. 7, no. 1, pp. 31–42, 2010.
- [37] J. T. Wang, Z. A. Medress, and B. A. Barres, "Axon degeneration: molecular mechanisms of a self-destruction pathway," *The Journal of Cell Biology*, vol. 196, no. 1, pp. 7–18, 2012.
- [38] A. Ferreira, "Calpain dysregulation in alzheimer's disease," *ISRN Biochemistry*, vol. 2012, Article ID 728571, 12 pages, 2012.
- [39] C. A. Matos, L. P. de Almeida, and C. Nóbrega, "Proteolytic cleavage of polyglutamine disease-causing proteins: Revisiting the toxic fragment hypothesis," *Current Pharmaceutical Design*, vol. 23, no. 5, pp. 753–775, 2017.
- [40] S. Samantaray, S. Ray, and N. Banik, "Calpain as a potential therapeutic target in parkinsons disease," *CNS & Neurological Disorders - Drug Targets*, vol. 7, no. 3, pp. 305–312, 2008.
- [41] A. L. Wright and B. Vissel, "CAST your vote: Is calpain inhibition the answer to ALS?" *Journal of Neurochemistry*, vol. 137, no. 2, pp. 140–141, 2016.
- [42] B. M. Dufty, L. R. Warner, S. T. Hou et al., "Calpain-cleavage of α -synuclein: Connecting proteolytic processing to disease-linked aggregation," *The American Journal of Pathology*, vol. 170, no. 5, pp. 1725–1738, 2007.
- [43] J. Gafni and L. M. Ellerby, "Calpain activation in huntington's disease," *The Journal of Neuroscience*, vol. 22, no. 12, pp. 4842–4849, 2002.
- [44] A. Haacke, F. U. Hartl, and P. Breuer, "Calpain inhibition is sufficient to suppress aggregation of polyglutamine-expanded ataxin-3," *The Journal of Biological Chemistry*, vol. 282, no. 26, pp. 18851–18856, 2007.

- [45] J. Hübener, J. J. Weber, C. Richter et al., "Calpain-mediated ataxin-3 cleavage in the molecular pathogenesis of spinocerebellar ataxia type 3 (SCA3)," *Human Molecular Genetics*, vol. 22, no. 3, pp. 508–518, 2013.
- [46] T. Yamashita, T. Hideyama, K. Hachiga et al., "A role for calpain-dependent cleavage of TDP-43 in amyotrophic lateral sclerosis pathology," *Nature Communications*, vol. 3, p. 1307, 2012.
- [47] L. E. Clemens, J. J. Weber, T. T. Wlodkowski et al., "Olesoxime suppresses calpain activation and mutant huntingtin fragmentation in the BACHD rat," *Brain*, vol. 138, no. 12, pp. 3632–3653, 2015.
- [48] M. Diepenbroek, N. Casadei, H. Esmer et al., "Over expression of the calpain-specific inhibitor calpastatin reduces human alpha-Synuclein processing, aggregation and synaptic impairment in [A30P]αSyn transgenic mice," *Human Molecular Genetics*, vol. 23, no. 15, pp. 3975–3989, 2014.
- [49] J. Gafni, E. Hermel, J. E. Young, C. L. Wellington, M. R. Hayden, and L. M. Ellerby, "Inhibition of calpain cleavage of Huntingtin reduces toxicity: accumulation of calpain/caspase fragments in the nucleus," *The Journal of Biological Chemistry*, vol. 279, no. 19, pp. 20211–20220, 2004.
- [50] A. T. Simões, N. Gonçalves, A. Koeppen et al., "Calpastatin-mediated inhibition of calpains in the mouse brain prevents mutant ataxin 3 proteolysis, nuclear localization and aggregation, relieving Machado-Joseph disease," *Brain*, vol. 135, no. 8, pp. 2428–2439, 2012.
- [51] J. J. Weber, M. Golla, G. Guaitoli et al., "A combinatorial approach to identify calpain cleavage sites in the Machado-Joseph disease protein ataxin-3," *Brain*, vol. 140, no. 5, pp. 1280–1299, 2017.
- [52] M. V. Rao, P. S. Mohan, C. M. Peterhoff et al., "Marked calpastatin (CAST) depletion in Alzheimer's disease accelerates cytoskeleton disruption and neurodegeneration: Neuroprotection by CAST overexpression," *The Journal of Neuroscience*, vol. 28, no. 47, pp. 12241–12254, 2008.
- [53] M. V. Rao, J. Campbell, A. Palaniappan, A. Kumar, and R. A. Nixon, "Calpastatin inhibits motor neuron death and increases survival of hSOD1G93A mice," *Journal of Neurochemistry*, vol. 137, no. 2, pp. 253–265, 2016.
- [54] M. V. Rao, M. K. McBrayer, J. Campbell et al., "Specific calpain inhibition by calpastatin prevents tauopathy and neurodegeneration and restores normal lifespan in tau P301L Mice," *The Journal of Neuroscience*, vol. 34, no. 28, pp. 9222–9234, 2014.
- [55] Y. Wang, J. Hersheson, D. Lopez et al., "Defects in the CAPN1 gene result in alterations in cerebellar development and cerebellar ataxia in mice and humans," *Cell Reports*, vol. 16, no. 1, pp. 79–91, 2016.
- [56] C. H. Ji and Y. T. Kwon, "Crosstalk and interplay between the ubiquitin-proteasome system and autophagy," *Molecules and Cells*, vol. 40, no. 7, pp. 441–449, 2017.
- [57] A. Lilienbaum, "Relationship between the proteasomal system and autophagy," *International Journal of Biochemistry and Molecular Biology*, vol. 4, no. 1, pp. 1–26, 2013.
- [58] G. L. Grice and J. A. Nathan, "The recognition of ubiquitinated proteins by the proteasome," *Cellular and Molecular Life Sciences*, vol. 73, no. 18, pp. 3497–3506, 2016.
- [59] A. Ciechanover, "Proteolysis: from the lysosome to ubiquitin and the proteasome," *Nature Reviews Molecular Cell Biology*, vol. 6, no. 1, pp. 79–87, 2005.
- [60] S. Kaushik, U. Bandyopadhyay, S. Sridhar et al., "Chaperone-mediated autophagy at a glance," *Journal of Cell Science*, vol. 124, no. 4, pp. 495–499, 2011.
- [61] J. F. Dice, "Chaperone-mediated autophagy," *Autophagy*, vol. 3, no. 4, pp. 295–299, 2007.
- [62] W. W. Li, J. Li, and J. K. Bao, "Microautophagy: lesser-known self-eating," *Cellular and Molecular Life Sciences*, vol. 69, no. 7, pp. 1125–1136, 2012.
- [63] B. Boland, A. Kumar, S. Lee et al., "Autophagy induction and autophagosome clearance in neurons: relationship to autophagic pathology in Alzheimer's disease," *The Journal of Neuroscience*, vol. 28, no. 27, pp. 6926–6937, 2008.
- [64] C. He and D. J. Klionsky, "Regulation mechanisms and signaling pathways of autophagy," *Annual Review of Genetics*, vol. 43, pp. 67–93, 2009.
- [65] Z. Xie and D. J. Klionsky, "Autophagosome formation: core machinery and adaptations," *Nature Cell Biology*, vol. 9, no. 10, pp. 1102–1109, 2007.
- [66] D. Egan, J. Kim, R. J. Shaw, and K.-L. Guan, "The autophagy initiating kinase ULK1 is regulated via opposing phosphorylation by AMPK and mTOR," *Autophagy*, vol. 7, no. 6, pp. 643–644, 2011.
- [67] J. Kim, M. Kundu, B. Viollet, and K. Guan, "AMPK and mTOR regulate autophagy through direct phosphorylation of Ulk1," *Nature Cell Biology*, vol. 13, no. 2, pp. 132–141, 2011.
- [68] J.-M. Park, C. H. Jung, M. Seo et al., "The ULK1 complex mediates MTORC1 signaling to the autophagy initiation machinery via binding and phosphorylating ATG14," *Autophagy*, vol. 12, no. 3, pp. 547–564, 2016.
- [69] R. C. Russell, Y. Tian, H. Yuan et al., "ULK1 induces autophagy by phosphorylating Beclin-1 and activating VPS34 lipid kinase," *Nature Cell Biology*, vol. 15, no. 7, pp. 741–750, 2013.
- [70] Y. Ohsumi, "Molecular dissection of autophagy: Two ubiquitin-like systems," *Nature Reviews Molecular Cell Biology*, vol. 2, no. 3, pp. 211–216, 2001.
- [71] N. Fujita, T. Itoh, H. Omori, M. Fukuda, T. Noda, and T. Yoshimori, "The Atg16L complex specifies the site of LC3 lipidation for membrane biogenesis in autophagy," *Molecular Biology of the Cell (MBoC)*, vol. 19, no. 5, pp. 2092–2100, 2008.
- [72] J. Hemelaar, V. S. Lelyveld, B. M. Kessler, and H. L. Ploegh, "A single protease, Apg4B, is specific for the autophagy-related ubiquitin-like proteins GATE-16, MAPI-LC3, GABARAP, and Apg8L," *The Journal of Biological Chemistry*, vol. 278, no. 51, pp. 51841–51850, 2003.
- [73] N. Mizushima, A. Kuma, Y. Kobayashi et al., "Mouse Apg16L, a novel WD-repeat protein, targets to the autophagic isolation membrane with the Apg12-Apg5 conjugate," *Journal of Cell Science*, vol. 116, no. 9, pp. 1679–1688, 2003.
- [74] N. Mizushima, A. Yamamoto, M. Hatano et al., "Dissection of autophagosome formation using Apg5-deficient mouse embryonic stem cells," *The Journal of Cell Biology*, vol. 152, no. 4, pp. 657–667, 2001.
- [75] V. Cohen-Kaplan, I. Livneh, N. Avni et al., "p62- and ubiquitin-dependent stress-induced autophagy of the mammalian 26S proteasome," *Proceedings of the National Academy of Sciences of the United States of America*, vol. 113, no. 47, pp. E7490–E7499, 2016.
- [76] L. Galluzzi, E. H. Baehrecke, A. Ballabio et al., "Molecular definitions of autophagy and related processes," *EMBO Journal*, vol. 36, no. 13, pp. 1811–1836, 2017.
- [77] I. Kim, S. Rodriguez-Enriquez, and J. J. Lemasters, "Selective degradation of mitochondria by mitophagy," *Archives of Biochemistry and Biophysics*, vol. 462, no. 2, pp. 245–253, 2007.

- [78] T. Johansen and T. Lamark, "Selective autophagy mediated by autophagic adapter proteins," *Autophagy*, vol. 7, no. 3, pp. 279–296, 2011.
- [79] A. Stolz, A. Ernst, and I. Dikic, "Cargo recognition and trafficking in selective autophagy," *Nature Cell Biology*, vol. 16, no. 6, pp. 495–501, 2014.
- [80] K. Lu, I. Psakhye, and S. Jentsch, "A new class of ubiquitin-Atg8 receptors involved in selective autophagy and polyQ protein clearance," *Autophagy*, vol. 10, no. 12, pp. 2381–2382, 2014.
- [81] F. M. Menzies, A. Fleming, A. Caricasole et al., "Autophagy and Neurodegeneration: Pathogenic Mechanisms and Therapeutic Opportunities," *Neuron*, vol. 93, no. 5, pp. 1015–1034, 2017.
- [82] Y. Tanaka, G. Guhde, A. Suter et al., "Accumulation of autophagic vacuoles and cardiomyopathy LAMP-2-deficient mice," *Nature*, vol. 406, no. 6798, pp. 902–906, 2000.
- [83] A. Ciechanover and Y. T. Kwon, "Degradation of misfolded proteins in neurodegenerative diseases: therapeutic targets and strategies," *Experimental & Molecular Medicine*, vol. 47, no. 3, p. e147, 2015.
- [84] N. Mizushima, B. Levine, A. M. Cuervo, and D. J. Klionsky, "Autophagy fights disease through cellular self-digestion," *Nature*, vol. 451, no. 7182, pp. 1069–1075, 2008.
- [85] G. Kroemer and B. Levine, "Autophagic cell death: the story of a misnomer," *Nature Reviews Molecular Cell Biology*, vol. 9, no. 12, pp. 1004–1010, 2008.
- [86] A. T. Vessoni, E. C. Filippi-Chiela, C. F. M. Menck, and G. Lenz, "Autophagy and genomic integrity," *Cell Death & Differentiation*, vol. 20, no. 11, pp. 1444–1454, 2013.
- [87] J. M. M. Levy, C. G. Towers, and A. Thorburn, "Targeting autophagy in cancer," *Nature Reviews Cancer*, vol. 17, no. 9, pp. 528–542, 2017.
- [88] G. Maria Fimia, A. Stoykova, A. Romagnoli et al., "Ambral regulates autophagy and development of the nervous system," *Nature*, vol. 447, no. 7148, pp. 1121–1125, 2007.
- [89] M. Komatsu, J. W. Qing, G. R. Holstein et al., "Essential role for autophagy protein Atg7 in the maintenance of axonal homeostasis and the prevention of axonal degeneration," *Proceedings of the National Academy of Sciences of the United States of America*, vol. 104, no. 36, pp. 14489–14494, 2007.
- [90] C. Wang, C.-C. Liang, Z. C. Bian, Y. Zhu, and J.-L. Guan, "FIP200 is required for maintenance and differentiation of postnatal neural stem cells," *Nature Neuroscience*, vol. 16, no. 5, pp. 532–542, 2013.
- [91] A. Kuma, M. Hatano, M. Matsui et al., "The role of autophagy during the early neonatal starvation period," *Nature*, vol. 432, no. 7020, pp. 1032–1036, 2004.
- [92] S. Carloni, G. Buonocore, and W. Balduini, "Protective role of autophagy in neonatal hypoxia-ischemia induced brain injury," *Neurobiology of Disease*, vol. 32, no. 3, pp. 329–339, 2008.
- [93] S. Erlich, A. Alexandrovich, E. Shohami, and R. Pinkas-Kramarski, "Rapamycin is a neuroprotective treatment for traumatic brain injury," *Neurobiology of Disease*, vol. 26, no. 1, pp. 86–93, 2007.
- [94] T. Hara, K. Nakamura, M. Matsui et al., "Suppression of basal autophagy in neural cells causes neurodegenerative disease in mice," *Nature*, vol. 441, no. 7095, pp. 885–889, 2006.
- [95] M. Komatsu, S. Waguri, T. Chiba et al., "Loss of autophagy in the central nervous system causes neurodegeneration in mice," *Nature*, vol. 441, no. 7095, pp. 880–884, 2006.
- [96] D. C. Rubinsztein, G. Mariño, and G. Kroemer, "Autophagy and aging," *Cell*, vol. 146, no. 5, pp. 682–695, 2011.
- [97] E. Wong and A. M. Cuervo, "Autophagy gone awry in neurodegenerative diseases," *Nature Neuroscience*, vol. 13, no. 7, pp. 805–811, 2010.
- [98] D. C. Rubinsztein, M. DiFiglia, N. Heintz et al., "Autophagy and its possible roles in nervous system diseases, damage and repair," *Autophagy*, vol. 1, no. 1, pp. 11–22, 2005.
- [99] A. Sittler, M.-P. Muriel, M. Marinello, A. Brice, W. den Dunnen, and S. Alves, "Deregulation of autophagy in postmortem brains of Machado-Joseph disease patients," *Neuropathology*, vol. 38, no. 2, pp. 113–124, 2018.
- [100] X.-J. Zhang, S. Chen, K.-X. Huang, and W.-D. Le, "Why should autophagic flux be assessed?" *Acta Pharmacologica Sinica*, vol. 34, no. 5, pp. 595–599, 2013.
- [101] E. Sapp, C. Schwarz, K. Chase et al., "Huntingtin localization in brains of normal and Huntington's disease patients," *Annals of Neurology*, vol. 42, no. 4, pp. 604–612, 1997.
- [102] E. Nagata, A. Sawa, C. A. Ross, and S. H. Snyder, "Autophagosome-like vacuole formation in Huntington's disease lymphoblasts," *NeuroReport*, vol. 15, no. 8, pp. 1325–1328, 2004.
- [103] S. Sarkar and D. C. Rubinsztein, "Huntington's disease: Degradation of mutant huntingtin by autophagy," *FEBS Journal*, vol. 275, no. 17, pp. 4263–4270, 2008.
- [104] M. Martinez-Vicente, Z. Tallozy, E. Wong et al., "Cargo recognition failure is responsible for inefficient autophagy in Huntington's disease," *Nature Neuroscience*, vol. 13, no. 5, pp. 567–576, 2010.
- [105] A. Hodges, A. D. Strand, A. K. Aragaki et al., "Regional and cellular gene expression changes in human Huntington's disease brain," *Human Molecular Genetics*, vol. 15, no. 6, pp. 965–977, 2006.
- [106] M. Shibata, T. Lu, T. Furuya et al., "Regulation of intracellular accumulation of mutant huntingtin by beclin 1," *The Journal of Biological Chemistry*, vol. 281, no. 20, pp. 14474–14485, 2006.
- [107] S. Subramaniam and S. H. Snyder, "Huntington's Disease is a disorder of the corpus striatum: Focus on Rhes (Ras homologue enriched in the striatum)," *Neuropharmacology*, vol. 60, no. 7–8, pp. 1187–1192, 2011.
- [108] S. Sarkar, B. Ravikumar, R. A. Floto, and D. C. Rubinsztein, "Rapamycin and mTOR-independent autophagy inducers ameliorate toxicity of polyglutamine-expanded huntingtin and related proteinopathies," *Cell Death & Differentiation*, vol. 16, no. 1, pp. 46–56, 2009.
- [109] B. Ravikumar, C. Vacher, Z. Berger et al., "Inhibition of mTOR induces autophagy and reduces toxicity of polyglutamine expansions in fly and mouse models of Huntington disease," *Nature Genetics*, vol. 36, no. 6, pp. 585–595, 2004.
- [110] A. Fleming, T. Noda, T. Yoshimori, and D. C. Rubinsztein, "Chemical modulators of autophagy as biological probes and potential therapeutics," *Nature Chemical Biology*, vol. 7, no. 1, pp. 9–17, 2011.
- [111] F. M. Menzies, J. Huebener, M. Renna, M. Bonin, O. Riess, and D. C. Rubinsztein, "Autophagy induction reduces mutant ataxin-3 levels and toxicity in a mouse model of spinocerebellar ataxia type 3," *Brain*, vol. 133, no. 1, pp. 93–104, 2010.
- [112] P. Spilman, N. Podlutskaya, M. J. Hart et al., "Inhibition of mTOR by rapamycin abolishes cognitive deficits and reduces amyloid-beta levels in a mouse model of Alzheimer's disease," *PLoS ONE*, vol. 5, no. 4, p. e9979, 2010.
- [113] B. Spencer, R. Potkar, M. Trejo et al., "Beclin 1 gene transfer activates autophagy and ameliorates the neurodegenerative pathology in α -synuclein models of Parkinson's and Lewy body

- diseases," *The Journal of Neuroscience*, vol. 29, no. 43, pp. 13578–13588, 2009.
- [114] M. S. Kindy, J. Yu, H. Zhu, S. S. El-Amouri, V. Hook, and G. R. Hook, "Deletion of the cathepsin B gene improves memory deficits in a transgenic alzheimer's disease mouse model expressing A β PP containing the wild-type β -secretase site sequence," *Journal of Alzheimer's Disease*, vol. 29, no. 4, pp. 827–840, 2012.
- [115] T. Ratovitski, E. Chighladze, E. Waldron, R. R. Hirschhorn, and C. A. Ross, "Cysteine proteases bleomycin hydrolase and cathepsin Z mediate N-terminal proteolysis and toxicity of mutant huntingtin," *The Journal of Biological Chemistry*, vol. 286, no. 14, pp. 12578–12589, 2011.
- [116] J. S. Steffan, "Does Huntingtin play a role in selective macroautophagy?" *Cell Cycle*, vol. 9, no. 17, pp. 3401–3413, 2010.
- [117] J. Ochaba, T. Lukacsovich, G. Csikos et al., "Potential function for the Huntingtin protein as a scaffold for selective autophagy," *Proceedings of the National Academy of Sciences of the United States of America*, vol. 111, no. 47, pp. 16889–16894, 2014.
- [118] Y.-N. Rui, Z. Xu, B. Patel et al., "Huntingtin functions as a scaffold for selective macroautophagy," *Nature Cell Biology*, vol. 17, no. 3, pp. 262–275, 2015.
- [119] A. Ashkenazi, C. F. Bento, T. Ricketts et al., "Polyglutamine tracts regulate beclin 1-dependent autophagy," *Nature*, vol. 545, no. 7652, pp. 108–111, 2017.
- [120] I. Onofre, N. Mendonça, S. Lopes et al., "Fibroblasts of Machado Joseph Disease patients reveal autophagy impairment," *Scientific Reports*, vol. 6, no. 1, p. 28220, 2016.
- [121] M. M. Lipinski, B. Zheng, T. Lu et al., "Genome-wide analysis reveals mechanisms modulating autophagy in normal brain aging and in Alzheimer's disease," *Proceedings of the National Academy of Sciences of the United States of America*, vol. 107, no. 32, pp. 14164–14169, 2010.
- [122] F. Pickford, E. Masliah, M. Britschgi et al., "The autophagy-related protein beclin 1 shows reduced expression in early Alzheimer disease and regulates amyloid β accumulation in mice," *The Journal of Clinical Investigation*, vol. 118, no. 6, pp. 2190–2199, 2008.
- [123] M. S. Uddin, A. Stachowiak, A. Al Mamun et al., "Autophagy and Alzheimer's disease: From molecular mechanisms to therapeutic implications," *Frontiers in Aging Neuroscience*, vol. 10, p. 04, 2018.
- [124] D.-S. Yang, P. Stavrides, P. S. Mohan et al., "Reversal of autophagy dysfunction in the TgCRND8 mouse model of Alzheimer's disease ameliorates amyloid pathologies and memory deficits," *Brain*, vol. 134, no. 1, pp. 258–277, 2011.
- [125] F. Gao, J. Yang, D. Wang et al., "Mitophagy in parkinson's disease: pathogenic and therapeutic implications," *Frontiers in Neurology*, vol. 8, p. 527, 2017.
- [126] B. Wang, N. Abraham, G. Gao, and Q. Yang, "Dysregulation of autophagy and mitochondrial function in Parkinson's disease," *Translational Neurodegeneration*, vol. 5, no. 1, p. 19, 2016.
- [127] C. Malagelada, Z. H. Jin, V. Jackson-Lewis, S. Przedborski, and L. A. Greene, "Rapamycin protects against neuron death in vitro and in vivo models of Parkinson's disease," *The Journal of Neuroscience*, vol. 30, no. 3, pp. 1166–1175, 2010.
- [128] E. Santini, M. Heiman, P. Greengard, E. Valjent, and G. Fisone, "Inhibition of mTOR signaling in parkinson's disease prevents L-DOPA-induced dyskinesia," *Science Signaling*, vol. 2, no. 80, p. ra36, 2009.
- [129] Y. C. Wong and E. L. F. Holzbaur, "Optineurin is an autophagy receptor for damaged mitochondria in parkin-mediated mitophagy that is disrupted by an ALS-linked mutation," *Proceedings of the National Academy of Sciences of the United States of America*, vol. 111, no. 42, pp. E4439–E4448, 2014.
- [130] P. M. Sullivan, X. Zhou, A. M. Robins et al., "The ALS/FTLD associated protein C9orf72 associates with SMCR8 and WDR41 to regulate the autophagy-lysosome pathway," *Acta Neuropathologica Communications*, vol. 4, no. 1, p. 51, 2016.
- [131] A. Williams, S. Sarkar, P. Cuddon et al., "Novel targets for Huntington's disease in an mTOR-independent autophagy pathway," *Nature Chemical Biology*, vol. 4, no. 5, pp. 295–305, 2008.
- [132] P. Rivero-Ríos, J. Madero-Pérez, B. Fernández, and S. Hilfiker, "Targeting the autophagy/lysosomal degradation pathway in Parkinson's disease," *Current Neuropharmacology*, vol. 14, no. 3, pp. 238–249, 2016.
- [133] H. G. Xia, L. Zhang, G. Chen et al., "Control of basal autophagy by calpain1 mediated cleavage of ATG5," *Autophagy*, vol. 6, no. 1, pp. 61–66, 2010.
- [134] S. Yousefi, R. Perozzo, I. Schmid et al., "Calpain-mediated cleavage of Atg5 switches autophagy to apoptosis," *Nature Cell Biology*, vol. 8, no. 10, pp. 1124–1132, 2006.
- [135] J.-S. Kim, T. Nitta, D. Mohuczy et al., "Impaired autophagy: a mechanism of mitochondrial dysfunction in anoxic rat hepatocytes," *Hepatology*, vol. 47, no. 5, pp. 1725–1736, 2008.
- [136] R. Russo, L. Berliocchi, A. Adornetto et al., "Calpain-mediated cleavage of Beclin-1 and autophagy deregulation following retinal ischemic injury in vivo," *Cell Death & Disease*, vol. 2, no. 4, p. e144, 2011.
- [137] Q. Zhao, Z. Guo, W. Deng et al., "Calpain 2-mediated autophagy defect increases susceptibility of fatty livers to ischemia-reperfusion injury," *Cell Death & Disease*, vol. 7, no. 4, p. e2186, 2016.
- [138] J. M. Norman, G. M. Cohen, and E. T. W. Bampton, "The in vitro cleavage of the hAtg proteins by cell death proteases," *Autophagy*, vol. 6, no. 8, pp. 1042–1056, 2010.
- [139] A. Colunga, D. Bollino, A. Schech, and L. Aurelian, "Calpain-dependent clearance of the autophagy protein p62/SQSTM1 is a contributor to Δ pK oncolytic activity in melanoma," *Gene Therapy*, vol. 21, no. 4, pp. 371–378, 2014.
- [140] C. Kim, N. Yun, Y. M. Lee et al., "Gel-Based protease proteomics for identifying the novel calpain substrates in dopaminergic neuronal cell," *The Journal of Biological Chemistry*, vol. 288, no. 51, pp. 36717–36732, 2013.
- [141] C. Gerónimo-Olvera, T. Montiel, R. Rincon-Heredia, S. Castro-Obregón, and L. Massieu, "Autophagy fails to prevent glucose deprivation/glucose reintroduction-induced neuronal death due to calpain-mediated lysosomal dysfunction in cortical neurons," *Cell death & disease*, vol. 8, no. 6, p. e2911, 2017.
- [142] G. E. Villalpando Rodriguez and A. Torriglia, "Calpain 1 induce lysosomal permeabilization by cleavage of lysosomal associated membrane protein 2," *Biochimica et Biophysica Acta (BBA) - Molecular Cell Research*, vol. 1833, no. 10, pp. 2244–2253, 2013.
- [143] F. Demarchi, C. Bertoli, T. Copetti, E.-L. Eskelinen, and C. Schneider, "Calpain as a novel regulator of autophagosome formation," *Autophagy*, vol. 3, no. 3, pp. 235–237, 2007.
- [144] F. Demarchi, C. Bertoli, T. Copetti et al., "Calpain is required for macroautophagy in mammalian cells," *The Journal of Cell Biology*, vol. 175, no. 4, pp. 595–605, 2006.
- [145] E. Marcassa, M. Raimondi, T. Anwar et al., "Calpain mobilizes Atg9/Bif-1 vesicles from golgi stacks upon autophagy induction by thapsigargin," *Biology Open*, vol. 6, no. 5, pp. 551–562, 2017.

- [146] U.-J. P. Zimmerman, L. Boring, U. H. Pak, N. Mukerjee, and K. K. W. Wang, "The calpain small subunit gene is essential: Its inactivation results in embryonic lethality," *IUBMB Life*, vol. 50, no. 1, pp. 63–68, 2000.
- [147] K. Pillay and P. Govender, "Amylin uncovered: A review on the polypeptide responsible for type II diabetes," *BioMed Research International*, vol. 2013, Article ID 826706, 17 pages, 2013.
- [148] M. Masini, M. Bugliani, R. Lupi et al., "Autophagy in human type 2 diabetes pancreatic beta cells," *Diabetologia*, vol. 52, no. 6, pp. 1083–1086, 2009.
- [149] J. F. Rivera, S. Costes, T. Gurlo, C. G. Glabe, and P. C. Butler, "Autophagy defends pancreatic β cells from human islet amyloid polypeptide-induced toxicity," *The Journal of Clinical Investigation*, vol. 124, no. 8, pp. 3489–3500, 2014.
- [150] T. Gurlo, S. Costes, J. D. Hoang, J. F. Rivera, A. E. Butler, and P. C. Butler, " β Cell-specific increased expression of calpastatin prevents diabetes induced by islet amyloid polypeptide toxicity," *JCI Insight*, vol. 1, no. 18, p. e89590, 2016.
- [151] C. J. Huang, T. Gurlo, L. Haataja et al., "Calcium-activated calpain-2 is a mediator of beta cell dysfunction and apoptosis in type 2 diabetes," *The Journal of Biological Chemistry*, vol. 285, no. 1, pp. 339–348, 2010.
- [152] M. V. Hoang, L. E. Smith, and D. R. Senger, "Calpain inhibitors reduce retinal hypoxia in ischemic retinopathy by improving neovascular architecture and functional perfusion," *Biochimica et Biophysica Acta (BBA) - Molecular Basis of Disease*, vol. 1812, no. 4, pp. 549–557, 2011.
- [153] V. Kohli, W. Gao, C. A. Camargo, and P. A. Clavien, "Calpain is a mediator of preservation-reperfusion injury in rat liver transplantation," *Proceedings of the National Academy of Sciences of the United States of America*, vol. 94, no. 17, pp. 9354–9359, 1997.
- [154] C. Neuhof and H. Neuhof, "Calpain system and its involvement in myocardial ischemia and reperfusion injury," *World Journal of Cardiology*, vol. 6, no. 7, pp. 638–652, 2014.
- [155] L. Yang, P. Li, S. Fu, E. S. Calay, and G. S. Hotamisligil, "Defective hepatic autophagy in obesity promotes ER stress and causes insulin resistance," *Cell Metabolism*, vol. 11, no. 6, pp. 467–478, 2010.
- [156] S. K. Bhutia, R. Dash, S. K. Das et al., "Mechanism of autophagy to apoptosis switch triggered in prostate cancer cells by antitumor cytokine melanoma differentiation-associated gene 7/interleukin-24," *Cancer Research*, vol. 70, no. 9, pp. 3667–3676, 2010.
- [157] S. Lépine, J. C. Allegood, Y. Edmonds, S. Milstien, and S. Spiegel, "Autophagy induced by deficiency of sphingosine-1-phosphate phosphohydrolase 1 is switched to apoptosis by calpain-mediated autophagy-related gene 5 (Atg5) cleavage," *The Journal of Biological Chemistry*, vol. 286, no. 52, pp. 44380–44390, 2011.
- [158] B. Del Bello, D. Moretti, A. Gamberucci, and E. Maellaro, "Cross-talk between calpain and caspase-3/-7 in cisplatin-induced apoptosis of melanoma cells: A major role of calpain inhibition in cell death protection and p53 status," *Oncogene*, vol. 26, no. 19, pp. 2717–2726, 2007.
- [159] B. Del Bello, M. Toscano, D. Moretti, and E. Maellaro, "Cisplatin-induced apoptosis inhibits autophagy, which acts as a pro-survival mechanism in human melanoma cells," *PLoS ONE*, vol. 8, no. 2, p. e57236, 2013.
- [160] A. Marion, F.-X. Dieudonné, A. Patiño-García, F. Lecanda, P. J. Marie, and D. Modrowski, "Calpain-6 is an endothelin-1 signaling dependent protective factor in chemoresistant osteosarcoma," *International Journal of Cancer*, vol. 130, no. 11, pp. 2514–2525, 2012.
- [161] C. Andrique, L. Morardet, L. K. Linares et al., "Calpain-6 controls the fate of sarcoma stem cells by promoting autophagy and preventing senescence," *JCI Insight*, vol. 3, no. 17, 2018.
- [162] R. Santarelli, M. Granato, G. Pentassuglia et al., "KSHV reduces autophagy in THP-1 cells and in differentiating monocytes by decreasing CAST/calpastatin and ATG5 expression," *Autophagy*, vol. 12, no. 12, pp. 2311–2325, 2016.
- [163] D. D. O. Martin, R. J. Heit, M. C. Yap, M. W. Davidson, M. R. Hayden, and L. G. Berthiaume, "Identification of a post-translationally myristoylated autophagy-inducing domain released by caspase cleavage of huntingtin," *Human Molecular Genetics*, vol. 23, no. 12, pp. 3166–3179, 2014.
- [164] F. M. Menzies, M. Garcia-Arencibia, S. Imarisio et al., "Calpain inhibition mediates autophagy-dependent protection against polyglutamine toxicity," *Cell Death & Differentiation*, vol. 22, no. 3, pp. 433–444, 2015.
- [165] J. J. Weber, M. M. Ortiz Rios, O. Riess, L. E. Clemens, and H. P. Nguyen, "The calpain-suppressing effects of olesoxime in Huntington's disease," *Rare Diseases*, vol. 4, no. 1, p. e1153778, 2016.
- [166] M. Watchon, K. C. Yuan, N. Mackovski et al., "Calpain inhibition is protective in machado-joseph disease zebrafish due to induction of autophagy," *The Journal of Neuroscience*, vol. 37, no. 32, pp. 7782–7794, 2017.
- [167] S. Nuber, D. Tadros, J. Fields et al., "Environmental neurotoxic challenge of conditional alpha-synuclein transgenic mice predicts a dopaminergic olfactory-striatal interplay in early PD," *Acta Neuropathologica*, vol. 127, no. 4, pp. 477–494, 2014.
- [168] K. M. Chung, H. Park, S. Jung et al., "Calpain determines the propensity of adult hippocampal neural stem cells to autophagic cell death following insulin withdrawal," *Stem Cells*, vol. 33, no. 10, pp. 3052–3064, 2015.
- [169] J. J. Weber, S. J. Kloock, M. Nagel et al., "Calpastatin ablation aggravates the molecular phenotype in cell and animal models of Huntington disease," *Neuropharmacology*, vol. 133, pp. 94–106, 2018.
- [170] M. L. Tradewell and H. D. Durham, "Calpastatin reduces toxicity of SODIG93A in a culture model of amyotrophic lateral sclerosis," *NeuroReport*, vol. 21, no. 15, pp. 976–979, 2010.
- [171] A. S. Galvez, A. Diwan, A. M. Odley et al., "Cardiomyocyte degeneration with calpain deficiency reveals a critical role in protein homeostasis," *Circulation Research*, vol. 100, no. 7, pp. 1071–1078, 2007.
- [172] F. Wan, E. Letavernier, C. J. Le Saux et al., "Calpastatin overexpression impairs postinfarct scar healing in mice by compromising reparative immune cell recruitment and activation," *American Journal of Physiology-Heart and Circulatory Physiology*, vol. 309, no. 11, pp. H1883–H1893, 2015.
- [173] J.-S. Kim, J.-H. Wang, T. G. Biel et al., "Carbamazepine suppresses calpain-mediated autophagy impairment after ischemia/reperfusion in mouse livers," *Toxicology and Applied Pharmacology*, vol. 273, no. 3, pp. 600–610, 2013.
- [174] A. Liu, E. Guo, J. Yang et al., "Ischemic preconditioning attenuates ischemia/reperfusion injury in rat steatotic liver: Role of heme oxygenase-1-mediated autophagy," *Oncotarget*, vol. 7, no. 48, pp. 78372–78386, 2016.



Olfactory bulb atrophy and caspase activation observed in the BACHD rat models of Huntington disease

M. Lessard-Beaudoin^{a,1}, L. Yu-Taeger^{b,c,1}, M. Laroche^a, E. Singer^b, O. Riess^b, H.H.P. Nguyen^{b,c}, R.K. Graham^{a,*}

^a Research Center on Aging, Department of Pharmacology and Physiology, University of Sherbrooke, Sherbrooke, Canada

^b Institute for Medical Genetics and Applied Genomics, University of Tuebingen, Tuebingen, Germany

^c Department of Human Genetics, Ruhr University, Bochum, Germany

ARTICLE INFO

Keywords:

Caspases
Olfactory system
Apoptosis
Huntington disease
BACHD rats

ABSTRACT

Olfactory dysfunction is observed in several neurological disorders, including Huntington disease (HD), and correlates with global cognitive performance, depression and degeneration of olfactory regions in the brain. Despite clear evidence demonstrating olfactory dysfunction in HD patients, only limited details are available in murine models and the underlying mechanisms are unknown. In order to determine if alterations in the olfactory bulb (OB) are observed in HD we assessed OB weight or area from 3 to 12 months of age in the BACHD transgenic lines (TG5 and TG9). A significant decrease in the OB was observed at 6 and 12 months of age compared to WT. We also detected increased mRNA and protein expression of mutant huntingtin (mHTT) in the OB of TG5 compared to TG9 at specific ages. Despite the higher expression of mHTT in the TG5 OBs, there was increased nuclear accumulation of mHTT in the OB of TG9 compared to WT and TG5 rats. As we observed atrophy of the OB in the BACHD rats we assessed for caspase activation, a known mechanism underlying the cell death observed in HD. We characterized caspase-3, -6, -8 and -9 mRNA and protein expression levels in the OB of the BACHD transgenic lines at 3, 6 and 12 months of age. Alterations in caspase mRNA and protein expression were detected in the TG5 and TG9 lines. However, the changes observed in the mRNA and protein levels are in some cases discordant, suggesting that the caspase protein modifications detected may be more attributable to post-translational modifications. The caspase activation studies support that cell death may be increased in the rodent HD OB and further our understanding of the olfactory dysfunction and the role of caspases in the pathogenesis of HD.

1. Introduction

Huntington disease (HD), an autosomal dominant neurodegenerative disease caused by expansion of CAG repeats in exon 1 of the HD gene named as *HTT*, results in motor (Jankovic and Roos, 2014), cognitive and psychiatric symptoms (Burns et al., 1990; Cummings, 1995; Ross et al., 2014). Furthermore, substantial data in the literature demonstrates that olfactory dysfunction is observed in HD (Bylsma et al., 1997; Hamilton et al., 1999; Larsson et al., 2006; Nordin et al., 1995; Tabrizi et al., 2009) and indeed that it may be an early symptom and prior to the onset of motor symptoms (Moberg et al., 1987; Paulsen

et al., 2008; Paulsen et al., 2014; Pirogovsky et al., 2007; Tabrizi et al., 2009). The olfactory deficits observed in HD include a decrease in olfactory sensitivity, odor discrimination, odor recognition memory and odor identification ability compared to healthy controls (Bacon Moore et al., 1999; Moberg and Doty, 1997; Moberg et al., 1987; Nordin et al., 1995). Moreover, in HD patients, the quality of odor discrimination negatively correlates with the number of CAG repetitions in the HD gene (Larsson et al., 2006). Olfactory dysfunction is also observed in other neurodegenerative diseases and is accompanied by structural abnormalities of the olfactory epithelium, the olfactory bulb (OB) and the olfactory cortices (Barresi et al., 2012; Doty, 2012a; Menalled et al.,

Abbreviation: HD, Huntington disease; BAC, Bacterial artificial chromosome; OB, olfactory bulb; HTT, huntingtin; mHTT, mutant huntingtin; WT, wild-type; Trp, transient Receptor Potential; GCL, granule cell layer; IPL, internal plexiform layer; EPL, external plexiform layer; MCL, mitral cell layer; GL, glomerular layer.

* Corresponding author at: Department of Pharmacology and Physiology, Faculty of Medicine and Health Sciences, Research Centre on Aging, University of Sherbrooke, 3001 12e Avenue Nord, Sherbrooke J1H 5N4, Canada.

E-mail address: Rona.Graham@USherbrooke.ca (R.K. Graham).

¹ M.L.B and Y-T. L contributed equally to this work.

<https://doi.org/10.1016/j.nbd.2019.02.002>

Received 9 July 2018; Received in revised form 14 December 2018; Accepted 4 February 2019

Available online 06 February 2019

0969-9961/ © 2019 Published by Elsevier Inc.

2003; Thomann et al., 2009; Youssef et al., 2008).

Olfactory system deficits are also observed in murine models of HD and include decreases in olfactory sensitivity (R6/1) and olfactory discrimination (HdhQ111) in the early and late stages of the disease (Holter et al., 2013; Mo et al., 2015). Furthermore, activation of brain regions in response to an olfactory stimulus shows a gene dose effect in the HD knock-in mouse model (Ferris et al., 2014). In the YAC128 HD mice, a decrease has been observed in the olfactory bulb volume (Carroll et al., 2011), an area which has previously been reported to correlate with olfactory functions (Buschhuter et al., 2008; Hummel et al., 2011).

Mutant huntingtin (mHTT) aggregates have also been detected in several olfactory regions in the HD human and rodent brain (Hamilton et al., 1999; Kohl et al., 2010; Menalled et al., 2003). One of the primary functions of the OB is the generation of new neurons, thus the olfactory deficits observed in HD may be an early sign of a defect in neurogenesis and potentially be involved in the neurodegenerative processes. Indeed, impaired neurogenesis is observed in human and murine HD brain (Curtis et al., 2003; Curtis et al., 2005; Fedele et al., 2011; Kohl et al., 2010; Lazic et al., 2007), and other neurodegenerative conditions (Han et al., 2016; Wirths, 2017).

Several models of HD have been created in order to reproduce the symptoms of the disease with the most fidelity. Among them, the BACHD rats display a robust, early onset and progressive HD-like phenotype including motor deficits and anxiety-related symptoms (Abada et al., 2013; Yu-Taeger et al., 2012). There are two lines characterized (TG5 and TG9) and both express the complete human mHTT sequence, including regulatory elements and the human *HTT* promoter. Overall, the TG5 line expresses higher levels of mHTT (in copy number, mRNA and protein) in the whole brain and presents with motor deficits on the accelerated rotarod test by 1 month of age (Yu-Taeger et al., 2012). An abnormal walking strategy is observed at 3 months in line TG5 and at 5 months in TG9 line consistent with the mHTT dosage effect (Yu-Taeger et al., 2012).

Several proteases (caspase-1, -3, -6, -7 et -8, calpains and aspartyl-proteases) have been shown to cleave HTT both in vitro and in vivo and the resulting fragments containing the expanded polyglutamine repeat are found in human and rodent HD brain (Gafni et al., 2004; Goldberg et al., 1996; Hermel et al., 2004a; Kim et al., 2002; Lunkes et al., 2002; Mende-Mueller et al., 2001; Wellington et al., 2002b). Caspase activation, in particular caspase-6, is known to be a critical step in the pathogenesis of HD. Mice expressing mHTT resistant to cleavage by caspase-6, maintain normal neuronal function and do not develop striatal neurodegeneration (Graham et al., 2010; Graham et al., 2012; Graham et al., 2006a; Metzler et al., 2010; Milnerwood et al., 2010; Pouladi et al., 2009). Alterations of other caspases have also been implicated in the pathogenesis of HD including caspase-3, -8, -9 and -10, and in other expanded polyglutamine diseases (Gervais et al., 2002; Kiechle et al., 2002; Rigamonti et al., 2001; Sanchez et al., 1999b; Toulmond et al., 2004; U et al., 2001). Importantly, caspase activity has been shown to be an essential step in maintaining the normal turnover of OB cells through neurogenesis (Mouret et al., 2009). As caspases are key components in the pathogenesis of HD, and the functions related to the OB are impaired in the disease, we assessed OB weight and caspase expression profiles in the OB of the two lines of the BACHD (TG5 and TG9) rodent model in order to determine if activation of caspases may provide an explanation for the olfactory dysfunction and olfactory system atrophy observed in HD.

2. Material and methods

2.1. Animals

The olfactory bulbs (OB) were collected from two lines of the BACHD rat model (TG5 and TG9), transgenic rat models expressing human mutant full-length *HTT* gene with 97 CAG/CAA repeats, at 3, 6

and 12 months of age (Yu-Taeger et al., 2012). The rats were fed ad libitum and kept in a normal light and dark cycle. All experiments were approved by the local ethics committee at Regierungspräsidium Tuebingen (HG2/10), and carried out in accordance with the German Animal Welfare Act and the guidelines of the Federation of European Laboratory Animal Science Associations, based on European Union legislation (Directive 2010/63/EU).

2.2. Quantification of OB weight and area

The weight of the OBs of the BACHD rats and WT rats were obtained using an analytic balance (Denver instrument, SI-64) at 3 and 6 months of age. The area of the OB of the BACHD rats and WT rats were assessed at 12 months of age as following: rats were perfused with 4% paraformaldehyde in saline buffer followed by post-fixation of the brains in the same fixative. Nissl staining was performed to visualize different layers of the OB using 40- μ m thick coronal cryosections. Three olfactory bulb sections with 960 μ m intervals were chosen for the quantification of the OB area. We analyzed three areas separately: i) the total area of the mitral cell layer (MCL), internal plexiform layer (IPL) and granule cell layer (GCL); ii) area of the external plexiform layer (EPL); iii) area of the glomerular layer (GL). The region of interest (ROI) of the MCL + IPL + GCL was outlined along the outer edge of MCL of the OB and images were acquired. The area was determined using ImageJ. The area of the EPL was assessed by subtracting the total area of MCL + IPL + GCL from the area outlined along the outer edge of EPL. The area of the GL was calculated by subtracting the area outlined along the outer edge of EPL from the area outlined along the outer edge of GL. The area values of the three sections of each animal were averaged and compared among the groups.

2.3. Real-Time Quantitative RT-PCR

Total RNA was extracted from the OBs with RNeasy mini kit (QIAGEN) and cDNA was prepared using ProtoScript Reverse transcriptase II (#M0368X, New England BioLabs). Quantification was done using Mx3005P QPCR Systems (Stratagene) with rat-specific primers for caspase-3 (Forward: 5'-GGACCTGTGGACCTGAAAAA-3'; Reverse: 5'-GCATGCCATATCATCGTCAG-3'), caspase-6 (Forward: 5'-ACGTTGGATCATCAGACA-3'; Reverse: 5'-GGAGCCGTTTACAGTCTCTC-3'), caspase-8 (Forward: 5'-GGGGATGGCTACTGTGAAAA-3'; Reverse: 5'-CATGTTCTCGGGTTGTCTT-3'), caspase-9 (Forward: 5'-AAGACCA TGGCTTTGAGGTG-3'; Reverse: 5'-CAGGAACCGCTCTTCTTGTC-3'), and PgK1 (Forward: 5'-CCAAACAATCTGCTTAGCTCG-3'; Reverse: 5'-GATGAGAATGCAAAGACTGGC-3'). The primers designed to quantify transgenic mutant HTT were (Forward: 5'-ATCTTGAGCCACAGCT CCAGCCA-3'; Reverse: 5'-GGCCTCCGAGGCTTCATCAGG-3') and the primers used to quantify endogenous rat HTT were (Forward: 5'-ATC TTGAGCCACAGCTCCAGCCA-3'; Reverse: 5'-TCTGAAAAGCTGTGAGA CTTACCAGA-3'). Amplification of the references gene PgK1 was used to standardize the amount of sample RNA in the reaction. Gene-expression levels were measured using MxPro QPCR Software (Stratagene).

2.4. Western blot analysis

OBs were homogenized and sonicated in lysis buffer (0.32 mM Sucrose, 20 mM Tris pH 7.2, 1 mM MgCl₂, 0.5 mM EDTA pH 7.2) using a cocktail of protease inhibitors (Roche), PefaBloc SC (Roche) and Z-VAD-fmk (Enzo Lifes Sciences) and clarified by centrifugation at 13,000 rpm. The protein concentration was determined using the BCA (bicinchoninic acid) protein assay kit (Pierce). Protein lysates (50 μ g) were separated on 10% or 4–15% gels and transferred to PVDF membrane (PerkinElmer). The membranes were probed with caspase-3 (Cell Signalling, 9662, dilution: 1/1000), caspase-6 (Cell Signalling, 9762, dilution: 1/500), caspase-8, (Santa Cruz, sc-7890, dilution: 1/100), caspase-9 (Cell Signalling, 9508, dilution: 1/1000), huntingtin

(Millipore, MAB2166, dilution 1:500), Polyglutamine-Expansion disease marker (Millipore, 1:3000, MAB1574), Calnexin (Abcam, 1:2000, ab75801) or actin (Millipore, MAB1501, dilution 1/10000) antibodies. Peroxidase activity was detected and densitometry values were obtained with Odyssey Fc imaging system (Licor) using Luminata Crescendo Western HRP substrate (Millipore). Quantification of β -actin or calnexin was used to standardize the amount of protein in each lane.

2.5. HTT immunohistochemistry

Nuclear accumulation of mHTT was investigated by immunohistological staining using the antibody S830, a polyclonal antibody raised against HTT exon 1 recombinant protein with 53Q (kindly provided by Prof. Gillian P. Bates) (Sathasivam et al., 2001). Rat OB sections of two BACHD lines (TG5 and TG9) at 3, 6, 9 and 12 months of age were stained as described previously (Yu-Taeger et al., 2012). Sections were counterstained with thionin to visualize nuclei.

3. Results

3.1. Atrophy of the olfactory bulb in the BACHD transgenic lines

We assessed OB weight in the BACHD rats (TG5 and TG9) and WT rats at 3 and 6 months of age. A genotype effect was detected which showed a significantly lower OB weight in the TG5 rats (44%), and a trend decrease in the TG9 rats (34%), at 6 months of age compared to WT (Two-way ANOVA: interaction: $p = 0.16$; Age: $p = 0.71$; Genotype: $p = 0.002$; post hoc, 6 months WT vs. TG5, $p < 0.01$; Fig. 1A). A trend decrease is also observed at 3 months of age in TG5 OB compared with WT (t -test, $p < 0.01$). We also assessed specific areas within the OB including the i) MCL + IPL + GCL, ii) EPL and iii) GL at 12 months of age. An interaction between the genotypes and the OB layers was observed; suggesting that expression of mHTT may influence the size of specific layers in the OB (two-way ANOVA, Interaction $p = 0.004$; Genotype, $p < 0.0001$; Layers, $p < 0.0001$; Fig. 1B, C). Similar to the OB weight at 6 months of age, we observed a decreased area of the MCL, IPL and GCL in the TG5 and TG9 compared to WT (post hoc IPL and GCL: WT vs. TG5, $p < 0.0001$, WT vs. TG9, $p < 0.01$; Fig. 1C), while the area of the EPL was only decreased in TG5 compared to both WT (post hoc test, $p < 0.0001$) and TG9 rats (post hoc test, $p < 0.01$) (Fig. 1C). No variation in the glomerular layer was observed in either line compared to WT. As we observed a decrease in OB weight, using western blot analysis, we then evaluate the expression of NeuN, a marker of mature neurons. We observed a trend decrease in both lines in NeuN expression (data not shown, t -test WT vs. TG5, $p = 0.09$; WT vs. TG9, $p = 0.08$).

3.2. Differential HTT expression profiles between TG5 and TG9 BACHD rats

Strong evidence has demonstrated the opposing effects of wild-type and mutant HTT on cell death and neurogenesis pathways. Indeed, wild-type HTT plays a role in development, neurogenesis, anti-apoptotic pathways, protection against excitotoxic stress, and has been shown to reduce mutant HTT toxicity (Cattaneo et al., 2005; Gervais et al., 2002). As mutant HTT has a dose-dependent (de Almeida et al., 2002; Graham et al., 2006b; Hodgson et al., 1999; Reddy et al., 1998; Squitieri et al., 2003) and opposing effect vs. wild-type HTT, their expression levels may affect the OB atrophy differentially. We therefore evaluated *HTT* mRNA and protein expression levels of both mutant and wild-type HTT in these two lines at 3, 6 and 12 months of age. No difference in wild-type *HTT* OB mRNA levels were observed between BACHD rats and WT rats at any time points assessed (Fig. 2A, B, C). However, a trend increase in the mRNA expression of the HD gene was observed in TG9 rats compared to WT at 12 months (t -test: $p < 0.05$, Fig. 2C). The real-time quantification PCR analysis also revealed higher

expression of *mHTT* mRNA in the OB of the TG5 rats compared to TG9 at 3 months (ANOVA, $p < 0.001$, Fig. 2D) and 12 months of age (ANOVA, $p < 0.05$, Fig. 2F). Although we did not detect any significant variation in mRNA levels of wild-type *HTT* in the OB at 3 months of age between genotypes, we did detect a decrease in wild-type *HTT* protein expression in TG9 vs. WT rats at that age (ANOVA $p = 0.016$, post hoc, $p < 0.05$, Fig. 3A, B, Sup. Fig. 1). Correlating with the *mHTT* mRNA results at 3 months of age, we detected increased OB mHTT protein levels in TG5 compared to TG9 at this time point (ANOVA, Fig. 3C-E, Sup. Fig. 1). At 6 and 12 months of age, no difference in endogenous or mHTT protein expression levels was observed between TG5 and TG9 (Fig. 3F-L, Sup. Fig. 1). However, the mHTT/wild-type *HTT* ratio in the OB of TG5 rats was increased compared to TG9 at 3 and 12 months of age (Fig. 3E t -test, $p < 0.0001$, M t -test, $p < 0.001$, Sup. Fig. 1).

Despite the higher protein expression of mHTT in TG5 rats compared to the TG9 at 3 months of age, nuclear accumulation of mHTT, assessed using the S830 antibody, was observed earlier in the TG9 OB (3 months of age) compared to TG5 rats (6 months of age) (Fig. 4). By the age of 9–12 months, TG9 rats clearly display more intense nuclear immunoreactivity of mHTT in the OB than TG5 (Fig. 4). The quantification of mHTT nuclear accumulation shows an interaction by two-way ANOVA indicating that the increase in the nuclear immunostaining of mHTT occurs earlier in TG9 OB compared to TG5 (two-way ANOVA, Interaction, $p < 0.0001$: Genotype, $p < 0.0001$, Age $p < 0.0001$. Of note, the nuclear accumulation was almost exclusively observed in the IPL, GCL and MCL of the OB (Fig. 4, Sup. Fig. 2).

3.3. Increase in mRNA levels of specific caspases in BACHD olfactory bulb

As we observed atrophy of the OB in the BACHD lines, we next performed a temporal investigation of caspase expression profiles in the OB of the BACHD TG5 and TG9 rats. At 6 and 12 months of age, an increase in caspase-3 mRNA expression levels was observed in the OB of the TG9 rats compared to WT (6 months: ANOVA $p = 0.03$, post hoc: WT vs. TG9 $p < 0.05$, TG5 vs. TG9, $p < 0.05$; Fig. 5C, 12 months: ANOVA $p = 0.02$, post hoc: WT vs. TG9 $p < 0.05$, Fig. 5B-C). Furthermore, an increase in the expression of caspase-6 mRNA was observed in the OB of TG9 rats compared to WT at 3 months of age (ANOVA $p = 0.059$, t -test: WT vs. TG9 $p < 0.05$, Fig. 5D). However, at 6 and 12 months, no difference between genotype was observed (Fig. 5E-F). No variation in caspase-8 mRNA expression levels was detected between the BACHD lines and WT OB at any age (Fig. 5G-I). In contrast to the increased mRNA expression observed for caspase-3 and -6 in TG9 OB, a decrease in caspase-9 mRNA expression was observed in TG5 OB at 6 months of age compared to WT OB (ANOVA $p = 0.04$, post hoc: WT vs. TG5, $p < 0.05$, Fig. 5K) and there was a trend decrease in caspase-9 in TG9 OB at 3 months of age (ANOVA $p = 0.08$, t -test: TG5 vs. TG9, $p < 0.05$, Fig. 5J).

3.4. Alterations in caspase protein expression profiles in BACHD olfactory bulb

At the protein level, the p30 and p19 fragments of caspase-3 tend to increase in the TG9 OB compared to WT at 3 months of age, while no further variation was observed at 6 and 12 months of age (p30: ANOVA $p = 0.07$; p19: ANOVA $p = 0.09$, Fig. 6A-C, Sup. Fig. 3). While no change in the percentage of active caspase-3 was detected by ANOVA at 3 months of age between genotypes, a trend increase in active caspase-3 was observed in TG9 OB compared to WT (t -test, $p < 0.05$, Sup. Fig. 4). Furthermore, there was a significant decrease in the caspase-6 p20p10 fragment, an intermediate fragment in the path of activation, in both TG5 and TG9 OB, and a trend decrease in the caspase-6 proform in TG5 OB compared to WT at 3 months (Proform: ANOVA $p = 0.09$, t -test: WT vs. TG5 $p < 0.05$; p20p10: ANOVA $p = 0.003$, post hoc: WT vs. TG5, $p < 0.05$; WT vs. TG9, $p < 0.05$, Fig. 6D, Sup. Fig. 3). Despite

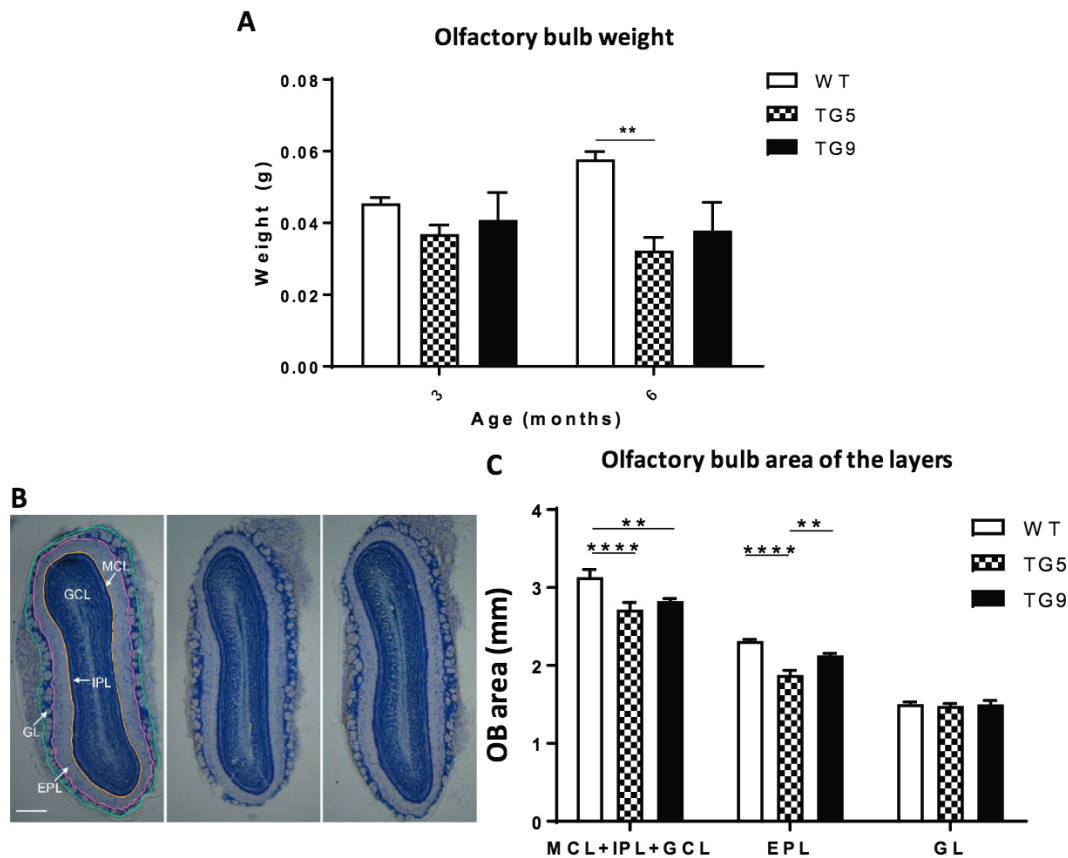


Fig. 1. Atrophy of the olfactory bulb in BACHD rodents. **A)** A significant effect of genotype showing a global decrease in olfactory bulb (OB) weight is observed in BACHD rats at 6 months of age compared to WT rats (Two-way ANOVA: Interaction $p = 0.16$, Age $p = 0.71$, Genotype $p = 0.002$; 3 months: WT $n = 10$, TG5 $n = 8$ and TG9 $n = 9$; 6 months: WT $n = 8$, TG5 $n = 6$ and TG9 $n = 4$). Tukey post hoc revealed a significant weight reduction in the TG5 compared to WT at 6 months of age. **B)** Representative images of coronal OB sections with Nissl staining of BACHD rats and WT controls at 12 months of age are shown. Scale bar: 0.5 mm. **C)** The average area of the MCL + IPL + GCL is decreased in the TG5 and TG9 compared to WT at 12 months of age. Furthermore, the EPL averaged area is lower in TG5 rats compared to WT and TG9 (two-way ANOVA, Interaction $p = 0.004$; Genotype, $p < 0.0001$; Layers, $p < 0.0001$, WT, $n = 4$; TG5, $n = 5$; TG9, $n = 4$). Tukey post hoc are presented on the graph. IPL = Internal plexiform layer, GCL = Granule cell layer, EPL = External plexiform layer, MCL = Mitral cell layer, GL = Glomerular layer. Error bar: SEM, post hoc between genotypes are presented on the graph.

the absence of variation detected in caspase-8 mRNA expression, a significant increase in the caspase-8 proform and p18 active fragment was observed at 3 months of age in the TG9 OB compared to WT (Proform: ANOVA $p = 0.013$, post hoc: WT vs. TG9, $p < 0.05$; p18: ANOVA $p = 0.003$, post hoc: WT vs. TG9, $p < 0.01$; TG5 vs. TG9, $p < 0.05$, Fig. 6G, Sup. Fig. 3), and a trend increase was also observed with the p43/41 fragments (p43/41: ANOVA $p = 0.08$, Fig. 6G, Sup. Fig. 3). Although no difference in the percent of active caspase-8 was detected between genotypes, a trend increase in the percentage of active caspase-8 was detected in 3-month-old TG9 OB compared to WT and TG5 OB (t-test, $p < 0.05$, Sup. Fig. 4). There was no further variation in caspase-3, -6 and -8 expression levels at 6 and 12 months of age (Fig. 6B-C, E-F, H-I, Sup. Fig. 3). In contrast to all the other caspases assessed, a significant increase in caspase-9 proform protein expression levels was observed only at the late time point (12 months of age) in the TG5 OB compared to WT (ANOVA $p = 0.003$, post hoc: WT vs. TG5, $p < 0.05$, Fig. 6J-L, Sup. Fig. 3). No cleaved fragments of caspase-9 were detected. In light of the alterations observed in the caspase expression profiles, we performed a TUNEL analysis of the OB at 12 months of age. We detected an increase in TUNEL-positive cells in the TG9 OB only, suggesting activation of the programmed cell death pathway is occurring in the TG9 line (Sup. Fig. 5, ANOVA Interaction, $p = 0.04$; Genotype, $p = 0.08$; Layers, $p < 0.045$). The increased number of TUNEL-positive cells are observed in the internal layers of the TG9 OB compared to WT and TG5 (post hoc: WT vs. TG9, $p < 0.05$;

TG5 vs. TG9, $p < 0.05$).

4. Discussion

Assessment of olfactory dysfunction is described as a promising diagnostic marker for Mild Cognitive Impairment, Alzheimer's disease and Parkinson's disease, and may provide a sensitive measure of the early disease process in HD (Bahar-Fuchs et al., 2011; Barresi et al., 2012; Christen-Zaech et al., 2003; Delmaire et al., 2012; Djordjevic et al., 2008; Doty, 2012b; Mitchell et al., 2005; Moberg et al., 1987). Furthermore, in early grade human HD brain, there is a significant correlation between olfactory function and volume reduction of brain regions related to olfaction (Barrios et al., 2007). It therefore becomes important to determine the underlying mechanisms of the olfactory dysfunction in HD. As programmed cell death is an integral part of normal OB development and neuronal precursor evolution (Cowan and Roskams, 2004; Mori, 2014; Yan et al., 2001), and caspase activation has been shown to be an underlying mechanism in the striatal and cortical pathology in HD (Graham et al., 2006a; Ona et al., 1999; Rigamonti et al., 2001; Uribe et al., 2012; Wellington et al., 2002a; Wong et al., 2015), we assessed OB morphology and expression profiles of caspases and HTT in the BACHD rats. We demonstrate that there is atrophy of the OB in the TG5 and TG9 lines at specific time points and in specific layers of the OB. We also show enhanced cell death, and alterations in caspases protein expression profiles in the HD rat models

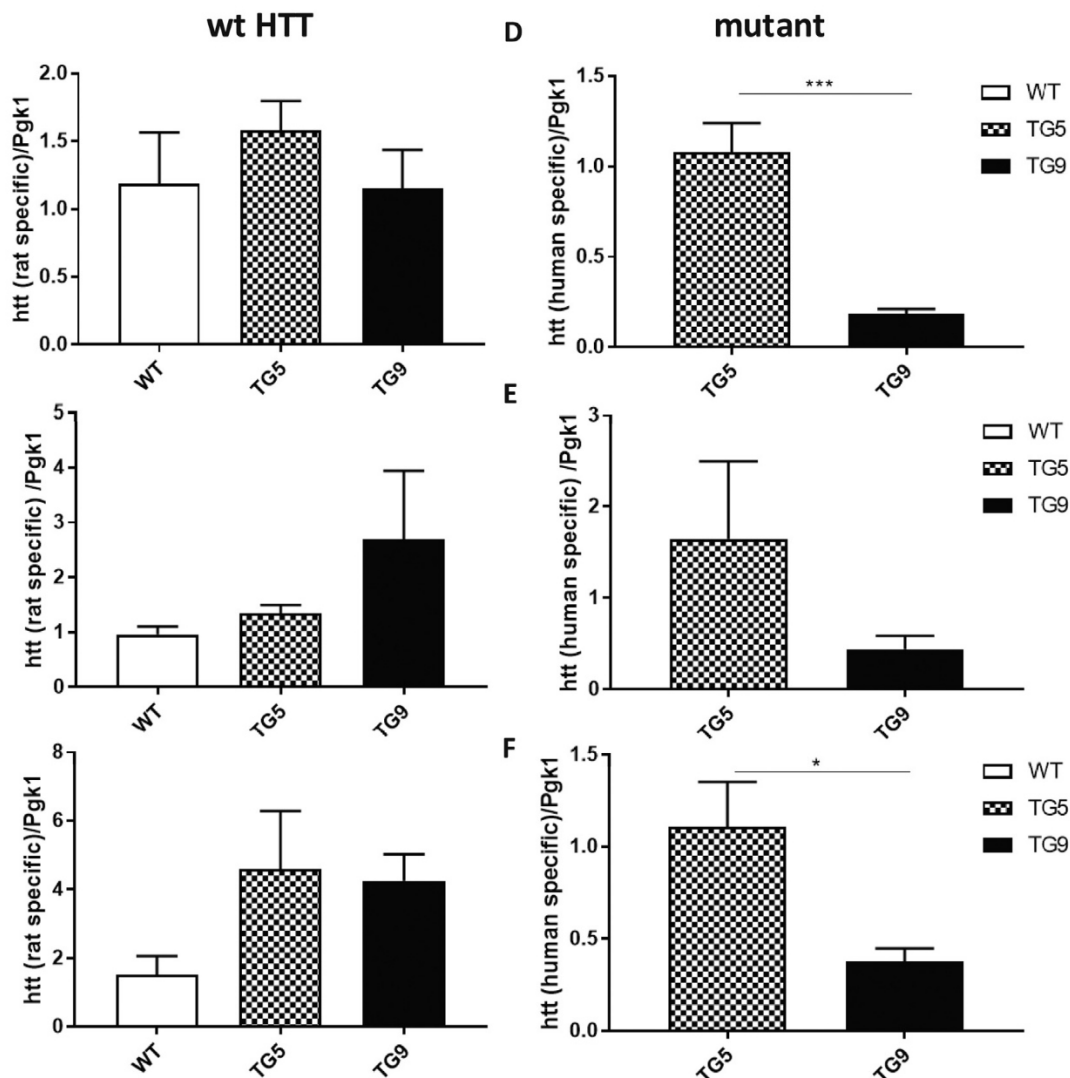


Fig. 2. Increased expression of mHTT mRNA in TG5 olfactory bulb compared to TG9 rats. A,B,C) No difference in endogenous HTT mRNA levels were observed at any age. However, a trend increase in TG9 vs. WT was observed at 12 months of age (t-test, $p < 0.05$). Increased mRNA expression of mHTT is observed in the OB of the TG5 line compared to TG9 at D) 3 ($p < 0.001$) and F) 12 months of age ($p < 0.05$). 3 months: WT $n = 4$, TG5 $n = 6$ and TG9 $n = 5$; 6 months: WT $n = 4$, TG5 $n = 3$ and TG9 $n = 3$; 12 months: WT $n = 6$, TG5 $n = 4$ and TG9 $n = 6$, relative measurements of HTT/pgk1 are \pm SEM.

that do not correlate with their respective mRNA expression patterns (Table 1).

While the presence of olfactory impairment is widely observed in human HD, only limited studies on olfactory behaviour have been done in models of HD. Impaired olfactory sensitivity and odor discrimination has been observed in the R6/1 (Mo et al., 2014; Mo et al., 2015) and HdhQ111/+ HD mice respectively (Holter et al., 2013). As the morphology of several olfactory-related brain regions correlate with levels of olfactory function (Barrios et al., 2007; Buschhuter et al., 2008; Hummel et al., 2011), we analyzed the OB in the BACHD lines. Our results show a significant decrease in OB weight in the TG5 line, and a trend decrease in the TG9 rats, by 6 months of age. Further analysis of the area of the OB layers at 12 months of age shows that both lines display atrophy of the mitral cell, internal plexiform and granule cell layers, while atrophy of the external plexiform is only significant in the TG5 line. These results are concordant with previous studies demonstrating that OB atrophy is a common event in neurodegenerative diseases which display signs of olfactory dysfunction (Brodoehl et al., 2012; Chen et al., 2014; Servello et al., 2015; ter Laak et al., 1994; Thomann et al., 2009; Wang et al., 2011) and in HD murine models (Carroll et al., 2011; Smail et al., 2016) (Carroll et al., 2011; Smail

et al., 2016). As alterations in the development of the mitral cell layer can affect odor discrimination (Bastakis et al., 2015), the atrophy of the internal layers (MCL, IPL and GCL) observed here could be involved in the olfaction impairment observed in HD. Furthermore, an increase in apoptosis of granule cells may be an important process for the olfactory information processing by eliminating the specific Granule cells and therefore reducing the signal-to-noise ratio which may help the olfactory learning and memory (Yamaguchi et al., 2013). The internal layers contain a population of immature cells. It is therefore possible that the decrease in the internal layers of the OB in the BACHD lines could also reflect a neurogenesis impairment previously observed in HD (Curtis et al., 2003; Fedele et al., 2011; Kohl et al., 2010; Phillips et al., 2005; Simpson et al., 2011). Indeed, we observed a trend decrease in OB NeuN (marker of mature neurons) protein expression at 6 months of age in both lines indicating that neurogenesis may be impaired.

Significant evidence in the literature supports a mHTT dose-dependent neurodegenerative effect (de Almeida et al., 2002; Graham et al., 2006; Hodgson et al., 1999; Reddy et al., 1998; Squitieri et al., 2003). This has also been demonstrated in the BACHD models with the TG5 line showing higher mHTT expression overall (this study and Yu-Taeger et al., 2012) and earlier motor deficits compared to the TG9 line

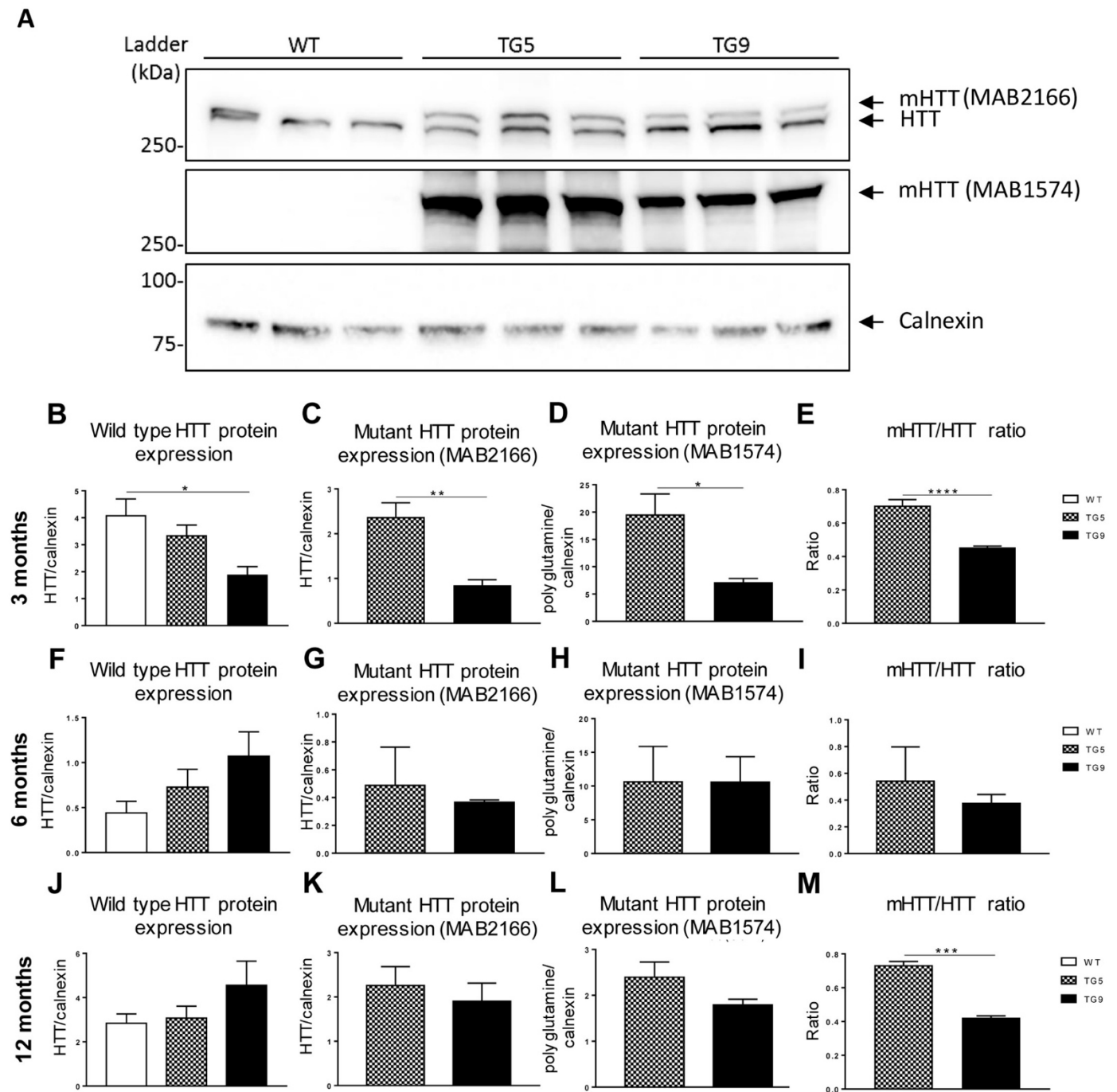
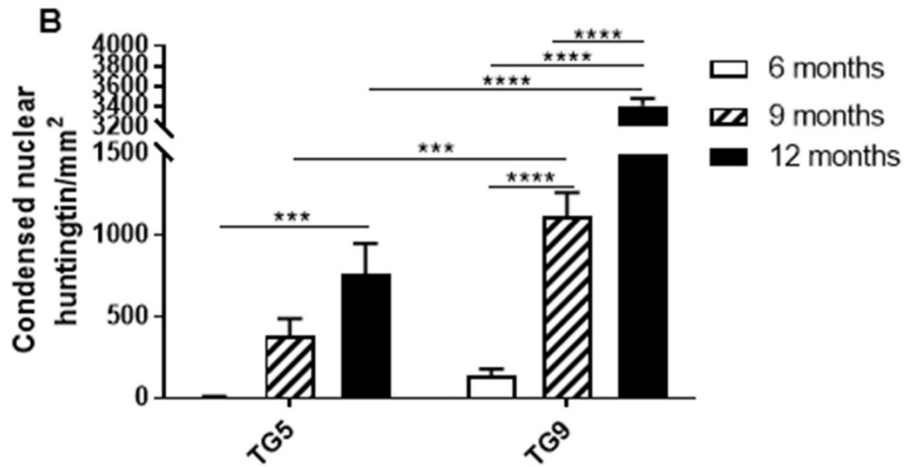
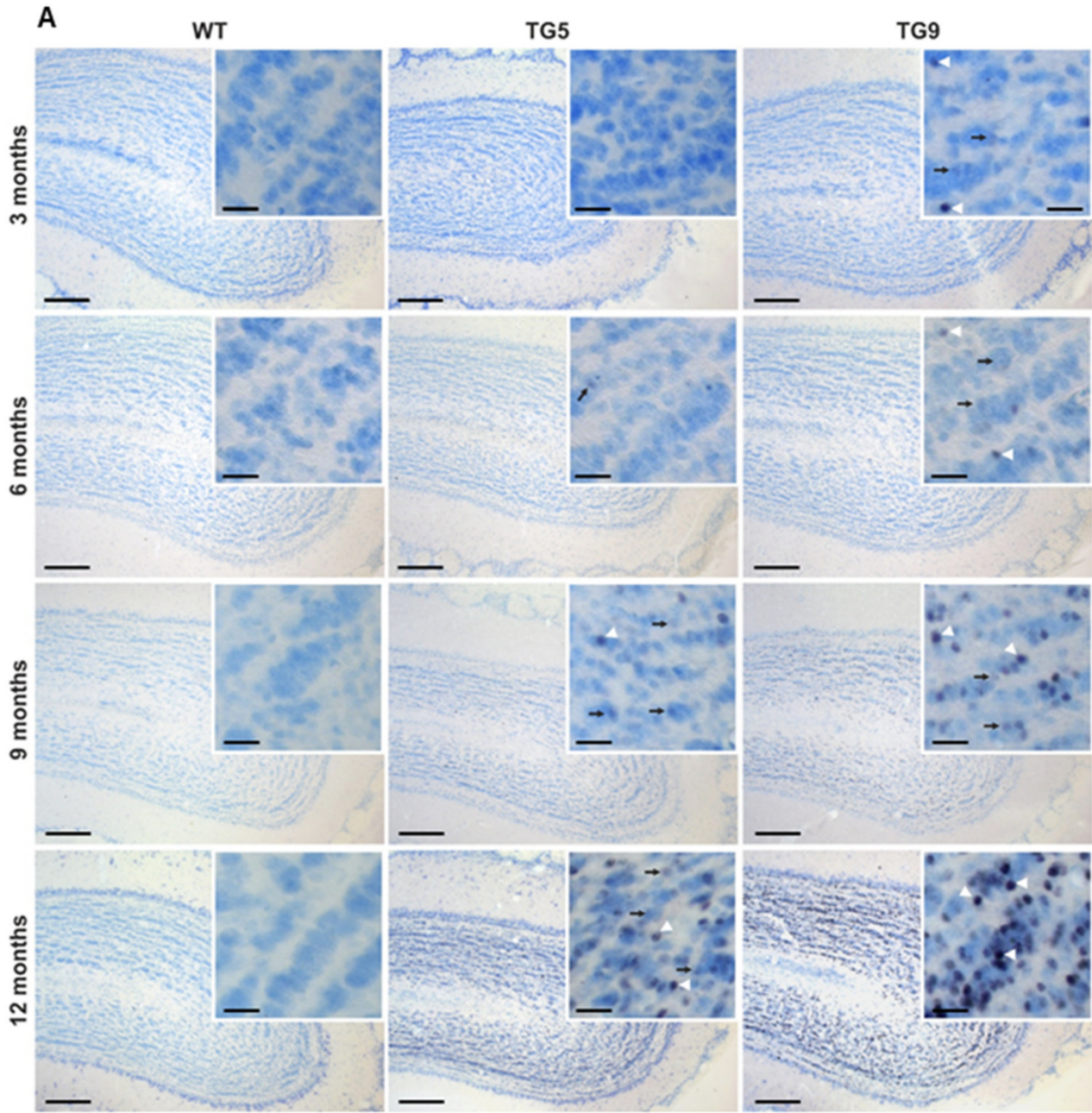


Fig. 3. Age-specific alterations in the protein expression of HTT in TG5 and TG9 olfactory bulb. **A)** Representative images of western blots for HTT and mHTT obtained with MAB2166 (first panel) and MAB1574 (second panel) antibodies on 12-month old OB lysates. The reference protein used is calnexin. **B)** At 3 months of age, decreased expression of wild type HTT is observed in the TG9 OB compared to WT (ANOVA $p = 0.016$, post hoc WT vs. TG9, $p < 0.05$). A higher expression of mHTT is observed by western blot in TG5 compared to TG9 OB when using **C)** MAB2166 (t-test, $p < .01$) and **D)** MAB1574 (t-test, $p < 0.05$) antibodies. **E)** A lower mHTT/HTT ratio is observed in TG9 when compared to TG5 (t-test, $p < 0.0001$, MAB2166). **F–I)** No significant variation in the expression of endogenous or mHTT is observed between genotypes at 6 months of age. **J–L)** At 12 months of age, no variation was detected in the wild type HTT or mHTT protein expression between genotypes. **M)** A lower mHTT/HTT ratio is observed in TG9 OB when compared to TG5 (t-test, $p < 0.001$, MAB2166) at 12 months of age. Mean measurements and densitometric ratios of mHTT/endogenous HTT are \pm SEM, $n = 6$ for all genotypes at 3 months of age and $n = 3$ for all genotypes at 6 and 12 months of age. MAB2166: Anti-huntingtin, MAB1574: Anti-Polyglutamine-Expansion disease marker.

(Yu-Taeger et al., 2012). Furthermore, mHTT gradually affects the volume of several brain regions (Aylward et al., 1994; Aylward et al., 1996). The same gradual decrease was observed in the OB weight of TG5 rats. In the TG9 line, which expresses less mHTT in the OB overall than the TG5 line, there is also atrophy but less than in TG5 (albeit the difference is subtle).

The expression of several caspases is deregulated in HD and active fragments of caspases are found in postmortem HD brains (Graham et al., 2010; Kiechle et al., 2002; Kim et al., 2001; Wanker, 2002; Wellington et al., 2002a). This deregulation in caspase activation could lead to not only cell death but also alterations in neurogenesis and development of the OB. Indeed, half of the newborn interneurons are



(caption on next page)

Fig. 4. Prominent nuclear accumulation of mHTT in BACHD TG9 rats. A) Nuclear accumulation of mHTT was investigated by immunohistochemistry using the antibody S830 against HTT (black color) in the OB of BACHD lines TG5 and TG9 at 3, 6, 9 and 12 months of age. Sections were counterstained with thionine to visualize nuclei (blue color). Transgenic rats of TG9 exhibit condensed nuclear accumulation (arrow heads) starting at 3 months of age which dramatically increase with age, while transgenic rats of TG5 show only a weak nuclear staining (arrows) by S830 staining at 6 months of age. Until 12 months of age the immunoreactivity of anti-HTT S830 antibody is more intense in rats of the TG9 line compared to rats of TG5. WT littermates serve as negative controls and show no positive signal for mHTT in all time points investigated. Scale bar = 20 and 200 μ m. B) The quantification of the nuclear accumulation of mHTT in TG5 compared to TG9 demonstrates there is an interaction between the genotype ($p < 0.0001$), an effect of the age ($p < 0.0001$), and an effect of the genotype ($p < 0.0001$) by two-way ANOVA. Sidak's post hoc are presented in the graph. Results are presented \pm SEM. (For interpretation of the references to color in this figure legend, the reader is referred to the web version of this article.)

eliminated by apoptosis before their incorporation into specific locations in the OB (Mori, 2014). The analysis of OB caspases expression profiles in the TG5 and TG9 HD rat models shows an increase or a trend increase in cleavage fragments of caspase-3 and -8 in TG9, implying the activation of these caspases by 3 months of age. This increase in active caspase fragments may explain the atrophy observed later. At older ages, increases in caspase-3 mRNA was also observed in this line. However, this did not translate into increases at the protein level at those time-points. In our results, the caspase protein expression data does not follow the same trend as the mRNA levels. Changes in mRNA may be buffered by translational changes or post-translational modifications of the protein as previously shown (Ishikawa et al., 2017; Perl et al., 2017). Furthermore, although the activation of caspase-3 has previously been observed in human HD striatum (Graham et al., 2010; Kim et al., 2001) and indeed used as a routine marker of cell death (Chen et al., 2015; Karamitopoulou et al., 2007; Mazumder et al., 2008), it is not clear whether the activation of caspase-3 observed in our results reflects impending cell death or issues with neurodevelopment. It has been previously demonstrated that the presence of caspase-3 affects the structural development of the OB as a deficiency in murine caspase-3 leads to abnormal development of the OB (Cowan and Roskams, 2004).

Similar to our results, an increase in caspase-8 has been previously reported in human HD caudate and caspase-8 shown to be required in cell death pathways caused by an expanded polyglutamine disease (Sanchez et al., 1999a). In contrast to the other caspases, a decrease in the proform and the p20p10 fragment of caspase-6 is observed in the OB of the BACHD lines. The p20p10 fragment is not an active fragment per se, rather it is an intermediate fragment of caspase-6, lacking the pro-domain, that has been shown to be required for the activation of caspase-6 and is further cleaved into the activated form (Klaiman et al., 2009). It is important to point out that some in vivo caspase active fragments, such as for caspase-6, are difficult to visualize by Western Blot (Warby et al., 2008). Therefore, we cannot rule out the possibility that the increase in caspase-6 gene expression, combined with the decrease in the proform and p20p10 fragment of caspase-6, may reflect the activation of caspase-6. This is concordant with the caspase-6 activation observed in the striatum and cortex of human and murine HD brain (Graham et al., 2010; Hermel et al., 2004b).

The activation of caspases observed in TG9 does correlates with the atrophy observed in this line. However, as cell death is an important part of the development of the OB and neurogenesis, the activation of the caspases observed predominantly at 3 months of age may also reflect an impairment in development that is occurring at that age which then persists. This is supported by the observation that in the WT OBs, there is a 21% increase in OB weight between 3 and 6 months of age which is not found in the BACHD OBs (TG5: -14% and TG9: -8%). An impairment in proliferation pathways may cause the decreases in OB weight and trend decrease in the NeuN expression at 6 months of age. It is also possible that the area of the cell may shrink in the presence of mHTT leading to the decrease in OB weight, as previously observed in an HD striatal cell line and human HD cortex (Rajkowska et al., 1998; Singer et al., 2017).

Our results do show that there is increased TUNEL positive cells, and therefore cell death, at the 12 month time point in the TG9 OB which correlates with the increases in caspase-3 mRNA and atrophy

observed. However, we do not see changes in the other caspases assessed at this time point. It is possible that these changes may have occurred prior, and/or different caspases may be implicated. Furthermore, it is possible that the variation in caspases expression is not uniform throughout the OB and is only observed in specific layers of the bulb, as suggested by the absence of atrophy in the glomerular layer. As the entire OB was used for the caspase expression analysis, this may have diluted any specific effects. It is also important to mention that the alterations observed in caspase expression in our results may reflect not only the death of OB cells in general, but also affect the cellular composition of the OB and therefore ultimately olfactory function.

In our results, the immunostaining of mHTT (using S830 antibody), which has been reported to correlate with disease progression (Acton, 2013), shows early and substantially more nuclear accumulation of mHTT in the internal layers of TG9 OBs compared to TG5. As some N-terminal fragments of HTT interact with the Trp protein and decrease the nuclear export of HTT (Cornett et al., 2005), the difference in the nuclear accumulation of HTT in the BACHD lines may be caused by an increased production of the caspase generated N-terminal fragments of HTT in the TG9 OBs. This correlates with the decrease in full length HTT and caspase-3 activation observed in this line. As wild type HTT has been shown to inhibit caspase-3 activation (Zhang et al., 2006), it is possible that the decrease in wild type HTT observed may have affected its inhibitory affect on caspase-3 thus influencing its activation. As mHTT aggregates can interact with transcription factor via their polyglutamine sequence (Boutell et al., 1999; Li et al., 2016; Shimohata et al., 2000; Steffan et al., 2000), mHTT accumulation in the TG9 line may alter the transcription process and lead to the increased cell death observed by TUNEL. Moreover, it has been shown that caspase-3, -8, -10 and -12, (in contrast to caspase-9) interact and are activated by expanded polyglutamine motifs (Gervais et al., 2002; Kouroku et al., 2002; Kouroku et al., 2000; Miyashita et al., 1999; Sanchez et al., 1999a; U et al., 2001). Of note, the interaction with caspase-8 occurs predominantly in the nuclear aggregates containing fragments of polyQ repeats (U et al., 2001). The increased accumulation of mHTT in the nucleus, along with the activation of caspase-3, -6 and -8, in the TG9 line and absence of any caspase-9 proteolytic fragments, may contribute to the atrophy observed in the TG9 OB and cell death observed by TUNEL.

A key question is why caspase-3 and -8 activation are only observed in the TG9 line. This is not due to differences in the transgene or the CAG size (Yu-Taeger et al., 2012). One reason may be related to the increased mHTT accumulation as the accumulation of misfolded protein impairs cell function (Vilchez et al., 2014). Another reason may be the spatial and temporal expression pattern of HTT and mHTT in these lines. A study has shown that the chromosomal location of a transgenes can create disparities in the molecular phenotypes between lines created with the same transgene and can affect the expression of the transgene in an organ-related manner (Hatada et al., 1999). Therefore, the differential expression and activation of caspases may be due to the insertion site of the HD gene in these models. Similar to the increase observed at the mRNA and protein level in our results, it has previously been shown that the TG5 line expresses overall more mHTT (Yu-Taeger et al., 2012). It is possible that some enhancers near the insertion site alter the expression of mHTT in the TG5 line in some brain regions. A

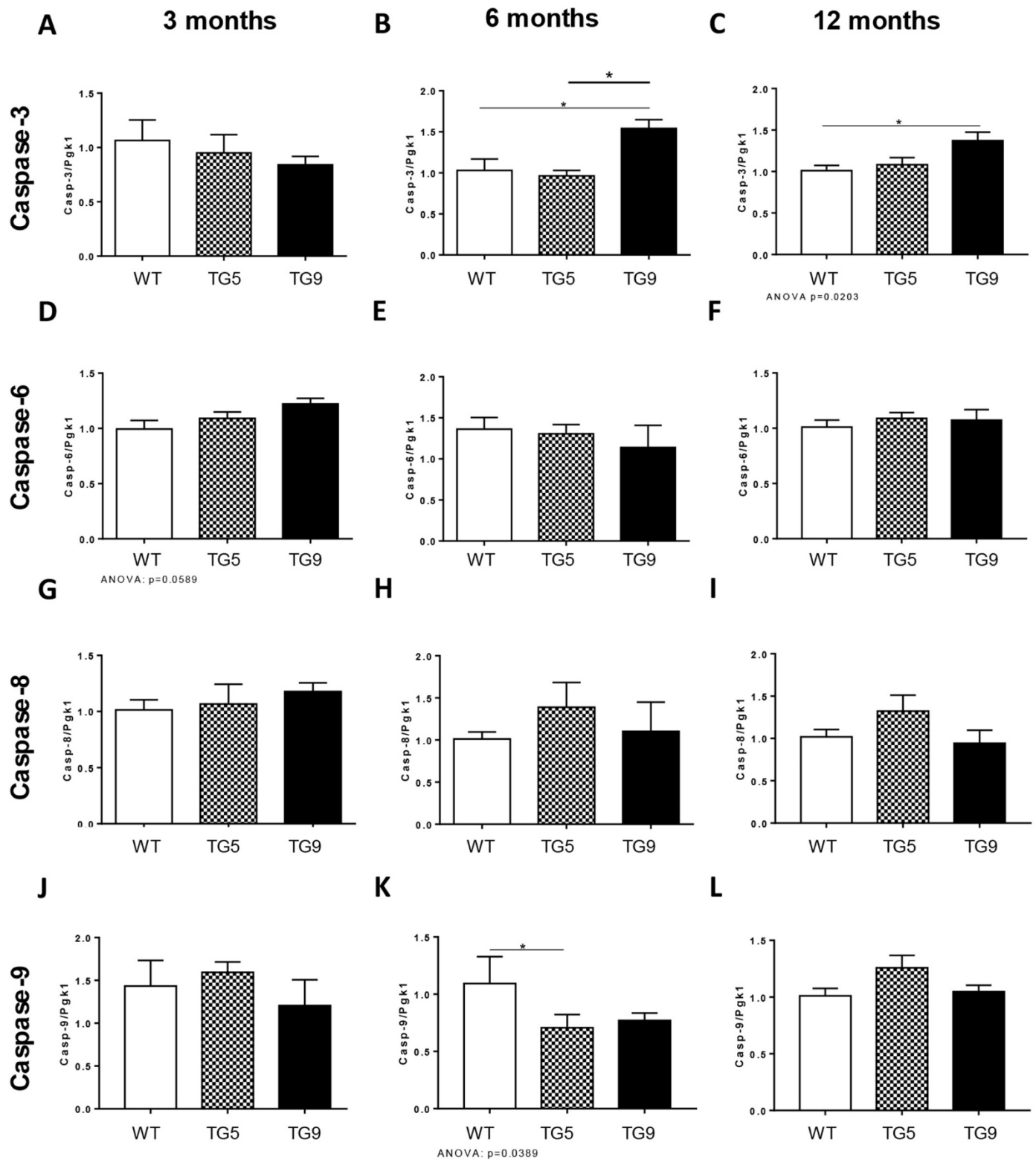
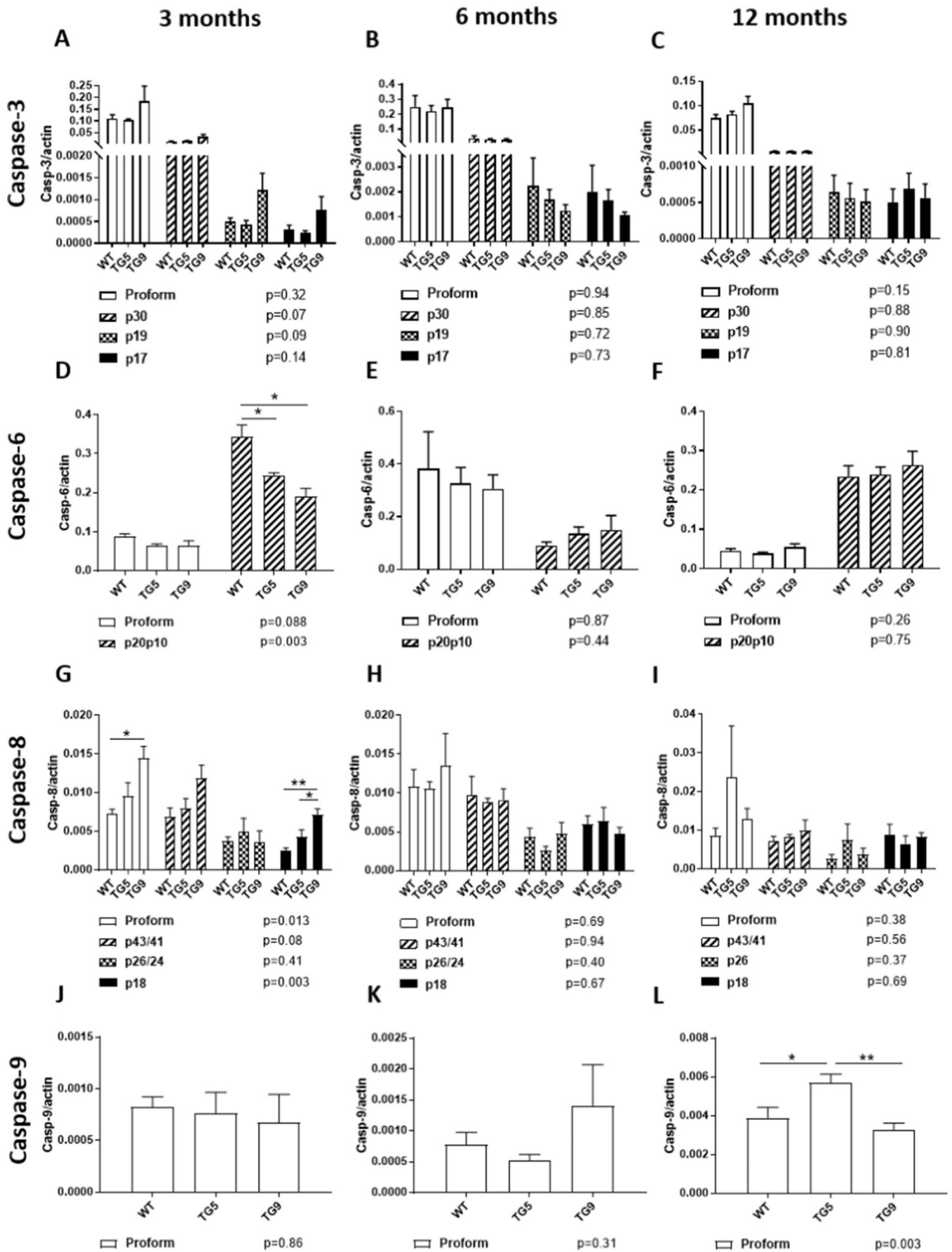


Fig. 5. Variations in caspase mRNA expression profiles in the olfactory bulb of BACHD models. A-C) Real-time quantitative RT-PCR shows an increase in caspase-3 mRNA expression levels in TG9 OB at 6 and 12 months of age compared to WT (6 months: ANOVA $p = 0.03$, post hoc: WT vs TG9 $p < 0.05$; 12 months: ANOVA $p = 0.02$, post hoc: WT vs TG9 $p < 0.05$). D-F) A trend increase in OB caspase-6 mRNA expression levels is observed at 3 months of age in TG9 vs. WT (ANOVA $p = 0.059$, t-test: WT vs TG9 $p < 0.05$). G-I) No variation in caspase-8 mRNA expression levels is detected in TG5 and TG9 OB compared to WT at any age assessed. J-L) A decrease is observed in caspase-9 mRNA expression levels in TG5 at 6 months of age and a trend decrease observed at 3 months of age in TG9 OB compared to WT (3 months: ANOVA $p = 0.08$, t-test: WT vs TG9, $p < 0.05$; 6 months: ANOVA $p = 0.04$, post hoc, WT vs. TG5, $p < 0.05$). 3 months: WT $n = 6$, TG5 $n = 6$ and TG9 $n = 6$; 6 months: WT $n = 4$, TG5 $n = 3$ and TG9 $n = 3$ 12 months: WT $n = 6$, TG5 $n = 4$ and TG9 $n = 6$; Dunnet post hoc are presented on graph. Pgk1 used as reference control. Relative measurements of caspase/pgk1 are \pm SEM.



(caption on next page)

Fig. 6. Early changes in caspase protein expression in the olfactory bulb of BACHD rats. A-C) A tendency to an increase in caspase-3 active fragment is observed at 3 months of age in TG9 OB, no further variation is observed at a later time point (p30: ANOVA $p = 0.07$; p19: ANOVA $p = 0.09$). D-F) A decrease, or a trend decrease in caspase-6 proform and p20p10 expression levels is observed at 3 months of age in TG5 and TG9 compared to WT OB (Proform: ANOVA $p = 0.09$, t-test: WT vs. TG5 $p < 0.05$; p20p10: ANOVA $p = 0.003$, post hoc: WT vs. TG5, $p < 0.05$; WT vs. TG9, $p < 0.05$). G-I) Increased expression of the caspase-8 proform, p43/41 and p18 fragments are detected in TG9 OB when compared to WT at 3 months of age (Proform: ANOVA $p = 0.013$, post hoc: WT vs. TG9, $p < 0.05$; p43/41: ANOVA $p = 0.08$, t-test: WT vs. TG9 $p = .052$; p18: ANOVA $p = 0.003$, post hoc: WT vs. TG9, $p < 0.01$; TG5 vs. TG9, $p < 0.05$). J-L) In sharp contrast to the other caspases, an increase in caspase-9 proform is observed only at 12 months of age in TG5 OB compared to WT (ANOVA $p = 0.003$, post hoc: WT vs. TG5, $p < 0.05$). The reference protein used is actin. The p values of the one-way ANOVA are presented below the graph for each form. Mean measurements and densitometric ratios of caspases/actin are \pm SEM, 3 months: WT $n = 4$ for all genotypes; 6 months: WT $n = 4$, TG5 $n = 3$ and TG9 $n = 3$; 12 months: WT $n = 6$, TG5 $n = 6$ and TG9 $n = 7$.

Table 1

Summary of huntingtin and caspase expression profiles in TG5 and TG9 BACHD OB compared to WT.

		3 months vs WT		6 months vs WT		12 months vs WT	
		TG5	TG9	TG5	TG9	TG5	TG9
Huntingtin	mRNA - wt htt	–	–	–	–	–	↑
	mRNA - mhhtt	↑ vs TG9	↓ vs TG5	–	–	↑ vs TG9	↓ vs TG5
	wild type htt	–	↓	–	–	–	–
	mhhtt (MAB2166)	↑ vs TG9	↓ vs TG5	–	–	–	–
	mhhtt (MAB1574)	↑ vs TG9	↓ vs TG5	–	–	–	–
	Ratio mhhtt/htt	↑ vs TG9	↓ vs TG5	–	–	↑ vs TG9	↓ vs TG5
	Nuclear htt accumulation	–	↑	↑	↑↑	↑↑	↑↑↑
Caspase 3	mRNA	–	–	–	↑	–	↑
	Proform	–	–	–	–	–	–
	p30	–	↑	–	–	–	–
	p19	–	↑	–	–	–	–
	p17	–	–	–	–	–	–
	% active caspase	–	↑ vs TG5	–	–	–	–
	Caspase 6	mRNA	–	↑	–	–	–
Proform		↓	–	–	–	–	–
p20p10		↓	↓	–	–	–	–
% active caspase		–	–	–	–	–	–
Caspase 8		mRNA	–	–	–	–	–
	Proform	–	↑	–	–	–	–
	p43/41	–	↑	–	–	–	–
	p26/24	–	–	–	–	–	–
	p18	–	↑	–	–	–	–
	% active caspase	–	↑	–	–	–	–
Caspase 9	mRNA	–	↓	–	–	–	–
	Proform	–	–	–	–	↑	–
Cell death	TUNEL-positive cells	ND	ND	ND	ND	–	↑

Caspase-3: p30 = 30 kDa fragment, p19 = 19 kDa fragment, p17 = 17 kDa fragment, Caspase-6: p20p10 = CASP6 without the prodomain, Caspase-8: p43/41 = 43 and 41 kDa fragments, p26/24 = 26 and 24 kDa fragments, p18 = 18 kDa fragment. Proform = full-length form of the caspase protein. The sign « – » represents no significant variation between the BACHD rat model and the WT. ND = Not Done.

difference in the spatial distribution of mHTT in TG5 vs. TG9 lines may explain the discrepancy observed in the behaviour and brain pathology between them. Indeed, in addition to the differences observed in this study (lack of caspase-3 and -8 activation in the TG5 OB and reduced OB mHTT nuclear accumulation compared to TG9) the TG5 line displays earlier motor deficits (accelerated rotarod, gait analysis) and decreased rearing activities compared to TG9. However, both lines display similar deficits in ambulatory activities, reduced food intake and HD gene expression signatures of a similar magnitude (Yu-Taeger et al., 2017; Yu-Taeger et al., 2012). These results highlight the necessity of comparing different lines and strains in animal models.

5. Conclusion

Our results show a significant decrease in the OB at specific time points in the BACHD transgenic lines. The atrophy is predominantly detected in the internal layers of the OB while the glomerular layer area is not affected. Furthermore, variations in caspase mRNA expression levels, and alterations in caspase protein expression levels are observed. We also detected a differential expression and localization profile of normal and mutant HTT in TG5 compared to the TG9 line. Despite the increase in mHTT expression in the TG5 OBs, TG9 rats demonstrate caspase-3 and -8 activation in the OB, more accumulation of HTT in the nucleus and more cell death. These data provide important information

regarding the olfactory dysfunction observed in HD and further implicate alterations in apoptosis and neurogenesis as underlying mechanisms in the pathogenesis of HD.

Acknowledgements

This research was undertaken with a research grant from the Huntington Society of Canada, Research Centre on Aging, and, in part, by the Canada Research chairs program. Support was also provided by the European Union 7th Framework Program (FP7/2012), Project “SWITCH-HD”, under grant agreement No. 324495 to H.P.N. RKG holds the Canada Research Chair in Neurodegenerative diseases.

Appendix A. Supplementary data

Supplementary data to this article can be found online at <https://doi.org/10.1016/j.nbd.2019.02.002>.

References


- Abada, Y.S., et al., 2013. Motor, emotional and cognitive deficits in adult BACHD mice: a model for Huntington's disease. *Behav. Brain Res.* 238, 243–251.
- Acton, Q.A., 2013. *Huntington's Disease: New Insights for the Healthcare Professional*. ScholarlyEditions, Atlanta, Georgia.
- Aylward, E.H., et al., 1994. Reduced basal ganglia volume associated with the gene for

- Huntington's disease in asymptomatic at-risk persons. *Neurology* 44, 823–828.
- Aylward, E.H., et al., 1996. Basal ganglia volume and proximity to onset in presymptomatic Huntington disease. *Arch. Neurol.* 53, 1293–1296.
- Bacon Moore, A.S., et al., 1999. A test of odor fluency in patients with Alzheimer's and Huntington's disease. *J. Clin. Exp. Neuropsychol.* 21, 341–351.
- Bahar-Fuchs, A., et al., 2011. Awareness of olfactory deficits in healthy aging, amnesic mild cognitive impairment and Alzheimer's disease. *Int. Psychogeriatr.* 23, 1097–1106.
- Barresi, M., et al., 2012. Evaluation of olfactory dysfunction in neurodegenerative diseases. *J. Neurol. Sci.* 323, 16–24.
- Barrios, F.A., et al., 2007. Olfaction and neurodegeneration in HD. *Neuroreport* 18, 73–76.
- Bastakis, G.G., et al., 2015. Tag1 deficiency results in olfactory dysfunction through impaired migration of mitral cells. *Development* 142, 4318–4328.
- Boutell, J.M., et al., 1999. Aberrant interactions of transcriptional repressor proteins with the Huntington's disease gene product, huntingtin. *Hum. Mol. Genet.* 8, 1647–1655.
- Brodoehl, S., et al., 2012. Decreased olfactory bulb volume in idiopathic Parkinson's disease detected by 3.0-tesla magnetic resonance imaging. *Mov. Disord.* 27, 1019–1025.
- Burns, A., et al., 1990. Clinical assessment of irritability, aggression, and apathy in Huntington and Alzheimer disease. *J. Nerv. Ment. Dis.* 178, 20–26.
- Buschhuter, D., et al., 2008. Correlation between olfactory bulb volume and olfactory function. *NeuroImage* 42, 498–502.
- Bylsma, F.W., et al., 1997. Odor identification in Huntington's disease patients and asymptomatic gene carriers. *J. Neuropsychiatry Clin. Neurosci.* 9, 598–600.
- Carroll, J.B., et al., 2011. Natural history of disease in the YAC128 mouse reveals a discrete signature of pathology in Huntington disease. *Neurobiol. Dis.* 43, 257–265.
- Cattaneo, E., et al., 2005. Normal huntingtin function: an alternative approach to Huntington's disease. *Nat. Rev. Neurosci.* 6, 919–930.
- Chen, S., et al., 2014. Imaging of olfactory bulb and gray matter volumes in brain areas associated with olfactory function in patients with Parkinson's disease and multiple system atrophy. *Eur. J. Radiol.* 83, 564–570.
- Chen, D.L., et al., 2015. Imaging caspase-3 activation as a marker of apoptosis-targeted treatment response in cancer. *Mol. Imaging Biol.* 17, 384–393.
- Christen-Zaech, S., et al., 2003. Early olfactory involvement in Alzheimer's disease. *Can. J. Neurol. Sci.* 30, 20–25.
- Cornett, J., et al., 2005. Polyglutamine expansion of huntingtin impairs its nuclear export. *Nat. Genet.* 37, 198–204.
- Cowan, C.M., Roskams, A.J., 2004. Caspase-3 and caspase-9 mediate developmental apoptosis in the mouse olfactory system. *J. Comp. Neurol.* 474, 136–148.
- Cummings, J.L., 1995. Behavioral and psychiatric symptoms associated with Huntington's disease. *Adv. Neurol.* 65, 179–186.
- Curtis, M.A., et al., 2003. Increased cell proliferation and neurogenesis in the adult human Huntington's disease brain. *Proc. Natl. Acad. Sci. U. S. A.* 100, 9023–9027.
- Curtis, M.A., et al., 2005. The distribution of progenitor cells in the subependymal layer of the lateral ventricle in the normal and Huntington's disease human brain. *Neuroscience* 132, 777–788.
- de Almeida, L.P., et al., 2002. Lentiviral-mediated delivery of mutant huntingtin in the striatum of rats induces a selective neuropathology modulated by polyglutamine repeat size, huntingtin expression levels, and protein length. *J. Neurosci.* 22, 3473–3483.
- Delmaire, C., et al., 2012. The structural correlates of functional deficits in early Huntington's disease. *Hum. Brain Mapp.* 34, 2141–2153.
- Djordjevic, J., et al., 2008. Olfaction in patients with mild cognitive impairment and Alzheimer's disease. *Neurobiol. Aging* 29, 693–706.
- Doty, R.L., 2012a. Olfaction in Parkinson's disease and related disorders. *Neurobiol. Dis.* 46, 527–552.
- Doty, R.L., 2012b. Olfactory dysfunction in Parkinson disease. *Nat. Rev. Neurol.* 8, 329–339.
- Fedele, V., et al., 2011. Neurogenesis in the R6/2 mouse model of Huntington's disease is impaired at the level of NeuroD1. *Neuroscience* 173, 76–81.
- Ferris, C.F., et al., 2014. Studies on the Q175 Knock-in Model of Huntington's Disease using Functional Imaging in Awake mice: evidence of Olfactory Dysfunction. *Front. Neurol.* 5, 94.
- Gafni, J., et al., 2004. Inhibition of calpain cleavage of huntingtin reduces toxicity: accumulation of calpain/caspase fragments in the nucleus. *J. Biol. Chem.* 279, 20211–20220.
- Gervais, F.G., et al., 2002. Recruitment and activation of caspase-8 by the Huntington-interacting protein Hip-1 and a novel partner Hippi. *Nat. Cell Biol.* 4, 95–105.
- Goldberg, Y.P., et al., 1996. Cleavage of huntingtin by apopain, a proapoptotic cysteine protease, is modulated by the polyglutamine tract. *Nat. Genet.* 13, 442–449.
- Graham, R.K., et al., 2006a. Cleavage at the caspase-6 site is required for neuronal dysfunction and degeneration due to mutant huntingtin. *Cell* 125, 1179–1191.
- Graham, R.K., et al., 2006b. Levels of mutant huntingtin influence the phenotypic severity of Huntington disease in YAC128 mouse models. *Neurobiol. Dis.* 21, 444–455.
- Graham, R.K., et al., 2010. Cleavage at the 586 amino acid caspase-6 site in mutant huntingtin influences caspase-6 activation in vivo. *J. Neurosci.* 30, 15019–15029.
- Graham, R.K., et al., 2012. Caspase-6-resistant mutant Huntingtin does not rescue the toxic effects of Caspase-Cleavable Mutant Huntingtin in vivo. *J. Huntingtons Dis.* 1, 243–260.
- Hamilton, J.M., et al., 1999. Odor detection, learning, and memory in Huntington's disease. *J. Int. Neuropsychol. Soc.* 5, 609–615.
- Han, M.H., et al., 2016. Current opinion on the role of neurogenesis in the therapeutic strategies for Alzheimer Disease, Parkinson Disease, and Ischemic Stroke; considering neuronal voiding function. *Int. Neurol.* J. 20, 276–287.
- Hatada, S., et al., 1999. The influence of chromosomal location on the expression of two transgenes in mice. *J. Biol. Chem.* 274, 948–955.
- Hermel, E., et al., 2004a. Specific caspase interactions and amplification are involved in selective neuronal vulnerability in Huntington's disease. *Cell Death Differ.* 11, 424–438.
- Hermel, E., et al., 2004b. Specific caspase interactions and amplification are involved in selective neuronal vulnerability in Huntington's disease. *Cell Death Differ.* 11, 424–438.
- Hodgson, J.G., et al., 1999. A YAC mouse model for Huntington's disease with full-length mutant huntingtin, cytoplasmic toxicity, and selective striatal neurodegeneration. *Neuron* 23, 181–192.
- Holter, S.M., et al., 2013. A broad phenotypic screen identifies novel phenotypes driven by a single mutant allele in Huntington's disease CAG knock-in mice. *PLoS One* 8, e80923.
- Hummel, T., et al., 2011. Correlation between olfactory bulb volume and olfactory function in children and adolescents. *Exp. Brain Res.* 214, 285–291.
- Ishikawa, K., et al., 2017. Post-translational dosage compensation buffers genetic perturbations to stoichiometry of protein complexes. *PLoS Genet.* 13, e1006554.
- Jankovic, J., Roos, R.A., 2014. Chorea associated with Huntington's disease: to treat or not to treat? *Mov. Disord.* 29, 1414–1418.
- Karamitopoulou, E., et al., 2007. Active caspase 3 and DNA fragmentation as markers for apoptotic cell death in primary and metastatic liver tumours. *Pathology* 39, 558–564.
- Kiechle, T., et al., 2002. Cytochrome C and caspase-9 expression in Huntington's disease. *NeuroMolecular Med.* 1, 183–195.
- Kim, Y.J., et al., 2001. Caspase 3-cleaved N-terminal fragments of wild-type and mutant huntingtin are present in normal and Huntington's disease brains, associate with membranes, and undergo calpain-dependent proteolysis. *Proc. Natl. Acad. Sci.* 98, 12784–12789.
- Kim, M.J., et al., 2002. Calpain-dependent cleavage of cain/cabin1 activates calcineurin to mediate calcium-triggered cell death. *Proc. Natl. Acad. Sci. U. S. A.* 99, 9870–9875.
- Klaiman, G., et al., 2009. Self-activation of Caspase-6 in vitro and in vivo: Caspase-6 activation does not induce cell death in HEK293T cells. *Biochim. Biophys. Acta* 1793, 592–601.
- Kohl, Z., et al., 2010. Impaired adult olfactory bulb neurogenesis in the R6/2 mouse model of Huntington's disease. *BMC Neurosci.* 11 (114-2202-11-114).
- Kouroku, Y., et al., 2000. Caspases that are activated during generation of nuclear polyglutamine aggregates are necessary for DNA fragmentation but not sufficient for cell death. *J. Neurosci. Res.* 62, 547–556.
- Kouroku, Y., et al., 2002. Polyglutamine aggregates stimulate ER stress signals and caspase-12 activation. *Hum. Mol. Genet.* 11, 1505–1515.
- Larsson, M., et al., 2006. Olfactory functions in asymptomatic carriers of the Huntington disease mutation. *J. Clin. Exp. Neuropsychol.* 28, 1373–1380.
- Lazic, S.E., et al., 2007. Olfactory abnormalities in Huntington's disease: decreased plasticity in the primary olfactory cortex of R6/1 transgenic mice and reduced olfactory discrimination in patients. *Brain Res.* 1151, 219–226.
- Li, L., et al., 2016. Real-time imaging of Huntingtin aggregates diverting target search and gene transcription. *elife* 5.
- Lunke, A., et al., 2002. Proteases acting on mutant huntingtin generate cleaved products that differentially build up cytoplasmic and nuclear inclusions. *Mol. Cell* 10, 259–269.
- Mazumder, S., et al., 2008. Caspase-3 activation is a critical determinant of genotoxic stress-induced apoptosis. *Methods Mol. Biol.* 414, 13–21.
- Menalled, L.B., et al., 2003. Time course of early motor and neuropathological anomalies in a knock-in mouse model of Huntington's disease with 140 CAG repeats. *J. Comp. Neurol.* 465, 11–26.
- Mende-Mueller, L.M., et al., 2001. Tissue-specific proteolysis of Huntingtin (htt) in human brain: evidence of enhanced levels of N- and C-terminal htt fragments in Huntington's disease striatum. *J. Neurosci.* 21, 1830–1837.
- Metzler, M., et al., 2010. Phosphorylation of huntingtin at Ser421 in YAC128 neurons is associated with protection of YAC128 neurons from NMDA-mediated excitotoxicity and is modulated by PPI and PPA. *J. Neurosci.* 30, 14318–14329.
- Milnerwood, A.J., et al., 2010. Early increase in extrasynaptic NMDA receptor signaling and expression contributes to phenotype onset in Huntington's disease mice. *Neuron* 65, 178–190.
- Mitchell, L.J., et al., 2005. Huntington's disease patients show impaired perception of disgust in the gustatory and olfactory modalities. *J. Neuropsychiatry Clin. Neurosci.* 17, 119–121.
- Miyashita, T., et al., 1999. Expression of extended polyglutamine sequentially activates initiator and effector caspases. *Biochem. Biophys. Res. Commun.* 257, 724–730.
- Mo, C., et al., 2014. Effects of chronic stress on the onset and progression of Huntington's disease in transgenic mice. *Neurobiol. Dis.* 71, 81–94.
- Mo, C., et al., 2015. Novel ethological endophenotypes in a transgenic mouse model of Huntington's disease. *Behav. Brain Res.* 276, 17–27.
- Moberg, P.J., Doty, R.L., 1997. Olfactory function in Huntington's disease patients and at-risk offspring. *Int. J. Neurosci.* 89, 133–139.
- Moberg, P.J., et al., 1987. Olfactory recognition: differential impairments in early and late Huntington's and Alzheimer's diseases. *J. Clin. Exp. Neuropsychol.* 9, 650–664.
- Mori, K., 2014. *The Olfactory System: From Odor Molecules to Motivational Behaviors*. Springer, Tokyo; New York.
- Mouret, A., et al., 2009. Turnover of newborn olfactory bulb neurons optimizes olfaction. *J. Neurosci.* 29, 12302–12314.
- Nordin, S., et al., 1995. Sensory- and memory-mediated olfactory dysfunction in Huntington's disease. *J. Int. Neuropsychol. Soc.* 1, 281–290.
- Ona, V.O., et al., 1999. Inhibition of caspase-1 slows disease progression in a mouse model of Huntington's disease. *Nature* 399, 263–267.
- Paulsen, J.S., et al., 2008. Detection of Huntington's disease decades before diagnosis: the Predict-HD study. *J. Neurol. Neurosurg. Psychiatry* 79, 874–880.

- Paulsen, J.S., et al., 2014. Clinical and biomarker changes in Premanifest Huntington Disease Show Trial Feasibility: a Decade of the PREDICT-HD Study. *Front. Aging Neurosci.* 6, 78.
- Perl, K., et al., 2017. Reduced changes in protein compared to mRNA levels across non-proliferating tissues. *BMC Genomics* 18, 305.
- Phillips, W., et al., 2005. Abnormalities of neurogenesis in the R6/2 mouse model of Huntington's disease are attributable to the in vivo microenvironment. *J. Neurosci.* 25, 11564–11576.
- Pirogovsky, E., et al., 2007. Impairments in source memory for olfactory and visual stimuli in preclinical and clinical stages of Huntington's disease. *J. Clin. Exp. Neuropsychol.* 29, 395–404.
- Pouladi, M.A., et al., 2009. Prevention of depressive behaviour in the YAC128 mouse model of Huntington disease by mutation at residue 586 of huntingtin. *Brain* 132, 919–932.
- Rajkowska, G., et al., 1998. Neuronal and glial somal size in the prefrontal cortex: a postmortem morphometric study of schizophrenia and Huntington disease. *Arch. Gen. Psychiatry* 55, 215–224.
- Reddy, P.H., et al., 1998. Behavioural abnormalities and selective neuronal loss in HD transgenic mice expressing mutated full-length HD cDNA. *Nat. Genet.* 20, 198–202.
- Rigamonti, D., et al., 2001. Huntingtin's neuroprotective activity occurs via inhibition of procaspase-9 processing. *J. Biol. Chem.* 276, 14545–14548.
- Ross, C.A., et al., 2014. Determinants of functional disability in Huntington's disease: role of cognitive and motor dysfunction. *Mov. Disord.* 29, 1351–1358.
- Sanchez, I., et al., 1999a. Caspase-8 is required for cell death induced by expanded polyglutamine repeats. *Neuron* 22, 623–633.
- Sanchez, I., et al., 1999b. Caspase-8 is required for cell death induced by expanded polyglutamine repeats. *Neuron* 22, 623–633.
- Sathasivam, K., et al., 2001. Centrosome disorganization in fibroblast cultures derived from R6/2 Huntington's disease (HD) transgenic mice and HD patients. *Hum. Mol. Genet.* 10, 2425–2435.
- Servello, A., et al., 2015. Olfactory dysfunction, olfactory bulb volume and Alzheimer's Disease: is there a correlation? A pilot Study1. *J. Alzheimers Dis.* 48, 395–402.
- Shimohata, T., et al., 2000. Interaction of expanded polyglutamine stretches with nuclear transcription factors leads to aberrant transcriptional regulation in polyglutamine diseases. *Neuropathology* 20, 326–333.
- Simpson, J.M., et al., 2011. Altered adult hippocampal neurogenesis in the YAC128 transgenic mouse model of Huntington disease. *Neurobiol. Dis.* 41, 249–260.
- Singer, E., et al., 2017. Reduced cell size, chromosomal aberration and altered proliferation rates are characteristics and confounding factors in the STHdh cell model of Huntington disease. *Sci. Rep.* 7, 16880.
- Smail, S., et al., 2016. Increased olfactory bulb BDNF expression does not rescue deficits in olfactory neurogenesis in the Huntington's Disease R6/2 Mouse. *Chem. Senses* 41, 221–232.
- Squitieri, F., et al., 2003. Homozygosity for CAG mutation in Huntington disease is associated with a more severe clinical course. *Brain* 126, 946–955.
- Steffan, J.S., et al., 2000. The Huntington's disease protein interacts with p53 and CREB-binding protein and represses transcription. *Proc. Natl. Acad. Sci. U. S. A.* 97, 6763–6768.
- Tabrizi, S.J., et al., 2009. Biological and clinical manifestations of Huntington's disease in the longitudinal TRACK-HD study: cross-sectional analysis of baseline data. *Lancet Neurol.* 8, 791–801.
- ter Laak, H.J., et al., 1994. The olfactory bulb in Alzheimer disease: a morphologic study of neuron loss, tangles, and senile plaques in relation to olfaction. *Alzheimer Dis. Assoc. Disord.* 8, 38–48.
- Thomann, P.A., et al., 2009. MRI-derived atrophy of the olfactory bulb and tract in mild cognitive impairment and Alzheimer's disease. *J. Alzheimers Dis.* 17, 213–221.
- Toulmond, S., et al., 2004. Neuroprotective effects of M826, a reversible caspase-3 inhibitor, in the rat malonate model of Huntington's disease. *Br. J. Pharmacol.* 141, 689–697.
- U, M., et al., 2001. Extended polyglutamine selectively interacts with caspase-8 and -10 in nuclear aggregates. *Cell Death Differ.* 8, 377–386.
- Uribe, V., et al., 2012. Rescue from excitotoxicity and axonal degeneration accompanied by age-dependent behavioral and neuroanatomical alterations in caspase-6-deficient mice. *Hum. Mol. Genet.* 21, 1954–1967.
- Vilchez, D., et al., 2014. The role of protein clearance mechanisms in organismal ageing and age-related diseases. *Nat. Commun.* 5, 5659.
- Wang, J., et al., 2011. Association of olfactory bulb volume and olfactory sulcus depth with olfactory function in patients with Parkinson disease. *AJNR Am. J. Neuroradiol.* 32, 677–681.
- Wanker, E.E., 2002. Hip1 and Hipp1 participate in a novel cell death-signaling pathway. *Dev. Cell* 2, 126–128.
- Warby, S.C., et al., 2008. Activated caspase-6 and caspase-6-cleaved fragments of huntingtin specifically colocalize in the nucleus. *Hum. Mol. Genet.* 17, 2390–2404.
- Wellington, C.L., et al., 2002a. Caspase cleavage of mutant huntingtin precedes neurodegeneration in Huntington's disease. *J. Neurosci.* 22, 7862–7872.
- Wellington, C.L., et al., 2002b. Caspase cleavage of mutant huntingtin precedes neurodegeneration in Huntington's disease. *J. Neurosci.* 22, 7862–7872.
- Wirhith, O., 2017. Altered neurogenesis in mouse models of Alzheimer disease. *Neurogenesis (Austin)* 4, e1327002.
- Wong, B.K., et al., 2015. Partial rescue of some features of Huntington disease in the genetic absence of caspase-6 in YAC128 mice. *Neurobiol. Dis.* 76, 24–36.
- Yamaguchi, M., et al., 2013. Reorganization of neuronal circuits of the central olfactory system during postprandial sleep. *Front. Neural Circuits.* 7, 132.
- Yan, X.X., et al., 2001. Expression of active caspase-3 in mitotic and postmitotic cells of the rat forebrain. *J. Comp. Neurol.* 433, 4–22.
- Youssef, I., et al., 2008. N-truncated amyloid-beta oligomers induce learning impairment and neuronal apoptosis. *Neurobiol. Aging* 29, 1319–1333.
- Yu-Taeger, L., et al., 2012. A novel BACHD transgenic rat exhibits characteristic neuropathological features of Huntington disease. *J. Neurosci.* 32, 15426–15438.
- Yu-Taeger, L., et al., 2017. Dysregulation of gene expression in the striatum of BACHD rats expressing full-length mutant huntingtin and associated abnormalities on molecular and protein levels. *Neuropharmacology* 117, 260–272.

Article

Intranasal Administration of Mesenchymal Stem Cells Ameliorates the Abnormal Dopamine Transmission System and Inflammatory Reaction in the R6/2 Mouse Model of Huntington Disease

Libo Yu-Taeger ^{1,2,†}, Janice Stricker-Shaver ^{1,2,†}, Katrin Arnold ^{3,4}, Patrycja Bambynek-Dziuk ^{1,2}, Arianna Novati ^{1,2}, Elisabeth Singer ^{1,2} , Ali Lourhmati ⁵, Claire Fabian ^{3,4}, Janine Magg ^{1,2}, Olaf Riess ^{1,2}, Matthias Schwab ^{5,6,7,8}, Alexandra Stolzing ^{3,9}, Lusine Danielyan ^{5,7,8} and Hoa Huu Phuc Nguyen ^{1,2,7,10,11,*}

¹ Institute of Medical Genetics and Applied Genomics, University of Tuebingen, D-72076 Tuebingen, Germany; Libo.Yu-Taeger@med.uni-tuebingen.de (L.Y.-T.); janice.strickershaver@gmail.com (J.S.-S.); Patrycja.Bambynek-Dziuk@med.uni-tuebingen.de (P.B.-D.); Arianna.Novati@med.uni-tuebingen.de (A.N.); Elisabeth.Singer@med.uni-tuebingen.de (E.S.); Janine.Magg@med.uni-tuebingen.de (J.M.); Olaf.Riess@med.uni-tuebingen.de (O.R.)

² Centre for Rare Diseases (ZSE), University of Tuebingen, D-72076 Tuebingen, Germany

³ Interdisciplinary Centre for Bioinformatics (IZBI), University of Leipzig, D-04107 Leipzig, Germany; katrin.arnold@izi.fraunhofer.de (K.A.); claire.fabian@izi.fraunhofer.de (C.F.); A.Stolzing@lboro.ac.uk (A.S.)

⁴ Fraunhofer Institute for Cell Therapy and Immunology (IZI), D-04103 Leipzig, Germany

⁵ Department of Clinical Pharmacology, University Hospital of Tuebingen, D-72076 Tuebingen, Germany; alilourhmati@yahoo.de (A.L.); Matthias.Schwab@ikp-stuttgart.de (M.S.); Lusine.Danielyan@med.uni-tuebingen.de (L.D.)

⁶ Dr. Margarete Fischer-Bosch Institute of Clinical Pharmacology, D-70376 Stuttgart, Germany

⁷ Departments of Biochemistry and Clinical Pharmacology, Yerevan State Medical University, 0025 Yerevan, Armenia

⁸ Laboratory of Neuroscience, Yerevan State Medical University, 0025 Yerevan, Armenia

⁹ Centre for Biological Engineering, School of Mechanical, Electrical and Manufacturing Engineering, Loughborough University, Loughborough LE11 3TU, UK

¹⁰ Department of Human Genetics, Ruhr University of Bochum, D-44801 Bochum, Germany

¹¹ Departments of Medical Chemistry and Biochemistry, Yerevan State Medical University, 0025 Yerevan, Armenia

* Correspondence: huu.nguyen-r7w@rub.de; Tel.: +49-234-32-23839

† The authors contributed equally to this work.

Received: 15 May 2019; Accepted: 13 June 2019; Published: 15 June 2019



Abstract: Intrastratial administration of mesenchymal stem cells (MSCs) has shown beneficial effects in rodent models of Huntington disease (HD). However, the invasive nature of surgical procedure and its potential to trigger the host immune response may limit its clinical use. Hence, we sought to evaluate the non-invasive intranasal administration (INA) of MSC delivery as an effective alternative route in HD. GFP-expressing MSCs derived from bone marrow were intranasally administered to 4-week-old R6/2 HD transgenic mice. MSCs were detected in the olfactory bulb, midbrain and striatum five days post-delivery. Compared to phosphate-buffered saline (PBS)-treated littermates, MSC-treated R6/2 mice showed an increased survival rate and attenuated circadian activity disruption assessed by locomotor activity. MSCs increased the protein expression of DARPP-32 and tyrosine hydroxylase (TH) and downregulated gene expression of inflammatory modulators in the brain 7.5 weeks after INA. While vehicle treated R6/2 mice displayed decreased Iba1 expression and altered microglial morphology in comparison to the wild type littermates, MSCs restored both, Iba1 level and the thickness of microglial processes in the striatum of R6/2 mice. Our results demonstrate

significantly ameliorated phenotypes of R6/2 mice after MSCs administration via INA, suggesting this method as an effective delivering route of cells to the brain for HD therapy.

Keywords: Huntington disease; cell therapy; mesenchymal stem cells; intranasal; R6/2 mice; dopamine transmission; microglia; neuroinflammation

1. Introduction

Huntington disease (HD) is an autosomal dominant neurodegenerative disorder that affects 4–10 individuals per 100,000 [1–4]. It is an adult-onset, chronically progressing disease manifested by motor dysfunction, cognitive decline, and psychiatric symptoms together with weight loss and sleep disturbance (reviewed in [5,6]). HD is caused by an expansion of the CAG (coding for glutamine) repeat region in exon 1 of the huntingtin (*HTT*) gene that encodes the huntingtin protein (HTT) [7]. In mutant HTT (mHTT), the polyglutamine tract contains more than 38 glutamines and the length of the tract correlates inversely with the age of disease onset, with longer tracts resulting in earlier onset [3,4]. The neuropathological hallmarks of HD feature a substantial accumulation of protein aggregates containing truncated N-terminal mHTT fragments in the cortex and striatum [8], and striatal atrophy that progressively extends to cerebral cortex and other brain regions [9,10].

At present, there is no effective treatment for disease prevention or slowing down disease progression [11,12]. Existing medications are limited and only alleviate the HD symptoms so as to improve the quality of life of the patients [3,12,13], but do not extend the life span of the patients. Recent therapeutic development for neurologic disorders explored the potentials of multipotent mesenchymal stem cells (MSCs) that possess regenerative properties and their preferential tropism to migrate to damaged brain regions in the degenerating central nervous system (CNS) [14,15]. In vivo testing reported that the therapeutic effects of MSCs are mainly attributed to their neuroprotective/immunomodulatory capacity and enhanced availability of bioactive factors including trophic and growth factors that could induce tissue repair and angiogenesis [16,17]. The therapeutic effects of MSCs were explored by intracerebral transplantation in animal models of HD [14,18–21], Parkinson's disease (PD) [22–27] and Alzheimer's disease (AD) [28–36], all of which ameliorated phenotypic impairments in MSC-treated animal models. It is, however, considered to have a limited translational potential [16]. While intracranial delivery enhances the number of cells reaching the targeted brain region when compared to systemic administration, the invasive nature of the delivery method poses high risk to the subject and restricts repeated cell administrations within a short period of time [37,38]. Later studies have hence utilized the innovative, non-invasive intranasal administration route for brain targeting [39,40]. We have previously shown that after MSCs crossed the cribriform plate, they either migrated into the olfactory bulb and subsequently to the other brain regions, or entered the cerebrospinal fluid (CSF) with movement along the surface of the cortex and then into the brain parenchyma [41], which has been recently confirmed [42]. Later we demonstrated the efficacy of intranasally administered MSCs in the 6-hydroxydopamine (6-OHDA) rat model of PD [43]. Likewise, beneficial effects of intranasally delivered MSCs were also reported in a rotenone-induced PD mouse model [44] and a spinal cord-lesioned rat model [45]. Based on the promising in vivo data and our technical expertise on intranasal MSC-treatment in neurological disease models, in this study we evaluated the therapeutic effects of MSCs administered via the intranasal route in HD using the R6/2 mouse model.

The R6/2 mouse model carries an N-terminal exon 1 fragment of the disease-causing human *HTT* gene that contains approximately 145 CAG repeats (length of polyglutamine expansion varies due to germ line instability) [46,47]. As a result, they display physiological and behavioral phenotypes that recapitulate symptoms of HD patients [48,49], including progressive weight loss, shortened life span [46,50,51], progressive motor dysfunction [50,52], cognitive decline [53,54] and

neuropsychiatric-like disturbances [55,56] such as disrupted circadian rhythm [57]. Brain volume reduction and neuronal intranuclear inclusions are also consistently observed in R6/2 mice, resembling the neuropathological features of human HD [46,51,52]. Furthermore, R6/2 mice have been reported to have a wide range of gene dysregulation in various brain areas. This includes the expression of multiple inflammation- and stress-related genes as well as genes related to neurodegeneration [58]. As in other neurodegenerative diseases, neuroinflammation was detected in HD patients as well as in HD animal models like the R6/2 mice [59–65], in which pro-inflammatory cytokines such as interleukin 6 (IL-6) and tumor necrosis factor alpha (TNF α) were significantly elevated. It is well known that MSCs exert immunomodulatory effects by affecting immune T- and B-cell responses, including suppression of T- and B-cell proliferation and the regulatory response of the T-cell, as well as activation of dendritic and natural killer cells [66–70]. Moreover, MSCs secrete various cytokines, trophic and growth factors that support neuronal survival and regeneration [71,72]. Cell migration deficits including impaired function of microglia and the decreased expression of microglia marker Ionized calcium-binding adapter molecule 1 (Iba1) have been observed in HD transgenic mice [73,74]. Besides, the dopaminergic neurotransmission system is also severely impaired [75,76], as shown by the decreased mRNA expressions of both D1 and D2 dopamine receptors and their electrophysiological responses to receptor activation [77].

In this study, MSCs isolated from the bone marrow of young eGFP mice were transplanted into the transgenic HD mouse model R6/2 via the intranasal delivery route at the early disease stage. MSCs were found to have a dynamic and widespread distribution in several major brain regions. Physiological and behavioral parameters were monitored in MSC-treated R6/2 mice longitudinally post-transplantation and were compared to the control groups (PBS-treated wild type (WT) and PBS-treated R6/2 mice). We found that intranasal MSC treatment extended the life span and alleviated the circadian activity disruption of the R6/2 mice. Expression analyses revealed that these functional improvements were attributed to ameliorated neuroinflammatory activation and improved dopaminergic signaling. Moreover, MSCs could restore the expression of Iba1 as a marker of microglia and the morphology of striatum-resident microglia in R6/2 mice. Altogether, our study provides evidence that intranasal administration of MSCs is an efficacious delivery route for HD treatment and has a high translational potential to the clinics for HD as well as other neurodegeneration-targeting therapies.

2. Materials and Methods

2.1. Isolation, Cultivation and Characterization of MSC *in Vitro*

Transgenic mice expressing eGFP (8–12 weeks old, male, C57Bl/6-Tg(UBC-GFP)30Scha/J (eGFP mice) were obtained from Jackson Laboratories (Bar Harbor, ME). Bone marrow was harvested from tibia and femur as described previously [78]. MSCs were cultivated in minimum essential medium (MEM) α , GlutaMAX™ (Gibco, 32561029) with 15% fetal calf serum (FCS) (Gibco, 10270106) and 1% penicillin/streptomycin (Gibco, 15070-063) supplemented with 20 ng/mL FGFB (Peprotech, 450-33). MSCs were harvested at passage 2 and frozen in 10% DMSO/90% cultivation medium until transplantation. All MSCs used for transplantations were at passage three. Cells were harvested at passage four and fixed with 2% (*v/v*) buffered paraformaldehyde (Pierce, 16% Formaldehyde, Methanol-free) for 15 min at room temperature. Mouse Mesenchymal Stem Cell Marker Antibody Panel (R&D Systems, SC018) was used according to the manufacturer's protocol. The panel consisted of the following antibodies: Anti-CD11b, anti-CD45, anti-Sca-1, anti-CD 106, anti-CD105, anti-CD73, anti-CD29, and anti-CD44, rat IgG2A (MAB006, Life Technologies) and rat IgG2B (MAB0061, Life Technologies). MSC were blocked in 5% BSA for 30 min at room temperature and then incubated with primary antibodies for 30 min at room temperature. MSC were washed two times with PBS and stained with secondary antibodies (1:200 dilution: Donkey anti-rat Cy3 (712-165-153, Dianova) or sheep anti-rat-NL557 (NL013, R&D)). After 30 min incubation at room temperature, cells were washed

two times and fluorescence was measured using BD-Influx. Gates were set according to appropriate isotype controls. Dot blot graphs were created using BD FACSTM Software.

2.2. HD Animals

For the animal experiments, female mice expressing exon 1 of mutant human *HTT* gene with approximately 145 CAG repeats were housed with littermates of mixed genotype in groups of four with 12 h light/dark cycle and free access to food and water. All experiments were approved by the local ethics committee at the Regierungspraesidium Tuebingen (License Number:PH8/13), and carried out in accordance with the German Animal Welfare Act and the guidelines of the Federation of European Laboratory Animal Science Associations based on European Union legislation (Directive 2010/63/EU).

Breeding was performed by crossing wild-type B6CBAF1/J males with ovary-transplanted R6/2 females (B6CBA-TgN(HDexon1)62Gbp/J) supplied by The Jackson Laboratory (Charles River Laboratory). Genotyped female R6/2 and wild-type (WT) littermates from each cohort were assigned to different treatment groups according to their body weight and rotarod test performance to counterbalance the potential litter effects. Animals were divided into three treatment groups and recruited to all behavioral experiments: (1) R6/2 mice treated with MSCs resuspended in phosphate-buffered saline (PBS) (R6/2-MSC); (2) R6/2 mice treated with PBS (R6/2-PBS) and; (3) WT mice treated with PBS (WT-PBS) ($n = 16$ per group). Animals were sacrificed at 7.5 weeks after intranasal MCS vs. PBS treatment. For the analysis of cell migration in the brain animals were sacrificed five days post-delivery of MSCs ($n = 3$).

2.3. Intranasal Cell Transplantation

Mice at four weeks of age were administered with MSCs of passage three as previously described [41]. The mice were held with a hand grip that allowed the animals to recline on their backs while immobilizing the skull, and the nose drop containing the substance/cell suspension was carefully placed on one nostril allowing it to be snorted naturally, and then the other nostril. One hundred units of hyaluronidase (Sigma-Aldrich Chemie GmbH, H3506) dissolved in 24 μ L sterile PBS was administered to the mouse nostrils (6 μ L/nostril, repeat once after 2 min) 30 min prior to the administration of MSCs or PBS. One million of vital MSCs were freshly prepared from frozen stocks and resuspended in 24 μ L of sterile PBS and applied to each mouse in the R6/2-MSC group using the same method as described for hyaluronidase, while R6/2-PBS and WT-PBS groups received the same amount of PBS only. Since the amount of living cells after the thawing procedure was highly variable for eGFP-MSC (50–75% survival), we thawed an excess of MSC, i.e., up to 2.5×10^6 cells. This ensured that the total number of cells applied contained 1×10^6 living cells, which was determined by the trypan blue staining immediately before cell administration. After three days, the administration was repeated so that each mouse in the R6/2-MSC group received two million of cells in total, whereas mice in the control groups received 24 μ L of vehicle buffer (PBS) for the second time.

2.4. Rotarod Test

R6/2-MSC and controls R6/2-PBS and WT-PBS were tested at 6, 8 and 10 weeks of age (2, 4 and 6 weeks after transplantation) on a rotarod apparatus (AccuScan Instruments). Mice were tested over 3 consecutive days [79]. On each day, the animals received a training trial of 5 min at 4 rpm on the rotarod. One hour later, the animals were tested for 3 consecutive accelerating trials of 5 min with the speed changing from 4 to 40 rpm over 360 s and a minimum of 30 min inter-trial interval. The latency to fall from the rotating rod was recorded. Mice remaining on the rod for more than 360 s were removed and their time scored as 360 s.

2.5. Locomotor Activities and Food Intake

Locomotor activities and feeding behavior were monitored by the LabMaster system which provided a home cage-like environment embedded in an infrared light frame (TSE system GmbH).

Animals were monitored for 22 h at 5 and 11 weeks of age ($n = 15$), and the data were collected automatically with 1 min intervals. As the animals were habituating to the new environment during the first two hours, these data were excluded from the analysis. Ambulatory activity was defined by the number of beam breaks along the x and y axes (horizontal activity), while beam breaks on z level were calculated as rearing (vertical activity). Fine movement was defined by repetitive beam breaks. Data were analyzed either by summing all activities in both phases as total activity or in the light phase and dark phase individually. Food intake was calculated as the food consumption over 22 h.

2.6. Quantitative PCR

RNA was extracted from mice tissues using peqGOLDTrifast™ reagent according to the manufacturer's instructions (PeqLab, 30-2040) and treated with DNase I (Life Technologies, EN0521). cDNA synthesis was performed using Superscript™ III Reverse Transcriptase (Life Technologies, 18080085) and Oligo(dT)₁₈-Primer (Thermo Scientific, SO132) at 50 °C for 1 h. cDNA (1:10 dilution) was used as PCR template with technical triplicate for every sample. Quantitative PCR was performed using the DNA engine CFX Connect™ Real-Time PCR Detection System (Biorad) according to published protocols [80].

2.7. Immunohistochemical Staining and Immunofluorescence Staining

Immunohistochemical analysis was performed on 11.5-week-old mice (7.5 weeks after MSCs administration). Mice were perfused transcardially with 4% paraformaldehyde in PBS (pH 7.4) and post fixed in the same fixatives overnight at 4 °C. Brains were serially cut into 25 µm-thick coronal sections, in which every 6th brain section was taken and pre-mounted on slices. All staining procedures were performed at room temperature. For the immunohistochemical staining, brain sections were incubated in 0.5% NaBH₄ for 30 min for blocking. After washing, the sections were permeabilized in 0.3% Triton X-100 in TBS buffer (25 mM Tris-HCl, 137 mM NaCl, 2.7 mM KCl). For staining mHTT aggregates, primary antibody EM48 (Millipore, MAB5374) incubation was carried out overnight at a concentration of 1:1000, followed by incubation with biotinylated anti-mouse antibody (1:500, Vector Laboratories, BA9200) for 2 h. Avidin-biotin complexes (1:200, Vector Laboratories, PK6100) with a single round of biotinylated tyramine amplification were used to enhance the signal intensity. For color development, sections were exposed to nickel-DAB-H₂O₂ (0.6%/nickel sulfate, 0.01% 3,3-diaminobenzidine (DAB), and 0.001% hydrogen peroxidase) until they reached an optimal staining intensity. For the immunofluorescence staining, brain sections were blocked with 5% normal goat serum (Vector Laboratories, S-1000), and incubated in one of the following primary antibodies: Anti-dopamine and cyclic AMP-regulated phosphoprotein (DARPP-32) at a concentration of 1:1000 (Epitomics, 1710-1), anti-eGFP at a concentration of 1:250 (NovusBio, NB600-308), anti-Iba1 at a concentration of 1:2000 (Wako, 019-1974), and anti-neuron-specific nuclear protein (NeuN) at a concentration of 1:200 (Merck Millipore, MAB377B) overnight. The secondary antibody anti-Rabbit Alexa 594 was used at 1:500 (Dianova, 711-585-152).

2.8. Quantification of Striatal Area

To compare the striatal volume, brain sections of WT-PBS, R6/2-PBS and R6/2-MSM mice were stained using anti-DARPP-32 to visualize striata ($n = 4$). Six sections containing the striatum starting from approximately Bregma 0.98 (2 sections are ~150 µm apart) were chosen for quantification. Images were analyzed by ImageJ (National Institutes of Health, USA) and the striatal area of each brain section was defined by the DARPP-32-positive area. The striatal area of each animal was calculated as the average of the striatal area of the 6 brain sections analyzed.

2.9. Western Blotting Analysis

Mice striatal tissues were homogenized in ice-cold 10 volumes *w/v* modified RIPA buffer (150 mM sodium chloride, 1.0% NP-40, 0.5% sodium deoxycholate, 0.1% SDS, 50 mM Tris, 5 mM EDTA pH 8.0) with Complete Proteinase Inhibitor Cocktail tablets (Sigma-Aldrich, 1873580) with a mechanical homogenizer.

After a further 5-min sonication step with a bath sonicator for shearing genomic DNA, the lysates were centrifuged at $16,200\times g$ at $4\text{ }^{\circ}\text{C}$ for 20 min to isolate the soluble protein. Protein samples were denatured in Lithium dodecyl sulfate (LDS) buffer (NP0007, Thermo Fisher, Darmstadt, Germany) containing 100 mM DTT and separated using NuPAGE Bis-Tris 12% gel (Thermo Fisher, NP0349BOX). Blots were incubated overnight at $4\text{ }^{\circ}\text{C}$ with the following primary antibodies: Anti-pro-brain-derived neurotrophic factor (BDNF) (1:500, Sigma-Aldrich, P1374-200UL), anti-nerve growth factor (NGF) (1:1000 Abcam, ab6199), anti-DARPP-32 (1:5000, Epitomics, 1710-1), anti-tyrosine hydroxylase (TH) at a concentration of 1:1000 (Merck Millipore, AB1542), anti-Iba1 at a concentration of 1:1000 (Wako, 019-1974), and anti-beta actin (1:5000, Sigma-Aldrich, A5441). Fluorescence-conjugated secondary antibodies, anti-rabbit and anti-mouse at a dilution of 1:10000 (Li-COR Bioscience, 926-32211 and 926-68070), were used to detect the signals utilizing Li-COR Odyssey imaging system (Li-COR Bioscience).

2.10. Statistical Analysis

Experimental results are expressed as means \pm SEM, except for the data on MSC phenotype analysis. Survival curves of the animals were analyzed using log rank test. Behavioral data were analyzed by two-way ANOVA with Tukey's post hoc test. Data from neuropathological analyses were analyzed by two-tailed student's *t*-tests for comparison between MSCs-treated and PBS-treated R6/2 mice, and between PBS-treated R6/2 mice and PBS-treated WT mice. A non-parametric Mann–Whitney test was performed for non-Gaussian distributions. A *p* value < 0.05 was considered statistically significant.

3. Results

3.1. Cell Characterization in Vitro

Mouse MSCs were characterized prior to transplantation and found to be positive for the following MSC markers: Sca-1, CD29, CD44, CD73, CD105 and CD106 and negative for hematopoietic markers including CD11b and CD45 (Figure 1A), showing a classical mesenchymal stem cell morphology at passage 4 (Figure 1B). In addition, we confirmed eGFP expression using fluorescence microscopy (Figure S1) and flow cytometry (Figure S2).

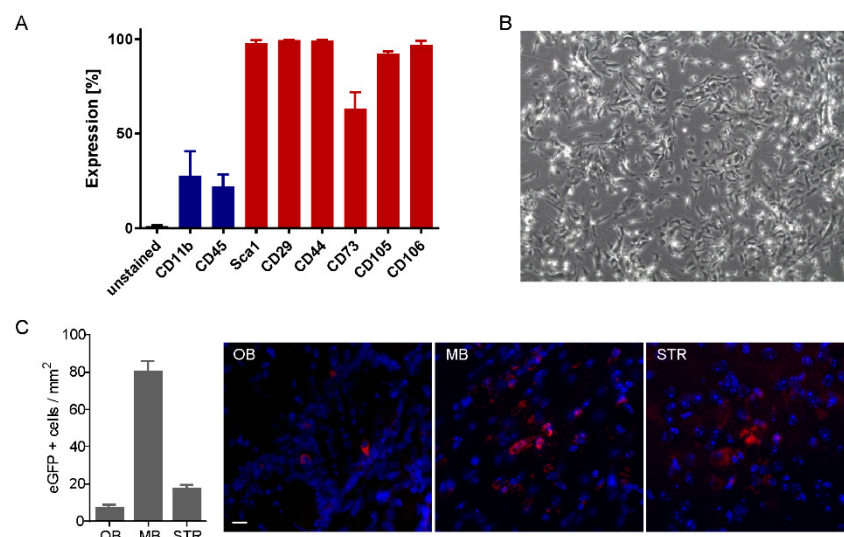


Figure 1. Characterization of mesenchymal stem cells (MSCs) in vitro and MSCs tracking post-delivery. (A) MSC phenotype was analyzed before transplantation by means of flow cytometry ($n = 3$, mean \pm SD). Blue bars represent negative markers (CD11b and CD45) whereas red bars are the positive markers. (B) Exemplary phase contrast image of eGFP-MSC at passage 2. (C) Quantification of GFP-positive cells and representative images showing GFP staining (pseudo-colored in red) in the olfactory bulb (OB), midbrain (MB) and striatum (STR) of R6/2 mice 5 days post-delivery of MSCs. Scale bar: $20\text{ }\mu\text{m}$.

3.2. Cell Tracking in the Brain after Intranasal Administration

To evaluate the migration of MSCs in different brain regions following intranasal delivery, we investigated the presence of the donor-specific eGFP signal in different brain regions using immunostaining in the mice 5 days ($n = 3$). Five days after the first transplantation, in the entire brain eGFP-expressing MSCs were only found in the midbrain, striatum, and olfactory bulb, whereas the amount of detectable MSCs was much lower in the olfactory bulb compared to the other two brain regions (Figure 1C). The presence of eGFP signal was also investigated 7.5 weeks after MSC administration. No GFP-positive signal was detected in any brain region (data not shown).

3.3. Intranasal Administration of MSCs Prolonged Survival of R6/2 Mice with Potentially Improved Motor Function

To assess the effect of intranasal administration of MSCs on the survival of R6/2 mice, 16 animals/group were monitored until the end of behavioral tests at 11 weeks of age. The survival curve showed that MSC-treated mice (R6/2-MSC) had a comparable survival rate as WT controls (WT-PBS) (100%), while the R6/2 mice receiving PBS only (R6/2-PBS) exhibited a significantly reduced survival rate of 75% (log rank test, $p = 0.0139$) (Figure 2A). Body weight of mice was monitored weekly. Two-way-ANOVA analysis revealed no significant difference among the 3 treatment groups, although R6/2 mice with PBS or MSCs treatment showed a trend of reduced body weight at 11 weeks of age when compared to WT controls (Figure 2B).

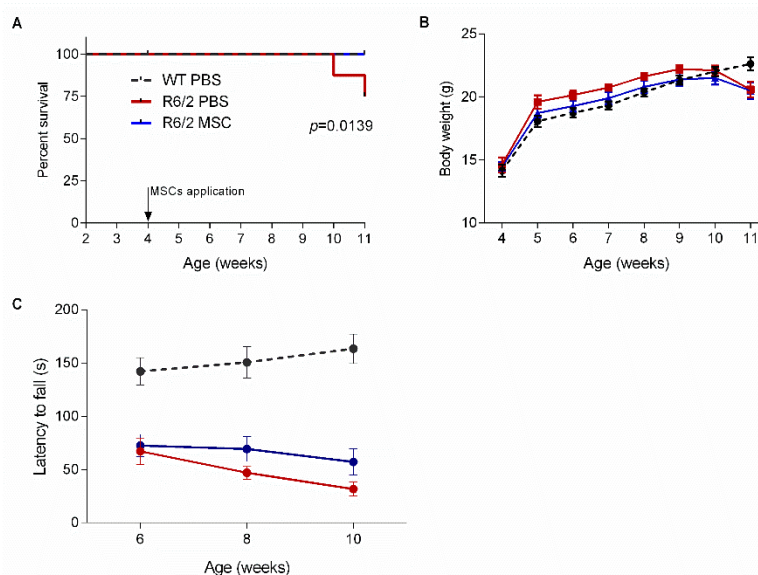


Figure 2. Longitudinal assessment after intranasal MSCs administration. (A) Kaplan–Meier survival curve of MSC-treated R6/2 mice and control groups ($n = 16$ for each group). (B) Body weight recorded from 4 to 11 weeks of age ($n = 16$ for R6/2-MSC and wild type (WT)-phosphate-buffered saline (PBS), $n = 12$ for R6/2-PBS). (C) Rotarod test performance of MSC-treated mice after MSCs administration ($n = 16$ for R6/2-MSC and WT-PBS, $n = 14$ for R6/2-PBS). R6/2-MSC displayed a trend towards improved latency to fall as compared to R6/2-PBS starting from 4 weeks post MSC delivery ($p = 0.1059$) and continued to 6 weeks after cell application ($p = 0.0848$). Data are expressed as mean \pm SEM.

It has been reported that R6/2 mice displayed motor deficits as early as 4 weeks of age as compared to WT littermates [81]. Motor function was assessed by rotarod test at 2, 4 and 6 weeks post intranasal MSCs application. The latency to fall was compared among the 3 treatment groups to evaluate the mice' performance on the rotating rod. R6/2 mice showed a highly significantly reduced latency to fall during the whole investigation period in comparison to the WT littermates (two-way ANOVA and Tukey's post-hoc test, $F(1.44) = 27.77$, $p < 0.001$). When we only compared the MSC-treated and

PBS-treated R6/2 mice using student's *t*-test, R6/2-MSC displayed a trend towards improved latency to fall as compared to R6/2-PBS starting from 4 weeks post MSC delivery ($p = 0.1059$) and continued to 6 weeks after cell application ($p = 0.0848$). These results suggested a potentially improved motor function in R6/2 mice after intranasal applications of MSCs (Figure 2C).

3.4. Ameliorated Circadian Rhythm in the MSC-Treated R6/2 Mice

Numerous studies have shown disrupted circadian rhythm in HD patients and animal models including R6/2 mice [82–84]. We tracked the locomotor behavior of the animals for 22 h (12 h dark phase and 10 h light phase) using LabMaster to evaluate their activities and circadian rhythms at 1 and 7 weeks after cell administration (i.e., 5 and 11 weeks of age, respectively). At 11 weeks of age, R6/2 mice with either MSC or PBS treatment showed an abnormal circadian rhythm with increased ambulatory activity during the light phase as compared to WT controls, although this phenotype was not observed at 5 weeks of age (1 week after cell administration) (Figure 3A,B). We therefore compared the sum of fine movement and total activity over the light phase. Two-way ANOVA and Tukey's post-hoc test revealed that both were significantly reduced in the MSC-treated R6/2 mice compared to R6/2-PBS mice at 11 weeks of age ($p < 0.05$ for both) (Figure 3C,D).

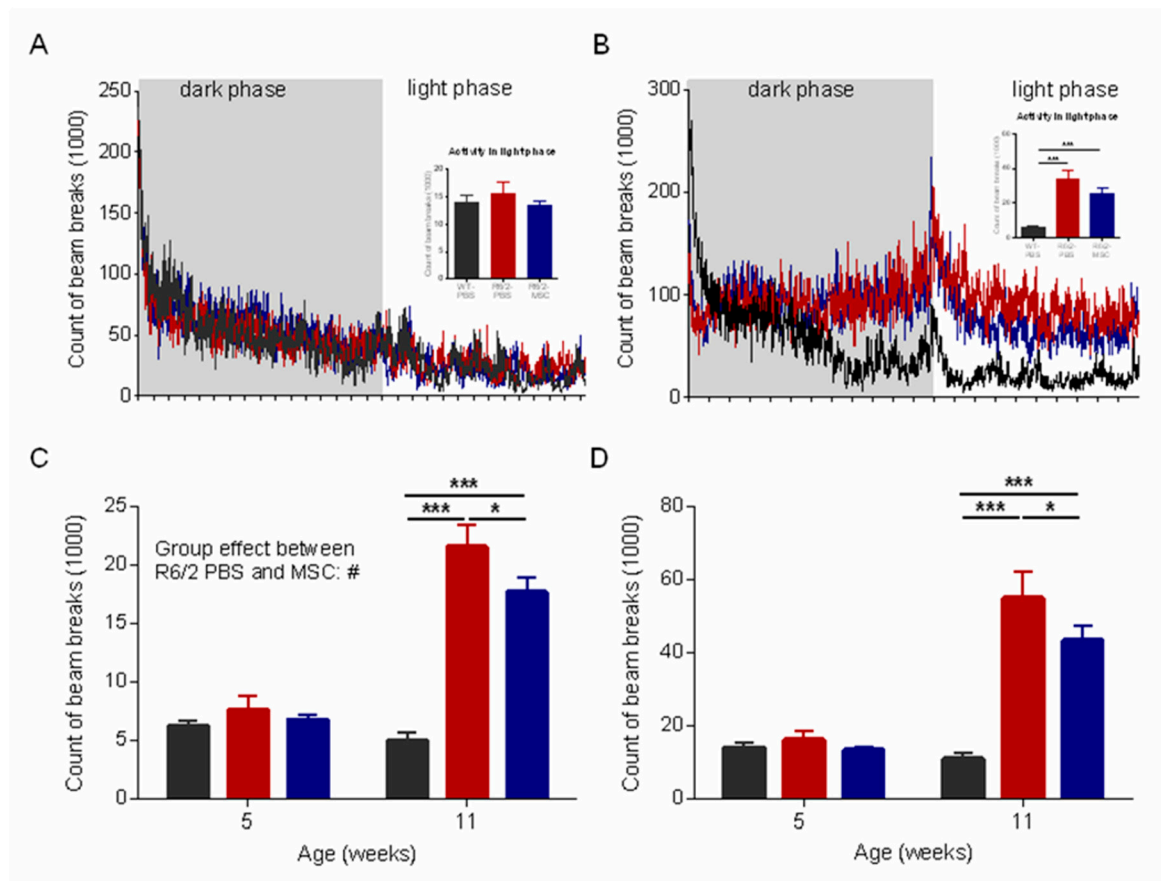


Figure 3. Ameliorated sleeping disturbance in the MSC-treated R6/2 mice at the later disease stage. Locomotor activities of mice were monitored using LabMaster at 5 and 11 weeks of age for 22 h ($n = 16$ for R6/2-MSC and WT-PBS groups, $n = 12$ for R6/2-PBS group). The counts of beam breaks represent the ambulatory activities during the whole recording period (22 h) at (A) 5 and (B) 11 weeks of age, and (C) fine movement and (D) total activities in the light phase at both 5 and 11 weeks of age. Data are represented as mean \pm SEM. *: $p < 0.05$; ***: $p < 0.001$.

3.5. Gene Expression Profiles of Inflammatory Regulators and Neurotrophic Factors

We analyzed the gene expression levels of inflammatory regulators and neurotrophic factors in the olfactory bulb, hippocampus, striatum and cortex at 11.5 weeks of age (7.5 weeks post-application of MSCs) (R6/2-MSC, $n = 8$, R6/2-PBS, $n = 6$ and WT-PBS, $n = 6$). Analyses of the gene expression levels of the inflammatory regulators including macrophage chemoattractant protein (MCP1), $\text{TNF}\alpha$, interleukin-6 (IL-6), C-C chemokine receptor type 5 (CCR5) and prostaglandin E2 receptor (PTGER2) revealed that these genes showed a general trend of increase in expression in the R6/2-PBS mice with the exception of MCP1 in hippocampus and IL-6 and CCR5 in cortex as compared to WT-PBS mice, and these aberrant increase in gene expressions were restored in the R6/2-MSC mice to comparable levels of the WT-PBS mice (Figure 4A). In particular, when compared to the WT-PBS group, CCR5 (student's t -test, $p < 0.05$) and PTGER2 (student's t -test, $p < 0.01$) were significantly upregulated in the olfactory bulb of R6/2-PBS, while MSC treatment in R6/2 mice (R6/2-MSC) led to a significant downregulation of MCP1 (student's t -test, $p < 0.05$) and PTGER2 (student's t -test, $p < 0.05$) gene expressions in the same brain area. However, such differences were neither detected in the striatum nor the cortex.

We also analyzed the gene expression levels of the neurotrophic factors, such as brain derived neurotrophic factor (BDNF), nerve growth factor (NGF) and vascular endothelial growth factor (VEGF). In comparison with WT-PBS, NGF was downregulated in all investigated brain regions of R6/2-PBS mice although the decrease did not reach statistical significance in cortex and striatum. MSC treatment (R6/2-MSC) further suppressed the mRNA expression of NGF in olfactory bulb, hippocampus and cortex. On the other hand, the expression of BDNF and VEGF were not significantly different among the 3 treatment groups in all analyzed brain regions although BDNF protein has been reported to be reduced in HD mouse brains [85] (Figure 4B). We have hence quantified the protein expression of BDNF in the hippocampus and cortex 7.5 weeks post-transplantation. Our results demonstrate that neither the glycosylated nor the non-glycosylated form of BDNF showed a significant difference among the treatment groups in the hippocampus (Figure S3A). In the cortex, the non-glycosylated form of BDNF was reduced in the R6/2-PBS mice when compared to the WT-PBS group (student's t -test, $p < 0.01$), whereas no change was found between MSC-treated and non-treated R6/2 mice (Figure S3B).

3.6. Microglial Changes in MSC-Treated R6/2 Mice

Analyses of the protein expression level of the microglial marker Iba1 in the striatum using western blot (11.5 weeks of age, $n = 4$ for each group) revealed an increased Iba1 in the R6/2-MSC mice compared to R6/2-PBS mice (student t -test, $p < 0.05$), while no significant difference was found between WT-PBS and R6/2-PBS control groups (Figure 5A). Morphological changes of microglia were examined using immunohistological staining with antibody against Iba1. In agreement with a previous report [86], microglial structural abnormalities such as thinner processes, decreased ramification and reduced Iba1 immunoreactivity were observed in R6/2-PBS mice compared to the WT-PBS littermates at 11.5 weeks. In contrast to R6/2-PBS mice, microglia of R6/2-MSC mice displayed increased process thickness and enhanced Iba1 immunoreactivity (Figure 5B).

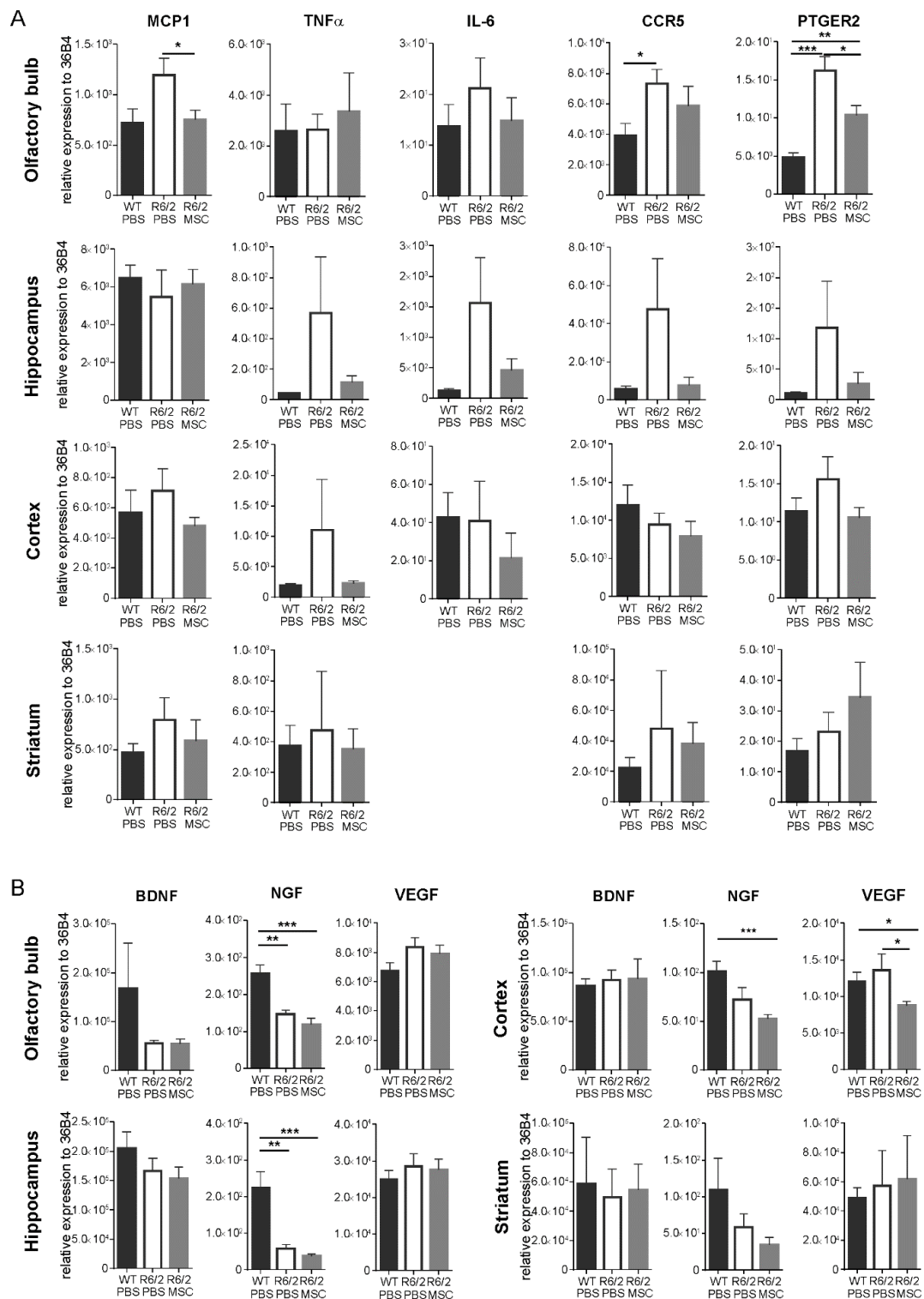


Figure 4. Altered gene expression of inflammation markers and neurotrophic factors in different brain regions. mRNA expression levels of (A) inflammatory regulators (MCP1, TNF α , IL-6, CCR5, and PTGER2) and (B) neurotrophic factors (BDNF, VEGF, and BDNF) were analyzed in 4 different brain parts (olfactory bulb, hippocampus, cortex and striatum) (WT-PBS, $n = 6$; R6/2-PBS, $n = 6$ and R6/2-MSC $n = 8$). Values were normalized to 36B4 level. Data are presented as mean \pm SEM. IL-6 was not detectable in the striatum and hence was not presented here. *: $p < 0.05$; **: $p < 0.01$; ***: $p < 0.001$.

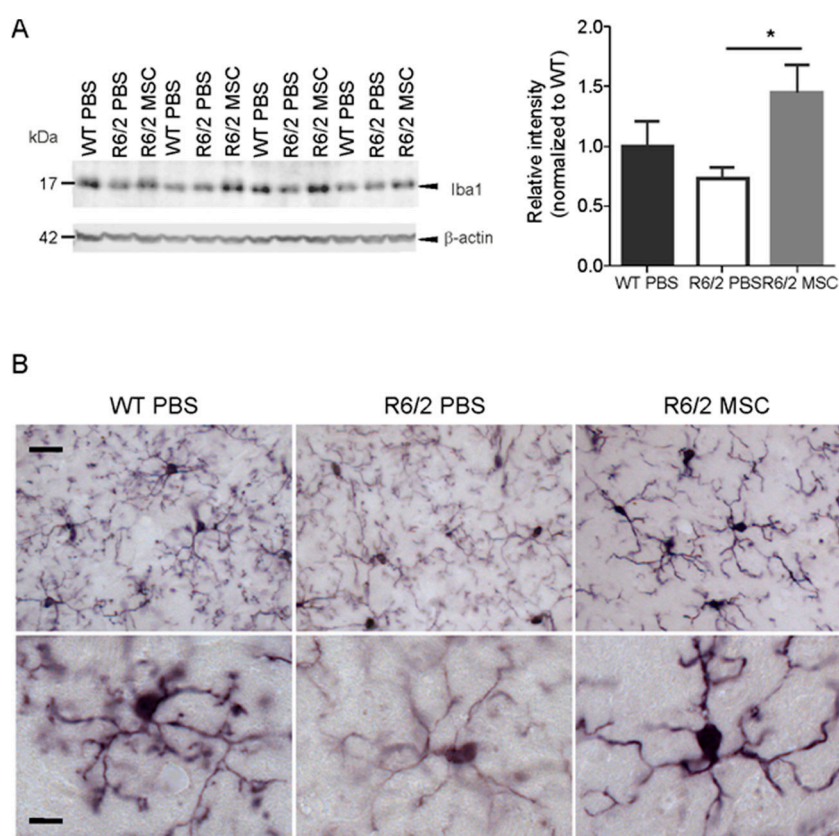


Figure 5. Enhanced expression of Iba1 and morphological changes of striatum-resident microglia in MSC-treated R6/2 mice. **(A)** Quantification of Iba1 protein expression level in the striatum using western blot. Intensity of Iba1-specific band at 17 kDa was compared among R6/2-MSC, R6/2-PBS and WT-PBS ($n = 4$ for each group) 7.5 weeks after MSC application. Values were normalized to the level of β -actin in each lane. Statistical analysis was performed using the student t -test. Data are presented as mean \pm SEM *: $p < 0.05$. Full western blots are shown in Figure S5A. **(B)** Representative images of Iba1 staining of striatum-resident microglia in the brain samples obtained in parallel to those analyzed using the western blot. When compared to WT-PBS mice, microglia of R6/2-PBS mice had thinner processes, less process ramification and reduced Iba1 immunoreactivity, whereas MSC treatment (i.e., R6/2-MSC mice) restored Iba1 expression and the thickness of microglial processes. Scale bar in the upper panel: 20 μ m, in the lower panel: 8 μ m.

3.7. Neuropathological Changes in MSC-Treated R6/2 Mice

As the striatum is the most affected brain region in HD, it is crucial to investigate the effects of intranasal MSC administration on neuronal survival in the striatum. DARPP-32, a widely used marker of mature medium spiny neurons (MSNs), has been reported to be reduced in the striatum of R6/2 mice as compared to WT littermates, indicating neuronal loss and dysfunction of MSNs in the striatum [87–89]. Hence, we quantified the protein levels of DARPP-32 in the WT-PBS, R6/2-PBS and R6/2-MSC groups using western blotting 7.5 weeks after MSC administration (11.5 weeks of age, $n = 4$ for each group) (Figure 6A). In agreement with previous studies [87–89], R6/2-PBS mice showed a strongly reduced protein level of DARPP-32 as compared to WT-PBS controls (student's t -test, $p < 0.01$), while R6/2-MSC mice exhibited a significantly increased DARPP-32 level when compared to R6/2-PBS mice (student's t -test, $p < 0.05$) (Figure 5A). This result was verified by immunofluorescence staining as indicated in the representative images of immunoreactivity of DARPP-32 in the striatum (Figure 6B). We have also investigated the protein expression levels of TH, the rate-limiting enzyme for dopamine biosynthesis, in the striatum of the same cohort. Consistent with a previous report [90], the expression

level of TH in the striatum of R6/2-PBS mice was significantly reduced as compared to WT-PBS mice (student's *t*-test, $p < 0.01$), and this reduction was significantly attenuated in the MSC-treated group (student's *t*-test, $p < 0.05$) (Figure 6A). We further quantified the protein expression levels of the synapse markers synaptophysin and PSD-95, and no significant difference could be detected among the treatment groups (Figure 6). Altogether, these results demonstrated an amelioration of the changes in the dopaminergic pathway in MSC-treated R6/2 mice via intranasal delivery.

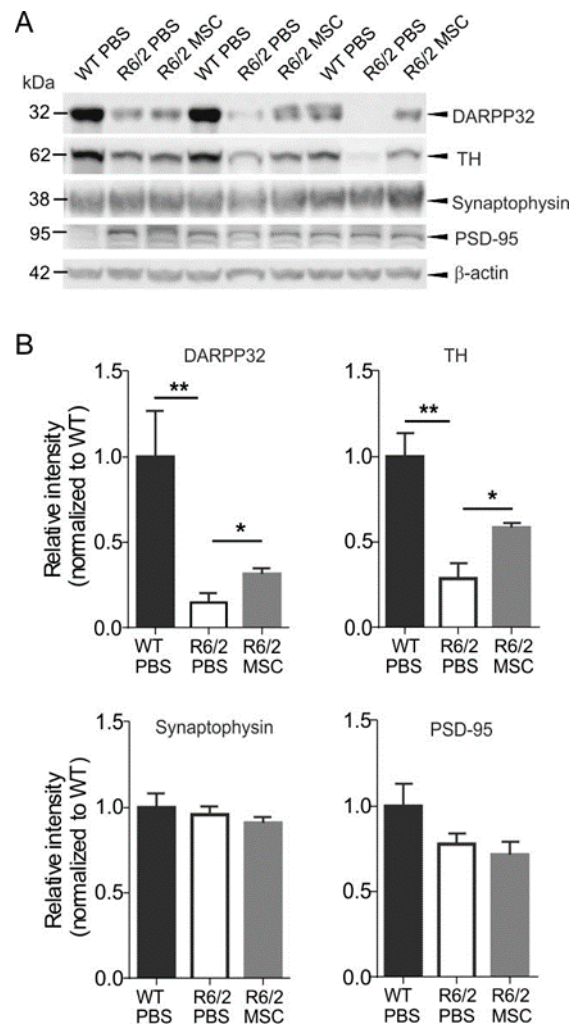


Figure 6. (A) Increased expression levels of DARPP-32 and tyrosine hydroxylase (TH) in the striatum of MSC-treated mice. The protein levels of DARPP-32 and TH were analyzed using mice striatal lysates and compared among R6/2-MSC, R6/2-PBS and WT-PBS ($n = 4$ for each group) 7.5 weeks after MSC application. (B) Both DARPP-32 and TH showed significantly reduced levels in R6/2-PBS mice as compared to WT-PBS mice (student's *t*-test), whereas these reductions were ameliorated as R6/2-MSC mice exhibited higher expression levels of DARPP-32 and TH (student's *t*-test). There is no difference in protein expression level of synaptic markers synaptophysin and PSD-95 among all three groups. Data are represented as mean \pm SEM. *: $p < 0.05$; **: $p < 0.01$. Full western blots are shown in Figure S5B.

As previous studies on intrastriatal administration of MSCs in HD animal models have reported the beneficial effect of MSCs might be associated with a decrease in mHTT aggregates formation [91,92], we analyzed mHTT aggregation using immunohistological staining with EM48 at the age of 11.5 weeks ($n = 4$ for each group). While R6/2-PBS mice displayed abundant nuclear inclusion bodies and neuropil aggregates in the striatum, we could not detect any difference in the abundance of nuclear inclusion bodies and neuropil aggregates in the striatum of the MSC-treated mice (Figure S4). Brain volume was

also quantified using the same cohort by stereology. Mean striatal area of 6 consecutive brain sections with a 150 μm interval (starting from Bregma 0.98) was analyzed and revealed no difference between R6/2-MSc and R6/2-PBS mice (data not shown).

4. Discussion

The main findings of the present study are: (1) MSCs delivered intranasally to R6/2 HD mice were able to migrate to and infiltrate into the olfactory bulb, midbrain and striatum 5 days post-delivery; (2) intranasal delivery of MSCs significantly increased survival rate and ameliorated sleep disturbance of R6/2 mice as well as showing a trend towards improved motor function; (3) MSCs treatment in R6/2 mice increased DARPP-32 expression in the striatum while the expression levels of synaptic markers and NeuN remained unchanged; (4) all investigated immunomodulators were either significantly restored or showed a trend towards restoration in most of the brain areas examined after MSCs treatment; and (5) neuroprotective effects of MSC were concomitant with increased expression of Iba1 in the striatum and restored morphology of striatum-resident microglia of R6/2 mice.

4.1. Migration Pattern and Survival of Intranasally Delivered MSCs in the Brain

Our results of cell tracking 5 days after intranasal delivery showed that the applied MSCs were distributed among the olfactory bulb, midbrain and striatum. This indicates that exogenous MSCs were able to migrate to the brain shortly after being delivered from the nose along the olfactory and trigeminal nerve pathways in R6/2 mice as reported previously for intranasal delivery of stem cells [41,44,92–94] and drugs or biologics in different models of CNS disorders [95–97]. MSCs were exclusively found in the striatum, olfactory bulb and midbrain 5 days post-transplantation, and they were more abundant in the midbrain than in the olfactory bulb. This more caudally directed distribution of MSC suggests their preferential migration to the lesioned regions as previously shown by intravenous administration of MSC in a model of brain injury [98]. Another explanation for rapid appearance of MSCs in deeper parts of the brain, such as striatum and midbrain, is their transportation via CSF, once they entered the subarachnoid space after crossing the cribriform plate as described previously [41]. It cannot be excluded that a portion of cells could reach the CNS via blood stream by entering the blood vessels of the nasal mucosa. However, in line with our observations, none of the previous studies could show intranasally delivered stem cells within the lumen of cerebral vessels [41,43,44,92–94].

Investigation on the engrafted MSCs 7.5 weeks post-cell-administration showed no detectable GFP signal in any brain area indicating a poor long-term survival rate as reported in previous studies [40,99]. In contrast, we found a wide range of readouts that were ameliorated including neuropathological and neurobehavioral changes at/until this time point. Although MSC possess the capacity of transdifferentiation to various cell types, a therapeutic effect has been proposed to be contributed by the secretion of vesicles and other molecules including cytokines and chemokines (reviewed in [100]). This hypothesis is supported by numerous pre-clinical studies demonstrating therapeutic effect upon administration of MSC-conditioned medium or -produced exosome [101–103]. Particularly, a study using a rat model with overactive bladder demonstrated increases of primitive progenitor cells genes and genes involved in stem cell trafficking processes in the bladder tissue transplanted with MSCs but no engraftment [104]. This finding suggests the activation of primitive progenitor cells by MSC paracrine effect as a possible mechanism for long-term therapeutic efficacy of MSCs.

4.2. Increased TH and DARPP-32 Expressions and Attenuated Circadian Rhythm Disturbances Indicate An Amelioration of Dopamine Signaling in MSC-Treated Mice

In this study, MSC treatment resulted in increased TH and DARPP-32 protein expressions, both of which are involved in dopamine biosynthesis and neurotransmission. As in HD patients, R6/2 mice displayed a decreased TH expression as its transcription was disrupted by mutant huntingtin [90].

Similarly, the immunoreactivity of DARPP-32 in the striatum had been reported to be reduced by approximately 50% even in the presymptomatic R6/2 mice as compared to WT animals [75,105] although the number of neurons in the striatum remained unaltered. In the dopaminergic pathway, TH is the rate-limiting enzyme for the conversion of tyrosine into the precursor of dopamine (i.e., L-3,4-dihydroxyphenylalanine (L-DOPA)), whereas DARPP-32 phosphorylation is bi-directionally modulated by dopamine receptors 1 and 2 in the neostriatum [106]. As a result, the reduction of TH and DARPP-32 expressions led to the impairment of dopaminergic signaling cascade [75]. This was rescued, at least partially, by MSC treatment, as demonstrated by the tendentially improved motor ability of the MSC-treated R6/2 mice. Another important behavioral improvement observed in MSC-treated R6/2 mice was their circadian activity pattern. Consistent with previous studies [57,83], our analyses showed that R6/2 mice suffered from sleep disturbance as they exhibited aberrant patterns of fine movement and ambulatory activities in light-dark phases, whereas MSC treatment markedly alleviated the disruption of the sleep-wake cycle. In mammals, the circadian clock is centrally regulated in the suprachiasmatic nuclei (SCN) [107–109] with an array of circadian genes widely expressed across the whole brain. Among these genes, the expressions of Per1 [110] and Per2 [83,111] are mediated by dopamine signaling. In particular, mPer2 expression was found to be significantly altered in the forebrain [57] and SCN [83] in R6/2 mice. As we have shown that the dopaminergic system in R6/2 mice benefited from the MSCs treatment, although we did not pursue deeper into the precise molecular mechanisms of MSCs treatment on circadian control in this study, the remedial effects of MSCs suggest a causal link between MSCs and circadian rhythm correction, probably via the restoration of functional dopamine signaling on circadian genes induction/expression. Another possible explanation could be the regulation of circadian genes by inflammatory cytokines [112,113], for instance, IL-6 is known to suppress the circadian clock [114].

4.3. Intranasal Administration of MSCs Reduced Neuroinflammation

As in HD patients [115], inflammatory factors are up-regulated in R6/2 mice [59]. In line with these studies, our data also showed trends of increased transcription of inflammatory modulators (MCP1, CCR5, IL6, PTGER2 and TNF α) in different brain regions of R6/2 mice. Intranasal administration of MSCs in R6/2 mice suppressed most of these abnormally up-regulated gene expressions attributed to the immunomodulatory properties of MSCs [68,116–119], and such immunomodulatory capacity was further enhanced in the inflammatory conditions [118,120,121]. Substantiated by the restored expressions of the investigated inflammatory modulators, our study validated the immunoregulatory ability of MSCs in HD as in other disorders [44,80,94]. Another neuroprotective potential of MSC is the secretion of neurotrophic factors, which has been reported in numerous studies including several MSC therapies for HD [91,121–123]. However, we did not detect any increased expressions of neurotrophic factors in R6/2-MSC mice as compared to the R6/2-PBS control group.

Interestingly, our results revealed an increased protein expression level of microglia marker Iba1 in MSC-treated R6/2 mice, indicating an activation of microglia, in contrast to the results of the ameliorated inflammatory modulators. Although it is a common feature that Iba1 expression is increased in both HD patients and symptomatic HD animal models, its expression is decreased in the pre-symptomatic stage of R6/2 mice [74]. Moreover, impaired migration and function of microglia have been reported in YAC128 and BACHD mice in response to brain injury [73]. These evidences suggest that mutant huntingtin protein affects microglial function under both basal and inflammatory conditions. Other reports showed that supplementation of normal microglia increased survival rate and electrophysiological properties of neurons expressing mHTT in vitro [124] and in vivo [125]. Since MSCs modulate the functional properties of microglia via TGF- β [126], TSG-6 [127], CX3CL1 [128], all of which are pro-inflammatory molecules, and microvesicles [129], MSCs could lead to microglia activation as shown by the increase in Iba1 expression in the MSC-treated R6/2 mice. In addition, it has been shown that the introduction of MSCs to primary rat microglia led to a shift of the active microglia phenotype from classical M1 to alternative M2 in vivo [126]. M1 secretes proinflammatory cytokines

causing toxic effects, whereas M2 promotes neuronal protection by releasing neurotrophic factors that led to reduced proinflammatory cytokines [130]. Besides, microglia are also involved in the modulation of synaptic plasticity and transmission (reviewed in [131]), its alteration potentially also contributes to the ameliorated dopamine transmission. In addition, our data demonstrate a thinning of microglial processes in the R6/2 mouse model of HD similar to that of transgenic Alzheimer's disease mice, which has been suggested to be associated with impaired microglial function [132]. This microglial morphology alteration has been successfully ameliorated by intranasal MSC treatment in R6/2 mice.

It is interesting to compare the treatment outcome of MSCs administrated via intranasal administration (INA) as an alternative non-invasive delivery route with MSCs applied via stereotactic injection, which directly delivers cells to the most affected brain regions. Intrastratial injection of bone marrow-derived MSCs at low passage (3–8) in R6/2 mice had a short two-week effect on spatial memory, while injection of MSCs at high passage (40–50) had a significant additional effect on rotarod performance and neuronal metabolism [123]. Another study reported an improved performance on the rotarod and increased striatal numbers of neurons in YAC128 HD mice injected with genetically engineered bone-marrow-derived MSCs that over-express BDNF, but these therapeutic effects were not observed in those injected with normal MSCs [133]. In comparison, the present study demonstrated the amelioration of both the behavioral phenotype and neuropathological changes in R6/2 HD mice after administration of bone-marrow-derived MSCs via INA. Moreover, MSCs were found in several major brain regions such as the olfactory bulb and striatum, suggesting a beneficial treatment effect attributed to multiple brain areas in intranasally treated mice.

5. Conclusions

Our results demonstrate significantly ameliorated behavioral and neuropathological phenotypes of R6/2 mice after intranasal MSC administration. This indicates that this method is an effective route for delivering MSCs for CNS-targeted HD therapy. Being non-invasive, intranasal delivery of MSCs can be repeatedly applied, resulting in a long-lasting therapeutic effect, overcoming the challenge of low cell survival and host immune response after surgical administration.

Supplementary Materials: The following are available online at <http://www.mdpi.com/2073-4409/8/6/595/s1>. Figure S1: Exemplary fluorescence images of cultured MSCs at passage 1, Figure S2: Exemplary flow cytometry data, Figure S3: Western blot analyses of protein expression levels of glycosylated and non-glycosylated BDNF in the hippocampus and cortex of mice at 11.5 weeks of age, Figure S4: Representative images of the staining of mutant huntingtin aggregates in the striatum of MSC-treated R6/2 mice and control groups, Figure S5: Full western blots used in Figures 5 and 6.

Author Contributions: Conceptualization, L.Y.-T., J.M., A.S., L.D. and H.H.P.N.; formal analysis, L.Y.-T. and C.F.; funding acquisition, A.S., L.D. and H.H.P.N.; investigation, L.Y.-T., J.S.-S., K.A., P.B.-D., A.N., E.S., A.L. and C.F.; project administration, A.S., L.D. and H.H.P.N.; resources, O.R., M.S. and H.H.P.N.; supervision, L.Y.-T., O.R., M.S., A.S., L.D. and H.H.P.N.; visualization, L.Y.-T. and C.F.; writing—original draft, L.Y.-T., J.S.-S., K.A., A.S., L.D. and H.H.P.N.; writing—review and editing, L.Y.-T., J.S.-S., C.F., O.R., M.S., A.S., L.D. and H.H.P.N. All authors read and approved the final manuscript.

Funding: This research was funded by the BMBF (Bundesministerium für Bildung und Forschung), the grant no. 031A575 (Project RESTRAIN), and in part by the Robert Bosch Stiftung, Stuttgart, Germany.

Acknowledgments: The authors wish to thank Michael Glaser for technical assistance and acknowledge the support by Deutsche Forschungsgemeinschaft and The Open Access Publishing Fund of The University of Tübingen.

Conflicts of Interest: The authors declare that they have no competing interests. The funder has no role in the design of the study; in the collection, analyses, or interpretation of data, in the writing of the manuscript, or in the decision of publishing the results.

References

1. Walker, F.O. Huntington's disease. *Lancet* **2007**, *369*, 218–228. [[CrossRef](#)]
2. Schapira, A.H.; Olanow, C.W.; Greenamyre, J.T.; Bezdard, E. Slowing of neurodegeneration in Parkinson's disease and Huntington's disease: Future therapeutic perspectives. *Lancet* **2014**, *384*, 545–555. [[CrossRef](#)]

3. Ross, C.A.; Tabrizi, S.J. Huntington's disease: From molecular pathogenesis to clinical treatment. *Lancet Neurol.* **2011**, *10*, 83–98. [[CrossRef](#)]
4. Albin, R.L.; Tagle, D.A. Genetics and molecular biology of Huntington's disease. *Trends Neurosci.* **1995**, *18*, 11–14. [[CrossRef](#)]
5. Ramaswamy, S.; Kordower, J.H. Gene therapy for Huntington's disease. *Neurobiol. Dis.* **2012**, *48*, 243–254. [[CrossRef](#)] [[PubMed](#)]
6. Mason, S.L.; Barker, R.A. Advancing pharmacotherapy for treating Huntington's disease: A review of the existing literature. *Expert Opin Pharm.* **2016**, *17*, 41–52. [[CrossRef](#)]
7. The Huntington's Disease Collaborative Research Group. A novel gene containing a trinucleotide repeat that is expanded and unstable on Huntington's disease chromosomes. The Huntington's disease collaborative research group. *Cell* **1993**, *72*, 971–983. [[CrossRef](#)]
8. DiFiglia, M.; Sapp, E.; Chase, K.O.; Davies, S.W.; Bates, G.P.; Vonsattel, J.P.; Aronin, N. Aggregation of huntingtin in neuronal intranuclear inclusions and dystrophic neurites in brain. *Science* **1997**, *277*, 1990–1993. [[CrossRef](#)]
9. Vonsattel, J.P.; Myers, R.H.; Stevens, T.J.; Ferrante, R.J.; Bird, E.D.; Richardson, E.P., Jr. Neuropathological classification of Huntington's disease. *J. Neuropathol. Exp. Neurol.* **1985**, *44*, 559–577. [[CrossRef](#)]
10. Rodda, R.A. Cerebellar atrophy in Huntington's disease. *J. Neurol. Sci.* **1981**, *50*, 147–157. [[CrossRef](#)]
11. Zielonka, D.; Mielcarek, M.; Landwehrmeyer, G.B. Update on Huntington's disease: Advances in care and emerging therapeutic options. *Parkinsonism Relat. Disord.* **2015**, *21*, 169–178. [[CrossRef](#)] [[PubMed](#)]
12. Frank, S. Treatment of Huntington's disease. *Neurother. J. Am. Soc. Exp. Neurother.* **2014**, *11*, 153–160. [[CrossRef](#)] [[PubMed](#)]
13. Handley, O.J.; Naji, J.J.; Dunnett, S.B.; Rosser, A.E. Pharmaceutical, cellular and genetic therapies for Huntington's disease. *Clin. Sci.* **2006**, *110*, 73–88. [[CrossRef](#)] [[PubMed](#)]
14. Jiang, Y.; Lv, H.; Huang, S.; Tan, H.; Zhang, Y.; Li, H. Bone marrow mesenchymal stem cells can improve the motor function of a Huntington's disease rat model. *Neurol. Res.* **2011**, *33*, 331–337. [[CrossRef](#)] [[PubMed](#)]
15. Aleynik, A.; Gernavage, K.M.; Mourad, Y.; Sherman, L.S.; Liu, K.; Gubenko, Y.A.; Rameshwar, P. Stem cell delivery of therapies for brain disorders. *Clin. Transl. Med.* **2014**, *3*, 24. [[CrossRef](#)] [[PubMed](#)]
16. Herberts, C.A.; Kwa, M.S.; Hermsen, H.P. Risk factors in the development of stem cell therapy. *J. Transl. Med.* **2011**, *9*, 29. [[CrossRef](#)] [[PubMed](#)]
17. Tanna, T.; Sachan, V. Mesenchymal stem cells: Potential in treatment of neurodegenerative diseases. *Curr. Stem Cell Res. Ther.* **2014**, *9*, 513–521. [[CrossRef](#)] [[PubMed](#)]
18. Lin, Y.T.; Chern, Y.; Shen, C.K.; Wen, H.L.; Chang, Y.C.; Li, H.; Cheng, T.H.; Hsieh-Li, H.M. Human mesenchymal stem cells prolong survival and ameliorate motor deficit through trophic support in Huntington's disease mouse models. *PLoS ONE* **2011**, *6*, e22924. [[CrossRef](#)]
19. Rossignol, J.; Boyer, C.; Leveque, X.; Fink, K.D.; Thinard, R.; Blanchard, F.; Dunbar, G.L.; Lescaudron, L. Mesenchymal stem cell transplantation and DMEM administration in a 3np rat model of Huntington's disease: Morphological and behavioral outcomes. *Behav. Brain Res.* **2011**, *217*, 369–378. [[CrossRef](#)]
20. Pollock, K.; Dahlenburg, H.; Nelson, H.; Fink, K.D.; Cary, W.; Hendrix, K.; Annett, G.; Torrest, A.; Deng, P.; Gutierrez, J.; et al. Human mesenchymal stem cells genetically engineered to overexpress brain-derived neurotrophic factor improve outcomes in Huntington's disease mouse models. *Mol. Ther.* **2016**, *24*, 965–977. [[CrossRef](#)]
21. Fink, K.D.; Rossignol, J.; Crane, A.T.; Davis, K.K.; Bombard, M.C.; Bavar, A.M.; Clerc, S.; Lowrance, S.A.; Song, C.; Lescaudron, L.; et al. Transplantation of umbilical cord-derived mesenchymal stem cells into the striata of r6/2 mice: Behavioral and neuropathological analysis. *Stem Cell Res. Ther.* **2013**, *4*, 130. [[CrossRef](#)] [[PubMed](#)]
22. Teixeira, F.G.; Carvalho, M.M.; Panchalingam, K.M.; Rodrigues, A.J.; Mendes-Pinheiro, B.; Anjo, S.; Manadas, B.; Behie, L.A.; Sousa, N.; Salgado, A.J. Impact of the secretome of human mesenchymal stem cells on brain structure and animal behavior in a rat model of Parkinson's disease. *Stem Cells Transl. Med.* **2017**, *6*, 634–646. [[CrossRef](#)] [[PubMed](#)]
23. Sadan, O.; Bahat-Stromza, M.; Barhum, Y.; Levy, Y.S.; Pisnevsky, A.; Peretz, H.; Ilan, A.B.; Bulvik, S.; Shemesh, N.; Krepel, D.; et al. Protective effects of neurotrophic factor-secreting cells in a 6-OHDA rat model of Parkinson disease. *Stem Cells Dev.* **2009**, *18*, 1179–1190. [[CrossRef](#)] [[PubMed](#)]

24. Levy, Y.S.; Bahat-Stroomza, M.; Barzilay, R.; Burshtein, A.; Bulvik, S.; Barhum, Y.; Panet, H.; Melamed, E.; Offen, D. Regenerative effect of neural-induced human mesenchymal stromal cells in rat models of Parkinson's disease. *Cytotherapy* **2008**, *10*, 340–352. [[CrossRef](#)] [[PubMed](#)]
25. Cova, L.; Armentero, M.T.; Zennaro, E.; Calzarossa, C.; Bossolasco, P.; Busca, G.; Lambertenghi Deliliers, G.; Polli, E.; Nappi, G.; Silani, V.; et al. Multiple neurogenic and neurorescue effects of human mesenchymal stem cell after transplantation in an experimental model of Parkinson's disease. *Brain Res.* **2010**, *1311*, 12–27. [[CrossRef](#)]
26. Blandini, F.; Cova, L.; Armentero, M.T.; Zennaro, E.; Levandis, G.; Bossolasco, P.; Calzarossa, C.; Mellone, M.; Giuseppe, B.; Deliliers, G.L.; et al. Transplantation of undifferentiated human mesenchymal stem cells protects against 6-hydroxydopamine neurotoxicity in the rat. *Cell Transplant.* **2010**, *19*, 203–217. [[CrossRef](#)] [[PubMed](#)]
27. Zhu, Q.; Ma, J.; Yu, L.; Yuan, C. Grafted neural stem cells migrate to substantia nigra and improve behavior in Parkinsonian rats. *Neurosci. Lett.* **2009**, *462*, 213–218. [[CrossRef](#)]
28. Bae, J.S.; Jin, H.K.; Lee, J.K.; Richardson, J.C.; Carter, J.E. Bone marrow-derived mesenchymal stem cells contribute to the reduction of amyloid-beta deposits and the improvement of synaptic transmission in a mouse model of pre-dementia Alzheimer's disease. *Curr. Alzheimer Res.* **2013**, *10*, 524–531. [[CrossRef](#)]
29. Yun, H.M.; Kim, H.S.; Park, K.R.; Shin, J.M.; Kang, A.R.; Lee, K.i.; Song, S.; Kim, Y.B.; Han, S.B.; Chung, H.M.; et al. Placenta-derived mesenchymal stem cells improve memory dysfunction in an abeta1-42-infused mouse model of Alzheimer's disease. *Cell Death Dis.* **2013**, *4*, e958. [[CrossRef](#)] [[PubMed](#)]
30. Chang, K.A.; Kim, H.J.; Joo, Y.; Ha, S.; Suh, Y.H. The therapeutic effects of human adipose-derived stem cells in Alzheimer's disease mouse models. *Neuro-Degener. Dis.* **2014**, *13*, 99–102. [[CrossRef](#)]
31. Lee, J.K.; Jin, H.K.; Bae, J.S. Bone marrow-derived mesenchymal stem cells reduce brain amyloid-beta deposition and accelerate the activation of microglia in an acutely induced Alzheimer's disease mouse model. *Neurosci. Lett.* **2009**, *450*, 136–141. [[CrossRef](#)] [[PubMed](#)]
32. Babaei, P.; Soltani Tehrani, B.; Alizadeh, A. Transplanted bone marrow mesenchymal stem cells improve memory in rat models of Alzheimer's disease. *Stem Cells Int.* **2012**, *2012*, 369417. [[CrossRef](#)] [[PubMed](#)]
33. Shin, J.Y.; Park, H.J.; Kim, H.N.; Oh, S.H.; Bae, J.S.; Ha, H.J.; Lee, P.H. Mesenchymal stem cells enhance autophagy and increase beta-amyloid clearance in Alzheimer disease models. *Autophagy* **2014**, *10*, 32–44. [[CrossRef](#)] [[PubMed](#)]
34. Lee, J.K.; Jin, H.K.; Endo, S.; Schuchman, E.H.; Carter, J.E.; Bae, J.S. Intracerebral transplantation of bone marrow-derived mesenchymal stem cells reduces amyloid-beta deposition and rescues memory deficits in Alzheimer's disease mice by modulation of immune responses. *Stem Cells* **2010**, *28*, 329–343. [[CrossRef](#)] [[PubMed](#)]
35. Yang, H.; Xie, Z.; Wei, L.; Yang, H.; Yang, S.; Zhu, Z.; Wang, P.; Zhao, C.; Bi, J. Human umbilical cord mesenchymal stem cell-derived neuron-like cells rescue memory deficits and reduce amyloid-beta deposition in an AbetaPP/PS1 transgenic mouse model. *Stem Cell Res. Ther.* **2013**, *4*, 76. [[CrossRef](#)] [[PubMed](#)]
36. Ma, T.; Gong, K.; Ao, Q.; Yan, Y.; Song, B.; Huang, H.; Zhang, X.; Gong, Y. Intracerebral transplantation of adipose-derived mesenchymal stem cells alternatively activates microglia and ameliorates neuropathological deficits in Alzheimer's disease mice. *Cell Transplant.* **2013**, *22* (Suppl. 1), S113–S126. [[CrossRef](#)]
37. Favre, J.; Taha, J.M.; Burchiel, K.J. An analysis of the respective risks of hematoma formation in 361 consecutive morphological and functional stereotactic procedures. *Neurosurgery* **2002**, *50*, 48–57. [[PubMed](#)]
38. Sansur, C.A.; Frysinger, R.C.; Pouratian, N.; Fu, K.M.; Bittl, M.; Oskouian, R.J.; Laws, E.R.; Elias, W.J. Incidence of symptomatic hemorrhage after stereotactic electrode placement. *J. Neurosurg.* **2007**, *107*, 998–1003. [[CrossRef](#)]
39. Frey, W.H., II. Method of Administering Neurologic Agents to the Brain. U.S. Patent 5,624,898, 29 April 1997.
40. Donega, V.; Nijboer, C.H.; van Velthoven, C.T.; Youssef, S.A.; de Bruin, A.; van Bel, F.; Kavelaars, A.; Heijnen, C.J. Assessment of long-term safety and efficacy of intranasal mesenchymal stem cell treatment for neonatal brain injury in the mouse. *Pediatr. Res.* **2015**, *78*, 520–526. [[CrossRef](#)]
41. Danielyan, L.; Schafer, R.; von Ameln-Mayerhofer, A.; Buadze, M.; Geisler, J.; Klopfer, T.; Burkhardt, U.; Proksch, B.; Verleysdonk, S.; Ayturan, M.; et al. Intranasal delivery of cells to the brain. *Eur. J. Cell Biol.* **2009**, *88*, 315–324. [[CrossRef](#)]

42. Galeano, C.; Qiu, Z.; Mishra, A.; Farnsworth, S.L.; Hemmi, J.J.; Moreira, A.; Edenhoffer, P.; Hornsby, P.J. The route by which intranasally delivered stem cells enter the central nervous system. *Cell Transplant.* **2018**, *27*, 501–514. [[CrossRef](#)] [[PubMed](#)]
43. Danielyan, L.; Schafer, R.; von Arnim-Mayerhofer, A.; Bernhard, F.; Verleysdonk, S.; Buadze, M.; Lourhmati, A.; Klopfer, T.; Schaumann, F.; Schmid, B.; et al. Therapeutic efficacy of intranasally delivered mesenchymal stem cells in a rat model of Parkinson disease. *Rejuvenation Res.* **2011**, *14*, 3–16. [[CrossRef](#)] [[PubMed](#)]
44. Salama, M.; Sobh, M.; Emam, M.; Abdalla, A.; Sabry, D.; El-Gamal, M.; Lotfy, A.; El-Husseiny, M.; Sobh, M.; Shalash, A.; et al. Effect of intranasal stem cell administration on the nigrostriatal system in a mouse model of Parkinson's disease. *Exp. Ther. Med.* **2017**, *13*, 976–982. [[CrossRef](#)] [[PubMed](#)]
45. Ninomiya, K.; Iwatsuki, K.; Ohnishi, Y.; Ohkawa, T.; Yoshimine, T. Intranasal delivery of bone marrow stromal cells to spinal cord lesions. *J. Neurosurg. Spine* **2015**, *23*, 111–119. [[CrossRef](#)] [[PubMed](#)]
46. Davies, S.W.; Turmaine, M.; Cozens, B.A.; DiFiglia, M.; Sharp, A.H.; Ross, C.A.; Scherzinger, E.; Wanker, E.E.; Mangiarini, L.; Bates, G.P. Formation of neuronal intranuclear inclusions underlies the neurological dysfunction in mice transgenic for the HD mutation. *Cell* **1997**, *90*, 537–548. [[CrossRef](#)]
47. Mangiarini, L.; Sathasivam, K.; Mahal, A.; Mott, R.; Seller, M.; Bates, G.P. Instability of highly expanded cag repeats in mice transgenic for the Huntington's disease mutation. *Nat. Genet.* **1997**, *15*, 197–200. [[CrossRef](#)]
48. Sathasivam, K.; Hobbs, C.; Mangiarini, L.; Mahal, A.; Turmaine, M.; Doherty, P.; Davies, S.W.; Bates, G.P. Transgenic models of Huntington's disease. *Philos. Trans. R. Soc. Lond. B Biol. Sci.* **1999**, *354*, 963–969. [[CrossRef](#)]
49. Stricker-Shaver, J.; Novati, A.; Yu-Taeger, L.; Nguyen, H.P. Genetic rodent models of Huntington disease. In *Polyglutamine Disorders*; Nóbrega, C., Pereira de Almeida, L., Eds.; Springer: Cham, Switzerland, 2018; Volume 1049, pp. 29–57.
50. Carter, R.J.; Lione, L.A.; Humby, T.; Mangiarini, L.; Mahal, A.; Bates, G.P.; Dunnett, S.B.; Morton, A.J. Characterization of progressive motor deficits in mice transgenic for the human Huntington's disease mutation. *J. Neurosci. J. Soc. Neurosci.* **1999**, *19*, 3248–3257. [[CrossRef](#)]
51. Stack, E.C.; Kubilus, J.K.; Smith, K.; Cormier, K.; Del Signore, S.J.; Guelin, E.; Ryu, H.; Hersch, S.M.; Ferrante, R.J. Chronology of behavioral symptoms and neuropathological sequela in R6/2 Huntington's disease transgenic mice. *J. Comp. Neurol.* **2005**, *490*, 354–370. [[CrossRef](#)]
52. Mangiarini, L.; Sathasivam, K.; Seller, M.; Cozens, B.; Harper, A.; Hetherington, C.; Lawton, M.; Trotter, Y.; Lehrach, H.; Davies, S.W.; et al. Exon 1 of the HD gene with an expanded CAG repeat is sufficient to cause a progressive neurological phenotype in transgenic mice. *Cell* **1996**, *87*, 493–506. [[CrossRef](#)]
53. Lione, L.A.; Carter, R.J.; Hunt, M.J.; Bates, G.P.; Morton, A.J.; Dunnett, S.B. Selective discrimination learning impairments in mice expressing the human Huntington's disease mutation. *J. Neurosci. Off. J. Soc. Neurosci.* **1999**, *19*, 10428–10437. [[CrossRef](#)]
54. Bolivar, V.J.; Manley, K.; Messer, A. Exploratory activity and fear conditioning abnormalities develop early in r6/2 Huntington's disease transgenic mice. *Behav. Neurosci.* **2003**, *117*, 1233–1242. [[CrossRef](#)] [[PubMed](#)]
55. Pla, P.; Orvoen, S.; Saudou, F.; David, D.J.; Humbert, S. Mood disorders in Huntington's disease: From behavior to cellular and molecular mechanisms. *Front. Behav. Neurosci.* **2014**, *8*, 135. [[CrossRef](#)] [[PubMed](#)]
56. Hickey, M.A.; Gallant, K.; Gross, G.G.; Levine, M.S.; Chesselet, M.F. Early behavioral deficits in r6/2 mice suitable for use in preclinical drug testing. *Neurobiol. Dis.* **2005**, *20*, 1–11. [[CrossRef](#)] [[PubMed](#)]
57. Maywood, E.S.; Fraenkel, E.; McAllister, C.J.; Wood, N.; Reddy, A.B.; Hastings, M.H.; Morton, A.J. Disruption of peripheral circadian timekeeping in a mouse model of Huntington's disease and its restoration by temporally scheduled feeding. *J. Neurosci. J. Soc. Neurosci.* **2010**, *30*, 10199–10204. [[CrossRef](#)] [[PubMed](#)]
58. Luthi-Carter, R.; Hanson, S.A.; Strand, A.D.; Bergstrom, D.A.; Chun, W.; Peters, N.L.; Woods, A.M.; Chan, E.Y.; Kooperberg, C.; Krainc, D.; et al. Dysregulation of gene expression in the r6/2 model of polyglutamine disease: Parallel changes in muscle and brain. *Hum. Mol. Genet.* **2002**, *11*, 1911–1926. [[CrossRef](#)]
59. Dalrymple, A.; Wild, E.J.; Joubert, R.; Sathasivam, K.; Bjorkqvist, M.; Petersen, A.; Jackson, G.S.; Isaacs, J.D.; Kristiansen, M.; Bates, G.P.; et al. Proteomic profiling of plasma in Huntington's disease reveals neuroinflammatory activation and biomarker candidates. *J. Proteome Res.* **2007**, *6*, 2833–2840. [[CrossRef](#)]
60. Silvestroni, A.; Faull, R.L.; Strand, A.D.; Moller, T. Distinct neuroinflammatory profile in post-mortem human Huntington's disease. *Neuroreport* **2009**, *20*, 1098–1103. [[CrossRef](#)]
61. Moller, T. Neuroinflammation in Huntington's disease. *J. Neural Transm.* **2010**, *117*, 1001–1008. [[CrossRef](#)]

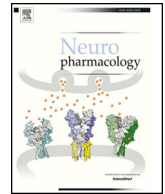
62. Hsiao, H.Y.; Chiu, F.L.; Chen, C.M.; Wu, Y.R.; Chen, H.M.; Chen, Y.C.; Kuo, H.C.; Chern, Y. Inhibition of soluble tumor necrosis factor is therapeutic in Huntington's disease. *Hum. Mol. Genet.* **2014**, *23*, 4328–4344. [[CrossRef](#)]
63. Yang, H.M.; Yang, S.; Huang, S.S.; Tang, B.S.; Guo, J.F. Microglial activation in the pathogenesis of Huntington's disease. *Front. Aging Neurosci.* **2017**, *9*, 193. [[CrossRef](#)] [[PubMed](#)]
64. Singhrao, S.K.; Neal, J.W.; Morgan, B.P.; Gasque, P. Increased complement biosynthesis by microglia and complement activation on neurons in Huntington's disease. *Exp. Neurol.* **1999**, *159*, 362–376. [[CrossRef](#)] [[PubMed](#)]
65. Sapp, E.; Kegel, K.B.; Aronin, N.; Hashikawa, T.; Uchiyama, Y.; Tohyama, K.; Bhide, P.G.; Vonsattel, J.P.; DiFiglia, M. Early and progressive accumulation of reactive microglia in the Huntington disease brain. *J. Neuropathol. Exp. Neurol.* **2001**, *60*, 161–172. [[CrossRef](#)] [[PubMed](#)]
66. Glennie, S.; Soeiro, I.; Dyson, P.J.; Lam, E.W.; Dazzi, F. Bone marrow mesenchymal stem cells induce division arrest energy of activated T cells. *Blood* **2005**, *105*, 2821–2827. [[CrossRef](#)] [[PubMed](#)]
67. Jouhou, H.; Yamamoto, K.; Homma, A.; Hara, M.; Kaneko, A.; Yamada, M. Depolarization of isolated horizontal cells of fish acidifies their immediate surrounding by activating V-ATPase. *J. Physiol.* **2007**, *585*, 401–412. [[CrossRef](#)] [[PubMed](#)]
68. Corcione, A.; Benvenuto, F.; Ferretti, E.; Giunti, D.; Cappiello, V.; Cazzanti, F.; Risso, M.; Gualandi, F.; Mancardi, G.L.; Pistoia, V.; et al. Human mesenchymal stem cells modulate B-cell functions. *Blood* **2006**, *107*, 367–372. [[CrossRef](#)]
69. Burchell, J.T.; Strickland, D.H.; Stumbles, P.A. The role of dendritic cells and regulatory t cells in the regulation of allergic asthma. *Pharmacol. Ther.* **2010**, *125*, 1–10. [[CrossRef](#)] [[PubMed](#)]
70. Spaggiari, G.M.; Capobianco, A.; Becchetti, S.; Mingari, M.C.; Moretta, L. Mesenchymal stem cell-natural killer cell interactions: Evidence that activated NK cells are capable of killing mscs, whereas MSCs can inhibit IL-2-induced NK-cell proliferation. *Blood* **2006**, *107*, 1484–1490. [[CrossRef](#)] [[PubMed](#)]
71. Meyerrose, T.; Olson, S.; Pontow, S.; Kalomoiris, S.; Jung, Y.; Annett, G.; Bauer, G.; Nolte, J.A. Mesenchymal stem cells for the sustained in vivo delivery of bioactive factors. *Adv. Drug Deliv. Rev.* **2010**, *62*, 1167–1174. [[CrossRef](#)] [[PubMed](#)]
72. Wilkins, A.; Kemp, K.; Ginty, M.; Hares, K.; Mallam, E.; Scolding, N. Human bone marrow-derived mesenchymal stem cells secrete brain-derived neurotrophic factor which promotes neuronal survival in vitro. *Stem Cell Res.* **2009**, *3*, 63–70. [[CrossRef](#)] [[PubMed](#)]
73. Kwan, W.; Trager, U.; Davalos, D.; Chou, A.; Bouchard, J.; Andre, R.; Miller, A.; Weiss, A.; Giorgini, F.; Cheah, C.; et al. Mutant huntingtin impairs immune cell migration in Huntington disease. *J. Clin. Investig.* **2012**, *122*, 4737–4747. [[CrossRef](#)] [[PubMed](#)]
74. Alpaugh, M.; Galleguillos, D.; Forero, J.; Morales, L.C.; Lackey, S.W.; Kar, P.; Di Pardo, A.; Holt, A.; Kerr, B.J.; Todd, K.G.; et al. Disease-modifying effects of ganglioside GM1 in Huntington's disease models. *EMBO Mol. Med.* **2017**, *9*, 1537–1557. [[CrossRef](#)] [[PubMed](#)]
75. Bibb, J.A.; Yan, Z.; Svenningsson, P.; Snyder, G.L.; Pieribone, V.A.; Horiuchi, A.; Nairn, A.C.; Messer, A.; Greengard, P. Severe deficiencies in dopamine signaling in presymptomatic Huntington's disease mice. *Proc. Natl. Acad. Sci. USA* **2000**, *97*, 6809–6814. [[CrossRef](#)] [[PubMed](#)]
76. Callahan, J.W.; Abercrombie, E.D. In vivo dopamine efflux is decreased in striatum of both fragment (R6/2) and full-length (YAC128) transgenic mouse models of Huntington's disease. *Front. Syst. Neurosci.* **2011**, *5*, 61. [[CrossRef](#)] [[PubMed](#)]
77. Cha, J.H.; Kosinski, C.M.; Kerner, J.A.; Alsdorf, S.A.; Mangiarini, L.; Davies, S.W.; Penney, J.B.; Bates, G.P.; Young, A.B. Altered brain neurotransmitter receptors in transgenic mice expressing a portion of an abnormal human Huntington disease gene. *Proc. Natl. Acad. Sci. USA* **1998**, *95*, 6480–6485. [[CrossRef](#)] [[PubMed](#)]
78. Bach, M.; Schimmelpfennig, C.; Stolzing, A. Influence of murine mesenchymal stem cells on proliferation, phenotype, vitality, and cytotoxicity of murine cytokine-induced killer cells in coculture. *PLoS ONE* **2014**, *9*, e88115. [[CrossRef](#)] [[PubMed](#)]
79. Hockly, E.; Woodman, B.; Mahal, A.; Lewis, C.M.; Bates, G. Standardization and statistical approaches to therapeutic trials in the r6/2 mouse. *Brain Res. Bull.* **2003**, *61*, 469–479. [[CrossRef](#)]
80. Naaldijk, Y.; Jager, C.; Fabian, C.; Leovsky, C.; Bluher, A.; Rudolph, L.; Hinze, A.; Stolzing, A. Effect of systemic transplantation of bone marrow-derived mesenchymal stem cells on neuropathology markers in APP/PS1 Alzheimer mice. *Neuropathol. Appl. Neurobiol.* **2017**, *43*, 299–314. [[CrossRef](#)]

81. Menalled, L.; El-Khodori, B.F.; Patry, M.; Suarez-Farinas, M.; Orenstein, S.J.; Zahasky, B.; Leahy, C.; Wheeler, V.; Yang, X.W.; MacDonald, M.; et al. Systematic behavioral evaluation of Huntington's disease transgenic and knock-in mouse models. *Neurobiol. Dis.* **2009**, *35*, 319–336. [[CrossRef](#)]
82. Goodman, A.O.; Morton, A.J.; Barker, R.A. Identifying sleep disturbances in Huntington's disease using a simple disease-focused questionnaire. *PLoS Curr.* **2010**, *2*, RRN1189. [[CrossRef](#)]
83. Morton, A.J.; Wood, N.L.; Hastings, M.H.; Hurelbrink, C.; Barker, R.A.; Maywood, E.S. Disintegration of the sleep-wake cycle and circadian timing in Huntington's disease. *J. Neurosci. J. Soc. Neurosci.* **2005**, *25*, 157–163. [[CrossRef](#)] [[PubMed](#)]
84. Cuesta, M.; Aungier, J.; Morton, A.J. The methamphetamine-sensitive circadian oscillator is dysfunctional in a transgenic mouse model of Huntington's disease. *Neurobiol. Dis.* **2012**, *45*, 145–155. [[CrossRef](#)] [[PubMed](#)]
85. Zuccato, C.; Ciammola, A.; Rigamonti, D.; Leavitt, B.R.; Goffredo, D.; Conti, L.; MacDonald, M.E.; Friedlander, R.M.; Silani, V.; Hayden, M.R.; et al. Loss of huntingtin-mediated BDNF gene transcription in Huntington's disease. *Science* **2001**, *293*, 493–498. [[CrossRef](#)] [[PubMed](#)]
86. Ma, L.; Morton, A.J.; Nicholson, L.F. Microglia density decreases with age in a mouse model of Huntington's disease. *Glia* **2003**, *43*, 274–280. [[CrossRef](#)] [[PubMed](#)]
87. Spires, T.L.; Grote, H.E.; Varshney, N.K.; Cordery, P.M.; van Dellen, A.; Blakemore, C.; Hannan, A.J. Environmental enrichment rescues protein deficits in a mouse model of Huntington's disease, indicating a possible disease mechanism. *J. Neurosci. J. Soc. Neurosci.* **2004**, *24*, 2270–2276. [[CrossRef](#)] [[PubMed](#)]
88. Giralt, A.; Carreton, O.; Lao-Peregrin, C.; Martin, E.D.; Alberch, J. Conditional BDNF release under pathological conditions improves Huntington's disease pathology by delaying neuronal dysfunction. *Mol. Neurodegener.* **2011**, *6*, 71. [[CrossRef](#)] [[PubMed](#)]
89. Ellrichmann, G.; Blusch, A.; Fatoba, O.; Brunner, J.; Hayardeny, L.; Hayden, M.; Sehr, D.; Winklhofer, K.F.; Saft, C.; Gold, R. Laquinimod treatment in the R6/2 mouse model. *Sci. Rep.* **2017**, *7*, 4947. [[CrossRef](#)]
90. Yohrling, G.J.t.; Jiang, G.C.; DeJohn, M.M.; Miller, D.W.; Young, A.B.; Vrana, K.E.; Cha, J.H. Analysis of cellular, transgenic and human models of Huntington's disease reveals tyrosine hydroxylase alterations and substantia nigra neuropathology. *Brain Res. Mol. Brain Res.* **2003**, *119*, 28–36. [[CrossRef](#)] [[PubMed](#)]
91. Lee, S.T.; Chu, K.; Jung, K.H.; Im, W.S.; Park, J.E.; Lim, H.C.; Won, C.H.; Shin, S.H.; Lee, S.K.; Kim, M.; et al. Slowed progression in models of Huntington disease by adipose stem cell transplantation. *Ann. Neurol.* **2009**, *66*, 671–681. [[CrossRef](#)]
92. Linares, G.R.; Chiu, C.T.; Scheuing, L.; Leng, Y.; Liao, H.M.; Maric, D.; Chuang, D.M. Preconditioning mesenchymal stem cells with the mood stabilizers lithium and valproic acid enhances therapeutic efficacy in a mouse model of Huntington's disease. *Exp. Neurol.* **2016**, *281*, 81–92. [[CrossRef](#)] [[PubMed](#)]
93. Danielyan, L.; Beer-Hammer, S.; Stolzing, A.; Schafer, R.; Siegel, G.; Fabian, C.; Kahle, P.; Biedermann, T.; Lourhmati, A.; Buadze, M.; et al. Intranasal delivery of bone marrow-derived mesenchymal stem cells, macrophages, and microglia to the brain in mouse models of Alzheimer's and Parkinson's disease. *Cell Transplant.* **2014**, *23* (Suppl. 1), S123–S139. [[CrossRef](#)]
94. Fransson, M.; Piras, E.; Wang, H.; Burman, J.; Duprez, I.; Harris, R.A.; LeBlanc, K.; Magnusson, P.U.; Brittebo, E.; Loskog, A.S. Intranasal delivery of central nervous system-retargeted human mesenchymal stromal cells prolongs treatment efficacy of experimental autoimmune encephalomyelitis. *Immunology* **2014**, *142*, 431–441. [[CrossRef](#)] [[PubMed](#)]
95. Grassin-Delyle, S.; Buenestado, A.; Naline, E.; Faisy, C.; Blouquit-Laye, S.; Couderc, L.J.; Le Guen, M.; Fischler, M.; Devillier, P. Intranasal drug delivery: An efficient and non-invasive route for systemic administration: Focus on opioids. *Pharmacol. Ther.* **2012**, *134*, 366–379. [[CrossRef](#)] [[PubMed](#)]
96. Kumar, H.; Mishra, G.; Sharma, A.K.; Gothwal, A.; Kesharwani, P.; Gupta, U. Intranasal drug delivery: A non-invasive approach for the better delivery of neurotherapeutics. *Pharm. Nanotechnol.* **2017**, *5*, 203–214. [[CrossRef](#)] [[PubMed](#)]
97. Crowe, T.P.; Greenlee, M.H.W.; Kanthasamy, A.G.; Hsu, W.H. Mechanism of intranasal drug delivery directly to the brain. *Life Sci.* **2018**, *195*, 44–52. [[CrossRef](#)]
98. Mahmood, A.; Lu, D.; Qu, C.; Goussev, A.; Chopp, M. Long-term recovery after bone marrow stromal cell treatment of traumatic brain injury in rats. *J. Neurosurg.* **2006**, *104*, 272–277. [[CrossRef](#)] [[PubMed](#)]
99. Donega, V.; van Velthoven, C.T.; Nijboer, C.H.; van Bel, F.; Kas, M.J.; Kavelaars, A.; Heijnen, C.J. Intranasal mesenchymal stem cell treatment for neonatal brain damage: Long-term cognitive and sensorimotor improvement. *PLoS ONE* **2013**, *8*, e51253. [[CrossRef](#)]

100. Liang, X.; Ding, Y.; Zhang, Y.; Tse, H.F.; Lian, Q. Paracrine mechanisms of mesenchymal stem cell-based therapy: Current status and perspectives. *Cell Transplant.* **2014**, *23*, 1045–1059. [[CrossRef](#)]
101. Tsai, M.J.; Tsai, S.K.; Hu, B.R.; Liou, D.Y.; Huang, S.L.; Huang, M.C.; Huang, W.C.; Cheng, H.; Huang, S.S. Recovery of neurological function of ischemic stroke by application of conditioned medium of bone marrow mesenchymal stem cells derived from normal and cerebral ischemia rats. *J. Biomed. Sci.* **2014**, *21*, 5. [[CrossRef](#)]
102. Thomi, G.; Surbek, D.; Haesler, V.; Joerger-Messerli, M.; Schoeberlein, A. Exosomes derived from umbilical cord mesenchymal stem cells reduce microglia-mediated neuroinflammation in perinatal brain injury. *Stem Cell Res. Ther.* **2019**, *10*, 105. [[CrossRef](#)]
103. Long, Q.; Upadhyya, D.; Hattiangady, B.; Kim, D.K.; An, S.Y.; Shuai, B.; Prockop, D.J.; Shetty, A.K. Intranasal MSC-derived A1-exosomes ease inflammation, and prevent abnormal neurogenesis and memory dysfunction after status epilepticus. *Proc. Natl. Acad. Sci. USA* **2017**, *114*, E3536–E3545. [[CrossRef](#)] [[PubMed](#)]
104. Song, M.; Heo, J.; Chun, J.Y.; Bae, H.S.; Kang, J.W.; Kang, H.; Cho, Y.M.; Kim, S.W.; Shin, D.M.; Choo, M.S. The paracrine effects of mesenchymal stem cells stimulate the regeneration capacity of endogenous stem cells in the repair of a bladder-outlet-obstruction-induced overactive bladder. *Stem Cells Dev.* **2014**, *23*, 654–663. [[CrossRef](#)] [[PubMed](#)]
105. Hansson, O.; Petersen, A.; Leist, M.; Nicotera, P.; Castilho, R.F.; Brundin, P. Transgenic mice expressing a Huntington's disease mutation are resistant to quinolinic acid-induced striatal excitotoxicity. *Proc. Natl. Acad. Sci. USA* **1999**, *96*, 8727–8732. [[CrossRef](#)] [[PubMed](#)]
106. Nishi, A.; Snyder, G.L.; Greengard, P. Bidirectional regulation of DARPP-32 phosphorylation by dopamine. *J. Neurosci. J. Soc. Neurosci.* **1997**, *17*, 8147–8155. [[CrossRef](#)]
107. Meijer, J.H.; Rietveld, W.J. Neurophysiology of the suprachiasmatic circadian pacemaker in rodents. *Physiol. Rev.* **1989**, *69*, 671–707. [[CrossRef](#)] [[PubMed](#)]
108. Miller, J.D. On the nature of the circadian clock in mammals. *Am. J. Physiol.* **1993**, *264*, R821–R832. [[CrossRef](#)] [[PubMed](#)]
109. Rietveld, W.J. Neurotransmitters and the pharmacology of the suprachiasmatic nuclei. *Pharmacol. Ther.* **1992**, *56*, 119–130. [[CrossRef](#)]
110. Yujnovsky, I.; Hirayama, J.; Doi, M.; Borrelli, E.; Sassone-Corsi, P. Signaling mediated by the dopamine d2 receptor potentiates circadian regulation by CLOCK:BMAL1. *Proc. Natl. Acad. Sci. USA* **2006**, *103*, 6386–6391. [[CrossRef](#)] [[PubMed](#)]
111. Bussi, I.L.; Levin, G.; Golombek, D.A.; Agostino, P.V. Involvement of dopamine signaling in the circadian modulation of interval timing. *Eur. J. Neurosci.* **2014**, *40*, 2299–2310. [[CrossRef](#)]
112. Esposito, E.; Cuzzocrea, S. Antiinflammatory activity of melatonin in central nervous system. *Curr. Neuropharmacol.* **2010**, *8*, 228–242. [[CrossRef](#)]
113. Graybeal, J.J.; Bozzelli, P.L.; Graybeal, L.L.; Groeber, C.M.; McKnight, P.E.; Cox, D.N.; Flinn, J.M. Human ApoE epsilon4 alters circadian rhythm activity, IL-1beta, and GFAP in CRND8 mice. *J. Alzheimer's Dis.* **2015**, *43*, 823–834. [[CrossRef](#)] [[PubMed](#)]
114. Motzkus, D.; Albrecht, U.; Maronde, E. The human per1 gene is inducible by interleukin-6. *J. Mol. Neurosci.* **2002**, *18*, 105–109. [[CrossRef](#)]
115. Bjorkqvist, M.; Wild, E.J.; Thiele, J.; Silvestroni, A.; Andre, R.; Lahiri, N.; Raibon, E.; Lee, R.V.; Benn, C.L.; Soulet, D.; et al. A novel pathogenic pathway of immune activation detectable before clinical onset in Huntington's disease. *J. Exp. Med.* **2008**, *205*, 1869–1877. [[CrossRef](#)] [[PubMed](#)]
116. Puissant, B.; Barreau, C.; Bourin, P.; Clavel, C.; Corre, J.; Bousquet, C.; Taureau, C.; Cousin, B.; Abbal, M.; Laharrague, P.; et al. Immunomodulatory effect of human adipose tissue-derived adult stem cells: Comparison with bone marrow mesenchymal stem cells. *Br. J. Haematol.* **2005**, *129*, 118–129. [[CrossRef](#)] [[PubMed](#)]
117. Siegel, G.; Schafer, R.; Dazzi, F. The immunosuppressive properties of mesenchymal stem cells. *Transplantation* **2009**, *87*, S45–S49. [[CrossRef](#)] [[PubMed](#)]
118. Uccelli, A.; Moretta, L.; Pistoia, V. Immunoregulatory function of mesenchymal stem cells. *Eur. J. Immunol.* **2006**, *36*, 2566–2573. [[CrossRef](#)]
119. Selmani, Z.; Naji, A.; Zidi, I.; Favier, B.; Gaiffe, E.; Obert, L.; Borg, C.; Saas, P.; Tiberghien, P.; Rouas-Freiss, N.; et al. Human leukocyte antigen-G5 secretion by human mesenchymal stem cells is required to suppress T lymphocyte and natural killer function and to induce CD4+CD25highFOXP3+ regulatory T cells. *Stem Cells* **2008**, *26*, 212–222. [[CrossRef](#)]

120. Crop, M.J.; Baan, C.C.; Korevaar, S.S.; Ijzermans, J.N.; Pescatori, M.; Stubbs, A.P.; van Ijcken, W.F.; Dahlke, M.H.; Eggenhofer, E.; Weimar, W.; et al. Inflammatory conditions affect gene expression and function of human adipose tissue-derived mesenchymal stem cells. *Clin. Exp. Immunol.* **2010**, *162*, 474–486. [[CrossRef](#)]
121. Ren, G.; Zhao, X.; Zhang, L.; Zhang, J.; L'Huillier, A.; Ling, W.; Roberts, A.I.; Le, A.D.; Shi, S.; Shao, C.; et al. Inflammatory cytokine-induced intercellular adhesion molecule-1 and vascular cell adhesion molecule-1 in mesenchymal stem cells are critical for immunosuppression. *J. Immunol.* **2010**, *184*, 2321–2328. [[CrossRef](#)]
122. Hardy, S.A.; Maltman, D.J.; Przyborski, S.A. Mesenchymal stem cells as mediators of neural differentiation. *Curr. Stem Cell Res. Ther.* **2008**, *3*, 43–52.
123. Rossignol, J.; Fink, K.D.; Crane, A.T.; Davis, K.K.; Bombard, M.C.; Clerc, S.; Bavar, A.M.; Lowrance, S.A.; Song, C.; Witte, S.; et al. Reductions in behavioral deficits and neuropathology in the R6/2 mouse model of Huntington's disease following transplantation of bone-marrow-derived mesenchymal stem cells is dependent on passage number. *Stem Cell Res. Ther.* **2015**, *6*, 9. [[CrossRef](#)] [[PubMed](#)]
124. Kraft, A.D.; Kaltenbach, L.S.; Lo, D.C.; Harry, G.J. Activated microglia proliferate at neurites of mutant huntingtin-expressing neurons. *Neurobiol. Aging* **2012**, *33*, 621.e17–621.e33. [[CrossRef](#)] [[PubMed](#)]
125. Benraiss, A.; Wang, S.; Herrlinger, S.; Li, X.; Chandler-Militello, D.; Mauceri, J.; Burm, H.B.; Toner, M.; Osipovitch, M.; Jim Xu, Q.; et al. Human glia can both induce and rescue aspects of disease phenotype in Huntington disease. *Nat. Commun.* **2016**, *7*, 11758. [[CrossRef](#)] [[PubMed](#)]
126. Noh, M.Y.; Lim, S.M.; Oh, K.W.; Cho, K.A.; Park, J.; Kim, K.S.; Lee, S.J.; Kwon, M.S.; Kim, S.H. Mesenchymal stem cells modulate the functional properties of microglia via tgf-beta secretion. *Stem Cells Transl. Med.* **2016**, *5*, 1538–1549. [[CrossRef](#)] [[PubMed](#)]
127. Liu, Y.; Zhang, R.; Yan, K.; Chen, F.; Huang, W.; Lv, B.; Sun, C.; Xu, L.; Li, F.; Jiang, X. Mesenchymal stem cells inhibit lipopolysaccharide-induced inflammatory responses of BV2 microglial cells through TSG-6. *J. Neuroinflamm.* **2014**, *11*, 135. [[CrossRef](#)] [[PubMed](#)]
128. Giunti, D.; Parodi, B.; Usai, C.; Vergani, L.; Casazza, S.; Bruzzone, S.; Mancardi, G.; Uccelli, A. Mesenchymal stem cells shape microglia effector functions through the release of CX3CL1. *Stem Cells* **2012**, *30*, 2044–2053. [[CrossRef](#)]
129. Jaimes, Y.; Naaldijk, Y.; Wenk, K.; Leovsky, C.; Emmrich, F. Mesenchymal stem cell-derived microvesicles modulate lipopolysaccharides-induced inflammatory responses to microglia cells. *Stem Cells* **2017**, *35*, 812–823. [[CrossRef](#)]
130. Saijo, K.; Glass, C.K. Microglial cell origin and phenotypes in health and disease. *Nat. Rev. Immunol.* **2011**, *11*, 775–787. [[CrossRef](#)]
131. Welberg, L. Synaptic plasticity: A synaptic role for microglia. *Nat. Rev. Neurosci.* **2014**, *15*, 69. [[CrossRef](#)]
132. Baron, R.; Babcock, A.A.; Nemirovsky, A.; Finsen, B.; Monsonogo, A. Accelerated microglial pathology is associated with abeta plaques in mouse models of Alzheimer's disease. *Aging Cell* **2014**, *13*, 584–595. [[CrossRef](#)]
133. Dey, N.D.; Bombard, M.C.; Roland, B.P.; Davidson, S.; Lu, M.; Rossignol, J.; Sandstrom, M.I.; Skeel, R.L.; Lescaudron, L.; Dunbar, G.L. Genetically engineered mesenchymal stem cells reduce behavioral deficits in the YAC 128 mouse model of Huntington's disease. *Behav. Brain Res.* **2010**, *214*, 193–200. [[CrossRef](#)] [[PubMed](#)]





Brain-penetrant PQR620 mTOR and PQR530 PI3K/mTOR inhibitor reduce huntingtin levels in cell models of HD

Elisabeth Singer^{a,b}, Carolin Walter^{a,b}, Dorian Fabbro^c, Denise Rageot^d, Florent Beaufiles^c, Matthias P. Wymann^d, Nadine Rischert^{a,b}, Olaf Riess^{a,b}, Petra Hillmann^c, Huu Phuc Nguyen^{e,*}

^a Institute of Medical Genetics and Applied Genomics, University of Tuebingen, Calwerstrasse 7, Tuebingen, 72076, Germany

^b Centre for Rare Diseases (ZSE), University of Tuebingen, Calwerstrasse 7, Tuebingen, 72076, Germany

^c PIQUR Therapeutics AG, Hochbergerstrasse 60C, Basel, 4057, Switzerland

^d Department of Biomedicine, University of Basel, Mattenstrasse 28, Basel, 4056, Switzerland

^e Department of Human Genetics, Ruhr University Bochum, Universitaetsstrasse 150, Bochum, 44801, Germany

HIGHLIGHTS

- PI3K/mTORC and mTORC inhibitors reduce levels of soluble and aggregated huntingtin.
- Catalytic mTOR inhibition ameliorates protein aggregation in cellular models of HD.
- PQR530 and PQR620 cross the BBB and effectively inhibit mTOR signalling.

ARTICLE INFO

Keywords:

Huntington disease
Huntingtin
Neurodegeneration
Catalytic mTOR inhibition
Aggregation

ABSTRACT

One of the pathological hallmarks of Huntington disease (HD) is accumulation of the disease-causing mutant huntingtin (mHTT), which leads to the disruption of a variety of cellular functions, ultimately resulting in cell death. Induction of autophagy, for example by the inhibition of mechanistic target of rapamycin (mTOR) signaling, has been shown to reduce HTT levels and aggregates. While rapalogs like rapamycin allosterically inhibit the mTOR complex 1 (TORC1), ATP-competitive mTOR inhibitors suppress activities of TORC1 and TORC2 and have been shown to be more efficient in inducing autophagy and reducing protein levels and aggregates than rapalogs. The ability to cross the blood-brain barrier of first generation catalytic mTOR inhibitors has so far been limited, and therefore sufficient target coverage in the brain could not be reached. Two novel, brain penetrant compounds – the mTORC1/2 inhibitor PQR620, and the dual pan-phosphoinositide 3-kinase (PI3K) and mTORC1/2 kinase inhibitor PQR530 – were evaluated by assessing their potential to induce autophagy and reducing mHTT levels. For this purpose, expression levels of autophagic markers and well-defined mTOR targets were analyzed in *STHdh* cells and HEK293T cells and in mouse brains. Both compounds potently inhibited mTOR signaling in cell models as well as in mouse brain. As proof of principle, reduction of aggregates and levels of soluble mHTT were demonstrated upon treatment with both compounds. Originally developed for cancer treatment, these second generation mTORC1/2 and PI3K/mTOR inhibitors show brain penetrance and efficacy in cell models of HD, making them candidate molecules for further investigations in HD.

1. Introduction

Cellular homeostasis is crucial to cell survival. As cells and organisms age or with increasing disease burden, they become less resistant to stress and accumulations of excess and dysfunctional proteins. These

accumulations of proteins cause damage to cells and can lead to cell death (Ross and Poirier, 2004). The maintenance of homeostasis is of special importance to post-mitotic cells, like neurons. Protein accumulations are common characteristics of various neurodegenerative diseases, like Alzheimer disease (AD) (Bucciantini et al., 2002),

* Corresponding author.

E-mail addresses: elisabeth.singer@med.uni-tuebingen.de (E. Singer), carolin.futter@googlemail.com (C. Walter), Dorian.fabbro@piqur.com (D. Fabbro), denise.rageot@unibas.ch (D. Rageot), florent.beaufiles@piqur.com (F. Beaufiles), matthias.wymann@unibas.ch (M.P. Wymann), Nadine.Rischert@gmx.de (N. Rischert), olaf.riess@med.uni-tuebingen.de (O. Riess), petra.hillmann@piqur.com (P. Hillmann), huu.nguyen-r7w@rub.de (H.P. Nguyen).

<https://doi.org/10.1016/j.neuropharm.2019.107812>

Received 20 June 2019; Received in revised form 25 September 2019; Accepted 10 October 2019

Available online 14 October 2019

0028-3908/ © 2019 Published by Elsevier Ltd.

Parkinson disease (PD) (Hashimoto et al., 2003), Spinocerebellar Ataxia Type 3 (SCA3) (Seidel et al., 2012) and Huntington disease (HD) (DiFiglia et al., 1997). The latter is a monogenetic, neurodegenerative disorder caused by a CAG expansion in the *Huntingtin* (*HTT*) gene (The Huntington's Disease Collaborative Research Group, 1993). Patients expressing more than 39 of these CAGs will inevitably develop the autosomal dominantly inherited disease (Nance et al., 1998) with symptoms including dysfunctions of motor, metabolic and cognitive systems (Vonsattel and DiFiglia, 1998). The pathology on the molecular level is associated with the malformation (Ko et al., 2001; Poirier et al., 2002), malfunction (Duennwald et al., 2006; Ehrnhoefer et al., 2011), degradation prevention (Jana et al., 2001), toxic fragment formation (Lajoie and Snapp, 2010; Mende-Mueller et al., 2001) and aggregation (Bates, 2003; Bucciantini et al., 2002; DiFiglia et al., 1997; Li et al., 2001; Michalik and Van Broeckhoven, 2003) of mutant Huntingtin (mHTT). Even though promising new approaches to specifically lower HTT levels are currently in development (Wild and Tabrizi, 2017), to date no causative treatment is available for patients and the disease progression cannot be halted. The reduction of mHTT levels has been found to correlate with the amelioration of disease burden (Kordasiewicz et al., 2012; Wang et al., 2014). This can be achieved either by reducing the expression of the protein or by decreasing its half-life in the cell. Degradation of protein accumulations and aggregates can be achieved by the induction of autophagy (Kraft et al., 2010; Mizushima et al., 2008; Pankiv et al., 2007; Ravikumar et al., 2002; Sarkar and Rubinsztein, 2008; Zhang et al., 2007), one of the cell's two major protein degradation systems, besides the ubiquitin-proteasome system (UPS) (Kaganovich et al., 2008; Rubinsztein, 2006). Macroautophagy, the major subtype of autophagy, contributes to the cellular renewal process by the degradation of cytoplasmic proteins and large structures, like aggregates and organelles (Mizushima and Komatsu, 2011). For the brain this upkeeping of recycling processes is of special interest, because of the post-mitotic state of the neurons (Rubinsztein et al., 2005). Consequently, depletion of autophagic genes and the inhibition of autophagy leads to neurodegeneration-like phenotypes (Alirezai et al., 2008; Hara, 2006; Komatsu, 2006; Komatsu et al., 2007). Macroautophagy is regulated by mTOR (Pattingre et al., 2008), providing the cell with energy and amino acids in times of starvation. mTOR is a conserved serine/threonine kinase functioning as an integration hub for various environmental cues – growth factors, amino acids, oxygen and energy levels – thereby regulating cell metabolism and proliferation (Laplante and Sabatini, 2012). It forms at least two multi-protein complexes - mTOR complex 1 (mTORC1) and mTOR complex 2 (mTORC2) - both of which exert distinct regulatory cell functions. mTORC1 drives protein biosynthesis by phosphorylation of eIF4E binding protein (4E-BP1) and S6 ribosomal protein (S6RP) (Ma and Blenis, 2009). mTORC2 is responsible for the integration of growth factor signaling, driving cell survival, metabolism and cytoskeletal reorganization (Laplante and Sabatini, 2009). As mTOR is the regulatory inhibitor of autophagy, its pharmacological inhibition has been shown to induce autophagy (Sarkar et al., 2009) and to ameliorate disease symptoms in various neurodegenerative disorders (Menzies, 2010; Ravikumar et al., 2004; Santini et al., 2009; Spilman et al., 2010). There are two types of mTOR inhibitors available. The first type comprises rapalogs, allosteric inhibitors like rapamycin, a macrolide antibiotic and its derivatives, used in the before mentioned studies, that have limited effects on mTORC2 and certain mTORC1 functions (Feldman, 2009), undesirable physicochemical properties and poor tolerability. The second type are catalytic inhibitors (Zhou and Huang, 2012). This second generation of ATP site directed mTOR inhibitors was developed to overcome feedback activation of the mTOR pathway and poor bioavailability of rapalogs (Brandt et al., 2018). These inhibitors can either target mTOR specifically or mTOR and phosphoinositide 3-kinases (PI3Ks), an upstream regulator of AKT and mTOR in the signaling cascade. The catalytic mTOR/PI3K inhibitor NVP-BEZ235 has been tested previously in cell models of HD, where it reduced mHTT

aggregation (Rosic et al., 2011).

Both compounds tested in this study are catalytic inhibitors of mTOR (PQR620) and mTOR/PI3K (PQR530), originally designed as cancer drugs. PQR530 (Hillmann et al., 2017; Rageot et al., 2017) and PQR620 (Rageot et al., 2018; Tarantelli et al., 2016, 2019) have been evaluated for their potential of reducing levels of HTT in *in vitro* models of HD. Both drugs were able to block mTOR activity and to induce autophagy without affecting cell viability. Moreover, HTT levels were reduced in an eGFP-HTT-Exon1 expression model and a full-length cell model of HD. The brain penetration of both substances was demonstrated *in vivo*. This study is adding to the limited knowledge about ATP-competitive mTOR inhibitors in neurodegeneration making PQR530 and PQR620 ideal candidates for further development in HD.

2. Material and methods

All chemicals were purchased from Sigma, Merck KGaA, Darmstadt, Germany and reagents were purchased from Thermo Fisher Scientific, Waltham, MA, USA, where not stated differently.

2.1. Cell culture & treatment

STHdh cell lines (*STHdh*^{Q7/Q7} and *STHdh*^{Q111/Q111}) (Trettel et al., 2000), immortalized cells derived from murine striatal primordia, were obtained from Coriell Cell Repositories (Coriell Institute for Medical Research). The two progenitor cell lines either encode 7 polyglutamines in the wild-type mouse gene locus or 111 within the chimeric exon 1 of *HTT*, homozygously knocked into the mouse locus (Menalled, 2005). Cell passages 4–12 were used for the experiments. Human embryonic kidney cells from line 293 (HEK293T) were used in passages 25–40. All cell lines were maintained in Dulbecco's modified eagle medium (DMEM), supplemented with 10% fetal bovine serum and 1% penicillin/streptomycin at 37 °C in 5% CO₂. Medium for *STHdh* cells was further complemented with 1% geneticin (G418, A2912, Biochrome, Berlin, Germany). For differentiation into neuron-like cells, *STHdh* cells were treated with differentiation medium, as previously described (Trettel et al., 2000). All cell lines were routinely tested negatively for mycoplasma contamination by PCR (Venor®GeM Mycoplasma detection kit; Merck, Darmstadt, Germany). All substances for treatment were dissolved in 100% DMSO. Cells were seeded out one day before treatment in 100 mm dishes. At ~80% confluency *STHdh* cells were differentiated and treated with PQR530 (130 nM and 1230 nM) and PQR620 (200, 400 and 1230 nM) obtained from PIQUR Therapeutics (Basel, Switzerland). Rapamycin (400 nM, Merck, Darmstadt, Germany) and INK128 (100 nM, Biomol GmbH, Hamburg, Germany) were used as controls for mTOR inhibition. DMSO was used as negative control. All substances were prepared in working solutions at concentrations assuring equal DMSO concentrations within treatments. Final DMSO concentration did not exceed 0.4%. Bafilomycin A1 (Baf.A1) was added at 50 nM for autophagic flux assays. For MSD assays HEK293T cells were treated with 1 μM and 3 μM of PQR530 and PQR620, rapamycin (100 nM) and INK128 (3 μM).

2.2. Protein overexpression & cell transfection

Constructs for the expression of an HTT Exon1 fragment were generated to express 20Q or 49Q expansion. The fragments were inserted into the pEGFP-N1 vector (Clontech Laboratories, Mountain View, CA, USA) via XhoI and HindIII. HEK293T cell transfection was performed with Attractene reagent (Qiagen GmbH, Hilden, Germany) according to manufacturer's protocol for filter trap analysis and fluorescence microscopy and Lipofectamine 2000 for measurements of HTT protein levels and pathway inhibition. pEGFP-N1-TFEB was a gift from Shawn Ferguson (Addgene plasmid #38119; <http://n2t.net/addgene:38119>; RRID:Addgene_38119). pCI-Neo HA-HTT 15Q/128Q were a gift from Michael Hayden (CMMT, Vancouver, CN).

2.3. Western blot & immunodetection

For the analysis of protein markers for mTOR inhibition and induction of autophagy, protein lysates were generated from treated cells after 8 h, 24 h or 24 h + 4 h. Cells were disrupted by vortexing in RIPA lysis buffer (50 mM Tris-HCl pH 7.5, 150 mM NaCl, 1% NP-40, 0.5% sodium deoxycholate, 0.1% SDS), containing protease inhibitor (cOmplete, Roche, Basel, Switzerland) and phosphatase inhibitor (phosSTOP, Roche, Basel, Switzerland). Cell and brain homogenates were incubated for 30 min on ice and vortexed every 10 min. Lysates were obtained after centrifugation for 20 min, 13,200 × g at 4 °C. Protein concentration was determined spectrophotometrically by Bradford assay (Bradford reagent, Bio-Rad Laboratories, Inc., Hercules, CA, USA) and adjusted to 30 µg total protein per sample. Proteins were separated and blotted using standard protocols. Bolt™ 4–12% Bis-Tris Plus gels were used with MES buffer (2.5 mM MES, 2.5 mM Tris, 0.005% SDS, 50 µM EDTA) for all proteins except for 4E-BP1, which was separated in standard tris-glycine gels. Samples for HTT analysis were run on NuPAGE Tris-Acetate gels (7%). All proteins, except for LC3B were transferred onto 0.2 µm nitrocellulose membrane (Amersham Protran™ Premium, GE Healthcare, Little Chalfont, UK). LC3B was blotted onto 0.2 µm PVDF membrane (Amersham Hybond P, GE Healthcare, Little Chalfont, UK). Primary antibodies used were the following: LC3 (1:200, clone 5F10, NanoTools, Teningen, Germany), p62 (1:1000, #5114, Cell Signalling, Cambridge, UK), mTOR (1:1000, #2972, Cell Signalling, Cambridge, UK), P-mTOR (Ser2448) (1:1000, #2971, Cell Signaling, Cambridge, UK), S6 ribosomal protein (1:1000, 54D2, #2317, Cell Signalling, Cambridge, UK), P-S6 ribosomal protein (Ser235/236) (1:1000, #2211, Cell Signalling, Cambridge, UK), AKT (1:1000, #9272, Cell Signaling, Cambridge, UK), P-AKT (Ser473) (1:1000, #9271, Cell Signaling, Cambridge, UK) 4E-BP1 (1:1000, #9452, Cell Signaling, Cambridge, UK), P-4E-BP1 (Thr37/46) (1:1000, #9459, Cell Signaling, Cambridge, UK), anti-polyglutamine-expansion disease marker antibody, clone 5TF1-1C2 (1:2000, MAB1574, Merck KGaA, Darmstadt, Germany), Huntingtin (D7F7) (1:1000, #5656, Cell Signaling, Cambridge, UK), β-actin (1:20,000, A5441, Sigma-Aldrich, Saint Louis, Missouri, USA), vinculin (1:1000; clone E1E9 V, #13901, Cell Signaling; Cambridge, UK). For detection, respective secondary IRDye antibodies: goat anti-mouse 680LT, goat anti-mouse 800CW and goat anti-rabbit 800CW (1:10,000, LI-COR Biosciences, Bad Homburg, Germany) were incubated for 1 h and detected with the LI-COR ODYSSEY® FC (LI-COR Biosciences, Bad Homburg, Germany). Quantification of signal was performed with LI-COR Image Studio Lite software, version 4.0.21 and normalised to β-actin signal, where not stated differently.

2.4. MSD & TR-FRET assays

HEK293T cells were harvested 44/48 h post transfection and lysed in Evotec MSD Lysis Buffer (150 mM NaCl, 20 mM Tris, pH 7.5, 1 mM EDTA, 1 mM EGTA, 1% Triton-X-100) supplemented with 10 mM NaF, 1 mM PMSF, phosphatase inhibitor I and II, complete mini EDTA free protease inhibitor cocktail tablet (Roche, Basel, Switzerland) by vortexing and rotation of samples. The transfected HEK293T cell samples were analyzed for expanded soluble mutant HTT by TR-FRET. HEK293T cells were analyzed in technical duplicates. Expanded soluble HTT was measured in final concentrations of 0.1 µg/µl total protein. 10 µl of HEK293T cell lysate were applied to the assay. Protein concentrations were determined by BCA assay (Pierce BCA Protein Assay). To assess autophagosomal markers LC3-II and p62 (TR-FRET) samples were frozen at - 80 °C for 1 h and re-thawed as part of the homogenization. 5 µl sample was added to 1 µl antibody mix (Terbium and Alexa647-labeled antibodies for p62 and LC3II, respectively) in a white 384-well microplate with low volume (Greiner, Greiner Bio-One GmbH, Frickenhausen, Germany). The plate was sealed and incubated at room temperature on a shaker at 500 rpm. The readout was done after

20–24 h for p62 TR-FRET analysis, for LC3II TR-FRET analysis the plate was incubated at 4 °C for additional 20–24 h, reading was performed using a fluorescence reader (EnVision Multimode Plate Reader, PerkinElmer, Waltham MA, USA). For autophagy assays, internal positive and negative controls were applied for each assay run. For analysis of (P-)p70S6K (Thr389), (P-)S6RP (Ser240/244), (P-)GSK-3β (Ser9) and (P-)AKT (Ser473) by MSD the AKT Signaling Panel II Whole Cell Lysate Kit (MesoScale, Cat. No. K15177D, Meso Scale Diagnostics, LLC, Rockville, MD, USA) was used to measure activation of the AKT signaling pathway according to manufacturer's protocol.

2.5. Protein biosynthesis

Cells were seeded in four technical replicates per genotype and treatment on a 96-well plate. 50,000 cells were seeded per well. Click-iT® AHA was added to the cultured cells together with two different concentrations of PQR530 and PQR620, rapamycin (400 nM), INK128 (100 nM) or vehicle for 24 h. The fluorescent signal was detected using a fluorescence plate reader (EnVision Multimode Plate Reader, PerkinElmer, Waltham, MA, USA). The intensity was quantified relative to Hoechst staining. This measurement was repeated at least three times in independent experiments for each cell line.

2.6. Viability assays

Effects on cell viability and cytotoxicity by the compounds were determined with PrestoBlue® and Cytotoxicity Detection Kit (LDH) (Roche, Basel, Switzerland), respectively. The procedure was performed according to manufacturer's protocol. In brief, cells were seeded 10,000/well in 96-well plates and incubated for approximately 12 h before cells were differentiated and further incubated for up to 72 h. PrestoBlue® and LDH assay were performed in the same plates. Fluorescence intensity (PrestoBlue®) and absorption (LDH) were measured with MWGt Synergy HT plate reader (BioTek Instruments, Winooski, VT, USA) and analyzed with Gen5 2.01 software (BioTek Instruments, Winooski, VT, USA).

2.7. Fluorescence microscopy

HEK293T cells were seeded onto Poly-L-Lysine coated cover slips and transfected on the following day. Treatment started 48 h after transfection and lasted for 24 h for quantification of aggregation and 1 h for TFEB localization investigation. Cells were fixed with 4% PFA in DPBS for 20 min at room temperature. Cell nuclei were stained with DAPI (Vectashield® Mounting medium, Vecta Laboratories, Burlingame, CA, USA). Images were acquired using a Zeiss Axioplan microscope (40x/0.75 objective, AxioCam MRC) (Zeiss, Jena). Transfected cells and aggregates per cell were counted on 30 pseudo-randomized pictures per experiment; the average from 3 independent experiments was calculated. Per treatment approximately 500 cells were evaluated. For TFEB localization images were acquired at 63x with an Apotome (Zeiss, Jena). 100–150 cells per treatment were analyzed in 3 independent experiments.

2.8. Filter trap

HEK293T cells were transiently transfected with the eGFP-HTT-Exon1 -20Q/49Q constructs. or with HTT-128Q or 15Q constructs. Total expression time was 72 h; treatment with compounds started 24 h before harvest. Cells were detached with ice-cold DPBS and lysed in RIPA buffer (see Western blot), homogenates were prepared by sonication (Bandelin Sonopuls HD2070, BANDELIN electronic GmbH & Co. KG, Berlin, Germany). To detect SDS insoluble HTT aggregates, samples containing 15 µg of protein in DPBS with 2% SDS were applied to a nitrocellulose membrane (0.45 µM, Bio-Rad Laboratories, Inc., Hercules, CA, USA) for the detection of total PolyQ protein levels in a

Minifold® II Slot Blot System (Schleicher & Schuell, GmbH, Erdmannhausen, Germany). Membranes were washed in TBS, blocked in 5% skim milk powder and immunoprobed with 1C2 antibody, clone 5TF1-1C2 (1:2000, MAB1574, Merck KGaA, Darmstadt, Germany). For the detection of aggregates, nitrocellulose acetate membrane 0.2 µm (OE66, Sigma-Aldrich, Merck KGaA, Darmstadt, Germany) was pre-incubated in 2% SDS in DPBS for 5 min and 30 µg of protein were applied.

2.9. Pharmacodynamic

Male C57BL/6J mice received a single oral dose of 50 mg/kg PQR530, 50 mg/kg PQR620 or vehicle (DMSO/Tween80hydroxypropyl-beta-cyclodextrin 20% in water (10:10:80)). At each of 8 time points (0 min, 5 min, 10 min, 30 min, 60 min, 120 min, 240 min, 480 min post dose) 3 animals of each group were anesthetized with isoflurane for blood sampling for PK analysis (Brandt et al., 2018). Then mice were sacrificed by inhalation of an overdose of isoflurane and brains were collected immediately and snap-frozen in halves. Brain homogenates were generated from snap frozen half brains, thawed in RIPA buffer and homogenized with a Dounce Homogenizer (Thermo Fisher Scientific, Waltham, MA, USA). Lysates were prepared as described for cells.

2.10. Statistical analysis

All data are presented as individual measurements (grey shapes) with mean and standard deviation (SD). Statistical analysis was performed with GraphPad Prism 6.00 for Windows (GraphPad Software, Inc). Comparison of two groups was performed with unpaired, two-tailed *t*-test. Comparison of multiple treatments was performed by One-way/Two-way ANOVA, with multiple comparison correction (Dunnett's). Where normalization between independent experiments was necessary, values were normalised to rapamycin, which was excluded from the ANOVA in these cases. Significance level, α , was set to 0.05.

3. Results

3.1. PQR530 and PQR620 potently block PI3K/mTOR and mTOR target phosphorylation in neuronal cells

In situations of ample nutrients and amino acids, mTOR constitutively phosphorylates several targets in the PI3K/mTOR cascade to drive protein biosynthesis and cell proliferation. S6RP and 4E-BP1 are well studied effector proteins in this cascade and mTOR inhibition at the catalytic site results in the dephosphorylation of these kinase targets. They were used in this study to monitor the target coverage of the compounds. *STHdh* cell lines were chosen based on their striatal origin and the full-length huntingtin they express. In both striatal cell lines, PQR530 and PQR620 were tested at different concentrations, each, determined in previous experiments (Supplementary material: Fig. S1 (a)). Concentrations were chosen, which inhibited S6RP phosphorylation and elevated LC3B-II levels. Control substances, namely, rapamycin, INK128 and vehicle (DMSO) were used to compare effects on mTOR inhibition. Fig. 1 (a) shows the results in *STHdh*^{Q111/Q111} cells. We have not directly compared any dose effects between the *STHdh*^{Q7/Q7} and *STHdh*^{Q111/Q111} cell lines, as they diverge in terms of size as well as proliferation behavior, which has been previously addressed (Singer et al., 2017). Nonetheless, in both cell lines mTOR inhibition was observed for both substances (Supplementary material: Fig. S2). Levels of P-S6RP were reduced in a dose dependent manner (quantification of Fig. 1 (a) is shown in Supplementary material: Fig. S1 (b)). Potent mTOR inhibition is confirmed by the decrease in phosphorylation levels of 4E-BP1, which was not quantified as the ratio of phosphorylated to unphosphorylated form of the protein, since total 4E-BP1 levels were

also decreased. Instead, the level of the Thr37/46 hyperphosphorylated form 4E-BP1- γ was used as an indicator. If phosphorylation is increased, the mobility of 4E-BP1 is decreased in electrophoresis (Choo et al., 2008), therefore the hyperphosphorylated form (the upper of the three bands) of the protein was used as a measure of mTOR inhibition. Both drugs decreased total and phosphorylated 4E-BP1 levels in a dose dependent manner, with reduction of phosphorylation by more than 50% in *STHdh*^{Q111/Q111} cells (Supplementary material: Fig. S1 (b)). mTOR inhibition was further assessed after 8 h of treatment. Results are shown for both cell lines (Supplementary material: Fig. S2). Since 4E-BP1 was not detectable in brain tissue, we have used S6RP phosphorylation as a measure of mTOR phosphorylation in our *in vivo* experiment (Fig. 5). For quantification of mTOR inhibition (Fig. 1 (b)) cells were pre-treated with each drug for 24 h and then treated with fresh compound supplemented medium for another 4 h at a concentration of 1230 nM, which allows analysis of induction of autophagy, as well. Quantification of mTOR (Ser2448) levels in *STHdh*^{Q111/Q111} cells revealed a reduction of mTOR phosphorylation after treatment with both substances in comparison to DMSO, which can be a result of PI3K inhibition in the case of PQR530. In line with this, the same trends for decreased mTOR phosphorylation upon treatment with rapamycin and INK128 where observed (Fig. 1 (a)). Reduction of mTOR phosphorylation has been further described for rapamycin treatment by affecting p70S6K (Chiang and Abraham, 2005). P-p70S6K was reduced in the MSD assay after treatment with PQR compounds or comparator compounds (Supplementary material: Fig. S3). Both compounds also decreased S6RP phosphorylation at Ser235/236 by more than 50% at 1230 nM, suggesting a potent mTOR inhibition (Fig. 1 (a)). Bafilomycin A1 treatment had no effect on protein or phosphorylation levels of mTOR and S6RP (Fig. 1b). Inhibition of PI3K/mTOR signaling was further confirmed by an MSD assay in the transiently transfected HEK293T cell model, overexpressing HTT-Exon1 fragments (Fig. 1 (c)). The MSD AKT signaling panel showed strong reduction of P-AKT (Fig. 1 (c)), P-p70S6K and P-S6RP (Supplementary material: Fig. S3) for both drugs. AKT levels were affected by Bafilomycin A1 treatment. PQR530 additionally showed a reduction of P-GSK-3 β levels that was comparable to the control substance INK128 (Fig. 1 (c)). The results in Q49 and Q20 transfected cells were comparable.

3.2. PQR530 and PQR620 induce autophagy in *STHdh*^{Q111/Q111} cells

Inhibition of mTOR leads to the induction of autophagy. ATG proteins are recruited to form the autophagosomal membrane, which is decorated with the lipidated form, LC3B-II, of LC3B-I. p62 binds to HTT and other targets of autophagosomal degradation and directs the cargo to the forming autophagosome. Both, LC3B-II and p62, were used to determine the potential of PQR620 and PQR530 in inducing autophagy. LC3B-II was assessed in an autophagic flux assay, in which Bafilomycin A1 is used to block the fusion of autophagosomes and lysosomes and the acidification of the lysosomes. Therefore, late autophagosomes accumulate. Samples treated with Bafilomycin A1 show stronger increases in LC3B-II levels, when there are more autophagosomes forming upon induction of autophagy. Fig. 2 (a) shows the comparison of different concentrations with positive (rapamycin, INK128) and vehicle control in both *STHdh* cell lines. From these qualitative blots (Fig. 2 (a)) no concentration dependence became apparent. For quantification of LC3B-II and p62, samples were pre-incubated with mTOR inhibitors at 1230 nM for 24 h and were treated with Bafilomycin A1 for the autophagic flux assay for additional 4 h with fresh compound solution (Fig. 2 (b)). After 4 h the induction of autophagy should peak and side effects of Bafilomycin A1 should be less drastic. LC3B-II levels were increased with PQR530 but not statistically significant, whereas p62 levels in samples without Bafilomycin A1 were decreased, arguing for degradation in the autophagolysosomes. PQR620 showed elevated LC3B-II levels and a non-significant tendency to decreased p62 levels.

In HEK293T cells, LC3B-II levels and p62 levels were further

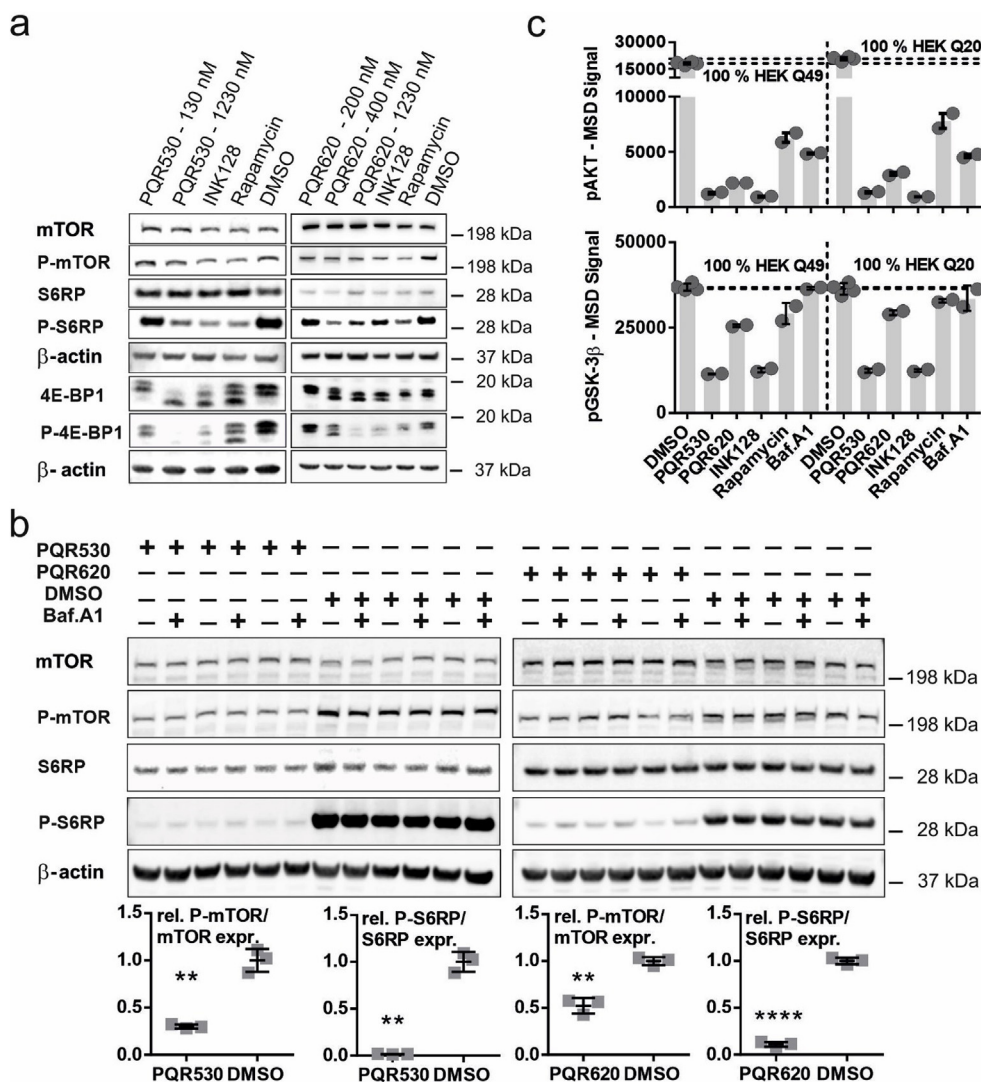


Fig. 1. PQR530 and PQR620 potentially block PI3K/mTOR and mTOR target phosphorylation. (a) representative western blots of mTOR and its targets after 24 h of treatment with PQR compounds, INK128 (100 nM), rapamycin (400 nM) and vehicle in *STHdh*^{Q111/Q111} cells. Protein levels relative to β -actin from three independent blots are shown in Supplementary material: Fig. S1(a). (b) Western blot analysis of mTOR and S6RP phosphorylation in *STHdh*^{Q111/Q111} cells after 24 h + 4 h of treatment. 3 replicates of either 1230 nM PQR530 or PQR620 were compared to vehicle. Protein levels are expressed relative to β -actin and as the ratio of phospho (P-) to total protein. BafilomycinA1 (Baf.A1) treated samples were not quantified. Unpaired, two-tailed *t*-test; PQR530-P-mTOR: ***p* = 0.0083; PQR530-P-S6RP: ***p* = 0.0039, PQR620-P-mTOR: ***p* = 0.0031; PQR620-P-S6RP: *****p* < 0.0001. (c) results of MSD Akt Signaling Panel II Whole Cell Lysate Kit for P-AKT and P-GSK-3 β levels from 2 technical replicates for transiently transfected HEK293T cells expressing either 49Q or 20Q. Cells were treated with 3 μ M of PQR530 and PQR620, 100 nM rapamycin and 3 μ M INK128. Grey circles represent technical duplicates.

analyzed by TR-FRET (Supplementary material: Fig. S4 (a)). Here, protein level reduction was compared to positive control, DMSO or Bafilomycin A1 treated samples, after 24 h of treatment. Bafilomycin A1 was added to one sample to demonstrate the increase of autophagosomes over time, excluding a deficit in autophagosome formation in the transiently transfected cells. A decrease of LC3B-II and p62 protein levels can be a further hint for increased autophagy, as it can be interpreted as an increase in lysosomal degradation of both proteins. Both assays showed a reduction of markers, comparable to INK128 in Q20 and Q49 transfected cells upon treatment with PQR530. PQR620 showed, comparable to rapamycin, a less prominent reduction of either protein marker. To further analyze the mTOR dependent effect, transcription factor EB (TFEB) localization was analyzed in HEK cells, transfected with GFP tagged TFEB (Fig. 2 (c)). Ferguson et al. have shown that ATP competitive inhibition of mTOR leads to the translocation of TFEB to the nucleus (Rocznik-Ferguson et al., 2012) and TFEB is considered a master regulator of lysosomal and autophagosomal genes (Settembre et al., 2011). DMSO treated cells showed mostly only cytoplasmic or nuclear TFEB signal that was equal to the cytoplasmic levels. With both PQR compounds the most striking observation was that almost all nuclei showed a TFEB signal demonstrating a translocation of TFEB to the nucleus. Moreover, there was an increase in strong GFP signal in the nuclei, which was significant for PQR530.

3.3. PQR530 and PQR620 decrease protein biosynthesis and show no cytotoxicity

As lowering of protein levels can be a result of enhanced protein turnover, it can just as likely be a product of reduced protein biosynthesis. Both, PQR530 and PQR620, did in fact lower the protein biosynthesis, as determined by an AHA Alexa 488 Click-iT assay (Fig. 3 (a)). Inhibition of protein biosynthesis was significant for PQR530 and PQR620 at the highest concentration after 24 h of treatment in both cell lines. Since both drugs were developed for cancer treatment, cytotoxicity and cell viability screening in the *STHdh* cells was performed, to eliminate the possibility of cytotoxicity. The cells were differentiated into neuron-like cells, as described before (Trettel et al., 2000) and immediately treated with the compounds and controls. The PrestoBlue[®] assay showed increased cell viability in both cell lines with the lower concentration of each substance after 72 h of treatment (Fig. 3 (b)). In contrast, a tendency to reduced cell viability was observed at the highest concentrations of PQR530 and PQR620 (1230 nM) in *STHdh*^{Q7/Q7} and *STHdh*^{Q111/Q111} cells. This minor decrease in viability was accompanied, however, by a decrease in cytotoxicity in the same concentrations in *STHdh*^{Q7/Q7} cells (Fig. 3 (c)) while no other changes were observed. The reasons for the decrease in PrestoBlue[®] may be explained by the reduced protein biosynthesis, since the assay relies on the enzymatic conversion in the mitochondria, which might be influenced by the reduction in protein biosynthesis. It could also be an effect of

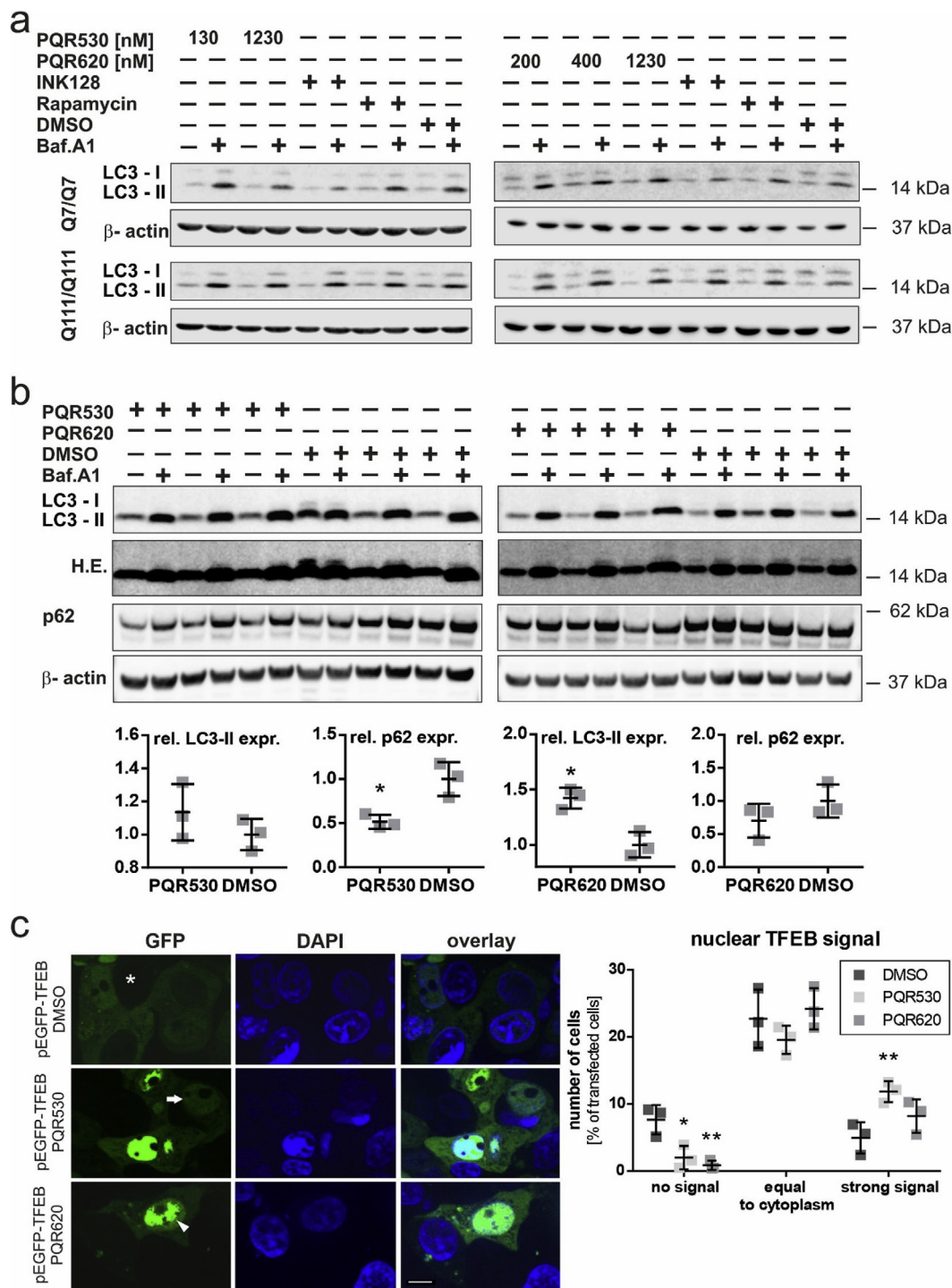


Fig. 2. PQR530 and PQR620 induce autophagy in *STHdh*^{Q111/Q111} cells (a) Western blot analysis of LC3B-II in an autophagic flux assay at different concentrations after 4 h of treatment with control substances. (b) Results of Western blot analysis of *STHdh*^{Q111/Q111} cells after 24 h + 4 h treatment with 1230 nM of PQR530 or PQR620. Protein levels of LC3B-II, from Baf.A1 treated samples, and p62, quantified from Baf.A1 untreated samples, are given relative to β-actin. H.E. = high exposure to detect LC3-I levels. Unpaired, two-tailed t-test; PQR530-p62: **p* = 0.0347; PQR620-LC3-II: ***p* = 0.0085. (c) Overexpression of pEGFP-N1-TFEB in HEK293T cells. Exemplary images and quantification of nuclear TFEB signal is shown. Asterisk = no signal in nucleus; arrow = signal, equal to cytoplasmic signal; arrowhead = strong nuclear signal. Cells were treated with PQR compounds 48 h post transfection for 1 h. Two-way ANOVA with multiple comparisons against DMSO and Dunnett's multiple comparison correction; *n* = 3; PQR530 – no signal **p* = 0.0226, - strong signal ***p* = 0.0061; PQR620 – no signal ***p* = 0.0067. Scale: 10 μm.

reduced proliferation, commonly observed for mTOR inhibition (Zheng and Jiang, 2015). In summary, these findings suggest unaltered cell viability and no apparent cytotoxic effects of these compounds on *STHdh* cells.

3.4. PQR530 and PQR620 reduce the levels of HTT in cell models of HD

A pathological hallmark of HD is the accumulation and aggregation of mHTT. The accumulation is a sequential process of protein malformation, proteofibril formation and oligomerization, which can form

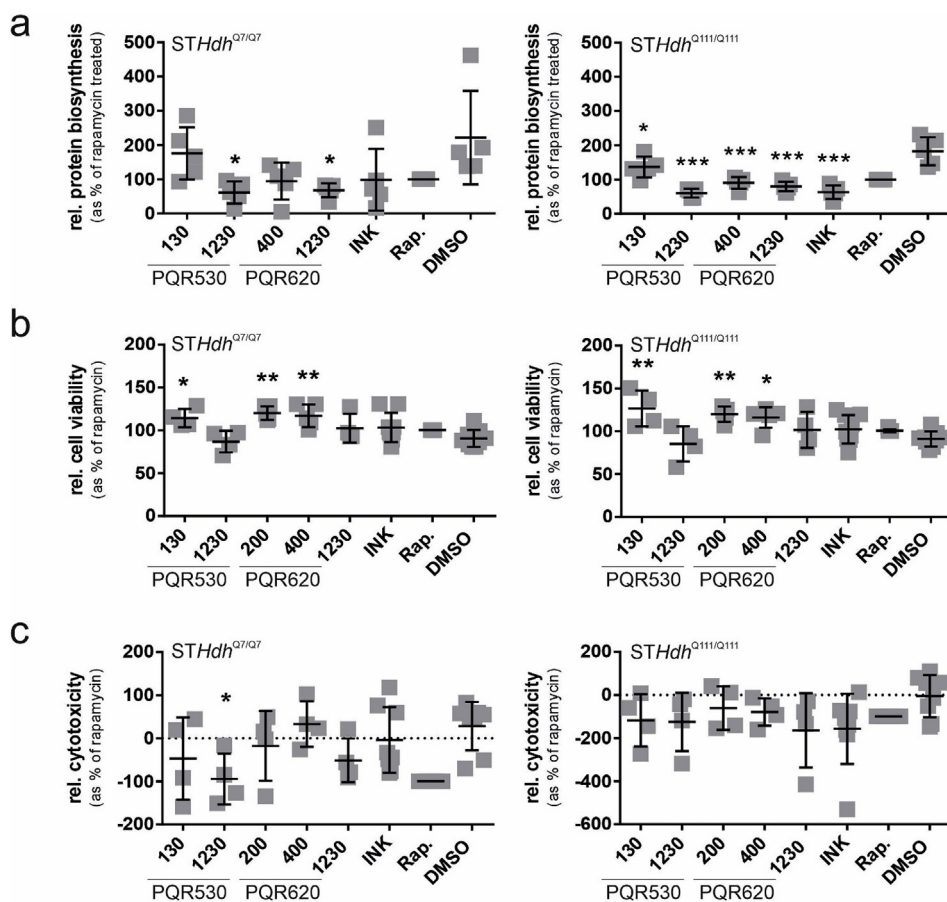


Fig. 3. PQR530 and PQR620 decrease protein biosynthesis and show no cytotoxicity (a) results of AHA Alexa488 Click it assay in *STHdh*^{Q7/Q7} (left) and *STHdh*^{Q111/Q111} cells (right) after 72 h of treatment, cells were differentiated. Values are shown relative to rapamycin treated cells. Rapamycin was excluded from One-way ANOVA with multiple comparisons against DMSO and Dunnett's multiple comparison correction; $n = 5$. *STHdh*^{Q7/Q7}: PQR530-1230 * $p = 0.015$; PQR620-1230 * $p = 0.0201$; *STHdh*^{Q111/Q111}: PQR530-130 ** $p = 0.0071$, *** $p < 0.001$ (b) cell viability analysis of both cell lines with PrestoBlue® assay. Values are shown relative to rapamycin treated cells. Rapamycin was excluded from One-way ANOVA with multiple comparisons against DMSO and Dunnett's multiple comparison correction; $n = 4$, results from PQR530 and PQR620 testing are plotted combined; *STHdh*^{Q7/Q7}: PQR530-130 * $p = 0.0258$, PQR620 - 200 ** $p = 0.0017$, - 400 ** $p = 0.0057$. *STHdh*^{Q111/Q111}: PQR530-130 ** $p = 0.0026$, PQR620 - 200 ** $p = 0.0092$, - 400 * $p = 0.0285$. (c) Measurement of cytotoxicity in form of LDH release in both cell lines with LDH assay. Values are shown relative to rapamycin treated cells. Rapamycin was excluded from One-way ANOVA with multiple comparisons against DMSO and Dunnett's multiple comparison correction; $n = 4$, results from PQR530 and PQR620 testing are plotted combined. PQR530-1230 * $p = 0.0402$.

dense protein aggregates that accumulate in the cell body and nuclei (Ross and Tabrizi, 2011). Autophagy is believed to reduce the amount of aggregates, either by aggrephagy directly or by the reduction of the amount of soluble HTT available in the cell to form and to contribute to aggregates. Reduction of HTT levels was analyzed in *STHdh*^{Q111/Q111} cells by Western blot. As *STHdh* cells do not present aggregate formation, levels of soluble mHTT were examined. Western blot detection with D7F7 antibody showed a strong reduction of mHTT levels for PQR530, but not for PQR620 in *STHdh*^{Q111/Q111} cells (Fig. 4 (a)). PQR620 showed slight decreases in huntingtin fragments, but this was not statistically significant. The reduction in PQR530 treated samples was consistent for the full-length protein, as well as the upper fragment of huntingtin (Fig. 4 (b)).

To analyze effects on aggregation, the Exon-1 overexpression model was used to confirm that reduction of protein synthesis and increase in autophagy leads to less aggregation. HEK293T cells were transiently transfected with a GFP-tagged fragment of HTT Exon1 and treated for 24 h (Fig. 4 c - e, g) to evaluate the reduction of HTT and aggregate formation. First, levels of soluble mHTT in the HEK293T cell model were analyzed by TR-FRET, which further confirmed the overall reduction of HTT levels and was in line with the results in *STHdh* cells, where PQR530 had a strong effect on soluble HTT levels (Fig. 4 (c)). PQR530 reduced the levels of soluble HTT to a comparable extend as INK128. The lower concentration of PQR530 and both tested concentrations of PQR620 had similar effects as rapamycin. Detection of HTT-Exon1-Q20 was much lower, but also showed a decrease of HTT levels by treatment with PQR530 and INK128. Cells transfected with HTT-Exon1-49Q constructs exhibited aggregate formation by the end of the experiment, after 72 h. Treating the cells with either substance for 24 h before harvest/fixation led to a reduction in the amount of aggregates and total amounts of PolyQ containing proteins. Nitrocellulose membrane was chosen for detection of total levels of PolyQ containing

proteins (Fig. 4 (d)) and aggregate detection was performed with nitrocellulose acetate membrane, because of the reduced overall protein binding capacity of this membrane (Fig. 4 (d)) and were further analyzed by fluorescence microscopy (Fig. 4 (e)-(f)). The quantification of the amount of SDS insoluble proteins in filter trap assay showed that lower protein levels were retained on the nitrocellulose membrane for PQR compounds and positive controls, than in DMSO treated samples (Fig. 4 (d)). The same was found for the measurement of aggregation by this method (Fig. 4 (e)). Here, we observed reduced aggregation levels in PQR and rapamycin treated samples that were as low as the 20Q background signal. Additionally, we used 128Q and 15Q HTT constructs to model more extreme forms of aggregation (Fig. 4 (f)). The 15Q background signal was almost undetectable because of the strong signal in the 128Q transfected samples and PQR compounds reduced the PolyQ specific signal. Quantification of aggregate number in transfected cells also confirmed significant reduction of aggregate counts for PQR530 and PQR620. Efficacy of comparator compounds INK128 and rapamycin was in the same range (Fig. 4 (g)). Altogether, both substances were found to potently decrease levels of HTT aggregates, while PQR530 has been more effective in the reduction of soluble levels of the protein.

3.5. PQR530 and PQR620 hit their target in the brain

Both compounds, second generation catalytic mTOR inhibitors, have improved properties enabling them to pass the blood brain barrier more efficiently as compared to rapalogs or competitor compounds. This was demonstrated by the evaluation of mTOR target engagement in mouse brain using Western blot analyses and recently in a model of chronic epilepsy (Brandt et al., 2018; Rageot et al., 2018). C57BL6 mice were treated orally with a single dose of 50 mg/kg with one of the substances. Markers of mTOR and PI3K inhibition, S6RP- and AKT

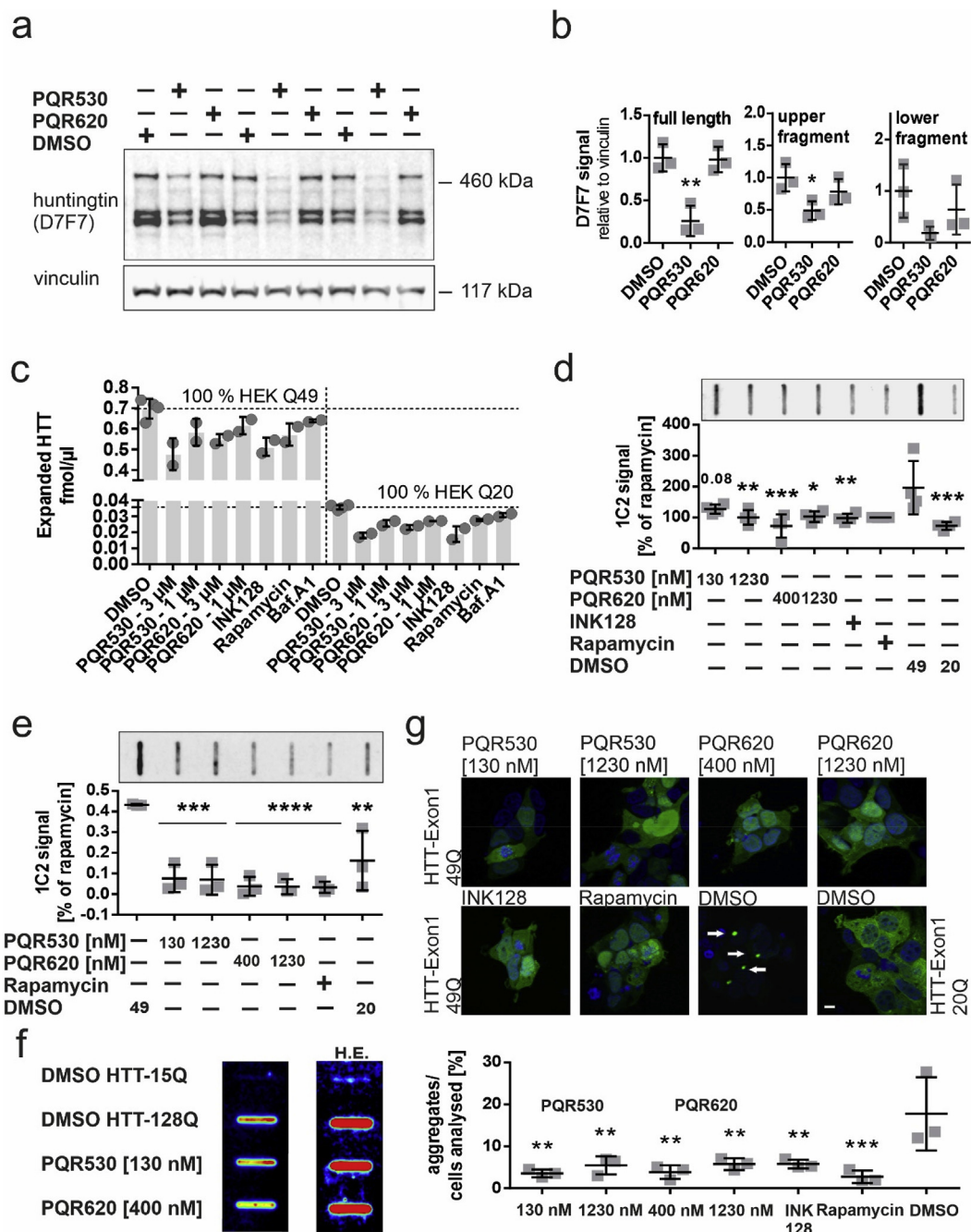


Fig. 4. PQR530 and PQR620 reduce the levels of HTT in cell models of HD (a) Western blot of HTT in *STHdh*^{Q111/Q111} cells after 48 h of treatment with PQR530 and PQR620 (1230 nM) and (b) quantification of relative HTT protein levels (D7F7) to vinculin. $n = 3$, One-way ANOVA with Dunnett's multiple comparison correction; full length $**p = 0.0028$, upper fragment $*p = 0.0342$ (c) results of TR-FRET measurements of soluble expanded HTT in HEK293T cells transfected with either 49Q or 20Q after 24 h treatment, two technical replicates. (d) total huntingtin levels - results of filter retardation assay after 24 h treatment, 1C2 signal was normalised to rapamycin treated samples, which were excluded from One-way ANOVA analysis, with Dunnett's multiple comparison against DMSO; $n = 4$, PQR530 – 1230 $**p = 0.0098$; PQR620-400 $***p = 0.0009$, -1230 $*p = 0.0121$, INK128 $**p = 0.008$, DMSO-20Q $***p = 0.001$, $**P < 0.01$ (e) aggregated huntingtin levels - results of filter retardation assay after 24 h treatment, One-way ANOVA analysis, with Dunnett's multiple comparison against DMSO 49Q; $n = 3$, PQR530 $***p = 0.0001$, PQR620 $****p < 0.0001$, DMSO-20Q $**p = 0.0017$ (f) aggregated huntingtin levels after 24 h treatment. 128Q HTT and 15Q control constructs were used for transfection. High exposure (H.E.) for detection of 15Q-HTT signal, red colour equals strong signal (g) fluorescence imaging of HTT-Exon1-49Q/20Q transfected HEK293T cells. Scale: 10 μ m; and quantification of aggregates. Cells were treated for 24 h after 48 h of transfection; ratio of aggregates per transfected cells in 30 fields of view were analyzed manually; One-way ANOVA analysis, with Dunnett's multiple comparison against DMSO; $n = 3$; PQR530-130 $**p = 0.0012$, -1230 $**p = 0.0043$; PQR620-400 $**p = 0.0015$, -1230 $**p = 0.0052$; INK $**p = 0.0052$, Rapamycin $***p = 0.0008$. (For interpretation of the references to colour in this figure legend, the reader is referred to the Web version of this article.)

phosphorylation, as well as autophagic markers, LC3B-II and p62 were analyzed (Fig. 5). PQR530 (Fig. 5 (a) and (b)) showed excellent inhibition of S6RP (Ser235/236) phosphorylation, as soon as half an hour after drug administration. The same trend was observed for AKT

(Ser473) phosphorylation, although not reaching statistical significance. p62 levels peaked first at 0.5 h before the levels decreased to a significant extent at 8 h post treatment LC3B-II levels showed more variance with a tendency to an increase between 0.5 and 8 h after

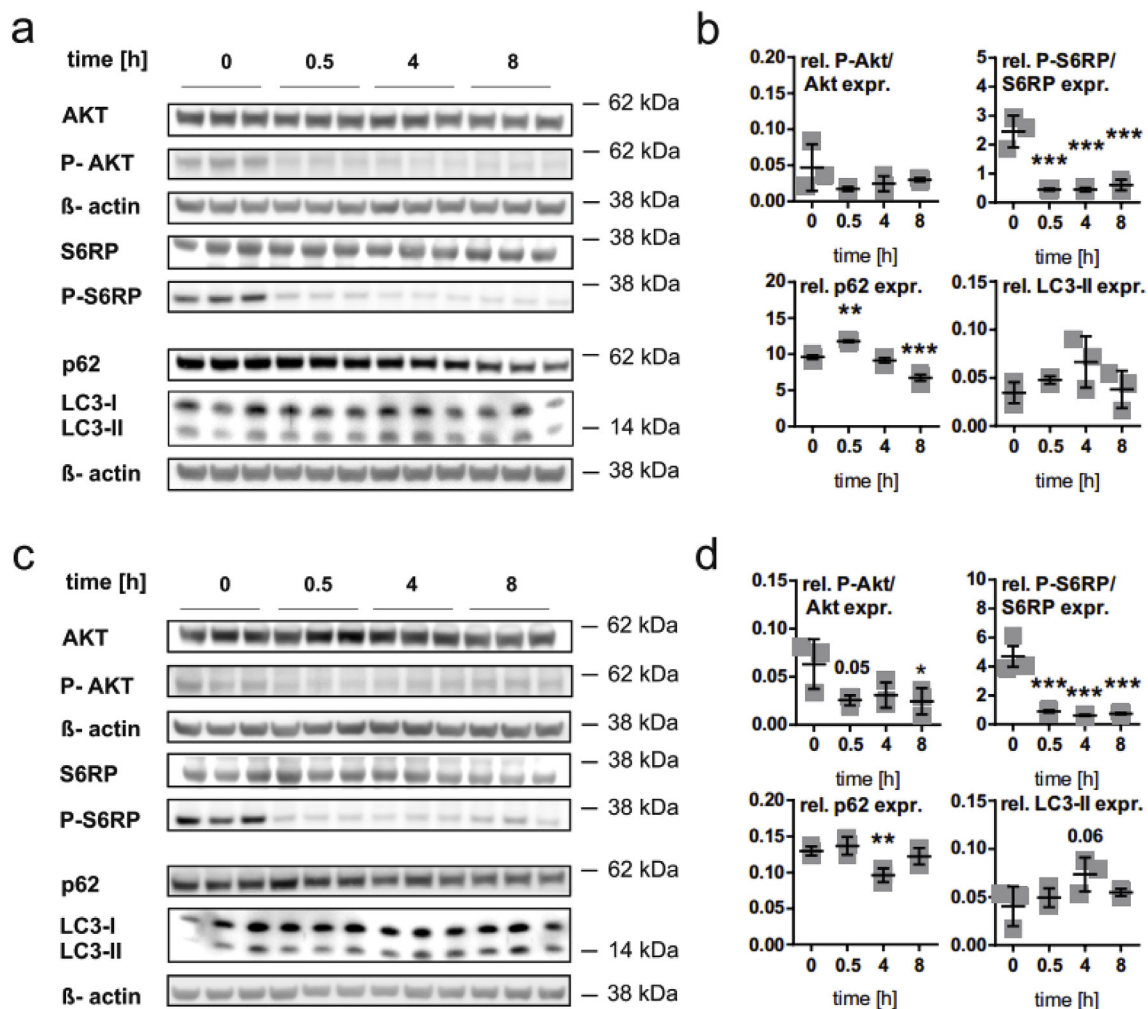


Fig. 5. PQR530 and PQR620 cover their target in brain (a) Western blot of mTOR and PI3K targets in brain lysates from C57/BL6 mice treated with PQR530 for up to 8 h and (b) quantification of relative protein levels to β-actin. $n = 3$, One-way ANOVA with Dunnett's multiple comparison correction; P-S6RP: 0.5 h, 4 h, 8 h $***p < 0.001$; p62: 0.5 h $**p = 0.0024$, 8 h $***p = 0.0004$. (c) Western blot of mTOR and PI3K targets in brain lysates from C57/B6 mice treated with PQR620 for up to 8 h and (d) quantification of relative protein levels to β-actin. $n = 3$, One-way ANOVA with Dunnett's multiple comparison correction; P-Akt: 8 h $*p = 0.047$; P-S6RP: 0.5 h, 4 h, 8 h $***p < 0.001$; p62: 4 h $**p = 0.0092$.

treatment. Levels of AKT (Ser473) and S6RP (Ser235/236) were reduced as well upon treatment with PQR620 (Fig. 5 (c) and (d)), starting from 0.5 h post treatment. p62 levels dropped at 4 h and recovered by 8 h post treatment. This drop in p62 levels was accompanied by an increase in LC3B-II levels at the same time point – indicating induction of autophagy in the brain.

4. Discussion

The inhibition of mTOR has been shown to alleviate HD pathology in *in vivo* models (Ravikumar et al., 2004). The same was found for other neurodegenerative disorders that are characterized by protein misfolding and accumulation (Menzies, 2010; Santini et al., 2009; Spilman et al., 2010). However, the compounds used for these experiments did only show limited bioavailability and were not administered orally. We found both ATP site directed inhibitors, PQR530 and PQR620, to lower huntingtin levels in cell models of Huntington disease. The substances showed target specificity and reduced protein biosynthesis, while autophagy was induced. Most importantly, oral administration of the compounds led to target inhibition in mouse brain, comparable to the effects observed in cell culture experiments. Reducing the levels of HTT or other PolyQ species has been reported to be achieved by mTOR inhibitors via the induction of autophagy

(Pandey et al., 2007; Ravikumar et al., 2002, 2004) or by the reduction of protein synthesis (King et al., 2008). Consistent with this we have found both pathways to be affected; protein biosynthesis was reduced, whereas autophagy was activated. We have not further investigated the contribution of each mechanism, as both will contribute to the reduction of Huntingtin protein levels and are well described for mTOR inhibitors (reviewed in Laplante and Sabatini, 2012 (Laplante and Sabatini, 2012)). The possibility to eliminate HTT from the adult CNS has recently been demonstrated (Grondin et al., 2012; Wang et al., 2016) and targeted therapies against HTT based on lowering the level of the protein mediated by anti-sense oligonucleotides (Kordasiewicz et al., 2012) have shown great potential, although many questions such as optimal delivery and distribution in the brain still need to be investigated (Wild and Tabrizi, 2017). Treatment with mTOR inhibitors will not lead to a specific reduction of HTT but nevertheless mTOR inhibition remains a promising treatment strategy. PQR530 and PQR620 outdo previous catalytic mTOR inhibitors in specificity and most importantly penetration over the blood brain barrier. Therefore, they are valuable tools to further investigate the contribution of mTOR signaling in the pathogenesis and potentially in treatment of HD. For this, several questions need to be addressed:

4.1. Is mTOR the right target?

mTOR hyperactivation has been described for HD models (Pryor et al., 2014), suggesting a contribution in the pathogenesis. This however is controversial, as decreased mTOR activity has been observed in patients and reinstating mTOR activity through Rheb was beneficial for HD models (Child et al., 2018; Lee et al., 2015). Increased autophagy has been observed in HD patients and models (Heng et al., 2010; Kegel et al., 2000; Martinez-Vicente et al., 2010), as well as other models of neurodegeneration (Nixon et al., 2005; Stefanis et al., 2001; Wang et al., 2006). An increase in autophagy in this disease context can be interpreted as a form of early stress response against proteotoxicity and ROS induced damage (Giordano et al., 2014). One possible explanation of these contradictory findings was provided by the observation that mTOR is sequestered in HTT aggregates, resulting in lower soluble mTOR protein levels and increased autophagy (Ravikumar et al., 2004; Sarkar and Rubinsztein, 2008). In line with this, HD cell models without aggregation of mHTT show higher levels of mTOR protein levels and activity (Walter et al., 2016). Moreover HTT itself is involved in the induction of selective autophagy (Rui et al., 2015a) and shares structural similarities with several ATG proteins (Ochaba et al., 2014; Steffan, 2010), highlighting the complex spatial and temporal relationship between the mTOR signaling cascade and the mHTT related aggregation and protein malfunction (Martin et al., 2015). Induction of macro-autophagy and therefore in-bulk cytoplasmic degradation can be achieved via modulation of the mTOR signaling cascade, either through starvation (Ehrnhoefer et al., 2017) or through pharmacological inhibition of mTOR, which has been proven effective before (Ravikumar et al., 2004; Santini et al., 2009; Spilman et al., 2010). But mTOR inhibition by catalytic inhibitors will not only affect HTT levels modulated by autophagy. This becomes obvious by the observed inhibition of protein biosynthesis. The question remains whether this approach is too close to be cracking a nut with a sledgehammer in regard of mTOR's crucial signaling functions in the cell (reviewed in (Laplante and Sabatini, 2009)). Early experiments have shown that the inhibition of protein biosynthesis leads to deficits in learning and memory formation (Alberini, 2008). In our experiments the block in protein biosynthesis was significant at 1.2 μM after 24 h. In future experiments it will be necessary to further address the question how persistent the inhibitory effect will be upon long-term treatment. So far, our findings and previous pre-clinical studies on both compounds suggest that positive effects might prevail. The substances have not shown severe signs of toxicity in GLP toxicology testing (Hillmann et al., 2017; Tarantelli et al., 2016). Similarly, compounds are not cytotoxic but rather cytostatic in a genotype independent manner, as expected for inhibitors of the PI3K/mTOR pathway. Moreover, the inhibition of protein biosynthesis could contribute to the reduction of HTT protein levels and additionally reduce mHTT mRNA levels, which have been attributed toxicity as well (Nalavade et al., 2013). mTOR modulation will be only beneficial, if the potential of transcriptional upregulation of autophagy related proteins is not exhausted. For example, declining beclin1 levels with age have been described, which were found to contribute to declining quality control in brain (Shibata et al., 2006) and will have to be considered for the right window of intervention. The more favorable tolerability of PQR620 in preclinical testing, particularly in terms of hyperglycemia – a class effect of PI3K inhibitors - might allow for maintaining life quality during the healthy life span or a prolonged treatment phase. In different mouse models treatment with rapamycin late in life was still sufficient to elongate lifespan (Harrison, 2009). mTOR inhibition most likely cannot be a continuous treatment form, because of the systemic effects. The immune suppression induced by rapalogs has made long term treatments difficult. On other, non-brain penetrant, catalytic inhibitors (e.g. AZD2014, PP242), less intense immunosuppression has been reported in first clinical trials (Fantus et al., 2017; Janes et al., 2010). From studies performed so far, it remains elusive whether a HTT holiday, a term coined by Carl Johnson in the

context of prolonged beneficial effects in ASOs therapy (Lu and Yang, 2012), could also be achieved by mTOR inhibition. In cell culture HTT lowering with PQR530 was very efficient, but long-term treatment effects, like inflammation need to be considered for the translation to *in vivo* models (Fruman et al., 2017). It will be interesting to see, whether a reduction of HTT protein levels by mTOR inhibitors for a short timeframe, will be sufficiently effective to prolong the healthy life span of HD models or to ameliorate disease symptoms, later in disease progression. Ultimately, this leaves both substances valuable for further elucidation of the complex interaction of mTOR and HTT (Martin et al., 2015; Rui et al., 2015a, 2015b), as well as the interaction of protein biosynthesis and degradation pathways.

4.2. Which of both substances is better suited for HD?

Both substances inhibit mTOR at the ATP directed site with high selectivity over other kinases. PQR530 additionally targets all isoforms of PI3K. The finding that it was still effective in the induction of autophagy is in part unexpected, because from literature the induction of autophagy by PI3K inhibitors is controversial. Wortmannin, a commonly used PI3K inhibitor, was used as a control for autophagy inhibition at the level of induction of autophagy (Blommaert et al., 1997). However, it has been shown, that this does not represent the full picture of the mechanism of action for PI3K inhibition (Benito-Cuesta et al., 2017). In our study we found further evidence that PI3K/mTOR inhibition can lead to the induction of autophagy, which is most likely time and concentration dependent. In our case, the induction of autophagy was observed after 4 h of treatment, with the same tendencies in brain tissue. Another important point is PI3K inhibition affecting AKT phosphorylation and subsequent activation. AKT plays a pivotal role in cell survival (Carloni et al., 2010; Downward, 1998; Dudek et al., 1997; Edinger and Thompson, 2002; Liu et al., 2006) and is therefore of special interest in cancer therapy. Inhibiting PI3K will decrease phosphorylation levels of AKT. AKT has been shown to be higher expressed and more active in HD models (Gines et al., 2003). However, genetic studies have shown that ablation of AKT results in increased apoptosis, whereas a drastic reduction of AKT activity is needed for this effect (Liu et al., 2006). Whilst this effect is desirable in cancer treatment, it remains unclear to what extent this might affect HD related complications. In neurodegenerative storage disease AKT inhibition by trehalose led to mTOR independent cellular clearance via transcription factor EB (TFEB) (Palmieri et al., 2017), which highlights the complexity of the interconnecting signaling pathways. Also, the inhibition of GSK-3 β , which is also affected by PI3K inhibition, has been shown to have beneficial effects on neurodegeneration (Carmichael et al., 2002; Giese, 2009), especially in Alzheimer's Disease (Sereno et al., 2009). We found a reduction of GSK-3 β phosphorylation upon treatment with PQR530, but the biological implications of this event would need further examination. PQR620, which is target specific only for mTOR, blocks the signaling events of both complexes, therefore also in this case AKT phosphorylation is decreased. Prolonged rapamycin treatment had surprisingly similar effects on AKT phosphorylation in cell culture (Sarbasov, 2006), through the signaling of mTORC2 (Bove et al., 2011). The effects of AKT inhibition and neuronal survival will need to be further assessed *in vivo*. The *in vitro* experiments showed no obvious differences in terms of cell viability, protein biosynthesis, mTOR inhibition and aggregation formation between both compounds, except PQR530 has shown stronger effects on soluble HTT levels. Further studies are needed to elucidate the mechanisms on HTT protein level reduction by PI3K inhibition.

4.3. What conclusions can be drawn from these experiments for *in vivo* models?

Clearly, both cell models do not represent the complexity of a whole organism and have certain limitations, which have been described. On

the cell line level, *STHdh*^{Q111/Q111} cells do not present aggregation or other features that are representative of the disease stage in which most neuronal vulnerability would be expected. Regarding autophagy, on the one hand these cells are aneuploid, which by itself has been shown to affect autophagy (Stingele et al., 2013). On the other hand, *STHdh*^{Q111/Q111} cells show increased autophagy and “empty” autophagosomes, as it was described for several other HD models (Martinez-Vicente et al., 2010; Walter et al., 2016). HEK293T cells also have chromosomal anomalies and are not derived from neurons. However, the high transfection efficiency makes them valuable for the kind of screening performed in this study. On the level of the disease-causing protein we could show in both cell models, one expressing the full-length protein and one an over-expressed Exon 1 fragment with a disease relevant CAG repeat length, that mTOR inhibition with PQR530 and PQR620 was beneficial regarding HTT levels and aggregation load. In our experiments the levels of HTT were lowered to an extent becoming apparent in Western blot. This argues for in bulk degradation and protein biosynthesis blockage being efficient enough to compensate for cargo loading defects. It further needs to be clarified, that autophagy is not the primary goal of this approach, but rather the reduction of excess protein and toxic protein species feeding into the system in the first place (Ravikumar and Rubinsztein, 2006; Ross and Tabrizi, 2011), which otherwise probably would be ending up in aggregates as a storage or protective form of unwanted protein (Arrasate et al., 2004; Saudou et al., 1998). Both compounds can be used for preliminary *in vivo* experiments. However, certain pitfalls with HD models need to be considered, too. Minor dose dependent toxicity has been observed: PQR530 was influencing the insulin and blood glucose levels in rats. Whilst this would be a manageable side effect in humans, in animal models, like the R6/2 mouse, which is known to develop hyperglycemia (Hurlbert et al., 1999), this might occlude readouts. Fox et al. have shown in the R6/2 model of HD that mTOR inhibition was insufficient to rescue the pathology of this model (Fox et al., 2010). This contrasts with other studies in HD and other neurodegenerative disorders and might be explained by the detrimental phenotype these animals present. Similar precautions need to be taken for animal models, which present severe weight loss, since PQR620 and PQR530 affected weight in rats. Another important question revolves about optimal dosage, since the threshold in battling cancer and neurodegeneration might diverge.

4.4. Conclusion

In conclusion, rare diseases can benefit greatly from the potential of drugs that have originally been developed for more common disorders. In our case the overlap of neurodegeneration mechanisms and cancer was of special interest. Inhibiting mTOR leads to the induction of autophagy and further decreases cell proliferation and protein biosynthesis. This has opened the field of neurodegenerative disorders that are characterized by the accumulation of protein aggregates, which can be degraded by autophagy. An obstacle in the treatment of animal models with mTOR inhibitors has been the weak blood-brain penetrance presented by rapalogs and second generation catalytic mTOR inhibitors. The oral application of PQR620 and PQR530 allows for testing that is more comparable to the desired form of application in humans.

Data availability statement

The datasets used and/or analyzed during the current study are available from the corresponding author on reasonable request.

Declaration of competing interest

D.F. and P.H. are employees of PIQR Therapeutics. M.P.W. and D.F. are shareholders of PIQR Therapeutics. ES and CW received funding from PIQR Therapeutics.

Acknowledgements

We would like to thank Kirsten Kuhlbrodt and Frank Herrmann (Evotec AG, Hamburg, Germany) for their work on the HEK293T cell model and the MSD and TR-FRET assays.

Appendix A. Supplementary data

Supplementary data to this article can be found online at <https://doi.org/10.1016/j.neuropharm.2019.107812>.

References

- Alberini, C.M., 2008. The role of protein synthesis during the labile phases of memory: revisiting the skepticism. *Neurobiol. Learn. Mem.* 89, 234–246.
- Alirezai, M., Kiosses, W.B., Flynn, C.T., Brady, N.R., Fox, H.S., 2008. Disruption of neuronal autophagy by infected microglia results in neurodegeneration. *PLoS One* 3, e2906.
- Arrasate, M., Mitra, S., Schweitzer, E.S., Segal, M.R., Finkbeiner, S., 2004. Inclusion body formation reduces levels of mutant huntingtin and the risk of neuronal death. *Nature* 431, 805.
- Bates, G., 2003. Huntingtin aggregation and toxicity in Huntington's disease. *Lancet* 361, 1642–1644.
- Benito-Cuesta, I., Diez, H., Ordoñez, L., Wandosell, F., 2017. Assessment of autophagy in neurons and brain tissue. *Cells* 6, 25.
- Blommaert, E.F., Krause, U., Schellens, J.P., Vreeling-Sindelárová, H., Meijer, A.J., 1997. The phosphatidylinositol 3-kinase inhibitors wortmannin and LY294002 inhibit autophagy in isolated rat hepatocytes. *FEBS J.* 243, 240–246.
- Bove, J., Martinez-Vicente, M., Vila, M., 2011. Fighting neurodegeneration with rapamycin: mechanistic insights. *Nat. Rev. Neurosci.* 12, 437–452.
- Brandt, C., Hillmann, P., Noack, A., Römermann, K., Öhler, L.A., Rageot, D., Beaufile, F., Melone, A., Sele, A.M., Wymann, M.P., 2018. The novel, catalytic mTORC1/2 inhibitor PQR620 and the PI3K/mTORC1/2 inhibitor PQR530 effectively cross the blood-brain barrier and increase seizure threshold in a mouse model of chronic epilepsy. *Neuropharmacology* 140, 107–120.
- Bucciantini, M., Giannoni, E., Chiti, F., Baroni, F., Formigli, L., Zurdo, J., Taddei, N., Ramponi, G., Dobson, C.M., Stefani, M., 2002. Inherent toxicity of aggregates implies a common mechanism for protein misfolding diseases. *Nature* 416, 507.
- Carloni, S., Girelli, S., Scopa, C., Buonocore, G., Longini, M., Balduini, W., 2010. Activation of autophagy and Akt/CREB signaling play an equivalent role in the neuroprotective effect of rapamycin in neonatal hypoxia-ischemia. *Autophagy* 6, 366–377.
- Carmichael, J., Sugars, K.L., Bao, Y.P., Rubinsztein, D.C., 2002. Glycogen synthase kinase-3 β inhibitors prevent cellular polyglutamine toxicity caused by the Huntington's disease mutation. *J. Biol. Chem.* 277, 33791–33798.
- Chiang, G.G., Abraham, R.T., 2005. Phosphorylation of mammalian target of rapamycin (mTOR) at ser-2448 is mediated by p70S6 kinase. *J. Biol. Chem.* 280, 25485–25490.
- Child, D.D., Lee, J.H., Pascua, C.J., Chen, Y.H., Mas Monteyes, A., Davidson, B.L., 2018. Cardiac mTORC1 dysregulation impacts stress adaptation and survival in huntington's disease. *Cell Rep.* 23, 1020–1033.
- Choo, A.Y., Yoon, S.-O., Kim, S.G., Roux, P.P., Blenis, J., 2008. Rapamycin differentially inhibits S6ks and 4E-BP1 to mediate cell-type-specific repression of mRNA translation. *Proc. Natl. Acad. Sci.* 105, 17414–17419.
- DiFiglia, M., Sapp, E., Chase, K.O., Davies, S.W., Bates, G.P., Vonsattel, J.P., Aronin, N., 1997. Aggregation of huntingtin in neuronal intranuclear inclusions and dystrophic neurites in brain. *Science* 277, 1990–1993.
- Downward, J., 1998. Mechanisms and consequences of activation of protein kinase B/Akt. *Curr. Opin. Cell Biol.* 10, 262–267.
- Dudek, H., Datta, S.R., Franke, T.F., Birnbaum, M.J., Yao, R., Cooper, G.M., Segal, R.A., Kaplan, D.R., Greenberg, M.E., 1997. Regulation of neuronal survival by the serine-threonine protein kinase Akt. *Science* 275, 661.
- Duennwald, M.L., Jagadish, S., Giorgini, F., Muchowski, P.J., Lindquist, S., 2006. A network of protein interactions determines polyglutamine toxicity. *Proc. Natl. Acad. Sci. U.S.A.* 103, 11051–11056.
- Edinger, A.L., Thompson, C.B., 2002. Akt maintains cell size and survival by increasing mTOR-dependent nutrient uptake. *Mol. Biol. Cell* 13, 2276–2288.
- Ehrnhoefer, D.E., Martin, D.D., Qiu, X., Ladha, S., Caron, N.S., Skotte, N.H., Nguyen, Y.T., Engemann, S., Franciosi, S., Hayden, M.R., 2017. Feeding Schedule and Proteolysis Regulate Autophagic Clearance of Mutant Huntingtin. *bioRxiv*.
- Ehrnhoefer, D.E., Sutton, L., Hayden, M.R., 2011. Small changes, big impact: post-translational modifications and function of huntingtin in Huntington disease. *The Neuroscientist* 17, 475–492.
- Fantus, D., Dai, H., Ono, Y., Watson, A., Yokota, S., Mohib, K., Yoshida, O., Ross, M.A., Watkins, S.C., Ramaswami, B., 2017. Influence of the novel ATP-competitive dual mTORC1/2 inhibitor AZD2014 on immune cell populations and heart allograft rejection. *Transplantation* 101, 2830–2840.
- Feldman, M.E., 2009. Active-site inhibitors of mTOR target rapamycin-resistant outputs of mTORC1 and mTORC2. *PLoS Biol.* 7, e38.
- Fox, J.H., Connor, T., Chopra, V., Dorsey, K., Kama, J.A., Bleckmann, D., Betschart, C., Hoyer, D., Frentzel, S., DiFiglia, M., 2010. The mTOR kinase inhibitor Everolimus decreases S6 kinase phosphorylation but fails to reduce mutant huntingtin levels in brain and is not neuroprotective in the R6/2 mouse model of Huntington's disease.

- Mol. Neurodegener. 5.
- Fruman, D.A., Chiu, H., Hopkins, B.D., Bagrodia, S., Cantley, L.C., Abraham, R.T., 2017. The PI3K pathway in human disease. *Cell* 170, 605–635.
- Giese, K.P., 2009. GSK-3: a key player in neurodegeneration and memory. *IUBMB Life* 61, 516–521.
- Gines, S., Ivanova, E., Seong, I.S., Saura, C.A., MacDonald, M.E., 2003. Enhanced Akt signaling is an early pro-survival response that reflects N-methyl-D-aspartate receptor activation in Huntington's disease knock-in striatal cells. *J. Biol. Chem.* 278, 50514–50522.
- Giordano, S., Darley-Usmar, V., Zhang, J., 2014. Autophagy as an essential cellular antioxidant pathway in neurodegenerative disease. *Redox Biology* 2, 82–90.
- Grondin, R., Kaytor, M.D., Ai, Y., Nelson, P.T., Thakker, D.R., Heisel, J., Weatherspoon, M.R., Blum, J.L., Burright, E.N., Zhang, Z., Kaemmerer, W.F., 2012. Six-month partial suppression of Huntingtin is well tolerated in the adult rhesus striatum. *Brain* 135, 1197–1209.
- Hara, T., 2006. Suppression of basal autophagy in neural cells causes neurodegenerative disease in mice. *Nature* 441, 885–889.
- Harrison, D.E., 2009. Rapamycin fed late in life extends lifespan in genetically heterogeneous mice. *Nature* 460, 392–395.
- Hashimoto, M., Rockenstein, E., Crews, L., Masliah, E., 2003. Role of protein aggregation in mitochondrial dysfunction and neurodegeneration in Alzheimer's and Parkinson's diseases. *NeuroMolecular Med.* 4, 21–35.
- Heng, M.Y., Duong, D.K., Albin, R.L., Tallaksen-Greene, S.J., Hunter, J.M., Lesort, M.J., 2010. Early autophagic response in a novel knock-in model of Huntington disease. *Hum. Mol. Genet.* 19.
- Hillmann, P., Rageot, D., Beaufils, F., Melone, A., Sele, A., Ettlin, R.A., Mestan, J., Cmilianovic, V., Lang, M., Singer, E., Walter, C., Nguyen, H.H., Hebeisen, P., Wymann, M.P., Fabbro, D., 2017. Abstract 159: pharmacological characterization of the selective, orally bioavailable, potent dual PI3K/mTORC1/2 inhibitor PQR530. *Cancer Res.* 77 159-159.
- Hurlbert, M.S., Zhou, W., Wasmeier, C., Kaddis, F.G., Hutton, J.C., Freed, C.R., 1999. Mice transgenic for an expanded CAG repeat in the Huntington's disease gene develop diabetes. *Diabetes* 48, 649–651.
- Jana, N.R., Zemskov, E.A., Wang, G.-h., Nukina, N., 2001. Altered proteasomal function due to the expression of polyglutamine-expanded truncated N-terminal huntingtin induces apoptosis by caspase activation through mitochondrial cytochrome c release. *Hum. Mol. Genet.* 10, 1049–1059.
- Janes, M.R., Limon, J.J., So, L., Chen, J., Lim, R.J., Chavez, M.A., Vu, C., Lilly, M.B., Mallya, S., Ong, S.T., 2010. Effective and selective targeting of leukemia cells using a TORC1/2 kinase inhibitor. *Nat. Med.* 16, 205.
- Kaganovich, D., Kopito, R., Frydman, J., 2008. Misfolded proteins partition between two distinct quality control compartments. *Nature* 454, 1088–1095.
- Kegel, K.B., Kim, M., Sapp, E., McIntyre, C., Castaño, J.G., Aronin, N., DiFiglia, M., 2000. Huntingtin expression stimulates endosomal-lysosomal activity, endosome tubulation, and autophagy. *J. Neurosci.* 20, 7268–7278.
- King, M.A., Hands, S., Hafiz, F., Mizushima, N., Tolkovsky, A.M., Wyttenbach, A., 2008. Rapamycin inhibits polyglutamine aggregation independently of autophagy by reducing protein synthesis. *Mol. Pharmacol.* 73, 1052–1063.
- Ko, J., Ou, S., Patterson, P.H., 2001. New anti-huntingtin monoclonal antibodies: implications for huntingtin conformation and its binding proteins. *Brain Res. Bull.* 56, 319–329.
- Komatsu, M., 2006. Loss of autophagy in the central nervous system causes neurodegeneration in mice. *Nature* 441, 880–884.
- Komatsu, M., Wang, Q.J., Holstein, G.R., Friedrich Jr., V.L., Iwata, J., Kominami, E., Chait, B.T., Tanaka, K., Yue, Z., 2007. Essential role for autophagy protein Atg7 in the maintenance of axonal homeostasis and the prevention of axonal degeneration. *Proc. Natl. Acad. Sci. U. S. A.* 104, 14489–14494.
- Kordasiewicz, Holly B., Stanek, Lisa M., Wancewicz, Edward V., Mazur, C., McAlonis, Melissa M., Pytel, Kimberly A., Artates, Jonathan W., Weiss, A., Cheng, Seng H., Shihabuddin, Lamya S., Hung, G., Bennett, C.F., Cleveland, Don W., 2012. Sustained therapeutic reversal of Huntington's disease by transient repression of huntingtin synthesis. *Neuron* 74, 1031–1044.
- Kraft, C., Peter, M., Hofmann, K., 2010. Selective autophagy: ubiquitin-mediated recognition and beyond. *Nat. Cell Biol.* 12, 836.
- Lajoie, P., Snapp, E.L., 2010. Formation and toxicity of soluble polyglutamine oligomers in living cells. *PLoS One* 5, e15245.
- Laplante, M., Sabatini, D.M., 2009. mTOR signaling at a glance. *J. Cell Sci.* 122, 3589–3594.
- Laplante, M., Sabatini, David M., 2012. mTOR signaling in growth control and disease. *Cell* 149, 274–293.
- Lee, J.H., Teecedor, L., Chen, Y.H., Monteys, A.M., Sowada, M.J., Thompson, L.M., Davidson, B.L., 2015. Reinstating aberrant mTORC1 activity in Huntington's disease mice improves disease phenotypes. *Neuron* 85, 303–315.
- Li, H., Li, S.H., Yu, Z.X., Shelbourne, P., Li, X.J., 2001. Huntingtin aggregate-associated axonal degeneration is an early pathological event in Huntington's disease mice. *J. Neurosci.* 21, 8473–8481.
- Liu, X., Shi, Y., Birnbaum, M.J., Ye, K., De Jong, R., Oltersdorf, T., Giranda, V.L., Luo, Y., 2006. Quantitative analysis of anti-apoptotic function of Akt in Akt1 and Akt2 double knock-out mouse embryonic fibroblast cells under normal and stressed conditions. *J. Biol. Chem.* 281, 31380–31388.
- Lu, X.-H., Yang, X.W., 2012. "Huntingtin holiday". Progress toward an antisense therapy for Huntington's disease. *Neuron* 74, 964–966.
- Ma, X.M., Blenis, J., 2009. Molecular mechanisms of mTOR-mediated translational control. *Nat. Rev. Mol. Cell Biol.* 10, 307–318.
- Martin, D.D.O., Ladha, S., Ehrnhoefer, D.E., Hayden, M.R., 2015. Autophagy in Huntington disease and huntingtin in autophagy. *Trends Neurosci.* 38, 26–35.
- Martinez-Vicente, M., Tallozy, Z., Wong, E., Tang, G., Koga, H., Kaushik, S., de Vries, R., Arias, E., Harris, S., Sulzer, D., Cuervo, A.M., 2010. Cargo recognition failure is responsible for inefficient autophagy in Huntington's disease. *Nat. Neurosci.* 13, 567–576.
- Menalled, L.B., 2005. Knock-in mouse models of Huntington's disease. *NeuroRx* 2, 465–470.
- Mende-Mueller, L.M., Toneff, T., Hwang, S.-R., Chesselet, M.-F., Hook, V.Y.H., 2001. Tissue-specific proteolysis of huntingtin (htt) in human brain: evidence of enhanced levels of N- and C-terminal htt fragments in Huntington's disease striatum. *J. Neurosci.* 21, 1830–1837.
- Menzies, F.M., 2010. Autophagy induction reduces mutant ataxin-3 levels and toxicity in a mouse model of spinocerebellar ataxia type 3. *Brain* 133, 93–104.
- Michalik, A., Van Broeckhoven, C., 2003. Pathogenesis of polyglutamine disorders: aggregation revisited. *Hum Mol Genet* 12 Spec No 2, R173–186.
- Mizushima, N., Komatsu, M., 2011. Autophagy: renovation of cells and tissues. *Cell* 147, 728–741.
- Mizushima, N., Levine, B., Cuervo, A.M., Klionsky, D.J., 2008. Autophagy fights disease through cellular self-digestion. *Nature* 451, 1069–1075.
- Nalavade, R., Griesche, N., Ryan, D.P., Hildebrand, S., Krauß, S., 2013. Mechanisms of RNA-induced toxicity in CAG repeat disorders. *Cell Death Disease* 4, e752.
- Nance, M.A., Seltzer, W., Ashizawa, T., Bennett, R., McIntosh, N., Myers, R.H., Potter, N.T., Shea, D.K., 1998. Laboratory guidelines for Huntington disease genetic testing. *Am. J. Hum. Genet.* 62, 1243–1247.
- Nixon, R.A., Wegiel, J., Kumar, A., Yu, W.H., Peterhoff, C., Cataldo, A., Cuervo, A.M., 2005. Extensive involvement of autophagy in Alzheimer disease: an immuno-electron microscopy study. *J. Neuropathol. Exp. Neurol.* 64, 113–122.
- Ochaba, J., Lukacsovich, T., Csikos, G., Zheng, S., Margulis, J., Salazar, L., Mao, K., Lau, A.L., Yeung, S.Y., Humbert, S., 2014. Potential function for the Huntingtin protein as a scaffold for selective autophagy. *Proc. Natl. Acad. Sci.* 111, 16889–16894.
- Palmieri, M., Pal, R., Nelvagal, H.R., Lotfi, P., Stinnett, G.R., Seymour, M.L., Chaudhury, A., Bajaj, L., Bondar, V.V., Bremner, L., Saleem, U., Tse, D.Y., Sanagasetti, D., Wu, S.M., Neilson, J.R., Pereira, F.A., Pautler, R.G., Rodney, G.G., Cooper, J.D., Sardiello, M., 2017. mTORC1-independent TFEB Activation via Akt Inhibition Promotes Cellular Clearance in Neurodegenerative Storage Diseases, vol. 8. pp. 14338.
- Pandey, U.B., Nie, Z., Batlevi, Y., McCray, B.A., Ritson, G.P., Nedelsky, N.B., Schwartz, S.L., DiProspero, N.A., Knight, M.A., Schuldiner, O., Padmanabhan, R., Hild, M., Berry, D.L., Garza, D., Hubbert, C.C., Yao, T.P., Baehrecke, E.H., Taylor, J.P., 2007. HDAC6 rescues neurodegeneration and provides an essential link between autophagy and the UPS. *Nature* 447, 859–863.
- Pankiv, S., Clausen, T.H., Lamark, T., Brech, A., Bruun, J.A., Outzen, H., Overvatn, A., Bjorkoy, G., Johansen, T., 2007. p62/SQSTM1 binds directly to Atg8/LC3 to facilitate degradation of ubiquitinated protein aggregates by autophagy. *J. Biol. Chem.* 282, 24131–24145.
- Pattingre, S., Espert, L., Biard-Piechaczyk, M., Codogno, P., 2008. Regulation of macroautophagy by mTOR and Beclin 1 complexes. *Biochimie* 90, 313–323.
- Poirier, M.A., Li, H., Macosko, J., Cai, S., Amzel, M., Ross, C.A., 2002. Huntingtin spheroids and protofibrils as precursors in polyglutamine fibrilization. *J. Biol. Chem.* 277, 41032–41037.
- Pryor, W.M., Biagioli, M., Shahani, N., Swarnkar, S., Huang, W.C., Page, D.T., MacDonald, M.E., Subramaniam, S., 2014. Huntingtin promotes mTORC1 signaling in the pathogenesis of Huntington's disease. *Sci. Signal.* 7, ra103.
- Rageot, D., Beaufils, F., Melone, A., Sele, A.M., Bohnacker, T., Lang, M., Mestan, J., Hillmann, P., Hebeisen, P., Fabbro, D., Wymann, M.P., 2017. Abstract 140: discovery and biological evaluation of PQR530, a highly potent dual pan-PI3K/mTORC1/2 inhibitor. *Cancer Res.* 77 140-140.
- Rageot, D., Bohnacker, T., Melone, A., Langlois, J.-B., Borsari, C., Hillmann, P., Sele, A.M., Beaufils, F., Zvelebil, M., Hebeisen, P., Loeschner, W., Burke, J.E., Fabbro, D., Wymann, M.P., 2018. Discovery and preclinical characterization of 5-[4,6-Bis(3-oxa-8-azabicyclo[3.2.1]octan-8-yl)-1,3,5-triazin-2-yl]-4-(difluoromethyl)pyridin-2-amine (PQR620), a highly potent and selective mTORC1/2 inhibitor for cancer and neurological disorders. *J. Med. Chem.*
- Ravikumar, B., Duden, R., Rubinsztein, D.C., 2002. Aggregate-prone proteins with polyglutamine and polyalanine expansions are degraded by autophagy. *Hum. Mol. Genet.* 11.
- Ravikumar, B., Rubinsztein, D.C., 2006. Role of autophagy in the clearance of mutant huntingtin: a step towards therapy? *Mol. Asp. Med.* 27, 520–527.
- Ravikumar, B., Vacher, C., Berger, Z., Davies, J.E., Luo, S., Oroz, L.G., 2004. Inhibition of mTOR induces autophagy and reduces toxicity of polyglutamine expansions in fly and mouse models of Huntington disease. *Nat. Genet.* 36.
- Roczniak-Ferguson, A., Petit, C.S., Froehlich, F., Qian, S., Ky, J., Angarola, B., Walther, T.C., Ferguson, S.M., 2012. The transcription factor TFEB links mTORC1 signaling to transcriptional control of lysosome homeostasis. *Sci. Signal.* 5, ra42.
- Roscic, A., Baldo, B., Crochemore, C., Marcellin, D., Paganetti, P., 2011. Induction of autophagy with catalytic mTOR inhibitors reduces huntingtin aggregates in a neuronal cell model. *J. Neurochem.* 119, 398–407.
- Ross, C.A., Poirier, M.A., 2004. Protein aggregation and neurodegenerative disease. *Nat. Med.* 10, S10.
- Ross, C.A., Tabrizi, S.J., 2011. Huntington's disease: from molecular pathogenesis to clinical treatment. *Lancet Neurol.* 10, 83–98.
- Rubinsztein, D.C., 2006. The roles of intracellular protein-degradation pathways in neurodegeneration. *Nature* 443, 780–786.
- Rubinsztein, D.C., DiFiglia, M., Heintz, N., Nixon, R.A., Qin, Z.-H., Ravikumar, B., Stefanis, L., Tolkovsky, A., 2005. Autophagy and its possible roles in nervous system diseases, damage and repair. *Autophagy* 1, 11–22.
- Rui, Y.-N., Xu, Z., Patel, B., Chen, Z., Chen, D., Tito, A., 2015a. Huntingtin functions as a scaffold for selective macroautophagy. *Nat. Cell Biol.* 17.

- Rui, Y.N., Xu, Z., Patel, B., Cuervo, A.M., Zhang, S., 2015b. HTT/Huntingtin in selective autophagy and Huntington disease: a foe or a friend within? *Autophagy* 11, 858–860.
- Santini, E., Heiman, M., Greengard, P., Valjent, E., Fisone, G., 2009. Inhibition of mTOR signaling in Parkinson's disease prevents L-DOPA-induced dyskinesia. *Sci. Signal.* 2, ra36.
- Sarbasov, D.D., 2006. Prolonged rapamycin treatment inhibits mTORC2 assembly and Akt/PKB. *Mol. Cell* 22, 159–168.
- Sarkar, S., Ravikumar, B., Floto, R.A., Rubinsztein, D.C., 2009. Rapamycin and mTOR-independent autophagy inducers ameliorate toxicity of polyglutamine-expanded huntingtin and related proteinopathies. *Cell Death Differ.* 16, 46–56.
- Sarkar, S., Rubinsztein, D.C., 2008. Huntington's disease: degradation of mutant huntingtin by autophagy. *FEBS J.* 275, 4263–4270.
- Saudou, F., Finkbeiner, S., Devys, D., Greenberg, M.E., 1998. Huntingtin acts in the nucleus to induce apoptosis but death does not correlate with the formation of intranuclear inclusions. *Cell* 95, 55–66.
- Seidel, K., Meister, M., Dugbartey, G., Zijlstra, M., Vinet, J., Brunt, E., van Leeuwen, F., Rüb, U., Kampinga, H., den Dunnen, W., 2012. Cellular protein quality control and the evolution of aggregates in spinocerebellar ataxia type 3 (SCA3). *Neuropathol. Appl. Neurobiol.* 38, 548–558.
- Sereno, L., Coma, M., Rodriguez, M., Sanchez-Ferrer, P., Sanchez, M., Gich, I., Agullo, J., Perez, M., Avila, J., Guardia-Laguarta, C., 2009. A novel GSK-3 β inhibitor reduces Alzheimer's pathology and rescues neuronal loss in vivo. *Neurobiol. Dis.* 35, 359–367.
- Settembre, C., Di Malta, C., Polito, V.A., Arcimbola, M.G., Vetrini, F., Erdin, S., Erdin, S.U., Huynh, T., Medina, D., Colella, P., Sardiello, M., Rubinsztein, D.C., Ballabio, A., 2011. TFEB links autophagy to lysosomal biogenesis. *Science* 332, 1429.
- Shibata, M., Lu, T., Furuya, T., Degterev, A., Mizushima, N., Yoshimori, T., MacDonald, M., Yankner, B., Yuan, J., 2006. Regulation of intracellular accumulation of mutant huntingtin by beclin 1. *J. Biol. Chem.* 281, 14474–14485.
- Singer, E., Walter, C., Weber, J.J., Krahl, A.-C., Mau-Holzmann, U.A., Rischert, N., Riess, O., Clemensson, L.E., Nguyen, H.P., 2017. Reduced cell size, chromosomal aberration and altered proliferation rates are characteristics and confounding factors in the STHdh cell model of Huntington disease. *Sci. Rep.* 7, 16880.
- Spilman, P., Podlitskaya, N., Hart, M.J., Debnath, J., Gorostiza, O., Bredesen, D., Richardson, A., Strong, R., Galvan, V., 2010. Inhibition of mTOR by rapamycin abolishes cognitive deficits and reduces amyloid- β levels in a mouse model of Alzheimer's disease. *PLoS One* 5, e9979.
- Stefanis, L., Larsen, K.E., Rideout, H.J., Sulzer, D., Greene, L.A., 2001. Expression of A53T mutant but not wild-type α -synuclein in PC12 cells induces alterations of the ubiquitin-dependent degradation system, loss of dopamine release, and autophagic cell death. *J. Neurosci.* 21, 9549–9560.
- Steffan, J.S., 2010. Does Huntingtin play a role in selective macroautophagy? *Cell Cycle* 9, 3401–3413.
- Stingele, S., Stoehr, G., Storchova, Z., 2013. Activation of autophagy in cells with abnormal karyotype. *Autophagy* 9, 246–248.
- Tarantelli, C., Gaudio, E., Hillmann, P., Spriano, F., Rinaldi, A., Kwee, I., Cascione, L., Fabbro, D., Stathis, A., Zucca, E., 2016. The novel mTORC1/2 inhibitor PQR620 has in vitro and in vivo activity in lymphomas. *Eur. J. Cancer* 69, S38.
- Tarantelli, C., Gaudio, E., Hillmann, P., Spriano, F., Sartori, G., Aresu, L., Cascione, L., Rageot, D., Kwee, I., Beauvais, F., 2019. The novel TORC1/2 kinase inhibitor PQR620 has anti-tumor activity in lymphomas as a single agent and in combination with venetoclax. *Cancers* 11, 775.
- The Huntington's Disease Collaborative Research Group, 1993. A novel gene containing a trinucleotide repeat that is expanded and unstable on Huntington's disease chromosomes. The Huntington's Disease Collaborative Research Group. *Cell* 72, 971–983.
- Trettel, F., Rigamonti, D., Hilditch-Maguire, P., Wheeler, V.C., Sharp, A.H., Persichetti, F., Cattaneo, E., MacDonald, M.E., 2000. Dominant phenotypes produced by the HD mutation in STHdhQ111 striatal cells. *Hum. Mol. Genet.* 9, 2799–2809.
- Vonsattel, J.P., DiFiglia, M., 1998. Huntington disease. *J. Neuropathol. Exp. Neurol.* 57, 369–384.
- Walter, C., Clemens, L.E., Muller, A.J., Fallier-Becker, P., Proikas-Cezanne, T., Riess, O., Metzger, S., Nguyen, H.P., 2016. Activation of AMPK-induced autophagy ameliorates Huntington disease pathology in vitro. *Neuropharmacology* 108, 24–38.
- Wang, G., Liu, X., Gaertig, M.A., Li, S., Li, X.-J., 2016. Ablation of huntingtin in adult neurons is nondeleterious but its depletion in young mice causes acute pancreatitis. *Proc. Natl. Acad. Sci.* 113, 3359–3364.
- Wang, N., Gray, M., Lu, X.-H., Cantle, J.P., Holley, S.M., Greiner, E., Gu, X., Shirasaki, D., Cepeda, C., Li, Y., Dong, H., Levine, M.S., Yang, X.W., 2014. Neuronal targets for reducing mutant huntingtin expression to ameliorate disease in a mouse model of Huntington's disease. *Nat. Med.* 20, 536.
- Wang, Q.J., Ding, Y., Kohtz, D.S., Kohtz, S., Mizushima, N., Cristea, I.M., 2006. Induction of autophagy in axonal dystrophy and degeneration. *J. Neurosci.* 26.
- Wild, E.J., Tabrizi, S.J., 2017. Therapies targeting DNA and RNA in Huntington's disease. *Lancet Neurol.* 16, 837–847.
- Zhang, L., Yu, J., Pan, H., Hu, P., Hao, Y., Cai, W., Zhu, H., Yu, A.D., Xie, X., Ma, D., Yuan, J., 2007. Small molecule regulators of autophagy identified by an image-based high-throughput screen. *Proc. Natl. Acad. Sci.* 104, 19023–19028.
- Zheng, Y., Jiang, Y., 2015. mTOR inhibitors at a glance. *Mol. Cell. Pharmacol.* 7, 15–20.
- Zhou, H.-Y., Huang, S.-L., 2012. Current development of the second generation of mTOR inhibitors as anticancer agents. *Chin. J. Canc.* 31, 8–18.

PQR530 and PQR620 reduce aggregation in the R6/2 mouse model but fail to ameliorate behavioral phenotype

Elisabeth Singer^{1,2}, Patrycja Bambynek-Dziuk^{1,2}, Libo Yu-Taeger^{1,2}, Dorian Fabbro³, Denise Rageot⁴, Florent Beaufigli³, Olaf Riess^{1,2}, Petra Hillmann³ and Huu P. Nguyen⁵

¹ *Institute of Medical Genetics and Applied Genomics, University of Tuebingen, Calwerstrasse 7, Tuebingen, 72076, Germany*

² *Centre for Rare Diseases (ZSE), University of Tuebingen, Calwerstrasse 7, Tuebingen, 72076, Germany*

³ *PIQUR Therapeutics AG, Hochbergerstrasse 60C, Basel, 4057, Switzerland*

⁴ *Department of Biomedicine, University of Basel, Mattenstrasse 28, Basel, 4056, Switzerland*

⁵ *Department of Human Genetics, Ruhr University Bochum, Universitaetsstrasse 150, Bochum, 44801, Germany*

Emails: elisabeth.singer@med.uni-tuebingen.de (Elisabeth Singer)

ABSTRACT

One of the pathological hallmarks of Huntington disease (HD) is the accumulation of the disease-causing mutant huntingtin protein (mHTT), which leads to the disruption of a variety of cellular functions, ultimately resulting in cell death. Induction of autophagy, for example by inhibition of mTOR signaling, has been shown to reduce HTT levels and aggregates. While rapalogs like rapamycin allosterically inhibit only part of the mTOR signaling pathway, ATP-competitive mTOR inhibitors suppress all functions of the mTOR complexes C1 and C2 and have been shown to be more efficient in inducing autophagy and reducing protein levels and aggregates than rapalogs. The ability of first generation catalytic mTOR inhibitors to cross the blood-brain barrier, so far has been limited and therefore sufficient target coverage in the brain could not be reached. Two novel, brain penetrant compounds – one mTORC1/2 inhibitor (PQR620) and one dual PI3K and mTORC1/2 inhibitor (PQR530) - were evaluated by assessing their potential in inducing autophagy and reducing mHTT levels in the Huntington Disease R6/2 mouse model.

Keywords: mTOR inhibition, R6/2 mouse, HD, Huntingtin, aggregation

Introduction

Huntington Disease (HD) is a neurodegenerative, fatal, autosomal dominantly inherited disorder that affects patients in mid-life and there is currently no cure available [1]. The disorder is caused by a triplet repeat expansion in the *Huntingtin* gene [2]. This mutation alters the protein's (mutant huntingtin; mHTT) conformation [3, 4], the interaction with other proteins [5] and ultimately the biological function. The huntingtin protein has many identified biological functions and the alteration of this "component" of the various intricate and interconnected processes, leads to a plethora of dysfunctions: (I) mHTT is cleaved distinctly from the wildtype (wt) form and certain cleavage products present toxic properties [6-8], e.g. affecting calcium homeostasis [9-11]; (II) mitochondrial dysfunction is caused directly and indirectly by mHTT and leads to energy disbalance and oxidative stress [12-14]; (III) protein degradation, via the UPS and autophagy, is altered in HD and the clearance of aggregates and other protein species is inefficient [15]. One strategy to reduce the disease burden on a cellular level is to reduce the amount of mutant protein. This can be achieved either by reducing the expression of the protein itself, which can be highly specific - by ASOs or RNAi [16, 17] - or a global reduction of protein expression [18]. The other option is to increase the rate at which proteins are degraded in the cell. This has been achieved by the induction of autophagy [19-21]. There are various means to increase autophagy: calorie restriction [22, 23], overexpression of components of the autophagic machinery [24,

25] and mTOR dependent and independently acting compounds [20, 26-28], which activate autophagic clearance. The best studied autophagy activator is rapamycin, a macrolide antibiotic, which induces autophagy by inhibiting mTOR, a molecular switch in the cell between anabolic and catabolic processes. The amelioration of HD phenotypes by rapalogs, derivatives of rapamycin, has been shown to be beneficial in various animal models of this and other neurodegenerative disorders [21, 29-34]. These compounds are however hydrophobic and do not pass the blood barrier efficiently. Rapalogs inhibit mTOR by binding to FKBP12, not by binding to the catalytic site, this can lead to side effects and resistances [35]. ATP-site directed, catalytic, mTOR inhibitors have been designed with improved bioavailability, which should be more potent inhibitors with more favorable tolerability [36]. In this study two novel compounds, which have been demonstrated to ameliorate aggregation and lower HTT levels in *in vitro* models of HD, were tested [28]. PQR530 is a dual PI3K/mTOR inhibitor of all PI3K isoforms [37, 38], while PQR620 targets mTOR solely [39-42]. Both substances demonstrate high selectivity over other kinases and cross the blood brain barrier effectively [28, 43]. In this study both compounds have been tested in the R6/2 mouse model of HD. R6/2 mice are the most commonly used model in pre-clinical testing [44, 45]. They present a severe motor phenotype, a peripheral HD phenotype and neuropathological changes, e.g. in form of aggregates, as soon as post-natal day 1 and a

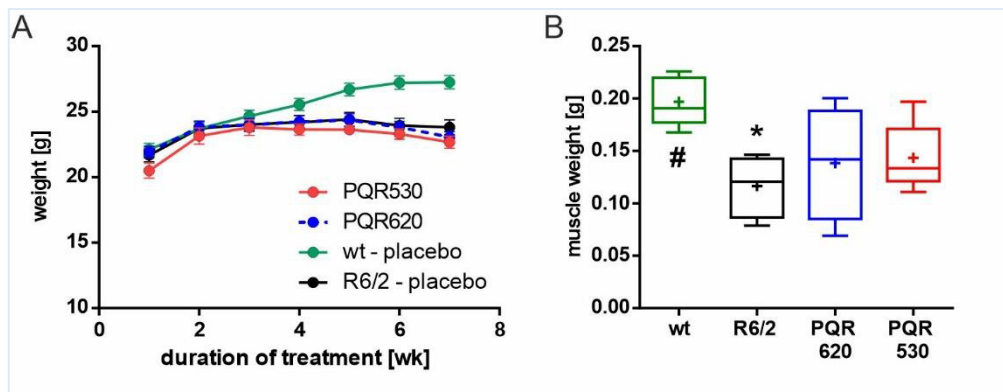


Figure 1: Effects of PQR530 and PQR620 on weight. (A) Body weight determination during the treatment phase. RM- 2way ANOVA, with Dunnett's multiple comparison correction for multiple testing. wt-placebo vs R6/2- placebo $p = 0.0249$; wt-placebo vs R6/2- PQR530 $p = 0.0019$; vs R6/2- PQR620 $p = 0.0202$ (B) muscle weight of *m. gastrocnemius* at the end of the experiment. One-way ANOVA, with Dunnett's multiple comparison correction for multiple testing: R6/2 vs. wild-type placebo* $p = 0.0123$. comparison to wt (*), comparison to placebo (#).

dramatic reduction in life span [46-50]. By treating these mice from 4 weeks of age until 12 weeks of age daily, we observed weight loss in the mice and no amelioration of the behavioral phenotype. However, we observed a reduction of mHTT aggregates, which was more prominent in PQR530 treated animals. This study is a first step to optimize treatment regimens of catalytic mTOR inhibitors in animal models of HD.

Results

PQR compounds induce weight loss and fail to rescue behavioural phenotype of R6/2 mice

R6/2 mice were treated with both compounds, to evaluate the effects on neuropathological markers and behavioral aspects. At weaning animals were separated into different treatment groups, based on genotype, litter and rotarod performance (Supplementary Figure 1). The rotarod test at this early time point was further used to familiarise the animals with the experimental set up. Body weight was measured once daily before treatment, which was performed at the same time of the day (Figure 1 A). The treatment led to an overall reduced weight gain in the treatment groups, especially

in the PQR530 group, which was not significantly different between the R6/2 treatment groups in the end of the experiment (R6/2 – placebo: $23.68 \text{ g} \pm 1.9$; R6/2 – PQR530: $22.95 \text{ g} \pm 1.5$; R6/2 – PQR620: $23.6 \text{ g} \pm 1.6$). There were also animals that experienced excessive weight loss (>15% of their maximum weight). These mice were excluded from the experiment. A relatively high fraction of the animals was susceptible to the weight loss, whereas the ones, which remained in the experiment (~ 60 %), had similar weight curves as the placebo treated, transgenic control group (Figure 1 A). Interestingly, the animals that were excluded because of weight loss, were the ones, which started the experiment with a higher body weight. Weight loss can also be an effect of muscle wasting. To assess this, muscle (*m. gastrocnemius*) was weighed. R6/2 mice show a drastic reduction of weight in comparison to wildtype animals (Figure 1 B). This difference was no longer statistically significant in the treatment groups. The mild improvement in

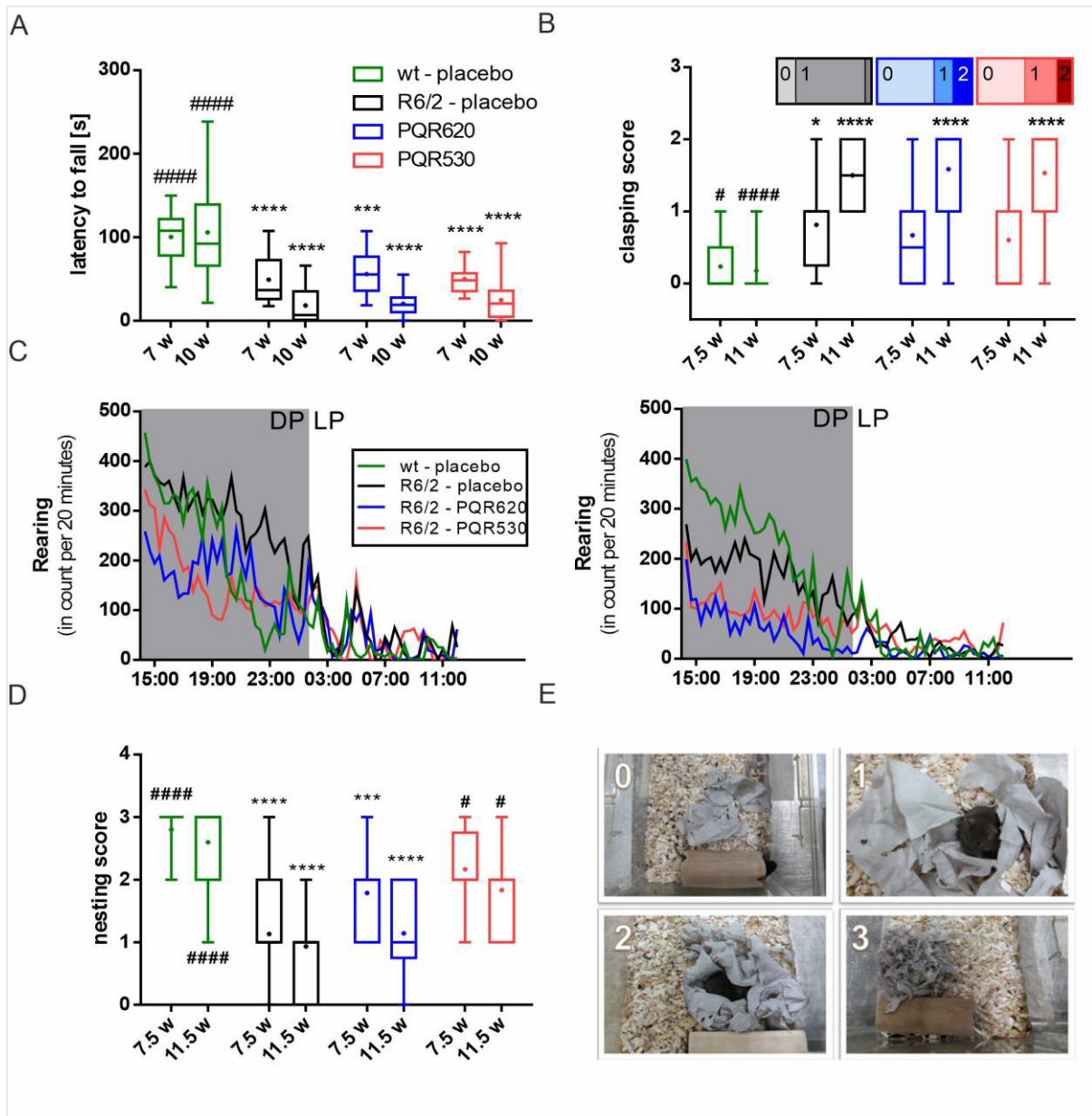


Figure 2: Effects of PQR530 and PQR620 on behavior. (A) Rotarod performance at 7 and 10 weeks of age. + indicates mean, line indicates median., RM Anova, 2-way, multiple comparisons against R6/2 (#) and wt (*). *** P < 0.001; **** P < 0.0001. (B) Clasping at 7.5 and 11 weeks of age. Score ranges from 0 – 2 points. + indicates mean, line indicates median.; * P < 0.05; **** P < 0.0001. Kruskal – Wallis test for One-way ANOVA, with nonparametric test multiple comparisons against wild type (*) and R6/2 (#); Dunn’s correction for multiple comparisons. Bar graphs represent score distribution at 7.5 weeks. (C) Rearing movements at 5 (left) and 11 weeks (right) of age. Average number of rearing movements over the 22-hour observation time. Mean values are plotted as 20-minute intervals. (D) Quantification of nesting scores. The quality of the nests built from the paper in the cage was scored at two different time points (7.5/ 11.5 weeks). + indicates mean, line indicates median * P < 0.05; **** P < 0.0001. Kruskal – Wallis test for One-way ANOVA, with nonparametric test multiple comparisons against wild type (*) and R6/2 placebo (#); Dunn’s correction for multiple comparisons. (E) Scoring scale examples. Only total values were given and scoring was performed blinded.

muscle weight had however no effect on the motor performance of the animals. Both compounds were additionally tested in the zQ175 mouse model of HD. Despite moderate weight loss, no complications comparable to the R6/2 mice were observed (personal

communication with PIQUR therapeutics). CAG lengths were checked in both experimental cohorts, which were generated from two different breeding groups of ovary transplanted females. Even though paternal transmission is known to be the cause of

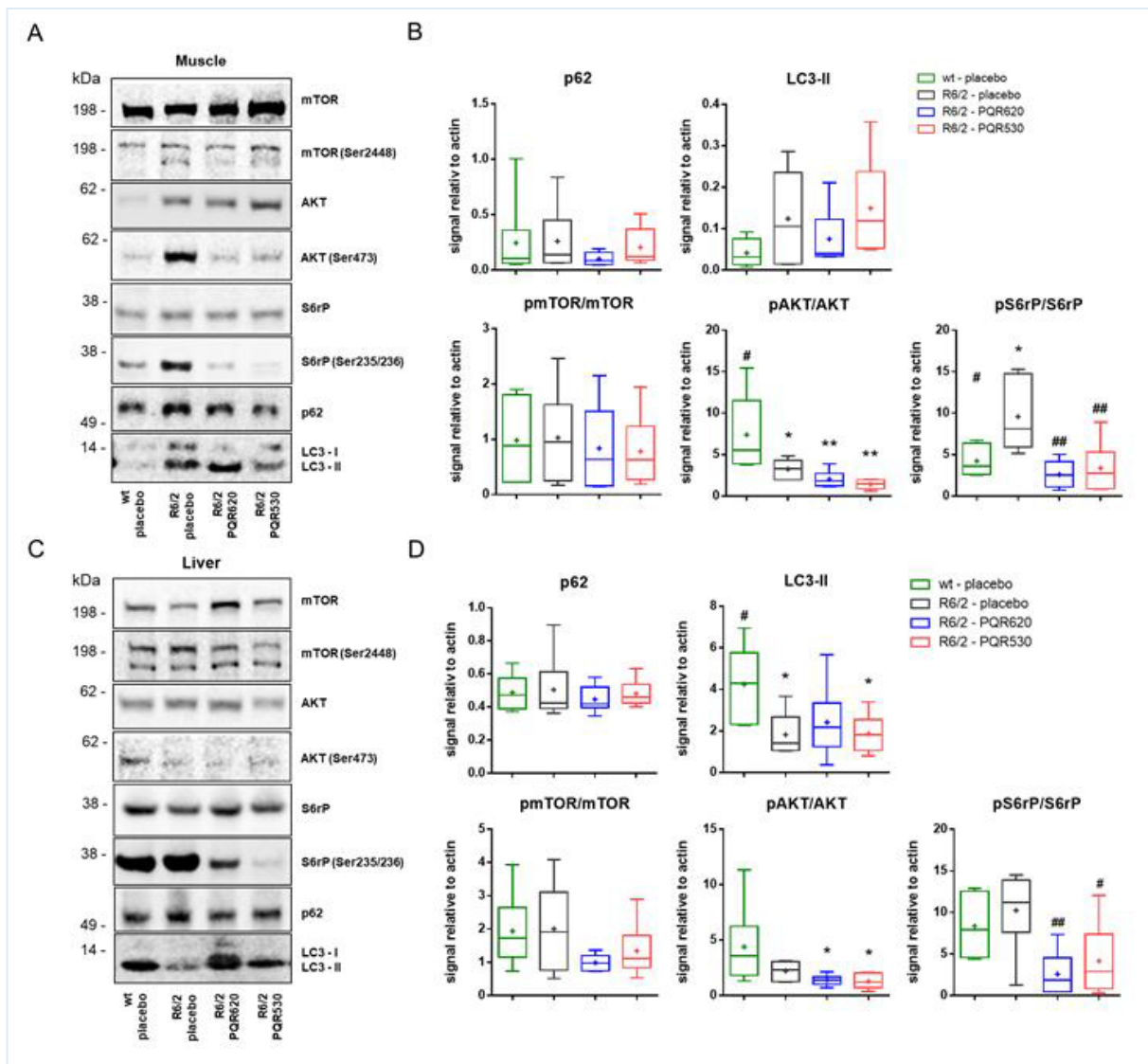


Figure 3: PQR compounds potently block mTOR inhibition in peripheral tissue. WB analysis of muscle (*m. gastrocnemius*) and liver 4 h after last treatment. Induction of autophagy was assessed by p62 and LC3-II. mTOR inhibition was monitored by phosphorylation of its downstream targets AKT and S6rP. Representative WB images are shown in A and C, with corresponding quantification of autophagy markers in B and D. + indicates mean, line indicates median; One-way ANOVA with multiple comparisons against R6/2 placebo (#) and wt-placebo (*); Dunnett's correction method for multiple comparisons. * $P < 0.05$; ** $P < 0.01$.

uncontrolled CAG expansions and therefore ovary transplanted females were bred with wild type males, we could detect a significant difference in the CAG length (Supplementary Figure 1 C). The motor phenotype of the R6/2 mouse, characterized by a motor coordination defect is detectable from a very early time point by rotarod. From 7 weeks of age onwards the R6/2 mice showed a deterioration of motor performance that was not affected by either compound (Figure 2A). Claspings is another

motor associated parameter that is routinely assessed in pre-clinical testing. From 9 weeks on, most R6/2 mice show immediate and total claspings of the hindlimbs, when suspended by the tail a few centimeters above the surface. Treatment with PQR530 and PQR620 led to a shift in proportion of mice claspings at an earlier timepoint, when claspings is not fully developed in all R6/2 mice (Figure 2 B). While the difference between wild type and R6/2 mice was significant at 7.5 weeks for the placebo

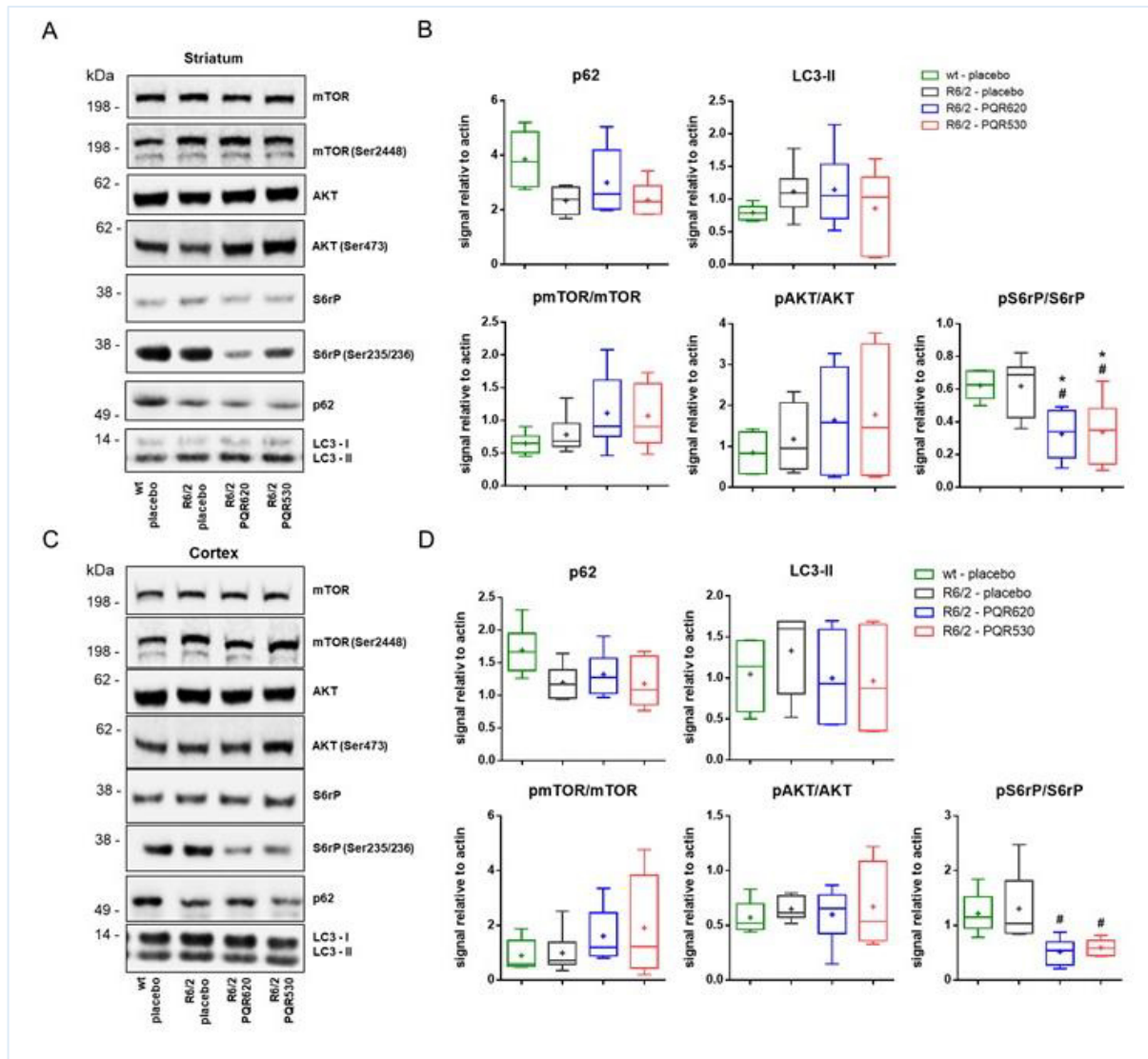


Figure 4: PQR compounds block mTOR signaling in the brain but fail to block AKT phosphorylation. WB analysis of striatum and cortex 4 h after last treatment. Induction of autophagy was assessed by p62 and LC3-II. mTOR inhibition was monitored by phosphorylation of its downstream targets AKT and S6rP. Representative WB images are shown in A and C, with corresponding quantification of autophagy markers in B and D. + indicates mean, line indicates median; One way – ANOVA with multiple comparisons against R6/2 placebo (#) and wt-placebo (*); Dunnet's correction method for multiple comparisons. * $P < 0.05$.

treated animals, PQR compound treated animals showed less clasping. In the second test at 11 weeks, all R6/2 mice showed moderate or complete clasping. Rearing, another parameter of motor performance was quantified over a time period of 22 hours in an automated home cage system (Figure 2 C). Overall activity of the mice in the cage and the distance moved in the cage were not different between the genotypes and treatments (data not shown). At 5 weeks of age PQR530 mice showed less rearing than the

R6/2 placebo group. This could be a combined effect of the hyperactivity described in young R6/2 mice and a reduced activity in the treated animals. Rearing during the first hour was additionally quantified, as the mice are exploring the unfamiliar cage with a lot of movements, also in the z-axis. At the older age, the difference between wildtype and R6/2 mice became apparent, whereas no difference between the treatment groups was observed. In the dark phase treated animals were rearing

tendentially less than the R6/2 placebo animals. Male mice are kept solitary in the cages for treatment studies to prevent any effects of fights or hierarchy. This allows to monitor the nest building abilities of the mice. The phenotype of the R6/2 model is complex and not limited to motoric abilities but further affects social interaction and behaviour. Building a nest is part of this social behaviour that is partly dependent on motoric skills, but also dependent on motivation and other factors that were not further assessed in this study [51] (Figure 2 D and E). The mixed background line of the R6/2 mice builds very elaborate, dome shaped nests from the material that is provided in the cages as an intact piece. A difference in this nest building behaviour can be observed from the beginning of the experiment, at 4 weeks of age and becomes more apparent with time. R6/2 mice differed from their wild-type litter mates regarding nesting behavior. This was clearly detectable at the age of 7.5 weeks and became more apparent with the progression of the phenotype (Figure 2 D). Interestingly, PQR530 treated animals did keep their ability to build a nest, which was significantly better than the placebo group. It is unclear to what extent these findings can be attributed to the treatment they were exposed to. It is unlikely that the results are a product of experimenter bias, since the pictures were taken and randomized several weeks before scoring took place; nevertheless, this experiment was based on subjective criteria (Figure 2 E).

PQR compounds inhibit mTOR and PQR530 leads to a reduction of mHTT load in the brain
The inhibition of mTOR with both substances,

PQR620 and PQR530, has been shown to induce autophagy in the *in vitro* experiments and markers of autophagy were indicative of induction of autophagy in wild type mice after 4 hours of treatment in preliminary experiments after a single dose of 50 mg/kg [28]. The inhibition of mTOR and the induction of autophagy was analysed in peripheral tissues (liver and muscle; Figure 3) and brain (striatum and cortex; Figure 4). The R6/2 mice show dysregulations in the mTOR pathway that have been described for HD models before. These are reduced levels of p62 in brain [52] and an increase in LC3-II levels in various tissues [52, 53]. However, the high flux in the autophagic process creates big variance in the samples, therefore most of the trends observed are not statistically significant. Furthermore, a dysregulation of AKT was observed in muscle [53]. In brain, AKT phosphorylation was unchanged after treatment with either compound (Figure 4) in contrast to muscle and liver (Figure 3). This was not observed in the preliminary experiments where mice were subjected to a single dose [28] and is interesting, because the inhibition of mTOR was shown by the dephosphorylation of ribosomal protein S6 (S6rP), in brain as well as in the peripheral tissue. The induction of autophagy however could not be shown in any of the tissues. Induction of autophagy would have theoretically led to a reduction of p62 and an increase in LC3. PQR620 did seem to bring the LC3 levels closer to the wild type level, especially in the cortex and muscle, but these changes are neither significant, nor is their biological relevance clear.

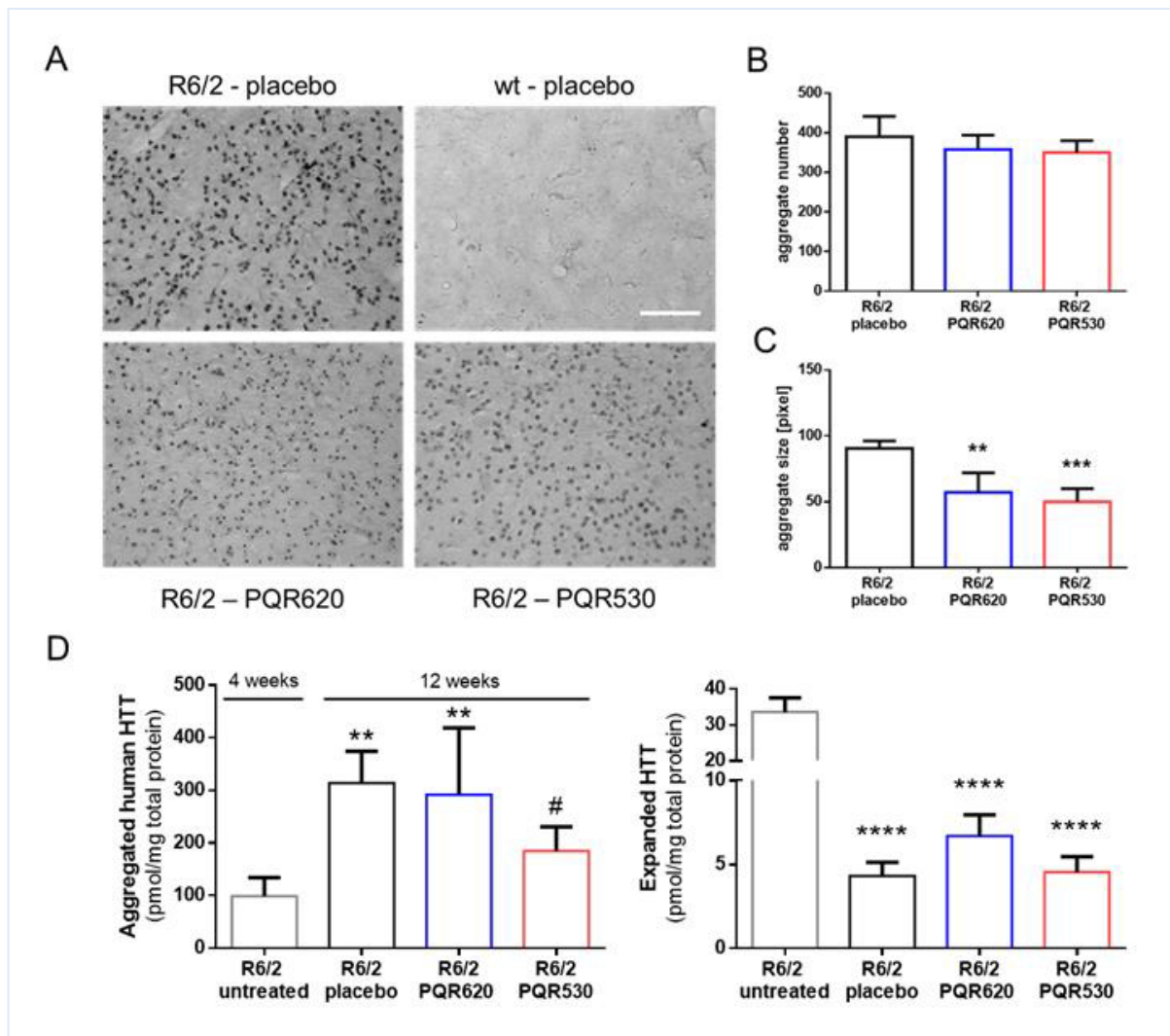


Figure 5: PQR compounds reduce the amount of aggregates in the brain. (A) EM48 staining of mHTT aggregates in striatal cryosections and (B) quantification of aggregate number and (C) size. (D) TR-FRET analysis of aggregated huntingtin (left) and MSD assay of soluble expanded HTT (right). Treatment groups are compared to samples from untreated R6/2 mice at 4 weeks of age. One way – ANOVA with multiple comparisons against R6/2 placebo (#) and 4 week old untreated animals (*); Dunnett's correction method for multiple comparisons. * P < 0.05; ** P < 0.01; *** P < 0.001; **** P < 0.0001.

R6/2 mice display intracellular and nuclear aggregates, as soon as post-natal day one. The aggregation is found throughout the entire brain. Differences in brain regions and size of the aggregates can be determined by immunohistochemistry. Analysis of striatum showed very strong staining for huntingtin positive aggregates (Figure 5 A). The number of aggregates between the different groups was comparable (Figure 5 B), whereas a size reduction was observed in R6/2 mice treated with PQR compounds (Figure 5 C). This

showed that aggregate size was reduced by both substances, by approximately 40%. These results were confirmed for PQR530 by TR-FRET. Aggregated (TR-FRET) and total amounts of soluble expanded huntingtin (MSD assay) were quantified (Figure 5 D) and both showed an increase in aggregated HTT levels in older animals. The levels of soluble expanded HTT were strongly decreased in the older animals and less affected by the treatment, which could be due to the low amount of soluble protein.

We could confirm with these findings that catalytic mTOR inhibition can be used to reduce the size of aggregates, and therefore the amount of aggregated protein in brain by oral administration.

Discussion

The results of the evaluation of PQR530 and PQR620 demonstrate their potential in reducing the amount of mHTT *in vivo*, confirming previous results from the *in vitro* characterization in HD cell models [28]. The reduction of size in the mostly nuclear aggregates was demonstrated with IHC and the reduction in aggregate load was shown with TR-FRET. In this regard, the reduction of aggregate size was as well demonstrated in the zQ175 mice, tested at a different institute (personal communication, unpublished data). The behavioral phenotype of the R6/2 model could not be ameliorated by the treatment. Behavioral testing was influenced by the effect of the drugs on the general condition of the animals. Weight loss and increased drinking combined with polyuria were observed. As the severity of side effects was not observed in previously tested wild type mice or zQ175 mice, HD related complications special to the R6/2 model could be the cause of the severity of the weight loss. R6/2 mice treated with pQR compounds developed symptoms of hyperglycemia before the onset in the placebo group, which was observed at around 9 weeks of age [54]. The weight loss in the R6/2 placebo group was less severe even at higher age. Animals with severe weight loss (>10% of their maximum weight) did perform worse in the rotarod test, possibly due to the lack of energy.

A contributing and interconnected factor to weight loss in the R6/2 model is muscle wasting. The presence of mHTT in the *gastrocnemius* has been shown to lead to an overactivation of mTOR and AKT and to an overall catabolic phenotype [55]. The muscle weight of the *m. gastrocnemius* was determined at the end of the experiment and the treatment groups did show slightly less reduction in muscle weight than the R6/2 – placebo group in comparison to wild type. The hyperphosphorylation of AKT in R6/2 mice was reduced in muscle after administration of PQR620 or PQR530. However, the improvement of the muscular phenotype did not affect the overall weight loss. R6/2 mice are a commonly used model in pre-clinical testing, as they present a very robust and fast-developing HD phenotype regarding behavior and the molecular markers [47]. A similar phenotype is also found in *HdhQ150* mice, confirming that exon1 is sufficient to trigger some aspects of the HD phenotype [56]. For this study, it is unclear, whether a less detrimental phenotype would have allowed for a better dissection of the contributing effects on the behavioral testing. R6/2 mice can be considered as a model for the severest form of HD, juvenile HD. This is because of the extreme early onset of disease (from post-natal day 1) and because of the severity of symptoms (seizures, extreme forms of dyskinesia) [57]. The R6/2 model develops aggregates and early disease symptoms and metabolic alterations already at a very early age, when the animals are still growing. In an animal model with a later onset of disease, at an adult age, the weight loss might be less severe.

Another option in such models would be to test, whether a treatment before disease onset would be sufficient to delay first symptoms. This can be supported by the trends in the data of this study. Signs of motor phenotypes (clasping, rotarod) were slightly better in the treatment groups at the earlier timepoints measured. Therefore, it could be beneficial treating a different animal model with a clear pre-symptomatic phase before disease onset, to reduce the aggregate levels, potentially delaying the point of overflow of toxic protein and relieving disease burden later. Also, defining the correct treatment regime could influence the outcome. Intermittent administration of everolimus has been shown to decrease the resistance to autophagy induction [58]. We could not assess autophagy induction indicated by levels of p62 and LC3-II. To reduce fluctuation of autophagic proteins, animals were treated exactly 4 hours before sacrificing them within 1.5 h at the same time of the day. For future experiments the use of autophagic flux blockers should be considered. The induction of autophagy at an old age is further limited by the declining levels of beclin1 and in HD by an increase of aggregate size and sequestration of autophagy regulating proteins in those aggregates [52, 59]. This could be another argument for a limited treatment phase at an earlier age and before the overt aggregation of huntingtin. Another interesting finding were the unaltered phosphorylation levels of AKT in brain at the end of the treatment period. Whereas the preliminary experiments in wild type animals showed that both compounds were able to reduce AKT

phosphorylation after a single oral administration [28], the animals treated for several weeks did not show the same effect in brain when they were dosed 4 hours before tissue collection. AKT phosphorylation has been described to increase upon mTOR inhibition in cancer cell lines [60] and an increase in p-AKT levels can generally be considered a positive pro-survival signal. In R6/1 mice increased p-AKT levels through PHLLP have been described as pro-survival mechanism [61, 62] together with the substantial role of AKT in brain. Phospho-S6rP levels were still decreased, which argues for enough target coverage. It is not clear, if AKT phosphorylation could be differentially regulated in brain after prolonged treatment, which could increase the survival of neurons through this signaling mechanism. AKT has further been shown to inhibit autophagy in a mTOR independent manner [63] by phosphorylating beclin1 and reducing autophagy initiation. This could be another contributing factor to the unchanged autophagy levels in brain.

In conclusion both compounds remain valid candidates for the reduction of mHTT in HD models. Further studies would be necessary to determine optimal dosing regimens and avoidance of overt weight loss.

Methods

R6/2 mice

B6CBA-Tg(HDexon1)62Gpb/3J mice (R6/2 mice) were obtained from 40 breeding pairs of wildtype males with ovarian transplant females purchased from Charles River (Charles River Laboratories, Sulzfeld, Germany). The pups are transgenic for the human N-terminal fragment

of the *HTT* gene. They carry a CAG repeat of approximately 150 CAGs [57].

Genotyping & fragment length analysis

All animals were genotyped at the beginning and the end of the experiments. Genotyping was performed by genomic DNA isolation (High Pure PCR Template Preparation Kit, Roche, Basel, Switzerland) and a standard PCR reaction. PCR reagents were purchased from Qiagen, Hilden, Germany.

Primer forward: 5' - atggcgacacctggaaaagctg

Primer reverse: 5' - aggtcgggtcagagagctcctc

Fragment length analysis was used to determine CAG size. In brief, PCR with fluorescently labelled primers for the sequence flanking the CAG repeats was performed. PCR product is run in capillary gel electrophoresis (Beckman Coulter, Brea, CA, USA) against a 600 bp size standard and CAG size is determined relative to unexpanded PCR product size.

Primer forward:

5' Cy5 – ccttcgagtcctccaagtccttc

Primer reverse: 5' - cggctgaggcagcagcggctgt

Housing conditions

The animal experiments were approved by the local ethics committee (Regierungspraesidium Tuebingen, Germany), in full compliance with the European Union legislation on the use of animals for scientific purposes (Directive 2010/63/EU). Male mice were used for this study. They were weaned and genotyped at 3 weeks of age and separated into single cages (euro norm: Type II L) at 3.5 weeks of age, to give them a short adaptation time before treatment began and housed under standard conditions, with standardized chew and water *ad libitum* in a 12/12 hours light/ dark cycle, switching at 2 am/ 2 pm. At 11 weeks of age or

when earlier weight-loss occurred, mice were additionally provided mashed chew.

Vehicle and preparation of dosing solution

40% SBECD (sulfobutylether-ether- β -cyclodextrin, Captisol[®], Dexolve[®]) solution was prepared (w/v) in water for injection (Ampuwa[®], Fresenius, Germany). The solution was mixed and sonicated. Vehicle and drug solution had a final concentration of 20% SBECD. PQR530 was added at 0.545% (w/v) to a 20% SBECD solution. PQR620 was added at 1.082% to the vehicle solution. Both dosing solutions were mixed and sonicated until no crystals were visible by light microscopy. pH was adjusted with 0.02 M HCl to 3.0 \pm 0.1. The dosing solutions were prepared always for 4 days in advance and were stored light protected at room temperature.

Treatment with PQR530 and PQR620

Treatment groups were established from genotype and measurement of weight, rotarod performance and litter. Genotype was confirmed at the end of the treatment. They were distributed equally over the four groups. Treatment began at four weeks of age and ended at 11 weeks, when mice were sacrificed. Mice were dosed 6 days per week once daily via oral gavage at the same time each day (10.30 am). Treatment groups were the following: wt placebo (20% SBECD solution), R6/2 placebo (SBECD solution), PQR530 (0.5% PQR530 in SBECD solution); PQR620 (1.0% PQR620 in SBECD solution). The experimenter was not blinded during drug administration.

Behavioral testing

All experiments were performed by the same person performing the treatment. For behavioral

testing, the animals were ordered according to a pre-set pseudo – randomized order and animal ID – cards were covered for blindness of the experimenter. n = 12-15.

Rotarod

Motor deficiencies were assessed at 7 weeks and at 10 weeks of age. Mice were tested on three consecutive days in the dark phase, starting at least 8 hours after the dosage. Mice were placed in the room, where the behavioral testing took place an hour before the start of the experiments. Experimenter was blinded to the treatment groups, genotypes become apparent from 6 weeks as motoric deficits develop. On each day of the testing, mice were placed on the rod (TSE systems, Bad Homburg, Germany) for a test run at a constant speed of 4 rpm for 300 seconds. The test run ended after 300 seconds or when the mice got off the rod a sixth time. This test run was followed by three runs with acceleration from 4 rpm to 40 rpm, as well for 300 seconds. Mice were only placed back, when the first period on the rod was shorter than 10 seconds, to exclude effects from positioning the mice on the rod. Time between each run was one hour. Time spent on the rod was recorded automatically, the average of the 3 runs was analyzed.

Labmaster – automated home cage

During the testing period, each day seven mice were recorded in the home-cage system (TSE system, Bad Homburg, Germany). Mice were assigned in a way that genotypes and treatments were mixed, and individual mice were not in the same groups at each time point and in a different cage. Recording was performed in the automated home-cage system LabMaster. Mice were recorded for a period of 22 hours from 2

pm to 11 am on the following day. Mice were given an acclimatization phase in the room of the behavioral testing of 1 hour. Mice were placed in the cages and monitoring started immediately. The measurements started approximately 10 minutes before the dark phase. Measurements were acquired in 1-minute intervals. Locomotion was analyzed by measurements of the beam breaks in the horizontal axes (ambulatory activity) and the distance travelled (Distance) and the vertical z-axis (rearing). Data analysis was performed with R (R: A Language and Environment for Statistical Computing, R Development Core Team, R Foundation for Statistical Computing, Vienna, Austria, 2011, ISBN 3-900051-07-0, <http://www.R-project.org>). The first 30 minutes of the 22-hour period were analyzed as the habituation time, the long – term measurements were summarized in 20 minutes intervals.

Clasping

Clasping behavior was assessed at two different time points. At 7.5 weeks this behavior starts to develop and at 11 weeks when almost all mice display this type of posture. Mice were suspended by the tail above a surface for a maximum of 30 seconds. The posture of the hind limbs is graded from 0 – 2 points for the severity of the clasping. The experimenter was blinded for the treatment groups and the genotype, even though the differences between R6/2 mice and wild – type mice become evident at 11 weeks.

Nesting

Pictures of the nests were taken at different time points of the day before the weekly exchange of the cages. Quality of the nest was scored by a grading system from 0 -3. The pictures were

labelled and ordered in a way that the experimenter was unable to identify genotype or treatment.

Sample collection

Mice were sacrificed on 4 consecutive days at the age of 11 weeks. Tissue was collected 4 hours post dosage. Mice were dosed in the same order as they were sacrificed. The maximum time between the first and the last animal per day was 1.5 hours for tissue collection. Perfusion was performed at 4 hours after dosage, as well; mice were dosed in 30 minutes intervals. Tissue was stored in PBS with 0.03% sodium acetate.

Immunohistological analysis of mHTT aggregation

To detect mHTT aggregates, immunostaining of striata was performed. Brains were fixed in 4% paraformaldehyde (SAV LP GmbH, Flintsbach am Inn, Germany). Before embedding in O.C.T (Sakura Finetek Germany GmbH, Staufen im Breisgau, Germany), whole brains were soaked in sucrose solution (30% w/v, Sigma-Aldrich, St. Louis; USA) for 3 days, snap frozen and fixed in Tissue-Tek® O.C.T (Sakura Finetek, Staufen im Breisgau, Germany). Brains were cut serially into 25 µm coronal sections on a cryostat (Leica CM-3050-S, Leica Biosystems Nussloch GmbH, Germany). Sections were stored in PBS, supplemented with 0.03% sodium acetate at 4°C. For free-floating staining, striatal sections were placed into fresh PBS. All steps were performed at room temperature. Blocking was performed in 0.5% sodium borohydride in PBS for 30 minutes and followed by washing with PBS. Primary antibody incubation with EM48 (MAB5374; Merck Chemicals GmbH,

Darmstadt, Germany) diluted 1:1000 was performed overnight. On the following day sections were washed with TBST and incubated with biotinylated goat anti-mouse IgG (Vecta BA9200, Vector Laboratories, Burlingame, USA) at a 1:1000 dilution for 2 hours. Avidin-biotin complex (Vectastain® Elite ABC Kit, Vector Laboratories, Burlingame, USA) was used at a 1:400 dilution. Incubation time was 1 hour. Biotinylated tyramine, supplemented with 0.001% H₂O₂ was administered for 8 minutes. For color development, sections were incubated for 4 minutes in a nickel-DAB- H₂O₂ containing buffer (0.6% nickel, 0.01% DAB and 0.001% H₂O₂ in 0.05 M Tris, 0.05 M imidazole). Reaction was stopped by placing the sections in TI buffer (0.05 M Tris, 0.05 M imidazole) and mounted in water, free floating. Sections were dehydrated by ethanol and xylol dilution row and sealed under coverslips with mounting medium (CV, Leica, Wetzlar, Germany). Images were acquired using a Zeiss Axioplan microscope (Plan-NEOFLUAR ×40/0.75 objective, AxioCam MRc) and Axiovision 4.8 software (Carl Zeiss Microscopy GmbH, Jena, Germany). 4 animals were analyzed per group. Per animal three subsequent sections of the striatum were analyzed. The EM48 positive structures were analyzed with the ImageJ built in particle analysis, with a fixed threshold for all pictures (ImageJ 1.47v; NIH, Bethesda, USA).
n = 4-5

Tissue sample preparation

Homogenates were prepared from the tissues collected with RIPA lysis buffer (50 mM Tris pH 7.5, 150 mM NaCl, 0.1% SDS, 0.5% sodium deoxycholate and 1% Igepal, containing

protease inhibitors and phosphatase inhibitors). Brain regions were homogenized for 30 seconds, muscle for 1 min with an ultra thurax. Muscle samples were minced in the frozen state before homogenization. Homogenized samples were incubated for 15 minutes on ice, during this time samples were sonicated for 10 seconds at 40% intensity and vortexed every five minutes. Samples were divided into homogenates and samples that were further processed to lysates. Therefore, they were transferred into pre-cooled reaction tubes and centrifuged for 13,200 g x 20 minutes at 4°C. To the supernatant 10 % glycerol of the total volume was added. Lysates and homogenates were kept at -80°C until further processing.

Analysis of markers of the mTOR pathway by Western Blot

Western blot was performed according to standard procedures. In brief, precast gradient gels (Novex® 4-12% Bis- Tris Mini Protein Gels, Invitrogen, USA) were used for the analysis of mTOR inhibition. Samples were prepared to contain 30 µg of protein. Running buffer was MES buffer (50 mM MES, 50 mM Tris, 0.1 % SDS ,1 mM EDTA) and gels were run at 150 V, constant. Proteins were transferred onto 0.2 µm nitrocellulose membrane by tank transfer in a TE22 Transfer Tank (Hofer, Serva Electrophoresis GmbH, Heidelberg, Germany) in either Bis- Tris transfer buffer (25 mM Bicine, 25 mM Bis-Tris, 1 mM EDTA) with 15% methanol. After transfer membranes were blocked in 5 % skim milk powder in TBST. n = 5-6 animals.

Antibodies for immunoblot analysis and detection method

Membranes were probed with the following

primary antibodies at 4°C, overnight.

Antibody	Dilution	Company
mTOR	1:1000	Cell signaling, Leiden, The Netherlands
mTOR (Ser2448)	1:1000	Cell signaling, Leiden, The Netherlands
AKT	1:1000	Cell signaling, Leiden, The Netherlands
AKT (Ser473)	1:1000	Cell signaling, Leiden, The Netherlands
P62	1:1000	Cell signaling, Leiden, The Netherlands
S6RP (54D2)	1:1000	Cell signaling, Leiden, The Netherlands
S6RP (Ser235/236)	1:1000	Cell signaling, Leiden, The Netherlands
LC3(0231-100/LC3-5F10)	1:200	nanoTools Antikörpertechnik GmbH & Co. KG; Teningen; Germany
MW8	1:100	DSHB Hybridoma Product; Iowa City, USA
Actin	1:20000	Sigma Aldrich; Saint Louis, MO, USA
Actin cardiac (A9357)	1:2000	Sigma Aldrich; Saint Louis, MO, USA

On the next day, membranes were washed with TBST and incubated for 1 hour with respective secondary IRDye antibodies goat anti-mouse 680LT, 800CW and goat anti-rabbit 800CW (all 1:10,000; LI-COR Biosciences). Fluorescence detection was performed with the LI-COR ODYSSEY® FC and quantified with Image Studio software version 2.1.10 (LI-COR Biosciences).

TR-FRET & MSD assays

To each sample 100 µl of Evotec MSD Lysis

Buffer was added (150 mM NaCl, 20 mM Tris, pH 7.5, 1 mM EDTA, 1 mM EGTA, 1% Triton-X-100 (Evotec MSD Lysis Buffer Stock Solution) supplemented with 10 mM NaF, 1 mM PMSF, 1x Phosphatase Inhibitor Cocktail 2, 1x Phosphatase Inhibitor Cocktail 3, 1x Protease Inhibitor Cocktail). Samples were homogenized in LYSING tubes CK15 (Precellys, Cat. # KT03961-1203.0.5) by using the FastPrep method (MP FastPrep homogenizer FastPrep-24, MP Biomedicals; 4 runs with 30 sec, 6 m/sec and settling time of app. 4 mins in between the runs). After centrifugation (15 min at 15700 RCF and 4° C; 2 x), the supernatant was transferred in pre-cooled tubes. Protein concentration of the tissue homogenate was determined by BCA (Pierce BCA Protein Assay, Thermo Scientific; Cat. No. 23225) and protein concentration was adjusted to 2 mg/ml. Aliquots were prepared and samples were pre-frozen on dry ice, then stored at -80° C until measurement of aggregated and expanded soluble mutant HTT levels (Evotec TR-FRET assay 13, Evotec MSD Assay 6). For detection of expanded soluble mutant HTT final concentrations of 0.1 µg/ µl total protein were used and applied to the assay (Evotec MSD assay 6). For detection of aggregated mutant HTT final concentrations of 1 µg/ µl total protein were used and applied to the assay (Evotec TR-FRET assay 13). n = 5-6. Samples were tested in technical duplicates.

The following recombinant standard proteins were used for quantification of HTT: Evotec MSD Assay 6 for detection of expanded soluble mutant HTT: Human HTT NF573Q73 (Biofocus) spiked into respective background

matrix (tissue homogenates of wild type whole brain; 0.2 mg/ml) and further diluted 1:1 in blocking buffer (2% (w/v) BSA / 0.2% (v/v) Tween20). Evotec TR-FRET Assay 13 for detection of aggregated mutant HTT: Thrombin digested aggregated exon1-Q46 spiked into respective background matrix (tissue homogenates of wild type whole brain; 2 mg/ml). Standard proteins were applied between 0.001 and 10 fmol/µl for Evotec MSD assay 6, and between 0.001 and 250 fmol/µl for Evotec TR-FRET assay 13.

Statistical analysis

Statistical analysis was performed with GraphPad Prism 6 (GraphPad Software Inc., La Jolla, CA, USA). One-way ANOVA was performed with multiple comparisons to the placebo group and Dunnett's correction method. Other used statistical methods are mentioned in figure legends. Significance level was set to 0.05.

Literature

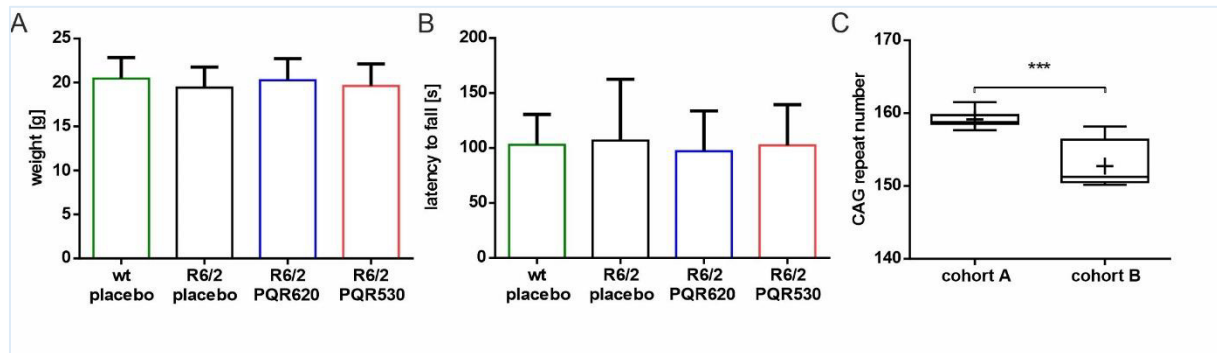
1. Vonsattel JP, DiFiglia M: **Huntington disease**. *Journal of neuropathology and experimental neurology* 1998, **57**(5):369-384.
2. The Huntington's Disease Collaborative Research Group: **A novel gene containing a trinucleotide repeat that is expanded and unstable on Huntington's disease chromosomes. The Huntington's Disease Collaborative Research Group**. *Cell* 1993, **72**(6):971-983.
3. Daldin M, Fodale V, Cariulo C, Azzollini L, Verani M, Martufi P, Spiezia MC, Deguire SM, Cherubini M, Macdonald D *et al*: **Polyglutamine expansion affects huntingtin conformation in multiple Huntington's disease models**. *Scientific Reports* 2017, **7**(1):5070.
4. Caron NS, Desmond CR, Xia J, Truant R: **Polyglutamine domain flexibility mediates the proximity between flanking sequences in huntingtin**. *Proceedings of the National Academy of Sciences* 2013, **110**(36):14610-14615.
5. Harjes P, Wanker EE: **The hunt for huntingtin function: interaction partners tell many different stories**. *Trends Biochem Sci* 2003, **28**(8):425-433.
6. Graham RK, Deng Y, Slow EJ, Haigh B, Bissada N, Lu G, Pearson J, Shehadeh J, Bertram L, Murphy Z: **Cleavage at the caspase-6 site is required for neuronal dysfunction and degeneration due to mutant huntingtin**. *Cell* 2006, **125**(6):1179-1191.
7. Lunkes A, Lindenberg KS, Ben-Haïem L, Weber C, Devys D, Landwehrmeyer GB, Mandel J-L, Trottier Y: **Proteases acting on mutant huntingtin generate cleaved products that differentially build up cytoplasmic and nuclear inclusions**. *Molecular cell* 2002, **10**(2):259-269.
8. Gafni J, Hermel E, Young JE, Wellington CL, Hayden MR, Ellerby LM: **Inhibition of calpain cleavage of huntingtin reduces toxicity accumulation of calpain/caspase fragments in the nucleus**. *Journal of Biological Chemistry* 2004, **279**(19):20211-20220.
9. Rockabrand E, Slepko N, Pantalone A, Nukala VN, Kazantsev A, Marsh JL, Sullivan PG, Steffan JS, Sensi SL, Thompson LM: **The first 17 amino acids of Huntingtin modulate its sub-cellular localization, aggregation and effects on calcium homeostasis**. *Human molecular genetics* 2006, **16**(1):61-77.
10. Zuccato C, Valenza M, Cattaneo E: **Molecular Mechanisms and Potential Therapeutical Targets in Huntington's Disease**. *Physiological Reviews* 2010, **90**(3):905.
11. Kolobkova YA, Vigont VA, Shalygin AV, Kaznacheeva EV: **Huntington's Disease: Calcium Dyshomeostasis and Pathology Models**. *Acta Naturae* 2017, **9**(2):34-46.
12. Quintanilla RA, Johnson GVW: **Role of mitochondrial dysfunction in the pathogenesis of Huntington's disease**. *Brain research bulletin* 2009, **80**(4-5):242-247.
13. Beal MF: **Mitochondrial dysfunction in neurodegenerative diseases**. *Biochimica et Biophysica Acta (BBA) - Bioenergetics* 1998, **1366**(1):211-223.
14. Panov AV, Gutekunst C-A, Leavitt BR, Hayden MR, Burke JR, Strittmatter WJ, Greenamyre JT: **Early mitochondrial calcium defects in Huntington's disease are a direct effect of polyglutamines**. *Nature neuroscience* 2002, **5**(8):731-736.
15. Rubinsztein DC: **The roles of intracellular protein-degradation pathways in neurodegeneration**. *Nature* 2006, **443**(7113):780.
16. Wild EJ, Tabrizi SJ: **Therapies targeting DNA and RNA in Huntington's disease**. *The Lancet Neurology* 2017, **16**(10):837-847.
17. Kordasiewicz Holly B, Stanek Lisa M, Wancewicz Edward V, Mazur C, McAlonis Melissa M, Pytel Kimberly A, Artates Jonathan W, Weiss A, Cheng Seng H, Shihabuddin Lamya S *et al*: **Sustained Therapeutic Reversal of Huntington's Disease by Transient Repression of Huntingtin Synthesis**. *Neuron* 2012, **74**(6):1031-1044.
18. Creus-Muncunill J, Badillos-Rodríguez R, Garcia-Forn M, Masana M, Garcia-Díaz Barriga G, Guisado-Corcoll A, Alberch J, Malagelada C, Delgado-García JM, Gruart A *et al*: **Increased translation as a novel pathogenic mechanism in Huntington's disease**. *Brain* 2019, **142**(10):3158-3175.
19. Ravikumar B, Duden R, Rubinsztein DC: **Aggregate-prone proteins with polyglutamine and polyalanine expansions are degraded by autophagy**. *Hum Mol Genet* 2002, **11**.

20. Berger Z: **Rapamycin alleviates toxicity of different aggregate-prone proteins.** *Hum Mol Genet* 2006, **15**:433-442.
21. Sarkar S, Ravikumar B, Floto RA, Rubinsztein DC: **Rapamycin and mTOR-independent autophagy inducers ameliorate toxicity of polyglutamine-expanded huntingtin and related proteinopathies.** *Cell Death Differ* 2009, **16**:46-56.
22. Bruce-Keller AJ, Umberger G, McFall R, Mattson MP: **Food restriction reduces brain damage and improves behavioral outcome following excitotoxic and metabolic insults.** *Annals of Neurology: Official Journal of the American Neurological Association and the Child Neurology Society* 1999, **45**(1):8-15.
23. Ehrnhoefer DE, Martin DD, Qiu X, Ladha S, Caron NS, Skotte NH, Nguyen YT, Engemann S, Franciosi S, Hayden MR: **Feeding Schedule And Proteolysis Regulate Autophagic Clearance Of Mutant Huntingtin.** *bioRxiv* 2017.
24. Spencer B, Potkar R, Trejo M, Rockenstein E, Patrick C, Gindi R, Adame A, Wyss-Coray T, Masliah E: **Beclin 1 gene transfer activates autophagy and ameliorates the neurodegenerative pathology in α -synuclein models of Parkinson's and Lewy body diseases.** *Journal of Neuroscience* 2009, **29**(43):13578-13588.
25. Mealer RG, Murray AJ, Shahani N, Subramaniam S, Snyder SH: **Rhes, a striatal-selective protein implicated in Huntington disease, binds beclin-1 and activates autophagy.** *Journal of Biological Chemistry* 2014, **289**(6):3547-3554.
26. Sarkar S, Davies JE, Huang Z, Tunnacliffe A, Rubinsztein DC: **Trehalose, a novel mTOR-independent autophagy enhancer, accelerates the clearance of mutant huntingtin and α -synuclein.** *J Biol Chem* 2007, **282**:5641-5652.
27. Walter C, Clemens LE, Muller AJ, Fallier-Becker P, Proikas-Cezanne T, Riess O, Metzger S, Nguyen HP: **Activation of AMPK-induced autophagy ameliorates Huntington disease pathology in vitro.** *Neuropharmacology* 2016, **108**:24-38.
28. Singer E, Walter C, Fabbro D, Rageot D, Beauflis F, Wymann MP, Rischert N, Riess O, Hillmann P, Nguyen HP: **Brain-penetrant PQR620 mTOR and PQR530 PI3K/mTOR inhibitor reduce huntingtin levels in cell models of HD.** *Neuropharmacology* 2019:107812.
29. Kraft C, Peter M, Hofmann K: **Selective autophagy: ubiquitin-mediated recognition and beyond.** *Nature cell biology* 2010, **12**:836.
30. Mizushima N, Levine B, Cuervo AM, Klionsky DJ: **Autophagy fights disease through cellular self-digestion.** *Nature* 2008, **451**(7182):1069-1075.
31. Ravikumar B, Vacher C, Berger Z, Davies JE, Luo S, Oroz LG: **Inhibition of mTOR induces autophagy and reduces toxicity of polyglutamine expansions in fly and mouse models of Huntington disease.** *Nat Genet* 2004, **36**.
32. Menzies FM: **Autophagy induction reduces mutant ataxin-3 levels and toxicity in a mouse model of spinocerebellar ataxia type 3.** *Brain* 2010, **133**:93-104.
33. Spilman P, Podlutskaya N, Hart MJ, Debnath J, Gorostiza O, Bredesen D, Richardson A, Strong R, Galvan V: **Inhibition of mTOR by Rapamycin Abolishes Cognitive Deficits and Reduces Amyloid- β Levels in a Mouse Model of Alzheimer's Disease.** *PLOS ONE* 2010, **5**(4):e9979.
34. Santini E, Heiman M, Greengard P, Valjent E, Fisone G: **Inhibition of mTOR signaling in Parkinson's disease prevents L-DOPA-induced dyskinesia.** *Sci Signal* 2009, **2**:ra36.
35. Guertin DA, Sabatini DM: **The Pharmacology of mTOR Inhibition.** *Science Signaling* 2009, **2**(67):pe24-pe24.
36. Cho DC: **Targeting the PI3K/Akt/mTOR Pathway in Malignancy: Rationale and Clinical Outlook.** *BioDrugs* 2014, **28**(4):373-381.
37. Hillmann P, Rageot D, Beauflis F, Melone A, Sele A, Ettlin RA, Mestan J, Cmiljanovic V, Lang M, Singer E: **Pharmacological characterization of the selective, orally bioavailable, potent dual PI3K/mTORC1/2 inhibitor PQR530.** In.: AACR; 2017.
38. Rageot D, Beauflis F, Melone A, Sele AM, Bohnacker T, Lang M, Mestan J, Hillmann P, Hebeisen P, Fabbro D: **Discovery and biological evaluation of PQR530, a highly potent dual pan-PI3K/mTORC1/2 inhibitor.** In.: AACR; 2017.
39. Beauflis F, Rageot D, Melone A, Sele A, Lang M, Mestan J, Ettlin RA, Hillmann P, Cmiljanovic V, Walter C: **Abstract 393A: Pharmacological characterization of the selective, orally bioavailable, potent mTORC1/2 inhibitor PQR620.** In.: AACR; 2016.

40. Rageot D, Bohnacker T, Melone A, Langlois J-B, Borsari C, Hillmann P, Sele AM, Beaufils F, Zvelebil M, Hebeisen P *et al*: **Discovery and Preclinical Characterization of 5-[4,6-Bis({3-oxa-8-azabicyclo[3.2.1]octan-8-yl})-1,3,5-triazin-2-yl]-4-(difluoromethyl)pyridin-2-amine (PQR620), a Highly Potent and Selective mTORC1/2 Inhibitor for Cancer and Neurological Disorders.** *Journal of Medicinal Chemistry* 2018.
41. Tarantelli C, Gaudio E, Hillmann P, Spriano F, Rinaldi A, Kwee I, Cascione L, Fabbro D, Stathis A, Zucca E: **The novel mTORC1/2 inhibitor PQR620 has in vitro and in vivo activity in lymphomas.** *European Journal of Cancer* 2016, **69**:S38.
42. Tarantelli C, Gaudio E, Hillmann P, Spriano F, Sartori G, Aresu L, Cascione L, Rageot D, Kwee I, Beaufils F: **The Novel TORC1/2 Kinase Inhibitor PQR620 Has Anti-Tumor Activity in Lymphomas as a Single Agent and in Combination with Venetoclax.** *Cancers* 2019, **11**(6):775.
43. Brandt C, Hillmann P, Noack A, Römermann K, Öhler LA, Rageot D, Beaufils F, Melone A, Sele AM, Wymann MP: **The novel, catalytic mTORC1/2 inhibitor PQR620 and the PI3K/mTORC1/2 inhibitor PQR530 effectively cross the blood-brain barrier and increase seizure threshold in a mouse model of chronic epilepsy.** *Neuropharmacology* 2018, **140**:107-120.
44. Li JY, Popovic N, Brundin P: **The Use of the R6 Transgenic Mouse Models of Huntington's Disease in Attempts to Develop Novel Therapeutic Strategies.** *NeuroRx* 2005, **2**(3):447-464.
45. Hockly E, Woodman B, Mahal A, Lewis CM, Bates G: **Standardization and statistical approaches to therapeutic trials in the R6/2 mouse.** *Brain Res Bull* 2003, **61**(5):469-479.
46. Luthi-Carter R, Hanson SA, Strand AD, Bergstrom DA, Chun W, Peters NL, Woods AM, Chan EY, Kooperberg C, Krainc D *et al*: **Dysregulation of gene expression in the R6/2 model of polyglutamine disease: parallel changes in muscle and brain.** *Human Molecular Genetics* 2002, **11**(17):1911-1926.
47. Hickey MA, Gallant K, Gross GG, Levine MS, Chesselet M-F: **Early behavioral deficits in R6/2 mice suitable for use in preclinical drug testing.** *Neurobiology of Disease* 2005, **20**(1):1-11.
48. Petersén Å, Renström E, Sundler F, Mulder H, Li J-Y, Gil J, Bacos K, Fex M, Björkqvist M, Popovic N *et al*: **The R6/2 transgenic mouse model of Huntington's disease develops diabetes due to deficient β -cell mass and exocytosis.** *Human Molecular Genetics* 2005, **14**(5):565-574.
49. Cepeda-Prado E, Popp S, Khan U, Stefanov D, Rodríguez J, Menalled LB, Dow-Edwards D, Small SA, Moreno H: **R6/2 Huntington's Disease Mice Develop Early and Progressive Abnormal Brain Metabolism and Seizures.** *The Journal of Neuroscience* 2012, **32**(19):6456-6467.
50. Wood NI, Goodman AOG, van der Burg JMM, Gazeau V, Brundin P, Björkqvist M, Petersén Å, Tabrizi SJ, Barker RA, Jennifer Morton A: **Increased thirst and drinking in Huntington's disease and the R6/2 mouse.** *Brain Research Bulletin* 2008, **76**(1-2):70-79.
51. Deacon RMJ: **Assessing nest building in mice.** *Nat Protocols* 2006, **1**(3):1117-1119.
52. Rue L, Lopez-Soop G, Gelpi E, Martinez-Vicente M, Alberch J, Perez-Navarro E: **Brain region- and age-dependent dysregulation of p62 and NBR1 in a mouse model of Huntington's disease.** *Neurobiol Dis* 2013, **52**:219-228.
53. She P, Zhang Z, Marchionini D, Diaz WC, Jetton TJ, Kimball SR, Vary TC, Lang CH, Lynch CJ: **Molecular characterization of skeletal muscle atrophy in the R6/2 mouse model of Huntington's disease.** *American Journal of Physiology - Endocrinology And Metabolism* 2011, **301**(1):E49-E61.
54. Hurlbert MS, Zhou W, Wasmeier C, Kaddis FG, Hutton JC, Freed CR: **Mice transgenic for an expanded CAG repeat in the Huntington's disease gene develop diabetes.** *Diabetes* 1999, **48**(3):649-651.
55. She P, Zhang Z, Marchionini D, Diaz WC, Jetton TJ, Kimball SR, Vary TC, Lang CH, Lynch CJ: **Molecular characterization of skeletal muscle atrophy in the R6/2 mouse model of Huntington's disease.** *American Journal of Physiology-Endocrinology and Metabolism* 2011, **301**(1):E49-E61.
56. Woodman B, Butler R, Landles C, Lupton MK, Tse J, Hockly E, Moffitt H, Sathasivam K,

- Bates GP: **The HdhQ150/Q150 knock-in mouse model of HD and the R6/2 exon 1 model develop comparable and widespread molecular phenotypes.** *Brain Research Bulletin* 2007, **72**(2):83-97.
57. Mangiarini L, Sathasivam K, Seller M, Cozens B, Harper A, Hetherington C, Lawton M, Trotter Y, Leach H, Davies SW *et al*: **Exon 1 of the HD gene with an expanded CAG repeat is sufficient to cause a progressive neurological phenotype in transgenic mice.** *Cell* 1996, **87**(3):493-506.
58. Kurdi A, De Doncker M, Leloup A, Neels H, Timmermans J-P, Lemmens K, Apers S, De Meyer GRY, Martinet W: **Continuous administration of the mTORC1 inhibitor everolimus induces tolerance and decreases autophagy in mice.** *British Journal of Pharmacology* 2016:n/a-n/a.
59. Shibata M, Lu T, Furuya T, Degtarev A, Mizushima N, Yoshimori T, MacDonald M, Yankner B, Yuan J: **Regulation of Intracellular Accumulation of Mutant Huntingtin by Beclin 1.** *Journal of Biological Chemistry* 2006, **281**(20):14474-14485.
60. O'Reilly KE, Rojo F, She Q-B, Solit D, Mills GB, Smith D, Lane H, Hofmann F, Hicklin DJ, Ludwig DL *et al*: **mTOR Inhibition Induces Upstream Receptor Tyrosine Kinase Signaling and Activates Akt.** *Cancer Research* 2006, **66**(3):1500-1508.
61. Saavedra A, García-Martínez JM, Xifró X, Giralt A, Torres-Peraza JF, Canals JM, Díaz-Hernández M, Lucas JJ, Alberch J, Pérez-Navarro E: **PH domain leucine-rich repeat protein phosphatase 1 contributes to maintain the activation of the PI3K/Akt pro-survival pathway in Huntington's disease striatum.** *Cell death and differentiation* 2009, **17**:324.
62. Faivre-Sarrailh C, Laval M, Liévens J-C, Iché M, Birman S: **AKT-sensitive or insensitive pathways of toxicity in glial cells and neurons in Drosophila models of Huntington's disease.** *Human Molecular Genetics* 2007, **17**(6):882-894.
63. Wang RC, Wei Y, An Z, Zou Z, Xiao G, Bhagat G, White M, Reichelt J, Levine B: **Akt-Mediated Regulation of Autophagy and Tumorigenesis Through Beclin 1 Phosphorylation.** *Science* 2012, **338**(6109):956-959.

Supplementary material



Supplementary Figure 1: Treatment group division and CAG length in 2 experimental cohorts. (A) equal group division by weight at 3 weeks of age. (B) equal rotarod performance in the different treatment groups at 3 weeks of age. (C) fragment length analysis for CAG number determination in both experimental cohorts.